

Investigation of Bacterial Cell Surface Accessibility and Peptidoglycan Interactions

Noel Jacqueline Ferraro

Washington, New Jersey

B.S. Chemistry, Moravian College (now University), 2016

A Dissertation presented to the Graduate Faculty of the University of Virginia in
Candidacy for the Degree of Doctor of Philosophy

Department of Chemistry

University of Virginia

December 2021

Abstract

Antibiotic resistance is a threat to public health that demands to be met with either new and innovative antibiotics or alternative therapies. The occurrence of antibiotic resistant bacteria is a multifactorial process but often involves improper use of antibiotics or sharing of genetic components that allow bacteria to survive when challenged with antimicrobial agents. Specific resistance mechanisms usually fall under one of the following categories: inactivation of drug, target modification, active efflux, and limiting uptake. As reviewed in Chapter 1, all of the antibiotics that have been assembled in arsenal against bacterial pathogens during the “Golden Age” of antibiotic discovery have been met with resistance and many are now losing clinical efficiency. The ongoing antibiotic crisis continues to worsen as challenges impede further drug discovery and development. There are two major challenges related to the process of bringing a new antibiotic to market, it is not only costly to develop and test but there are diminishing returns in mining natural products with new mechanisms of action. In order to develop new treatment options, a more in-depth understanding of bacterial biology and resistance mechanisms is needed.

As discussed in Chapter 2, an unappreciated mechanism of resistance that relates to limiting uptake is accessibility. It is evident that bacteria are actively protecting the cell surface, the site of many prominent antigens and binding sites, and that there is a lapse in understanding of the requirements to reach the surface of those cells. Chapter 3 describes a novel assay that aims to assess accessibility to the surface of live cells in a systematic and high-throughput way. Additionally, modulations to the bacterial cell surface were introduced in order to determine what factors, if any, impede accessibility. The assay workflow relies on site specific incorporation a free thiol handle onto the peptidoglycan layer of the cell wall and use of a library of compounds that range in size and flexibility with a bioorthogonal binding moiety and a fluorescent reporter molecule that can be tracked *via* flow cytometry. The assay is able to quantitatively report on the ability of each library member to reach the bacterial cell wall. Chapter 4 describes an application of the

accessibility assay to a screen of a transposon mutant library in effort to reveal genes that impact accessibility.

Chapter 5 describes a novel assay platform called SaccuFlow that allows for a high-throughput and quantitative investigation into bacterial peptidoglycan interactions with a range of molecules. For the first time whole native isolated peptidoglycan or sacculi from any organism is demonstrated to be compatible with flow cytometry analysis which is key to the assay. The utility of the assay is demonstrated in a high-throughput pilot screen for inhibitors of an important *Staphylococcus aureus* enzyme, sortase A which covalently installs bacterial proteins onto the cell wall. Sortase A is a promising target for anti-virulence drug discovery.

Acknowledgements

I would first like to thank my P.I. Dr. Pires for being the greatest mentor I could have ever asked for. I joined the graduate program at Lehigh feeling truly like a deer caught in headlights and I am leaving UVa an actual scientist, with accomplishments I am proud of and a confidence in myself and my knowledge base that I never could have done/found without your guidance. I may have gotten off to a late start, not even getting into a group in the first round, but you offered me an opportunity and I could not be more grateful. I hope accessibility has a long reign of ~~terror~~...fun in many projects to come and I am really going to miss working for you.

To my lady labmates, Alexis and Brianna, we came, we saw, we are conquering. I cannot believe for one last time I will step out of the lab and will not be coming back. Countless days of good mornings and see you tomorrows that felt never ending. I will miss you guys so very much and I hope I can make half as good of friends at my next job. I hope you two are so proud of yourselves and all the strides you have made, it has been so encouraging to work with fellow women in science and so exciting to see you both thrive. Do not be a stranger, I want to hear all the gossip.

To rest of the lab especially the new UVa chapter members, thank you so much for joining and carrying on the torch of great and exciting science. You are in the right place, it is hard to see sometimes but you will get to this point too and will not believe how far you have come nor how lucky you are to be in a lab with a P.I. who has as much dedication and passion as Dr. Pires. Make a few jokes for me at group meeting, a little laughter is good for the soul.

I also want to say thank you to my parents for supporting me the whole way through, your excitement for me just getting into graduate school meant a lot and getting to share in each milestone was even better. It has been a long haul but there is finally some light at the end of the tunnel. I hope I have made you proud and while I might not have become the type of doctor you might have hoped for in the beginning, I did technically still get there in the end. Very honored to be your

daughter: Noel Jacqueline Ferraro, PhD. I love you lots! And a special thank you to my sister Paulina. As big sisters tend to do, you set an awesome example for me growing up and I have been so lucky to go through this life with you. Thanks for being my best friend from birth and always being there for me. Emilie is so lucky to have a cool mom like you! I love you so much! And to Miss Emilie Noel, Auntie loves you and I cannot wait to see all the amazing things you will do, you are a wonderful little joy in all of our lives. And do not worry about becoming a big sister, I think I know someone who can show you the ropes.

Of course thank you to my friends from home, all of the texts, FaceTimes, and hang outs have kept me sane throughout graduate school. I could have never done it without you. You guys were my comfort and my relief from the hard parts of this process. It is rare to find friendships that last like ours. I am so lucky to have gotten to share in each of your lives. Raise a little glass tonight to everything we have been through and I will see you all so very soon.

Lastly I want to thank my sweet partner Alan. You and I had just barely started dating when I told you I had to move all the way to Virginia to finish what I started and somehow despite both of our fears we created this beautiful relationship and so much hope and plans for the future. Your support of me every step of the way through this program has been invaluable. I do not know how on Earth I got so blessed to have you by my side. Cheers to finally reaching the end of what has been the hardest and longest distance between us. I love you so very much, time to break out the Dom Pérignon!

Table of Contents

Abstract	III
Acknowledgements	V
Table of Contents	VII
Chapter 1	1
1.1 Antibiotic Resistance.....	1
1.2 Bacterial Cell Walls.....	2
1.3 Bacterial Resistance Mechanisms.....	5
1.4 <i>Staphylococcus aureus</i> Specific Resistance Mechanisms.....	10
1.5 References.....	13
Chapter 2	20
2.1 Accessibility as a Resistance Mechanism.....	20
2.2 Probing Accessibility.....	21
2.3 References.....	26
Chapter 3	30
3.1 Abstract.....	30
3.2 Introduction.....	30
3.3 Results and Discussion.....	32
3.4 Conclusion.....	55
3.5 Acknowledgements.....	55
3.6 References.....	56
3.7 Materials and Methods.....	64
3.8 References for Material and Methods.....	100

3.9 Extensions.....	101
3.10 References for Extensions.....	108
Chapter 4.....	110
4.1 Abstract.....	110
4.2 Introduction.....	110
4.3 Results and Discussion.....	113
4.4 Conclusion.....	124
4.5 Materials and Methods.....	124
4.6 References.....	129
Chapter 5.....	134
5.1 Abstract.....	134
5.2 Introduction.....	134
5.3 Results and Discussion.....	137
5.4 Conclusion.....	149
5.5 Materials and Methods.....	150
5.6 Acknowledgements.....	160
5.7 References.....	161

Chapter 1

1.1 Antibiotic Resistance

Bacterial resistance to antibiotics is a continuous challenge plaguing public health. The first antimicrobial agents to be developed, sulfonamides and penicillin, marked the beginning of not only the “Golden Age” of antibiotic discovery but the first understanding of this resistance phenomenon. The types of bacteria and the mechanisms used by those organisms to become resistant are highly diverse. In fact some forms of resistance arose in conjunction with the inception of the antibiotic. A large number of natural product antibiotics are sourced from bacteria engaging in bacterial warfare. In the competition for space and resources, bacteria in the environment evolved to biosynthesize highly effective antibiotics to ward off potential competitors. To counter this potentially lethal challenge from neighboring microorganisms, bacteria evolved various modes of resistance to reduce the efficacy and more effectively compete for the limited resources. For example, before it debuted in the clinical space, resistance to penicillin was already detected in an *Escherichia coli* (*E. coli*) strain that expresses an enzyme called penicillinase (more commonly known as β -lactamase). Penicillinase has the ability to chemically inactivate penicillin (and similar β -lactama antibiotics), a natural product antibiotic harvested from the *Penicillium chrysogenum* fungus. This chemical modification renders the antibiotic ineffective. The discovery of this resistance prior to use of the antibiotic as a therapeutic treatment option potentially indicates that the microorganism evolved the resistance mechanism in effort better equip themselves to survive in the fight for space and resources. These findings were swiftly followed by identification of penicillin resistance in *Staphylococcus aureus* (*S. aureus*) stains from hospitalized patients and in several additional organisms to follow.¹⁻⁴

Resistance can also emerge during treatment with antibiotics. During the course of administration of antibiotics for an infection, the susceptible population of bacterial cells will readily succumb to the therapeutic agent. However, those cells that possess genetic variations (or sometimes altered phenotypic features)

that confer a survival advantage can persist during the challenge of high levels of antibiotics. The surviving cells are able to propagate in the host, thus, leading to the rise of a resistant population. Throughout the Golden Age (1940 to 1980) many new classes of antibiotics were introduced to the clinical space in order to continue the fight against bacterial pathogens. However, the detection of drug-resistant strains across a wide range of bacterial species was discovered soon after the introduction of those agents into the clinic⁵

In the years following the Golden Age of antibiotics, there has been a lapse in the approval of new antibiotics by the FDA. While there are promising candidates currently under development, it is unlikely that the current rate of discovery can effectively compete with the critical need for new treatment options.⁶⁻⁸ Contributing to this lapse is the extensive amount of time (in excess of a decade) coupled with the high cost (up to billions of dollars) that is required to bring a promising antibiotic candidate through all stages of development.⁹ However, it is not just time and cost, most antibiotics are derived from natural products (with the others being synthetically produced) and a growing lack of biodiversity has made it challenging to discover novel natural products that result in the discovery of antibiotics with unique mechanisms of action.¹⁰ Still action must be taken because according to the Centers for Disease Control (CDC), in the U.S. alone an estimated 2.8 million people contract an antibiotic resistant infection and more than 35,000 people die due to those infections. This continued antibiotic crisis has created the need for either an antibiotic pipeline revitalization or alternative solutions to combat bacterial infections. However, for either of those to occur, a more comprehensive understanding of bacteria, their vulnerable molecular targets, and resistance mechanisms is urgently required.

1.2 Bacterial Cell Walls

Bacteria can be classified as Gram-positive, Gram-negative, or mycobacteria. The main factor for classification is the composition of the bacterial cell wall (**Figure 1.1**). Gram-positive bacteria have a cell wall that is composed of

a thick peptidoglycan (PG) layer followed by a cytoplasmic membrane. The PG layer provides structure to the cell wall and prevents cell lysis by internal turgor pressure. PG is a mesh-like polymer made up of repeating disaccharide units of *N*-acetylglucosamine (GlcNAc) and *N*-acetylmuramic acid (MurNAc). Off of each MurNAc unit is a short peptide, anywhere from 3 to 5 amino acids long, referred to as the stem peptide. The chemical composition of the stem peptide is prominently distinct from peptides produced by the ribosome, which include unusual connectivities and stereocenters. The typical sequence of a bacterial stem peptide is L-alanine-D-glutamic acid-meso-diaminopimelic acid (mDAP) (or L-lysine)-D-alanine-D-alanine. However, there are hundreds of possible stem peptide structures and amino acid substitutions across all of the diverse and naturally occurring bacterial species in existence. A unique feature of all known PG scaffolds is the crosslinking of the individual stem peptides. Crosslinking is an enzyme mediated reaction that occurs between neighboring stem peptide strands and the degree to which PG is crosslinked can influence the cell wall rigidity and integrity. The PG scaffold can be further diversified *via* the covalent incorporation of additional biomacromolecules. For example, polymers called teichoic acids (TAs) and proteins covalently decorate the PG of Gram-positive bacteria. These modifications can play important roles in the physiology of these organisms, including serving as virulence factors, regulating cell morphology and growth, aiding in adherence and colonization, and evading not only antibiotics but the immune system as well.¹¹⁻¹⁴

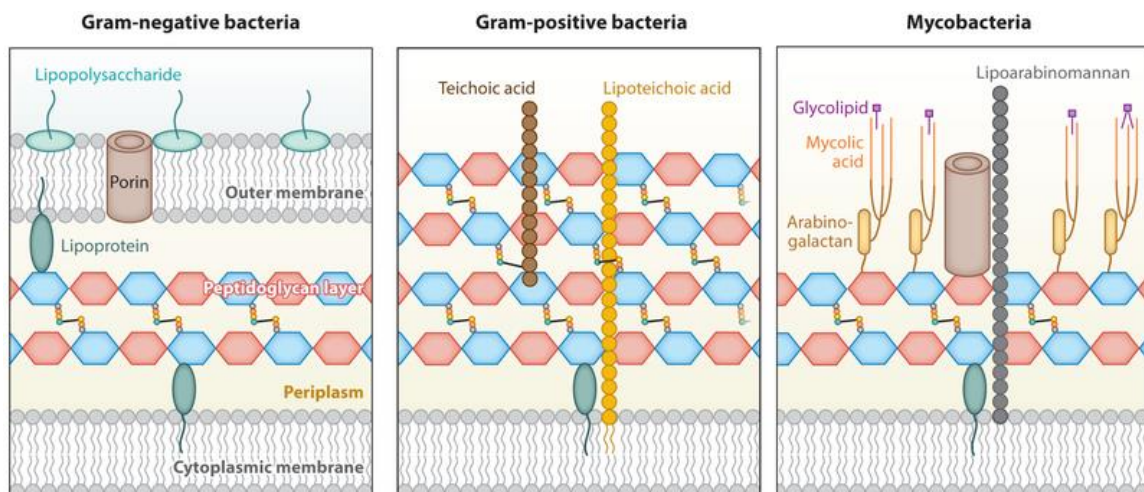


Figure 1.1 Bacterial Cell Wall Structures. Schematic representation of the bacterial cell wall components for Gram-negative, Gram-positive, and mycobacteria. Gram-negative bacterial cell walls are composed of an outer membrane, thin layer of peptidoglycan, and an inner membrane. Gram-positive bacterial cell walls consist of a thick peptidoglycan layer followed by a cytoplasmic membrane. Mycobacterial cell walls contain a mycomembrane, followed by an arabinogalactan layer, a peptidoglycan layer, and a cytoplasmic membrane.¹⁵

In contrast to Gram-positive bacteria, the PG scaffold of Gram-negative bacteria is not immediately accessible to the extracellular space. Instead, Gram-negative bacteria possess an outer membrane (OM) followed by a thin PG layer and an inner membrane (IM). The OM is an asymmetric bilayer, whereby the inner leaflet consists of canonical phospholipids but the outer leaflet is composed of glycolipids known as lipopolysaccharides (LPS). LPS is integral to the OM structure and stability. It also poses a large permeability barrier and differing compositions in the polysaccharide region of LPS known as O-antigen can aide bacterial pathogens in immune evasion. A high number of proteins are imbedded within the OM and are known as outer membrane proteins or OMPs. The most notable OMPs are those that act as porins, which allow for the passive diffusion of small polar molecules across the OM (including antibiotics). The OM is covalently

connected to the PG layer *via* a lipoprotein known as Lpp or Braun's lipoprotein and is generally considered a very formidable barrier.^{11, 16}

Mycobacteria have a unique cell wall structure consisting of the following layers: mycomembrane, arabinogalactan (AG), PG, and an inner membrane. The mycomembrane is composed of mycolic acids (MAs), which are long chain fatty acids and they are present in the mycomembrane as either free mycolic acids, covalently linked to the arabinogalactan, or attached to sugars forming trehalose monomycolate (TMM), trehalose dimycolate (TDM), or glucose monomycolate. The mycomembrane is also proposed to contain porins to facilitate the entry of small hydrophilic molecules into the cell and secretion machinery to potentially allow the release of virulence factors to the extracellular environment. Like the OM of Gram-negative bacteria, the mycomembrane is considered a barrier to permeability of many molecules including antibiotics. Another component of the mycobacterial cell wall is AG which is a highly branched polysaccharide primarily composed of arabinose and galactose. In a similar fashion to Gram-negative bacteria, mycobacteria possess a thin layer of PG. However, quite uniquely, the PG of mycobacteria is linked to the AG layer. A phosphodiester bond forms between a PG backbone sugar moiety and a sugar residue of the AG matrix, resulting in a covalent bond between the two. The mycobacterial cell wall is complex and there are many aspects related to its biology that remains poorly understood.¹⁷⁻¹⁹

1.3 Bacterial Resistance Mechanisms

Bacteria of any classification can potentially develop resistance to antibiotics and immune system components using any of the following mechanisms: 1) inactivation of drug, 2) target modification, 3) active efflux, and 4) limiting uptake.

In an act of defense, bacteria can express enzymes that will inactivate a drug by either modifying it or destroying it. The main target of enzymes that preform a modification are antibiotics that inhibit ribosomal protein synthesis. These

enzymes will catalyze various modifications such as acetylation, phosphorylation, and adenylation. The ultimate effect of the chemical modification of the antibiotic is the creation of a steric hindrance that reduces the binding ability of the drug to its target. A common example is the modification of the ribosome targeting antibiotic, chloramphenicol, by chloramphenicol acetyltransferases (CATs) which are typically expressed in Gram-negative bacteria. The CATs can perform acetylation on key hydroxyl groups of chloramphenicol, a modification that results in an abolishment of the affinity of the drug for the ribosome.²⁰ Then there are enzymes expressed by bacteria that function in the destruction of the antibiotic instead. An example of this can be found in the battle β -lactam antibiotics vs penicillinases or β -lactamases. β -lactams are the most widely used antibiotic class, a commonly prescribed β -lactam is penicillin. The mechanism of action of β -lactams relates to the structure of the antibiotic. To explain this further an understanding of PG biosynthesis is integral. Bacteria synthesize the PG wall with the help of an arsenal of enzymes, a critical group being penicillin-binding proteins (PBPs). PBPs catalyze the formation of crosslinks between neighboring stem peptides, a process known as transpeptidation. During transpeptidation, PBPs will specifically recognize the D-ala-D-ala motif of the stem peptide and an active site serine residue will attack the amide bond between the two D-alanines. This causes a release of a terminal D-alanine and the formation of an acyl enzyme intermediate between the PBP and the remaining stem peptide. The intermediate is then broken by a nucleophilic attack from a free amine on an adjacent stem peptide strand, forming a new amide bond, and covalently crosslinking the two strands together. If this enzyme is inhibited and transpeptidation cannot occur, the disruption in the biosynthesis of an essential cell wall component like PG can induce cell death. β -lactams have a structure that mirrors that of the D-ala-D-ala motif (**Figure 1.2**), however they possess a strained ring with a very reactive carbonyl that is susceptible to a nucleophilic attack. β -lactams can essentially act as a substrate of PBPs and an attack of this β -lactam ring by a PBP will result in a covalent linkage between the drug and enzyme, inhibiting PBP activity further. However, bacteria have cleverly armed themselves with an enzyme, β -lactamase, which will cleave

the amide bond in the β -lactam ring effectively destroying the active component of the drug before it can reach its target, the PBPs. This effective resistance strategy has plagued many generations of β -lactam antibiotics such as penicillins, cephalosporins, and carbapenems.²¹⁻²³

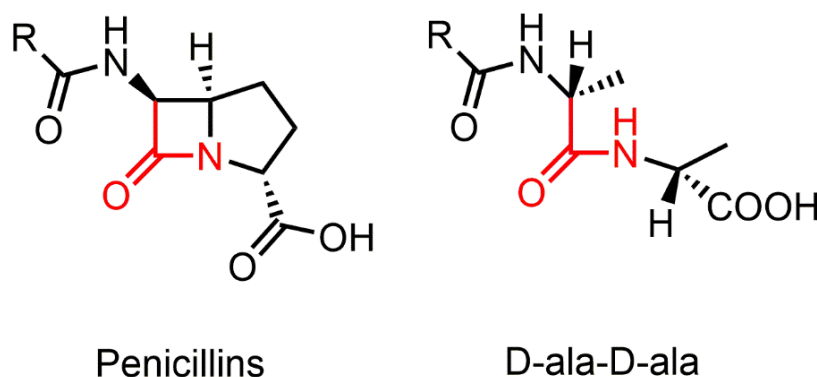


Figure 1.2 β -lactam Antibiotic Structure. General structure of a β -lactam antibiotic and the D-alanine-D-alanine motif of the PG stem peptide, highlighted in red is the site of enzymatic attack and serves in demonstrating the structure similarity of this site for both molecules.

Instead of targeting the drug, bacteria can modify the target site instead. Modification can occur by a few different methods, it is possible that the organism will evolve point mutations within the gene that encodes for the target, there can be alterations to the binding site (often enzyme catalyzed changes [e.g. methylation of a critical binding site residue]), or there can be a replacement or bypass/loss of the target. Point mutations and alterations in the binding site are efforts that both result in decreased binding affinity between the drug and its target, this has been seen in numerous examples with antibiotics such as rifamycin²⁴, fluoroquinolones²⁵, and macrolides.²⁶⁻²⁷ If the bacteria replace or bypass the target, they will adapt in order to produce a new target that can perform similar functions to the original but it is not affected by the antimicrobial agent. An interesting example of this occurs in enterococci and contributes to the development of vancomycin resistance. Similar to β -lactams, the glycopeptide class antibiotic

vancomycin also inhibits PG biosynthesis which can induce cell death. Vancomycin binds to the D-ala-D-ala motif early in the PG biosynthesis pathway on a precursor called lipid II. This binding is thought to prevent not only transpeptidation but also transglycosylation (a process carried out by enzymes to link together the PG sugar backbone).²⁸⁻²⁹ Some strains of enterococci bacteria, however, have acquired a gene cluster which encodes for PG machinery capable of remodeling the PG in response to vancomycin.³⁰⁻³¹ One phenotype resulting from this remodeling is the replacement of the terminal D-alanine in the stem peptide sequence for D-lactate or D-serine. These are tolerable alterations to the PG scaffold and allows the organism to survive vancomycin treatment by reducing its affinity (loss of a hydrogen binding partner).³²⁻³⁸ The other phenotype results in the removal of the terminal D-alanine, which reduces the number of binding sites available to vancomycin, rendering it less effective.^{23, 30, 39}

A different mechanism of resistance bacteria can use against antibiotics depends on a protein called an efflux pump. Efflux pumps function in the transport of harmful materials out of the bacterial cell and into the extracellular environment. There are six main families of efflux pumps: the ATP-binding cassette (ABC) family, the multidrug and toxin extrusion (MATE) family, the major facilitator superfamily (MFS), the proteobacterial antimicrobial compound efflux (PACE) family, the resistance-nodulation-cell division (RND) family, and the small multidrug resistance (SMR) family. These families differ by physical structure of the efflux pump (i.e. homo- and heterodimeric, tripartite/trimers, V-shaped), the trigger that incites pump function (i.e. adenosine triphosphate [ATP], ligand/proton binding event), the substances they are able to expel, and the classification of bacteria in which they are expressed.^{23, 40-42}

The last resistance mechanism that will be discussed in this chapter involves the ability of bacteria to limit the uptake of antimicrobials based on the structural components of their cell wall. Many antibiotics have intracellular targets so the understanding is that they will need to penetrate through the cell wall to be effective. For Gram-negative bacteria the OM is a physical barrier to permeation.

The LPS on the OM is responsible for the permeability challenge. To review, the outer leaflet of the OM is composed of LPS, a molecule consisting of a lipid base and a polysaccharide chain extending from that base. The lipid base, called lipid A, consists of densely packed saturated fatty acids which create a gel like layer with low levels of fluidity. LPS packing coupled with the high anionic charge of the polysaccharide region, makes diffusion through the OM extremely difficult.⁴³ Another prominent barrier of uptake in Gram-negative bacteria involves the porins that heavily decorate the OM. Porins are water filled channels in which hydrophilic molecules can diffuse through to gain access into the cell, however it is often seen that these hydrophilic agents are not actually effective against Gram-negative bacteria.⁴⁴⁻⁴⁵ Bacteria control porin-mediated resistance by either changing the type of porin expressed (selectivity, not all porins permit the same types of molecules to diffuse through), changing the level to which the porins are expressed, or inducing a shift in functional efficiency of the porin. While these changes typically result in low level resistance, they can be coupled with the power of an efflux pump to increase resistance capacity (as molecules diffuse in through the porins, the efflux pumps can shuttle them quickly back out).^{23, 46-51}

In mycobacteria the mycomembrane is lipid rich so hydrophobic molecules such as rifampicin and fluoroquinolones may gain passage through the membrane however any hydrophilic agents will struggle to penetrate through. Mycobacteria do express porins like Gram-negative bacteria, but they are expressed at low levels and are very size restrictive. There are many aspects related to permeation through the mycobacterial cell wall that are still unknown.⁵² Gram-positive bacteria lack an OM-type structure and are generally considered to be more permeable, however hints of uptake limitation have been observed. For example, in *S. aureus* the development of vancomycin resistance has been observed to be related to the production of a thickened cell wall (due to accelerated PG biosynthesis) that limits drug penetration through the PG to the lipid II target.⁵³⁻⁵⁵

1.4 *Staphylococcus aureus* Specific Resistance Mechanisms

S. aureus is a Gram-positive pathogen that is most commonly observed in skin infections. However, it can cause more severe infections such as that of the bloodstream and organs which can be fatal.⁵⁶⁻⁵⁷ According to the CDC, the hard to treat methicillin resistant strain of *S. aureus* (MRSA) infects an estimated 70,000 people and causes over 9,000 deaths a year, making it a serious health threat. A majority of the work presented in this dissertation centers around *S. aureus* so its specific mechanisms of resistance and evasion are of particular interest.

One way *S. aureus* circumvents immune response is through the use of a surface protein called protein A. Protein A is capable of binding to the fragment crystallizable (Fc) portion of any immunoglobulins present in the extracellular milieu. This binding allows for the surface of the bacterial cell to become coated with antibodies that are oriented in a manner that prevents immune recognition and phagocytosis of those cells.⁵⁸⁻⁵⁹ Another mechanism *S. aureus* employs to escape phagocytosis is the variable production of an extracellular capsule layer. The capsule is constructed from polysaccharide chains referred to as capsular polysaccharides (CPS). It can be advantageous for *S. aureus* to be encapsulated by CPS due to the proposed anti-phagocytic effect of the layer as a deterrent of opsonization, allowing for escape and survival.⁶⁰⁻⁶²

Most critical to survival, however, is cell wall integrity. For Gram-positive bacteria, cell wall integrity depends upon the degree of PG crosslinking. To review, crosslinking is an integral step of the PG biosynthesis pathway and is performed by enzymes called transpeptidases. If transpeptidases are inhibited, the cell wall biosynthesis is halted causing an inhibition of further cell growth.⁶³ *S. aureus* relies on four PBP transpeptidases. While these PBPs are susceptible to β -lactam antibiotics, there are strains that have adapted to survive this inhibition in order to protect their cell wall integrity. For example, in the case of the pathogenic MRSA, the bacteria have acquired the *mecA* gene which encodes for a fifth PBP, PBP2a, from an organism not of *S. aureus* origin. PBP2a is able to continue transpeptidase activity even in the presence of β -lactams due to its low affinity for those

antibiotics.⁶⁴ The thick layer of crosslinked PG resulting from biosynthesis creates a mesh-like network and there are pores that funnel through the PG to the cytoplasmic membrane. However, depending on the level of crosslinking, the pore sizes can vary. Most small molecules are able to sieve through the PG pores but large molecules or complexes can struggle, due to sterics, to penetrate through.⁶⁵ In fact this barrier-like function is thought to disarm one component of the complement system, the membrane attack complex (MAC). The MAC targets pathogen cell membranes and kills *via* lysis. The thick PG layer in Gram-positive bacteria, such as *S. aureus*, prevents the lytic MAC from accessing the cytoplasmic membrane.⁶⁶

There are also polymers on the cell surface termed teichoic acids (TA) that can function in antibiotic and immune system evasion. There are two types of TAs, lipoteichoic acids (LTA) and wall teichoic acids (WTA). LTAs are anchored in the cytoplasmic membrane and span the PG scaffold while WTAs are covalently attached to the PG. Compositionally, TAs are anionic, phosphate-rich glycopolymers which can undergo D-alanyl modification and glycosylation.^{61, 67} The presence of TAs and relevant modifications in *S. aureus* has been assigned a variety of roles but a major one is influencing resistance. For example the D-alanyl modification has been implicated in decreasing the overall net negative charge available for cationic antimicrobial peptide binding resulting in resistance.⁶⁸ Similarly, the altered surface charge due to D-alanylation is thought to also play a role in resistance to antibiotics of the glycopeptide class, such as vancomycin.⁶⁹ Alternatively, for the antibiotic daptomycin, resistance is thought to be the result of a thickened cell wall. Daptomycin resistant *S. aureus* strains present with upregulated WTA biosynthesis. This increases the density of those polymers on the surface potentially limiting the access of daptomycin to its target, the cytoplasmic membrane. Although another factor in daptomycin resistance may be altered surface charge as well.⁷⁰⁻⁷¹ Lytic enzymes (e.g. lysozyme) can be resisted by *S. aureus* and this is achieved by a culmination of increased PG crosslinking, O-acetylation of the MurNAc unit in the PG sugar backbone, and presence of WTAs.⁷² Lastly, there has been observed resistance to antimicrobial fatty acids

potentially due to the hydrophilicity of WTAs resulting in the exclusion of the typically hydrophobic fatty acids from penetrating and reaching their target, the cytoplasmic membrane.⁷³

There is still many facets about resistance mechanisms used by bacteria, like *S. aureus*, to evade antibiotics and the immune system that are unknown. This lack of understanding can potentially stymie the development of new and innovative therapies against these pathogens. The work discussed in this dissertation aims to provide more information on the underappreciated resistance mechanism of accessibility to bacterial cell surfaces.

1.5 References

1. Levy, S. B.; Marshall, B., Antibacterial resistance worldwide: causes, challenges and responses. *Nat Med* **2004**, *10* (12 Suppl), S122-9.
2. Davies, J.; Davies, D., Origins and evolution of antibiotic resistance. *Microbiol Mol Biol Rev* **2010**, *74* (3), 417-33.
3. Davies, J., Where have All the Antibiotics Gone? *Can J Infect Dis Med Microbiol* **2006**, *17* (5), 287-290.
4. Lobanovska, M.; Pilla, G., Penicillin's Discovery and Antibiotic Resistance: Lessons for the Future? *Yale J Biol Med* **2017**, *90* (1), 135-145.
5. Ventola, C. L., The antibiotic resistance crisis: part 1: causes and threats. *P T* **2015**, *40* (4), 277-83.
6. Hutchings, M. I.; Truman, A. W.; Wilkinson, B., Antibiotics: past, present and future. *Curr Opin Microbiol* **2019**, *51*, 72-80.
7. Durand-Reville, T. F.; Miller, A. A.; O'Donnell, J. P.; Wu, X.; Sylvester, M. A.; Guler, S.; Iyer, R.; Shapiro, A. B.; Carter, N. M.; Velez-Vega, C.; Moussa, S. H.; McLeod, S. M.; Chen, A.; Tanudra, A. M.; Zhang, J.; Comita-Prevoir, J.; Romero, J. A.; Huynh, H.; Ferguson, A. D.; Horanyi, P. S.; Mayclin, S. J.; Heine, H. S.; Drusano, G. L.; Cummings, J. E.; Slayden, R. A.; Tommasi, R. A., Rational design of a new antibiotic class for drug-resistant infections. *Nature* **2021**, *597* (7878), 698-702.
8. Ling, L. L.; Schneider, T.; Peoples, A. J.; Spoering, A. L.; Engels, I.; Conlon, B. P.; Mueller, A.; Schäberle, T. F.; Hughes, D. E.; Epstein, S.; Jones, M.; Lazarides, L.; Steadman, V. A.; Cohen, D. R.; Felix, C. R.; Fetterman, K. A.; Millett, W. P.; Nitti, A. G.; Zullo, A. M.; Chen, C.; Lewis, K., A new antibiotic kills pathogens without detectable resistance. *Nature* **2015**, *517* (7535), 455-459.
9. Farrell, L. J.; Lo, R.; Wanford, J. J.; Jenkins, A.; Maxwell, A.; Piddock, L. J. V., Revitalizing the drug pipeline: AntibioticDB, an open access database to aid antibacterial research and development. *J Antimicrob Chemother* **2018**, *73* (9), 2284-2297.
10. Neergheen-Bhujun, V.; Awan, A. T.; Baran, Y.; Bunnefeld, N.; Chan, K.; Dela Cruz, T. E.; Egamberdieva, D.; Elsasser, S.; Johnson, M. V.; Komai, S.; Konevega,

A. L.; Malone, J. H.; Mason, P.; Nguon, R.; Piper, R.; Shrestha, U. B.; Pesic, M.; Kagansky, A., Biodiversity, drug discovery, and the future of global health: Introducing the biodiversity to biomedicine consortium, a call to action. *J Glob Health* **2017**, *7* (2), 020304.

11. Silhavy, T. J.; Kahne, D.; Walker, S., The bacterial cell envelope. *Cold Spring Harb Perspect Biol* **2010**, *2* (5), a000414.

12. Vollmer, W.; Blanot, D.; de Pedro, M. A., Peptidoglycan structure and architecture. *FEMS Microbiol Rev* **2008**, *32* (2), 149-67.

13. Weidenmaier, C.; Peschel, A., Teichoic acids and related cell-wall glycopolymers in Gram-positive physiology and host interactions. *Nat Rev Microbiol* **2008**, *6* (4), 276-87.

14. Brown, S.; Santa Maria, J. P., Jr.; Walker, S., Wall teichoic acids of gram-positive bacteria. *Annu Rev Microbiol* **2013**, *67*, 313-36.

15. Radkov, A. D.; Hsu, Y. P.; Booher, G.; VanNieuwenhze, M. S., Imaging Bacterial Cell Wall Biosynthesis. *Annu Rev Biochem* **2018**, *87*, 991-1014.

16. Bertani, B.; Ruiz, N., Function and Biogenesis of Lipopolysaccharides. *EcoSal Plus* **2018**, *8* (1).

17. Nataraj, V.; Varela, C.; Javid, A.; Singh, A.; Besra, G. S.; Bhatt, A., Mycolic acids: deciphering and targeting the Achilles' heel of the tubercle bacillus. *Mol Microbiol* **2015**, *98* (1), 7-16.

18. Chiaradia, L.; Lefebvre, C.; Parra, J.; Marcoux, J.; Burlet-Schiltz, O.; Etienne, G.; Tropis, M.; Daffe, M., Dissecting the mycobacterial cell envelope and defining the composition of the native mycomembrane. *Sci Rep* **2017**, *7* (1), 12807.

19. Alderwick, L. J.; Harrison, J.; Lloyd, G. S.; Birch, H. L., The Mycobacterial Cell Wall--Peptidoglycan and Arabinogalactan. *Cold Spring Harb Perspect Med* **2015**, *5* (8), a021113.

20. Biswas, T.; Houghton, J. L.; Garneau-Tsodikova, S.; Tsodikov, O. V., The structural basis for substrate versatility of chloramphenicol acetyltransferase CATI. *Protein Sci* **2012**, *21* (4), 520-30.

21. Bush, K.; Bradford, P. A., beta-Lactams and beta-Lactamase Inhibitors: An Overview. *Cold Spring Harb Perspect Med* **2016**, *6* (8).

22. Macheboeuf, P.; Contreras-Martel, C.; Job, V.; Dideberg, O.; Dessen, A., Penicillin binding proteins: key players in bacterial cell cycle and drug resistance processes. *FEMS Microbiol Rev* **2006**, *30* (5), 673-91.
23. Munita, J. M.; Arias, C. A., Mechanisms of Antibiotic Resistance. *Microbiol Spectr* **2016**, *4* (2).
24. Floss, H. G.; Yu, T. W., Rifamycin-mode of action, resistance, and biosynthesis. *Chem Rev* **2005**, *105* (2), 621-32.
25. Hooper, D. C., Fluoropuinolone resistance among Gram-positive cocci. *Lancet Infect Dis* **2002**, *2* (9), 530-538.
26. Leclercq, R., Mechanisms of resistance to macrolides and lincosamides: Nature of the resistance elements and their clinical implications. *Clin Infect Dis* **2002**, *34* (4), 482-492.
27. Weisblum, B., Erythromycin resistance by ribosome modification. *Antimicrob Agents Chemother* **1995**, *39* (3), 577-85.
28. Barna, J. C.; Williams, D. H., The structure and mode of action of glycopeptide antibiotics of the vancomycin group. *Annu Rev Microbiol* **1984**, *38*, 339-57.
29. Reynolds, P. E., Structure, Biochemistry and Mechanism of Action of Glycopeptide Antibiotics. *Eur J Clin Microbiol* **1989**, *8* (11), 943-950.
30. Koteva, K.; Hong, H. J.; Wang, X. D.; Nazi, I.; Hughes, D.; Naldrett, M. J.; Buttner, M. J.; Wright, G. D., A vancomycin photoprobe identifies the histidine kinase VanSsc as a vancomycin receptor. *Nat Chem Biol* **2010**, *6* (5), 327-329.
31. Evers, S.; Courvalin, P., Regulation of VanB-type vancomycin resistance gene expression by the VanS(B)-VanR (B) two-component regulatory system in *Enterococcus faecalis* V583. *J Bacteriol* **1996**, *178* (5), 1302-9.
32. Bugg, T. D.; Wright, G. D.; Dutka-Malen, S.; Arthur, M.; Courvalin, P.; Walsh, C. T., Molecular basis for vancomycin resistance in *Enterococcus faecium* BM4147: biosynthesis of a depsipeptide peptidoglycan precursor by vancomycin resistance proteins VanH and VanA. *Biochemistry* **1991**, *30* (43), 10408-15.
33. Arthur, M.; Molinas, C.; Bugg, T. D.; Wright, G. D.; Walsh, C. T.; Courvalin, P., Evidence for in vivo incorporation of D-lactate into peptidoglycan precursors of

- vancomycin-resistant enterococci. *Antimicrob Agents Chemother* **1992**, *36* (4), 867-9.
34. Hubbard, B. K.; Walsh, C. T., Vancomycin assembly: nature's way. *Angew Chem Int Ed Engl* **2003**, *42* (7), 730-65.
35. Kahne, D.; Leimkuhler, C.; Lu, W.; Walsh, C., Glycopeptide and lipoglycopeptide antibiotics. *Chem Rev* **2005**, *105* (2), 425-48.
36. Arthur, M.; Depardieu, F.; Snaith, H. A.; Reynolds, P. E.; Courvalin, P., Contribution of VanY D,D-carboxypeptidase to glycopeptide resistance in *Enterococcus faecalis* by hydrolysis of peptidoglycan precursors. *Antimicrob Agents Chemother* **1994**, *38* (9), 1899-903.
37. Arthur, M.; Depardieu, F.; Cabanie, L.; Reynolds, P.; Courvalin, P., Requirement of the VanY and VanX D,D-peptidases for glycopeptide resistance in enterococci. *Mol Microbiol* **1998**, *30* (4), 819-30.
38. Reynolds, P. E.; Depardieu, F.; Dutka-Malen, S.; Arthur, M.; Courvalin, P., Glycopeptide resistance mediated by enterococcal transposon Tn1546 requires production of VanX for hydrolysis of D-alanyl-D-alanine. *Mol Microbiol* **1994**, *13* (6), 1065-70.
39. Arthur, M.; Molinas, C.; Courvalin, P., The VanS-VanR two-component regulatory system controls synthesis of depsipeptide peptidoglycan precursors in *Enterococcus faecium* BM4147. *J Bacteriol* **1992**, *174* (8), 2582-91.
40. Reygaert, W. C., An overview of the antimicrobial resistance mechanisms of bacteria. *AIMS Microbiol* **2018**, *4* (3), 482-501.
41. Du, D.; Wang-Kan, X.; Neuberger, A.; van Veen, H. W.; Pos, K. M.; Piddock, L. J. V.; Luisi, B. F., Multidrug efflux pumps: structure, function and regulation. *Nat Rev Microbiol* **2018**, *16* (9), 523-539.
42. Webber, M. A.; Piddock, L. J., The importance of efflux pumps in bacterial antibiotic resistance. *J Antimicrob Chemother* **2003**, *51* (1), 9-11.
43. Kumar, A.; Schweizer, H. P., Bacterial resistance to antibiotics: active efflux and reduced uptake. *Adv Drug Deliv Rev* **2005**, *57* (10), 1486-513.

44. Pages, J. M.; James, C. E.; Winterhalter, M., The porin and the permeating antibiotic: a selective diffusion barrier in Gram-negative bacteria. *Nat Rev Microbiol* **2008**, 6 (12), 893-903.
45. Blair, J. M.; Richmond, G. E.; Piddock, L. J., Multidrug efflux pumps in Gram-negative bacteria and their role in antibiotic resistance. *Future Microbiol* **2014**, 9 (10), 1165-77.
46. Thiolas, A.; Bornet, C.; Davin-Regli, A.; Pages, J. M.; Bollet, C., Resistance to imipenem, cefepime, and ceftazidime associated with mutation in Omp36 osmoporin of *Enterobacter aerogenes*. *Biochem Biophys Res Commun* **2004**, 317 (3), 851-6.
47. Hancock, R. E.; Brinkman, F. S., Function of pseudomonas porins in uptake and efflux. *Annu Rev Microbiol* **2002**, 56, 17-38.
48. Quinn, J. P.; Dudek, E. J.; DiVincenzo, C. A.; Lucks, D. A.; Lerner, S. A., Emergence of resistance to imipenem during therapy for *Pseudomonas aeruginosa* infections. *J Infect Dis* **1986**, 154 (2), 289-94.
49. Nikaido, H., Molecular basis of bacterial outer membrane permeability revisited. *Microbiol Mol Biol Rev* **2003**, 67 (4), 593-656.
50. Cornaglia, G.; Mazzariol, A.; Fontana, R.; Satta, G., Diffusion of carbapenems through the outer membrane of enterobacteriaceae and correlation of their activities with their periplasmic concentrations. *Microb Drug Resist* **1996**, 2 (2), 273-276.
51. Chow, J. W.; Shlaes, D. M., Imipenem resistance associated with the loss of a 40 kDa outer membrane protein in *Enterobacter aerogenes*. *J Antimicrob Chemother* **1991**, 28 (4), 499-504.
52. Lambert, P. A., Cellular impermeability and uptake of biocides and antibiotics in Gram-positive bacteria and mycobacteria. *J Appl Microbiol* **2002**, 92 Suppl, 46S-54S.
53. Pfeltz, R. F.; Singh, V. K.; Schmidt, J. L.; Batten, M. A.; Baranyk, C. S.; Nadakavukaren, M. J.; Jayaswal, R. K.; Wilkinson, B. J., Characterization of passage-selected vancomycin-resistant *Staphylococcus aureus* strains of diverse parental backgrounds. *Antimicrob Agents Chemother* **2000**, 44 (2), 294-303.

54. Cosgrove, S. E.; Carroll, K. C.; Perl, T. M., Staphylococcus aureus with reduced susceptibility to vancomycin. *Clin Infect Dis* **2004**, 39 (4), 539-45.
55. Cui, L.; Murakami, H.; Kuwahara-Arai, K.; Hanaki, H.; Hiramatsu, K., Contribution of a thickened cell wall and its glutamine nonamidated component to the vancomycin resistance expressed by Staphylococcus aureus Mu50. *Antimicrob Agents Chemother* **2000**, 44 (9), 2276-85.
56. Chambers, H. F.; Deleo, F. R., Waves of resistance: Staphylococcus aureus in the antibiotic era. *Nat Rev Microbiol* **2009**, 7 (9), 629-41.
57. Tong, S. Y.; Davis, J. S.; Eichenberger, E.; Holland, T. L.; Fowler, V. G., Jr., Staphylococcus aureus infections: epidemiology, pathophysiology, clinical manifestations, and management. *Clin Microbiol Rev* **2015**, 28 (3), 603-61.
58. Kobayashi, S. D.; DeLeo, F. R., Staphylococcus aureus protein A promotes immune suppression. *mBio* **2013**, 4 (5), e00764-13.
59. Foster, T. J.; Geoghegan, J. A.; Ganesh, V. K.; Hook, M., Adhesion, invasion and evasion: the many functions of the surface proteins of Staphylococcus aureus. *Nat Rev Microbiol* **2014**, 12 (1), 49-62.
60. O'Riordan, K.; Lee, J. C., Staphylococcus aureus capsular polysaccharides. *Clin Microbiol Rev* **2004**, 17 (1), 218-34.
61. Keinhorster, D.; George, S. E.; Weidenmaier, C.; Wolz, C., Function and regulation of Staphylococcus aureus wall teichoic acids and capsular polysaccharides. *Int J Med Microbiol* **2019**, 309 (6), 151333.
62. Willis, L. M.; Whitfield, C., Structure, biosynthesis, and function of bacterial capsular polysaccharides synthesized by ABC transporter-dependent pathways. *Carbohydr Res* **2013**, 378, 35-44.
63. Kong, K. F.; Schneper, L.; Mathee, K., Beta-lactam antibiotics: from antibiosis to resistance and bacteriology. *APMIS* **2010**, 118 (1), 1-36.
64. Fishovitz, J.; Hermoso, J. A.; Chang, M.; Mobashery, S., Penicillin-binding protein 2a of methicillin-resistant Staphylococcus aureus. *IUBMB Life* **2014**, 66 (8), 572-7.
65. Dijkstra, A. J.; Keck, W., Peptidoglycan as a barrier to transenvelope transport. *Journal of Bacteriology* **1996**, 178 (19), 5555-5562.

66. Tegla, C. A.; Cudrici, C.; Patel, S.; Trippe, R., 3rd; Rus, V.; Niculescu, F.; Rus, H., Membrane attack by complement: the assembly and biology of terminal complement complexes. *Immunol Res* **2011**, *51* (1), 45-60.
67. Atilano, M. L.; Pereira, P. M.; Yates, J.; Reed, P.; Veiga, H.; Pinho, M. G.; Filipe, S. R., Teichoic acids are temporal and spatial regulators of peptidoglycan cross-linking in *Staphylococcus aureus*. *Proc Natl Acad Sci U S A* **2010**, *107* (44), 18991-6.
68. Peschel, A.; Otto, M.; Jack, R. W.; Kalbacher, H.; Jung, G.; Gotz, F., Inactivation of the *dlt* operon in *Staphylococcus aureus* confers sensitivity to defensins, protegrins, and other antimicrobial peptides. *J Biol Chem* **1999**, *274* (13), 8405-10.
69. Peschel, A.; Vuong, C.; Otto, M.; Gotz, F., The D-alanine residues of *Staphylococcus aureus* teichoic acids alter the susceptibility to vancomycin and the activity of autolytic enzymes. *Antimicrob Agents Chemother* **2000**, *44* (10), 2845-7.
70. Bertsche, U.; Weidenmaier, C.; Kuehner, D.; Yang, S. J.; Baur, S.; Wanner, S.; Francois, P.; Schrenzel, J.; Yeaman, M. R.; Bayer, A. S., Correlation of daptomycin resistance in a clinical *Staphylococcus aureus* strain with increased cell wall teichoic acid production and D-alanylation. *Antimicrob Agents Chemother* **2011**, *55* (8), 3922-8.
71. Bertsche, U.; Yang, S. J.; Kuehner, D.; Wanner, S.; Mishra, N. N.; Roth, T.; Nega, M.; Schneider, A.; Mayer, C.; Grau, T.; Bayer, A. S.; Weidenmaier, C., Increased cell wall teichoic acid production and D-alanylation are common phenotypes among daptomycin-resistant methicillin-resistant *Staphylococcus aureus* (MRSA) clinical isolates. *PLoS One* **2013**, *8* (6), e67398.
72. Bera, A.; Biswas, R.; Herbert, S.; Kulauzovic, E.; Weidenmaier, C.; Peschel, A.; Gotz, F., Influence of wall teichoic acid on lysozyme resistance in *Staphylococcus aureus*. *J Bacteriol* **2007**, *189* (1), 280-3.
73. Kohler, T.; Weidenmaier, C.; Peschel, A., Wall teichoic acid protects *Staphylococcus aureus* against antimicrobial fatty acids from human skin. *J Bacteriol* **2009**, *191* (13), 4482-4.

Chapter 2

2.1 Accessibility as a Resistance Mechanism

As discussed in Chapter 1 when detailing the limiting uptake resistance mechanism, it is evident that bacteria are actively shielding the cell surface. This creates a challenge of accessibility to the antigens, ligands, and binding sites that are important to many antibiotics and immune system components to function. However the issue of accessibility is often unaccounted for in the literature. There are a few studies that touch on the topic but do not address accessibility directly.²⁻¹⁰ For example, one paper investigated antibody binding to an epitope called fluorescein isothiocyanate (FITC). This epitope was installed onto the peptidoglycan (PG) of *Staphylococcus aureus* (*S. aureus*) via sortase A, a *S. aureus* enzyme that covalently anchors proteins to the growing PG wall. The FITC moiety can be conjugated to a preferred substrate of sortase A. The now fluorescent substrate can be supplemented in during cell growth and sortase A will process it for placement onto the growing PG wall. The ability of the anti-FITC antibody to be recruited was determined in the presence of the prominent *S. aureus* surface polymers, wall teichoic acids (WTAs), and compared to cells with WTA biosynthesis inhibited. Without WTAs, antibody recruitment was significantly higher than the native cells with WTA. The authors specifically address that this is evidence that WTA is serving as a barrier to potential opsonin recruitment to the cell surface. They further clarify that surface charge and WTA density may sterically and/or electrostatically deter opsonins.¹ While this example touches on accessibility, it is not an explicit investigation of how powerful the challenge of accessibility can be, especially as it relates to our understanding of the ability of antibiotics or immune system components to interact with targets on bacterial cell surfaces.

Perhaps the strongest example to date that addresses accessibility is an investigation into the longstanding notion that peptidoglycan recognition proteins (PGRPs) are able to discriminate between different structures of PG. PGRPs are innate immunity molecules that can recognize and bind to PG. The PGRPs that

Drosophila (fruit flies) possess are well studied and binding of these PGRPs to PG signals several different responses such as the generation of antimicrobial agents and induction of phagocytosis. PGRPs can also act as amidases and hydrolyze the PG, which is documented to occur with both *Drosophila* and mammalian PGRPs. For *Drosophila* though, it is thought that the PGRPs they possess, PGRP-SA and PGRP-LC, can discriminate between and preferentially interact with PG that has lysine in the third position of the stem peptide or PG with meso-diaminopimelic acid (mDAP) at the third position instead. PGRP-SA is thought to interact with the lysine containing PG primarily and PGRP-LC interacts with mDAP-type. However they discover that when WTA is genetically deleted from *S. aureus*, lysine-type PG, and from *Bacillus subtilis* (*B. subtilis*) which contains mDAP-type PG, the binding of both PGRPs to either bacteria is increased. This majorly contradicts the supposed specificity of these proteins and points to the fact that accessibility of the cell wall plays a large role in the ability of the immune system, specifically PGRPs in this case, to respond to an infection.¹¹⁻¹²

Given that accessibility is able to mediate the interactions of an immune system component with a PG binding site, it may be reasonable to question if this may not be the only interaction that is being hindered and possibly misevaluated due to limited accessibility. The impact of accessibility needs to be understood and characterized more in-depth. There are numerous studies that investigate cell wall permeation which relates to accessibility but there seems to be a lack of a quantitative and systematic characterization of accessibility to live bacterial cell surfaces, information that could be vital in guiding future drug design.

2.2 Probing Accessibility

In effort to highlight the need of a novel assay that can assess accessibility, it is pertinent to understand what has already been done. Some of the earliest examples of permeation studies began being reported in the 1970s. One of the first investigations worked to devise a library of hydrophilic molecules and determined their permeation through whole cells by tracking molecular weight changes and disruption of osmotic stability in various solvents before and after

treatment with the library. Overall the study revealed only the smallest molecules in the library were allowed to achieve what they were determining to be permeation.¹³ In a similar vein other libraries have been tested for permeation into native isolated whole PG (sacculi) and spores. Instead of small molecule libraries however, these consisted of polymers of various lengths. One study used increasing chain lengths of polyethylene glycol while another used dextrans. Both studies looked at permeability or uptake by measuring pellet weight before and after treatment. These studies had similar conclusions, revealing that the longer the molecule is the less permeable. However measuring by mass is error prone and the sensitivity of detection of mass shifts is low.¹⁴⁻¹⁵ Strides were taken to improve the readout of permeation by first introducing a radioactive moiety attached to the polymer chain, one could then measure the radioactivity of the resulting cell pellet in order to deduce permeation levels. This study also concluded that smaller lengths diffuse into the cell faster. However the radiation is likely to induce DNA damage, if not cell death/lysis, so the integrity of the sample is in question.¹⁶ The final iteration of this assay and perhaps the most effective involved the creation of a library of fluorescein labeled dextrans that ranged in length. These were used to probe permeation into sacculi of *Escherichia coli* (*E. coli*) and *B. subtilis*. They measured the fluorescence of the sacculi pellet with a spectrofluorometer over the course of an hour. They did identify that smaller dextrans are more permeable however these results were only qualitative. For all of these studies it is also impossible to know where within the cell wall the molecules permeated to (no specificity).¹⁷

Around the same timeframe as the fluorescent dextran study a different way to assess permeability was being developed. This assay relies on the horseradish peroxidase (HRP) enzyme, which is typically used to amplify signals in a photometric assay by catalyzing the conversion of a chromogenic substrate to a product with a measurable absorbance. It also relies on hybridization, which is the process of combining two single strands of DNA or RNA by complimentary base pairing. This group created HRP linked oligonucleotide probes, one short in length and one longer, and these probes can get hybridized in bacterial cells should it be

able to permeate through the cell wall to the bacterial DNA. Once hybridized, a fluorescent HRP substrate can be added and that measurable fluorescence becomes a read out of permeability. This needs to be done on fixed cells however so there is a loss of the active metabolism and related processes that occur in live cells. The actual intent of the assay was to measure how permeable the cells become after treatment with autolysins (cell wall degrading enzymes) but there was a sample set that looked at the cells before autolysin treatment that showed the larger oligonucleotide could not hybridize in intact cells but the smaller probe did give a weak signal.¹⁸ Another study taking place at this time and is still widely used today involves the use of fluorescent dyes particularly ones that result in the staining of nucleic acids of bacterial cells and flow cytometry to track that staining. Uptake of the dye can be impacted by changes in permeability of the cell wall and that should be reflected in the cellular fluorescence levels. While this does not provide a systematic analysis of accessibility it can be an efficient read out of cell wall integrity, especially after treatment with an antimicrobial agent for example.¹⁹⁻

20

Another assay that reports on compound uptake and accumulation is one that has been used extensively for Gram-negative bacteria and involves the use of liquid chromatography with tandem mass spectrometry (LC-MS/MS). Essentially the bacteria can be treated with a library of compounds, harvested, washed to remove excess compound, lysed, and analyzed via LC-MS/MS. The LC can separate the components in the lysate and tandem MS can help identify the peaks with an eye towards picking out compounds from the screen that may have accumulated in the cell. However there is not a simple way to know where the compound has localized to within the cell wall unless each layer of the cell wall is extracted and analyzed separately.²¹⁻²⁴ However, there is a modified version of this assay that allows for specific accumulation in either the periplasmic or cytoplasmic space. This is done through use of the protein, streptavidin, which is expressed with a specific peptide tag that instructs the cell to export it to either the periplasmic or cytoplasmic space. The cell is then treated with biotin that has been functionalized with a cyclooctyne handle, which is capable of participating in strain-

promoted alkyne–azide cycloaddition (SPAAC), a copper free form of click chemistry. The functionalized biotin will bind to the streptavidin and the cell can be treated with a library of bioorthogonally functionalized (azide) molecules that can react with the click partner. In this assay set up the cells still need to be lysed and MS is still used to identify the hits.²⁵⁻²⁷ There is also another permeability assay that uses SPAAC partners. This assay uses an azide functionalized choline that can be incorporated into the outer membrane of Gram-negative bacteria. This functionalized choline can be labeled by a fluorophore linked cyclooctyne and the fluorescence level can be detected by flow cytometry. The aim of the assay however is to look at outer membrane integrity, the fluorescence labeling levels in intact cells is low, however if genes critical to outer membrane stability are knocked out or the cells are treated with outer membrane disrupters there should be an increase in signal due to an increase of accessibility of the azide functionalized choline.²⁸

Lastly many efforts have been made towards computational models that work to predict permeability of molecules and analyze the physiochemical properties of the hit compounds. This method has been extensively explored with the model organism being mycobacteria. While these models can be informative they need to be supported by experimental data. In tandem with these permeation models, minimum inhibitory concentration (MIC) assays are performed to validate the hits, which determines the lowest concentration of an antimicrobial agent that can be used to prevent visible growth of the bacteria of choice. However there is no clear indication from a MIC value that the molecule permeated into the cell wall and reached a target.²⁹⁻³²

The techniques in each of these examples do have their value. While the early permeability studies paved the way for interest in this area much could be improved upon with the technology that is available today. For instance, it would be more advantageous to assess surface accessibility of whole, live cells as opposed to the sacculi alone. In isolating the PG from native whole cells, there is a loss of important structural information that may impact the accessibility data. Also many of these studies rely on noncovalent interactions and that creates an

inability to identify where these library compounds localized to within the cell envelope. There is also a lack of quantitative data that can be achieved in a high-throughput manner. The HRP-based and nucleic acid dye assays provide valuable information on cell wall integrity but have not been employed in a way that allows for a systematic evaluation of cell surface accessibility. The LC-MS/MS assays could allow for more systematic characterization but the method is technically challenging and low throughput. Modeling provides excellent physiochemical data of the permeating molecules (in theory) but the tandem MIC assays only speak to cell death, it does not tell you where the compound actually localized to and imparted its effect. Chapter 3 will describe a novel assay that was designed to assess accessibility to the surface of PG in live *S. aureus* cells in a systematic way. Additionally, modulations to the bacterial cell surface were introduced in order to determine what factors, if any, are impeding accessibility. The general approach of the assay relies on the metabolic incorporation of an unnatural free thiol handle onto the stem peptide of the PG and the use of a library of compounds that range in size and flexibility. The library members are functionalized with a bioorthogonal binding handle and a fluorescent reporter molecule that can be tracked *via* flow cytometry. This results in quantitative data about the ability of each library member to reach the bacterial cell surface with the aim that this could be a guide for future drug design.

2.3 References

1. Gautam, S.; Kim, T.; Lester, E.; Deep, D.; Spiegel, D. A., Wall teichoic acids prevent antibody binding to epitopes within the cell wall of *Staphylococcus aureus*. *ACS Chem Biol* **2016**, *11* (1), 25-30.
2. Carvalho, F.; Atilano, M. L.; Pombinho, R.; Covas, G.; Gallo, R. L.; Filipe, S. R.; Sousa, S.; Cabanes, D., L-Rhamnosylation of *Listeria monocytogenes* Wall Teichoic Acids Promotes Resistance to Antimicrobial Peptides by Delaying Interaction with the Membrane. *PLoS Pathog* **2015**, *11* (5), e1004919.
3. Wu, X.; Paskaleva, E. E.; Mehta, K. K.; Dordick, J. S.; Kane, R. S., Wall Teichoic Acids Are Involved in the Medium-Induced Loss of Function of the Autolysin CD11 against *Clostridium difficile*. *Sci Rep* **2016**, *6*, 35616.
4. Wu, X.; Kwon, S. J.; Kim, D.; Zha, J.; Mora-Pale, M.; Dordick, J. S., Unprotonated Short-Chain Alkylamines Inhibit Staphylolytic Activity of Lysostaphin in a Wall Teichoic Acid-Dependent Manner. *Appl Environ Microbiol* **2018**, *84* (14).
5. Eugster, M. R.; Loessner, M. J., Wall teichoic acids restrict access of bacteriophage endolysin Ply118, Ply511, and PlyP40 cell wall binding domains to the *Listeria monocytogenes* peptidoglycan. *J Bacteriol* **2012**, *194* (23), 6498-506.
6. Kohler, T.; Weidenmaier, C.; Peschel, A., Wall teichoic acid protects *Staphylococcus aureus* against antimicrobial fatty acids from human skin. *J Bacteriol* **2009**, *191* (13), 4482-4.
7. Bertsche, U.; Yang, S. J.; Kuehner, D.; Wanner, S.; Mishra, N. N.; Roth, T.; Nega, M.; Schneider, A.; Mayer, C.; Grau, T.; Bayer, A. S.; Weidenmaier, C., Increased cell wall teichoic acid production and D-alanylation are common phenotypes among daptomycin-resistant methicillin-resistant *Staphylococcus aureus* (MRSA) clinical isolates. *PLoS One* **2013**, *8* (6), e67398.
8. Steen, A.; Buist, G.; Leenhouts, K. J.; El Khattabi, M.; Grijpstra, F.; Zomer, A. L.; Venema, G.; Kuipers, O. P.; Kok, J., Cell wall attachment of a widely distributed peptidoglycan binding domain is hindered by cell wall constituents. *J Biol Chem* **2003**, *278* (26), 23874-81.

9. Schlag, M.; Biswas, R.; Krismer, B.; Kohler, T.; Zoll, S.; Yu, W.; Schwarz, H.; Peschel, A.; Gotz, F., Role of staphylococcal wall teichoic acid in targeting the major autolysin Atl. *Mol Microbiol* **2010**, *75* (4), 864-73.
10. Lee, S. H.; Wang, H.; Labroli, M.; Koseoglu, S.; Zuck, P.; Mayhood, T.; Gill, C.; Mann, P.; Sher, X.; Ha, S.; Yang, S. W.; Mandal, M.; Yang, C.; Liang, L.; Tan, Z.; Tawa, P.; Hou, Y.; Kuvelkar, R.; DeVito, K.; Wen, X.; Xiao, J.; Batchlett, M.; Balibar, C. J.; Liu, J.; Murgolo, N.; Garlisi, C. G.; Sheth, P. R.; Flattery, A.; Su, J.; Tan, C.; Roemer, T., TarO-specific inhibitors of wall teichoic acid biosynthesis restore beta-lactam efficacy against methicillin-resistant staphylococci. *Sci Transl Med* **2016**, *8* (329), 329ra32.
11. Vaz, F.; Kounatidis, I.; Covas, G.; Parton, R. M.; Harkiolaki, M.; Davis, I.; Filipe, S. R.; Ligoxygakis, P., Accessibility to Peptidoglycan Is Important for the Recognition of Gram-Positive Bacteria in Drosophila. *Cell Rep* **2019**, *27* (8), 2480-2492 e6.
12. Atilano, M. L.; Yates, J.; Glittenberg, M.; Filipe, S. R.; Ligoxygakis, P., Wall teichoic acids of *Staphylococcus aureus* limit recognition by the drosophila peptidoglycan recognition protein-SA to promote pathogenicity. *PLoS Pathog* **2011**, *7* (12), e1002421.
13. Scherrer, R.; Gerhardt, P., Molecular sieving by the *Bacillus megaterium* cell wall and protoplast. *J Bacteriol* **1971**, *107* (3), 718-35.
14. Scherrer, R.; Cabrera Beaman, T.; Gerhardt, P., Macromolecular sieving by the dormant spore of *Bacillus cereus*. *J Bacteriol* **1971**, *108* (2), 868-73.
15. Sara, M.; Sleytr, U. B., Molecular sieving through S layers of *Bacillus stearothermophilus* strains. *J Bacteriol* **1987**, *169* (9), 4092-8.
16. Decad, G. M.; Nikaido, H., Outer membrane of gram-negative bacteria. XII. Molecular-sieving function of cell wall. *J Bacteriol* **1976**, *128* (1), 325-36.
17. Demchick, P.; Koch, A. L., The permeability of the wall fabric of *Escherichia coli* and *Bacillus subtilis*. *J Bacteriol* **1996**, *178* (3), 768-73.
18. Bidnenko, E.; Mercier, C.; Tremblay, J.; Tailliez, P.; Kulakauskas, S., Estimation of the state of the bacterial cell wall by fluorescent In situ hybridization. *Appl Environ Microbiol* **1998**, *64* (8), 3059-62.

19. Walberg, M.; Gaustad, P.; Steen, H. B., Uptake kinetics of nucleic acid targeting dyes in *S. aureus*, *E. faecalis* and *B. cereus*: a flow cytometric study. *J Microbiol Methods* **1999**, *35* (2), 167-76.
20. Campodonico, V. L.; Rifat, D.; Chuang, Y. M.; Ioerger, T. R.; Karakousis, P. C., Altered Mycobacterium tuberculosis Cell Wall Metabolism and Physiology Associated With RpoB Mutation H526D. *Front Microbiol* **2018**, *9*, 494.
21. Iyer, R.; Ye, Z.; Ferrari, A.; Duncan, L.; Tanudra, M. A.; Tsao, H.; Wang, T.; Gao, H.; Brummel, C. L.; Erwin, A. L., Evaluating LC-MS/MS To Measure Accumulation of Compounds within Bacteria. *ACS Infect Dis* **2018**, *4* (9), 1336-1345.
22. Widya, M.; Pasutti, W. D.; Sachdeva, M.; Simmons, R. L.; Tamrakar, P.; Krucker, T.; Six, D. A., Development and Optimization of a Higher-Throughput Bacterial Compound Accumulation Assay. *ACS Infect Dis* **2019**, *5* (3), 394-405.
23. Kim, T. H.; Tao, X.; Moya, B.; Jiao, Y.; Basso, K. B.; Zhou, J.; Lang, Y.; Sutaria, D. S.; Zavascki, A. P.; Barth, A. L.; Reeve, S. M.; Schweizer, H. P.; Deveson Lucas, D.; Boyce, J. D.; Bonomo, R. A.; Lee, R. E.; Shin, B. S.; Louie, A.; Drusano, G. L.; Bulitta, J. B., Novel Cassette Assay To Quantify the Outer Membrane Permeability of Five beta-Lactams Simultaneously in Carbapenem-Resistant *Klebsiella pneumoniae* and *Enterobacter cloacae*. *mBio* **2020**, *11* (1).
24. Prochnow, H.; Fetz, V.; Hotop, S. K.; Garcia-Rivera, M. A.; Heumann, A.; Bronstrup, M., Subcellular Quantification of Uptake in Gram-Negative Bacteria. *Anal Chem* **2019**, *91* (3), 1863-1872.
25. Spangler, B.; Dovala, D.; Sawyer, W. S.; Thompson, K. V.; Six, D. A.; Reck, F.; Feng, B. Y., Molecular Probes for the Determination of Subcellular Compound Exposure Profiles in Gram-Negative Bacteria. *ACS Infect Dis* **2018**, *4* (9), 1355-1367.
26. Baskin, J. M.; Prescher, J. A.; Laughlin, S. T.; Agard, N. J.; Chang, P. V.; Miller, I. A.; Lo, A.; Codelli, J. A.; Bertozzi, C. R., Copper-free click chemistry for dynamic in vivo imaging. *Proc Natl Acad Sci U S A* **2007**, *104* (43), 16793-7.

27. Jewett, J. C.; Sletten, E. M.; Bertozzi, C. R., Rapid Cu-free click chemistry with readily synthesized biarylazacyclooctynones. *J Am Chem Soc* **2010**, *132* (11), 3688-90.
28. Klobucar, K.; French, S.; Cote, J. P.; Howes, J. R.; Brown, E. D., Genetic and Chemical-Genetic Interactions Map Biogenesis and Permeability Determinants of the Outer Membrane of Escherichia coli. *mBio* **2020**, *11* (2).
29. Ferreira, R. J.; Kasson, P. M., Antibiotic Uptake Across Gram-Negative Outer Membranes: Better Predictions Towards Better Antibiotics. *ACS Infect Dis* **2019**, *5* (12), 2096-2104.
30. Hong, X.; Hopfinger, A. J., Molecular modeling and simulation of Mycobacterium tuberculosis cell wall permeability. *Biomacromolecules* **2004**, *5* (3), 1066-77.
31. Merget, B.; Zilian, D.; Muller, T.; Sotriffer, C. A., MycPermCheck: the Mycobacterium tuberculosis permeability prediction tool for small molecules. *Bioinformatics* **2013**, *29* (1), 62-8.
32. Janardhan, S.; Ram Vivek, M.; Narahari Sastry, G., Modeling the permeability of drug-like molecules through the cell wall of Mycobacterium tuberculosis: an analogue based approach. *Mol Biosyst* **2016**, *12* (11), 3377-3384.

Chapter 3. Systematic Assessment of Accessibility to the Surface of *Staphylococcus aureus*

Adapted from: Ferraro, N. J.; Kim, S.; Im, W.; Pires, M. M., Systematic Assessment of Accessibility to the Surface of *Staphylococcus aureus*. *ACS Chem Biol* **2021**.

3.1 Abstract

Proteins from bacterial foes, antimicrobial peptides, and host immune proteins must navigate past a dense layer of bacterial surface biomacromolecules to reach the peptidoglycan (PG) layer of Gram-positive bacteria. A subclass of molecules (e.g., antibiotics with intracellular targets) also must permeate through the PG (in a molecular sieving manner) to reach the cytoplasmic membrane. Despite the biological and therapeutic importance of surface accessibility, systematic analyses in live bacterial cells have been lacking. We describe a live cell fluorescence assay that reports on the permeability of molecules to and within the PG scaffold. The assay has robust reproducibility, is readily adoptable to any Gram-positive organism. Moreover, our study shows that teichoic acids impede the permeability of molecules of a wide range of sizes and chemical composition.

3.2 Introduction

Bacterial cell walls are essential barriers that protect bacteria against an onslaught of potentially lethal external insults. The therapeutic effectiveness of most antibiotics hinges on their ability to permeate through bacterial surface biomacromolecules to ultimately reach their target. At the same time, bacteria cell wall features have evolved in order to reduce the accessibility of antibacterial agents. For example, *Staphylococcus aureus* (*S. aureus*) resistance to vancomycin can result from cell wall thickening, which effectively captures vancomycin molecules and prevents their association with their lipid II target.¹ A molecular sieving concept through the dense cell wall has also been evoked to describe trends in antibacterial activities of synthetic mimics of antimicrobial peptides.² Similarly, central components of the human innate and adaptive immune system, such as lysozyme and antibodies, target cell surface components

and do not need to cross the membrane bilayer, yet they too can have their activities modulated by cell surface biopolymers.³⁻⁵

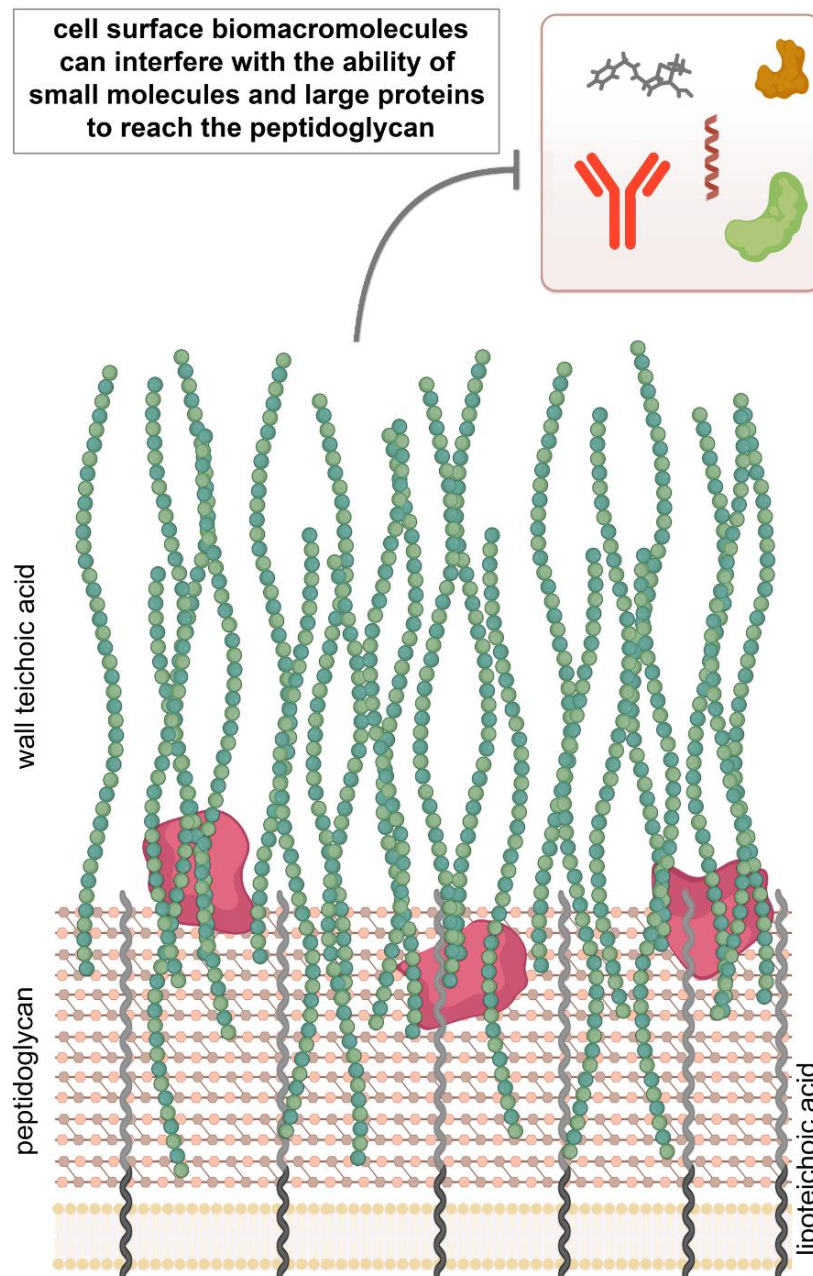


Figure 3.1 Schematic representation of the surface composition of *S. aureus* delineating key biomacromolecules that can potentially impact penetration of molecules.

Gram-positive bacteria have a cell wall that includes a thick PG layer on the exterior side of the cytoplasmic membrane (**Figure 3.1**). PG is a mesh-like polymer made up of repeating disaccharides N-acetylglucosamine (GlcNAc) and N-acetylmuramic acid (MurNAc). Each MurNAc unit is connected to a short and unusual peptide (stem peptide) with the canonical sequence of L-Ala-iso-D-Glu-L-Lys-D-Ala-D-Ala or meso-diaminopimelic acid (m-DAP) in place of L-Lys at the 3rd position.⁶ For all known bacteria, neighboring stem peptides are crosslinked to endow the PG matrix with rigidity and integrity. Cell walls are further decorated with a number of polymers and proteins that play important physiological roles such as regulating cell morphology and growth, serving as virulence factors, and aiding in adherence and colonization.⁷ Bacterial PG is an essential component of the bacterial cell wall and its unique structure makes it a prominent target for the innate immune system. Critically, a significant number of FDA-approved antibiotics also target PG by inhibiting the biosynthesis of it.⁸⁻⁹ Given the importance of PG in antibacterial therapy, a better understanding of the accessibility to this polymer is imperative.

3.3 Results and Discussion

Early seminal works have described a molecular sieving effect of polymers permeating through bacterial PG, which is likely a product of its lattice structure.¹⁰⁻¹¹ While illuminating, these experiments were performed in vitro with isolated PG (sacculi). In contrast, we set out to develop a method to systematically measure accessibility to the PG scaffold of live bacterial cells. The basis of the assay is a site selective incorporation of a reactive epitope within the PG of live cells followed by treatment with heterobifunctional reporter molecules of varying sizes that attach to the PG scaffold (**Figure 3.2**). The reporter molecules are linked to fluorophores, and, therefore, cellular fluorescence levels describe the ability of the probes to navigate through surface exposed biomacromolecules. Covalent PG tagging is expected to result in reliable measurements that can be readily quantified using standard techniques amendable to high throughput analyses (e.g., flow cytometry). We initially reasoned that a thiol functional group could be installed

within bacterial PG, which lacks native thiols, by the process of metabolic tagging of the PG with synthetic stem peptide analogs containing D-cysteine.¹²⁻¹⁶ During cell growth and division, synthetic PG analogs enter the biosynthetic pathway in place of endogenous building blocks, and this process provides a robust route to introduce non-native functional groups within bacterial PG.¹⁷

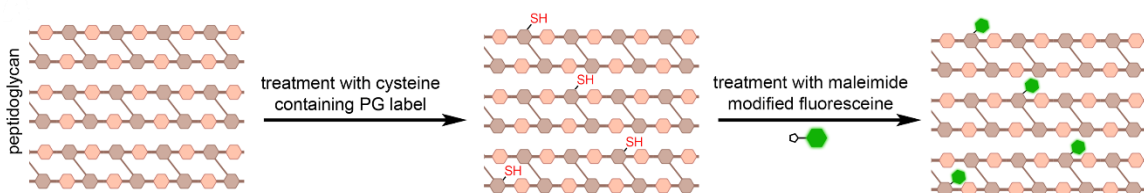


Figure 3.2 Proposed assay to tag the bacterial PG scaffold with thiol handles followed by a fluorescent probe that contains a bioorthogonal binding partner for the thiol handle.

A small panel of synthetic PG analogs was synthesized, each of which contained a cysteine residue (**Figure 3.3**). The panel contained three derivatives of the single D-amino acid, D-cysteine (**1**). During cell growth, single D-amino acids supplemented in the culture medium, such as D-cysteine, are swapped in the place of the D-alanine that occupies the 5th position within the stem peptide of *S. aureus* (**Figure 3.4**).^{12,18} A wide range of single D-amino acid PG probes have been developed to elucidate fundamental steps in bacterial cell wall biology.¹⁷⁻²⁸ We also included oxidized D-cystine (**2**) and D-cysteine amidated (**3**) at the C-terminus in an attempt to maximize PG tagging, which can result in higher levels of unnatural D-amino acid incorporation and/or retention.^{22,26} Alternatively, cell treatment with the dipeptide D-Cys-D-Ala (**4**) was expected to result in the incorporation of D-cysteine at the 4th position of the stem peptide.^{12,29-30} D-Cys-D-Ala mimics the D-Ala-D-Ala dipeptide PG precursor, therefore it should be processed intracellularly by the MurF enzyme to generate D-cysteine containing PG. Lastly, cysteine was placed at the N-terminus of a tetrapeptide (**5**) synthetic analog of the PG stem

peptide. We^{28,31} and others³²⁻³⁵ recently showed that structural analogs of PG stem peptides can be crosslinked into the growing PG scaffold of live cells.

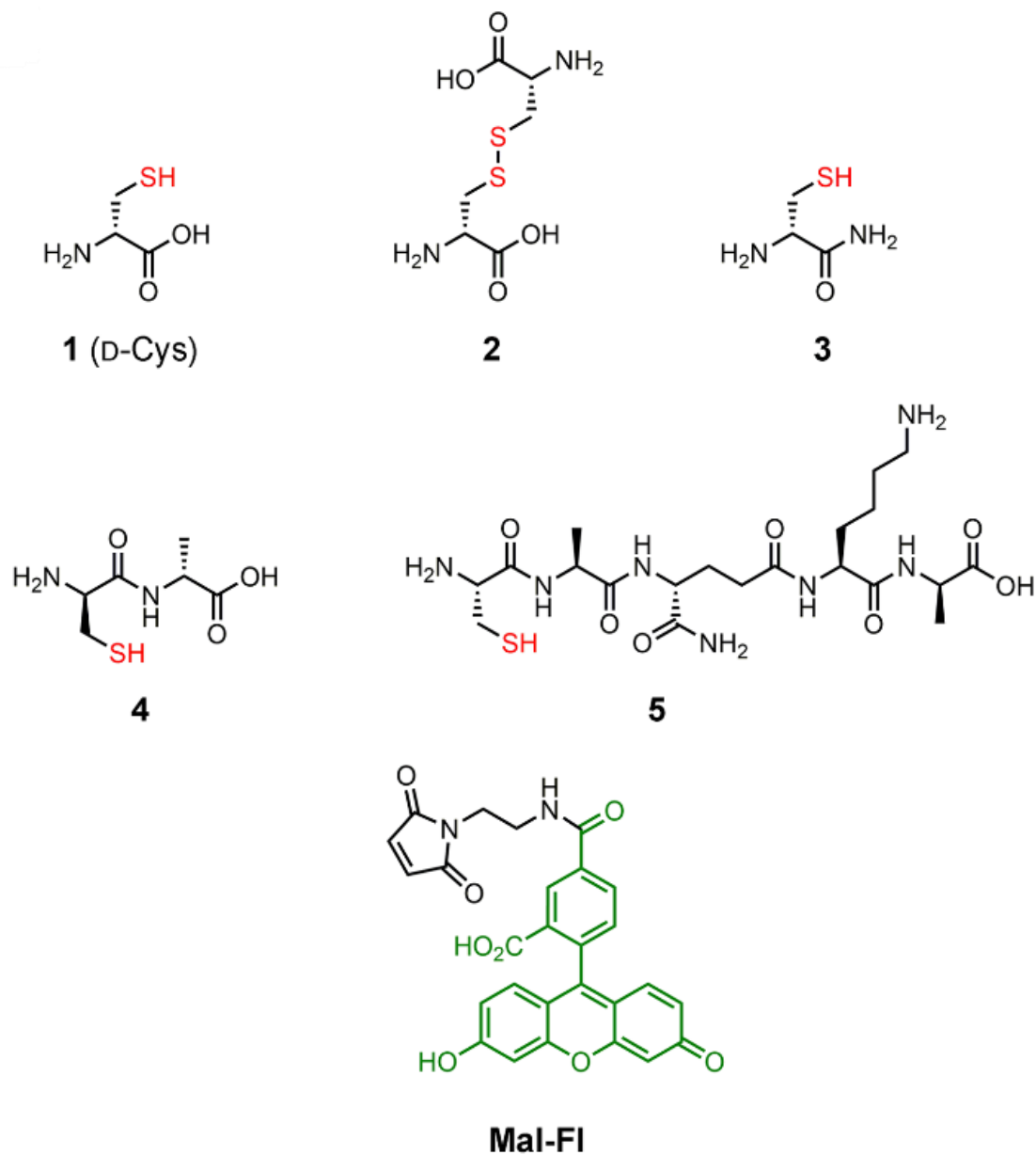


Figure 3.3 Chemical structure of PG analogs modified with a cysteine residue and the fluorescent reporter **Mal-FI**.

Our first goal was to identify which cysteine-based label would result in the highest level of thiol handles on the surface of *S. aureus*. To accomplish this, *S. aureus* cells were grown overnight in the presence of each PG analog to promote incorporation throughout the entire PG scaffold. Then, cells were treated with the reducing agent dithiothreitol (DTT) to unmask the thiols on the PG, which were expected to exist primarily as disulfides due to the oxidizing nature of the culture media. Cells were washed with PBS to remove excess reducing agent and incubated with maleimide-modified fluorescein (**Mal-FI**).

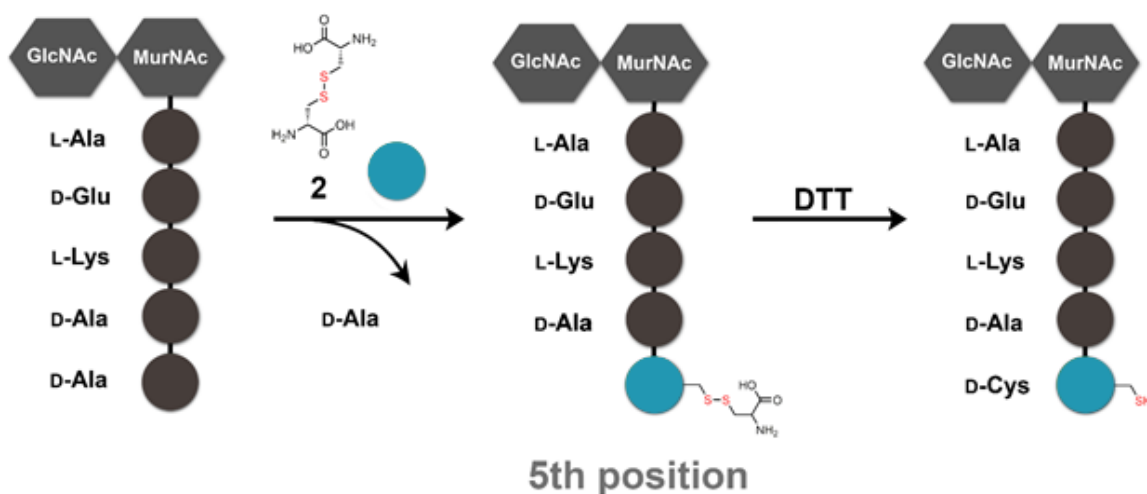


Figure 3.4 Modes of incorporation of single amino acids by swapping into the 5th position on the peptidoglycan stem peptide of *S. aureus* cells. D-cystine is incorporated (singly or doubly) within the PG scaffold and is subsequently reduced with DTT to generate D-cysteine.

Our results clearly showed that some of the PG metabolic tags resulted in significant increases in fluorescence levels (**Figure 3.5**). Incubation of cells with D-cystine (**2**) led to a ~12-fold increase in cellular fluorescence relative to DMSO treated cells. Interestingly, this large increase suggests that the total amount of cysteines within the modified PG are far greater than the number of cysteines found within endogenous *S. aureus* cell surface proteins. Likewise, treatment of *S.*

aureus cells with the enantiomeric L-cystine, which is not expected to be processed by PG transpeptidases, led to a minimal increase in cellular fluorescence compared to DMSO treated cells (**Figure 3.6A**). Next, a titration experiment was carried out and we found that 25 μ M was an optimum concentration of **Mal-FI** based on labeling levels (**Figure 3.6B**).

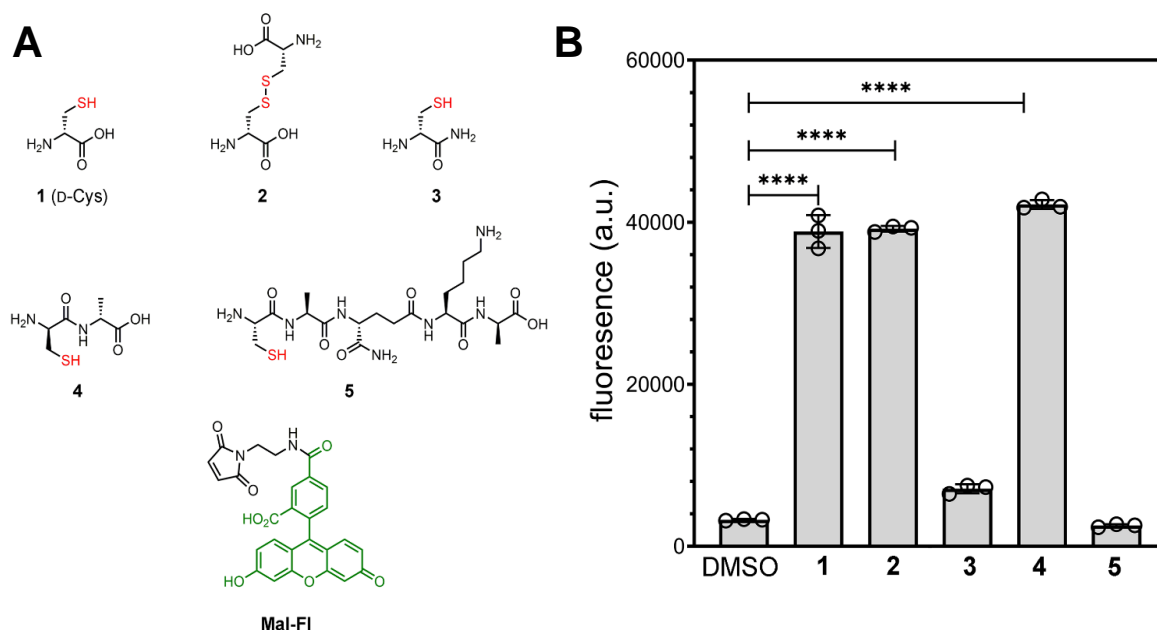


Figure 3.5 (A) Chemical structure of PG analogs modified with a cysteine residue and the fluorescent reporter **Mal-FI**. (B) Flow cytometry analysis of *S. aureus* (ATCC 25923) treated overnight with 1 mM of synthetic PG analogs, reduced with DTT (5 mM), and incubated with 25 μ M of **Mal-FI**. Data are represented as mean \pm SD (n = 3). P-values were determined by a two-tailed t-test (* denotes a p-value < 0.05, ** < 0.01, *** < 0.001, ns = not significant).

Although there were similar labeling levels observed with the other PG analogues, we expected that D-cystine, the disulfide form of D-cysteine, would result in more consistent labeling levels compared to the other compounds due to the fact that the others may exist at varying levels of oxidized product during the incubation period in the oxygenated media. It should be noted that larger

concentrations of D-amino acids in the culture media (e.g., 100-250 mM D-serine) has resulted in reduced levels of PG crosslinks.³⁶⁻³⁷ Based on these results, we selected the PG probe D-cystine for all subsequent assays that use the thiol-maleimide pair.

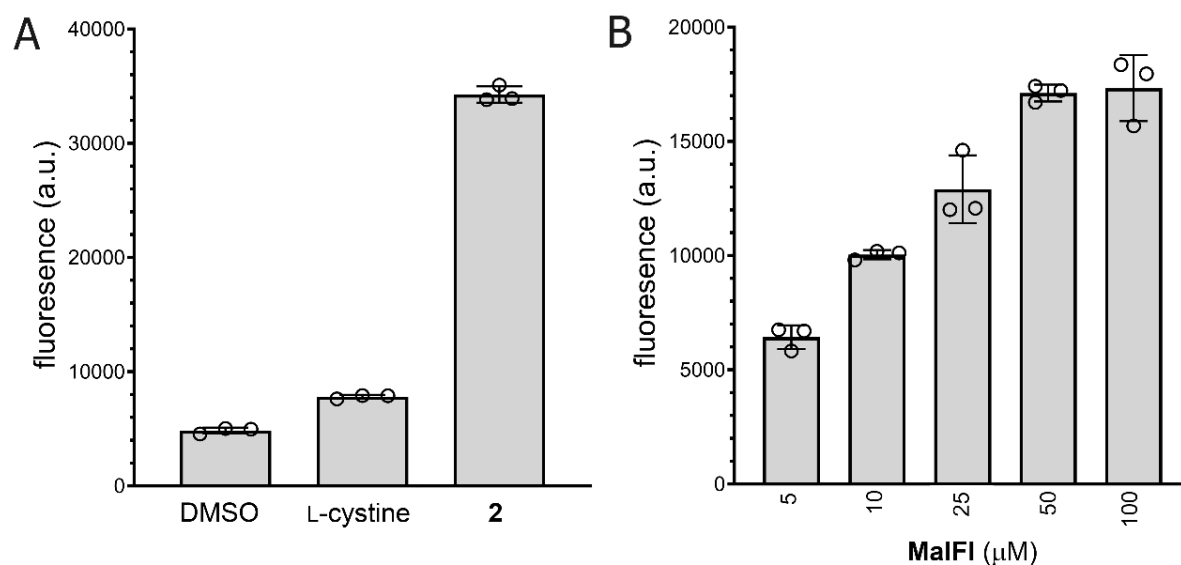


Figure 3.6 (A) Flow cytometry analysis of *S. aureus* (ATCC 25923) treated overnight with 1 mM of DMSO/L-cystine/D-cystine, reduced with DTT (5 mM), and incubated with 25 μM of **Mal-FI**. (B) Flow cytometry analysis of *S. aureus* (ATCC 25923) treated overnight with 1 mM of D-cystine, reduced with DTT (5 mM), and incubated with increasing concentrations **Mal-FI**. Data are represented as mean \pm SD (n = 3).

Localization studies were performed next to test whether the **Mal-FI** is imbedded within the bacterial PG scaffold after reacting with the thiol handle. Our laboratory had previously demonstrated that treatment of *S. aureus* with single D-amino acid probes resulted in the chemical modification of the stem peptide using a range of biochemical techniques.^{12, 18, 25} *S. aureus* cells were treated with D-cystine followed by **Mal-FI** and visualized by confocal microscopy. Our results

showed that the reporter probe had similar labeling profile as *S. aureus* labeled with the single amino acid probe **D-LysFI** (**Figure 3.7**). The same cells were subjected to a sacculi isolation procedure and imaged by confocal microscopy as well. Satisfyingly, the pattern of labeling in the isolated PG scaffold mirrored that of the whole cell and are suggestive of the probe being covalently attached to the PG scaffold.

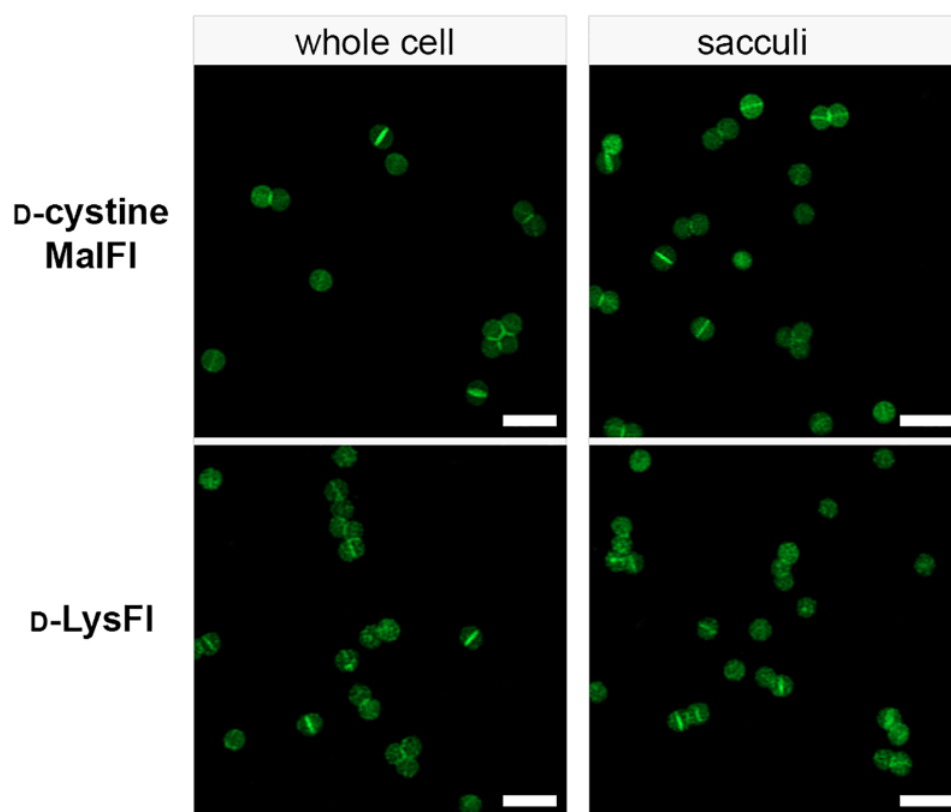


Figure 3.7 Confocal microscopy of *S. aureus* or isolated sacculi from *S. aureus*. *S. aureus* (ATCC 25923) treated overnight with 1 mM of D-cystine or **D-LysFI**. Cells treated with D-cystine were reduced with DTT (5 mM) and incubated with 25 μ M of **Mal-FI** and imaged. Scale bar = 5 μ m. Cells were either imaged by confocal microscopy or subjected to a secondary step in which the sacculi was isolated and imaged.

A second line of evidence of PG binding by the accessibility probe was provided by treatment of *S. aureus* with digestion enzymes (**Figure 3.8**). As before, *S. aureus* were labeled with D-cystine followed by **Mal-FI**, subjected to treatment with either proteinase K or mutanolysin, and cellular fluorescence was measured periodically. Mutanolysin is a muralytic enzyme that cleaves the polysaccharide backbone of PG, thus triggering the release of PG fragments from the cell. Fluorescent probes that are covalently attached to the PG should, likewise, separate from the cells upon treatment with mutanolysin, leading to a reduction in cellular fluorescence levels. As expected, *S. aureus* cells treated with mutanolysin demonstrated a fluorescence level that was half that of the starting level by 120 minutes. Conversely, fluorescence levels of *S. aureus* cells treated with proteinase K (a promiscuous protease that typically cleaves the peptide bond adjacent to aliphatic and aromatic amino acids) remained mostly unchanged over the course the entire experiment.

Two additional sets of experiments were performed to confirm the tagging of the PG scaffold by **Mal-FI**. First we performed BioOrthogonal Non-Canonical Amino acid Tagging (BONCAT) of *S. aureus* (WT) using L-azidohomoalanine (AHA), which is an analog of L-methionine.³⁸⁻⁴⁰ The substrate promiscuity of methionyl-tRNA synthetase allows for the incorporation of AHA into newly synthesized proteins, including those that are surface exposed in *S. aureus*. We anticipated that, likewise, proteins covalently anchored within the PG by sortase would be readily labeled by AHA. After overnight incubation with AHA, cells were washed and treated with **DBCO-FI**. Given the large size of **DBCO-FI**, we anticipated that protein tagging would occur primarily (but not exclusively) within surface exposed proteins. Our results showed that treatment with both mutanolysin and proteinase K resulted in a significant decrease in cellular fluorescence (**Figure 3.9A-B**). These results confirm that proteinase K can access, and release proteins tagged with fluorophores. Therefore, the lack of change in fluorescence levels in cells treated with D-cystine followed by **Mal-FI** are consistent with PG-specific labeling of D-cystine.

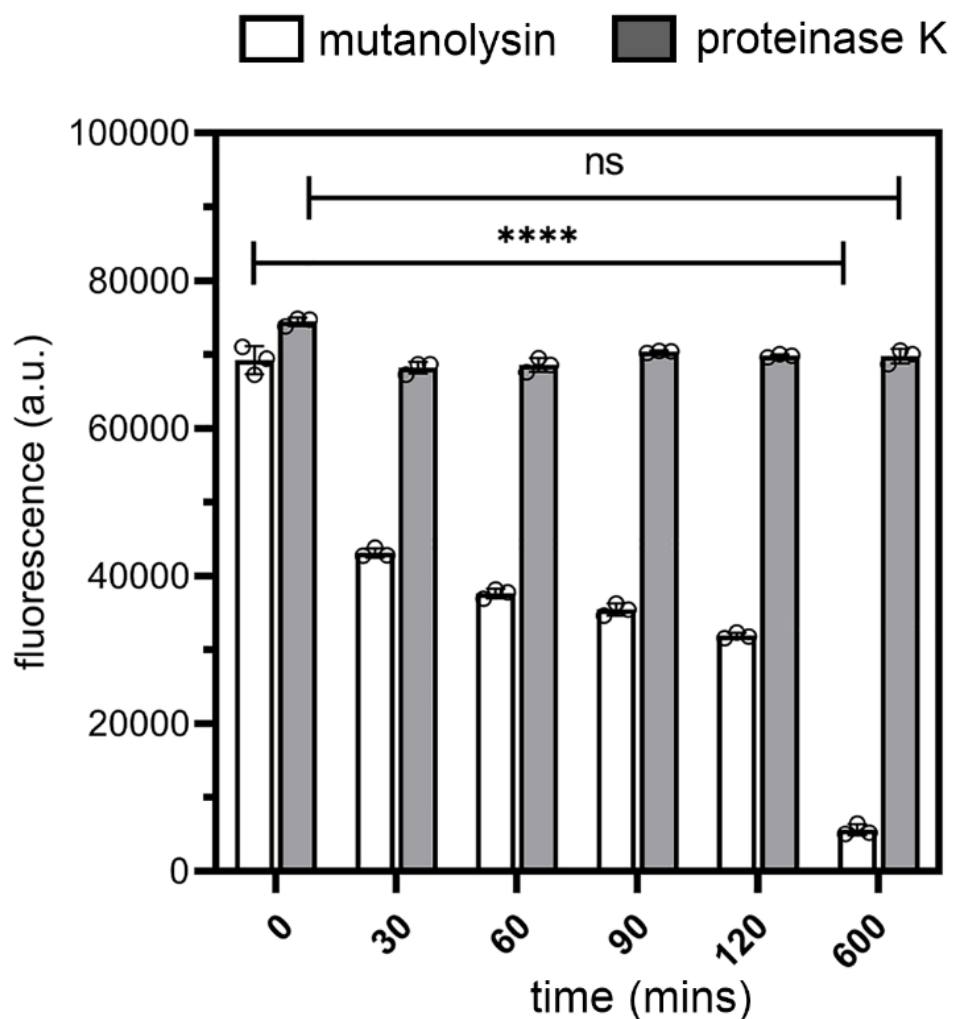


Figure 3.8 Flow cytometry analysis of surface labeled *S. aureus* (ATCC 25923) treated proteinase K (dark bars) or mutanolysin (clear bars). Labeled cells were treated with 1 mM of D-cystine, reduced with DTT (5 mM), and incubated with 25 μ M of **Mal-FI**. Data are represented as mean \pm SD ($n = 3$). P-values were determined by a two-tailed t-test (* denotes a p-value < 0.05 , ** < 0.01 , *** < 0.001 , ns = not significant).

Moreover, the isolated sacculus of *S. aureus* cells, treated with D-cystine followed by **Mal-FI**, was analyzed using an assay we recently described

(SaccuFlow).⁴¹ SaccuFlow enables the quantification of isolated PG fluorescence. Using this assay, we observed similar sensitivity of PG relative to whole cells upon treatment with mutanolysin and proteinase K (**Figure 3.9C**). Together, these results are strongly suggestive of the modification of bacterial PG following the two-step labeling procedure (installation of D-cystine within the PG scaffold followed by covalent attachment of the accessibility probe).

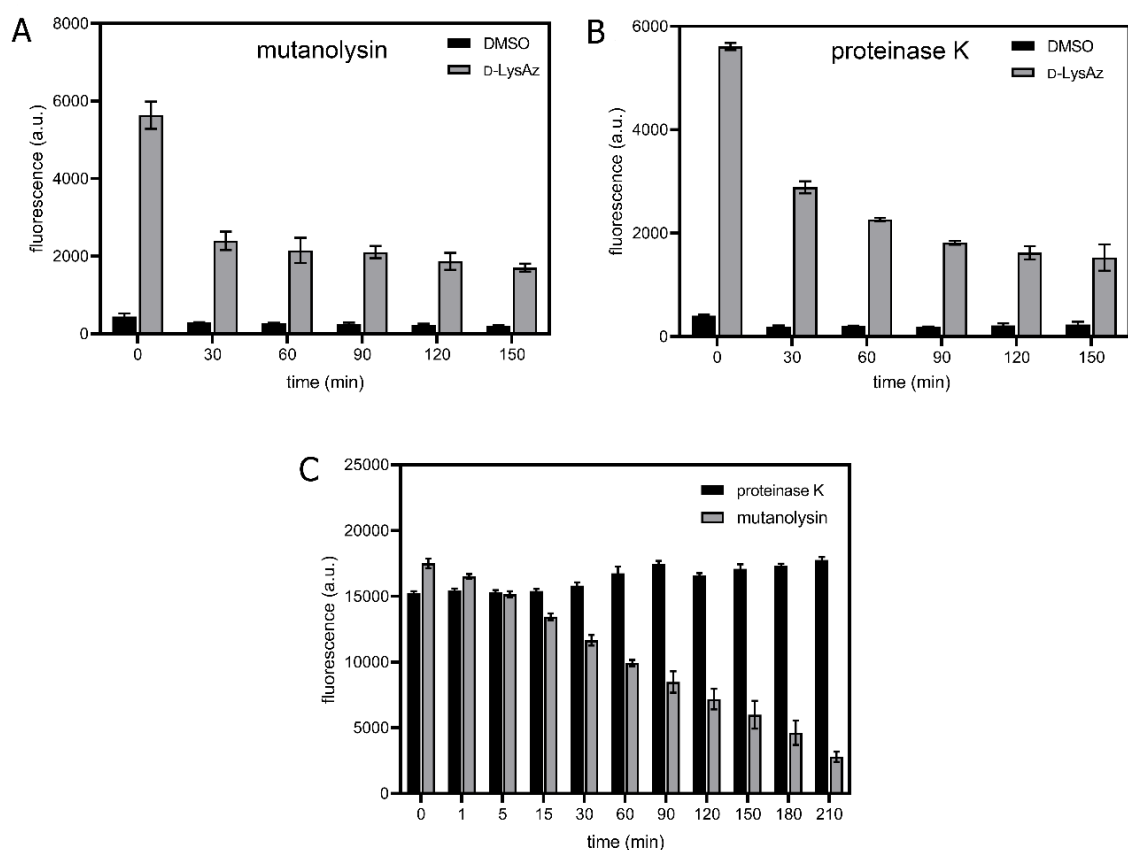


Figure 3.9 Flow cytometry analysis of *S. aureus* (ATCC 25923) treated with 50 µg/mL mutanolysin (A) or 500 µg/mL proteinase K (B). *S. aureus* cells were treated with 1 mM of L-azidohomoalanine and incubated with 25 µM of **DBCO-FI** before enzyme treatment. (C) Flow cytometry analysis of sacculi isolated from *S. aureus* (ATCC 25923) treated 500 µg/mL proteinase K (dark bars) or 50 µg/mL mutanolysin (clear bars). *S. aureus* cells were treated with 1 mM of D-cystine,

reduced with DTT (5 mM), and incubated with 25 μ M of **Mal-FI** prior to sacculi isolation procedure. Data are represented as mean \pm SD (n = 3).

Accessibility to the bacterial PG layer and permeation within the PG scaffold by molecules from the extracellular space should be tied to their physiochemical properties (e.g., charge, size, and flexibility). To test these concepts, we assembled two libraries of accessibility probes that, like **Mal-FI**, display maleimide and fluorescein functional groups. One library contained a flexible polar polyethylene glycol (PEG) spacer and while the other was composed of a rigid polyproline spacer, both of varying lengths (**Figure 3.10A-B**). As before, the PG scaffold of *S. aureus* cells was tagged with thiol handles by incubating with D-cystine. Accessibility to the PG scaffold was investigated by treating cells with members of both libraries and subsequently analyzing by flow cytometry (**Figure 3.10C-D**). A stark difference in surface accessibility was noted between the two libraries. Increasing the length of the spacer in **Mal-peg_n-FI** resulted in a gradual and consistent decrease in fluorescence, whereas there was a sharp decrease in cellular fluorescence with the series of **Mal-pro_n-FI**. These results indicate that rigidity of a molecule may not be favorable for reaching the PG scaffold of bacteria. Instead, flexibility may promote the maneuvering of molecules across surface biopolymers. A similar labeling profile was observed with two other strains of *S. aureus*, including the MRSA strain USA300 (**Figure 3.11**). These results likely reflect the conserved nature of D-cystine labeling in these organisms and could make this assay applicable to other *S. aureus* strains.

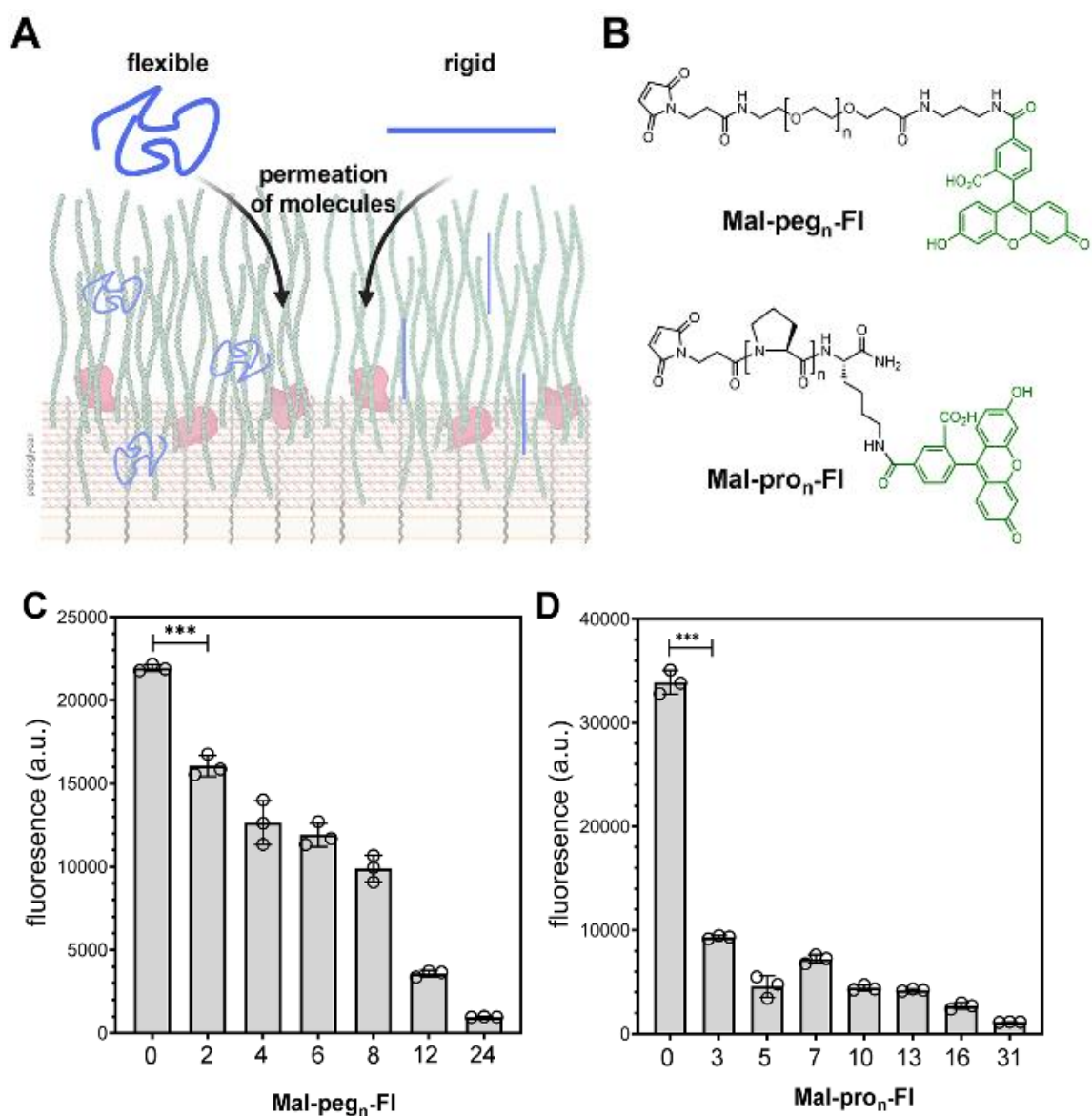


Figure 3.10 (A) Cartoon representation of the two libraries. (B) Chemical structures of accessibility probes. (C-D) Flow cytometry analysis of WT *S. aureus* (ATCC 25923) treated overnight with 1 mM of D-cystine, reduced with DTT (5 mM), and incubated with 25 μ M of designated accessibility probes. Data are represented as mean \pm SD ($n = 3$).

Molecular dynamics (MD) simulations were conducted to determine the conformational variations of the spacer of the **Mal-peg_n-FI** and **Mal-pro_n-FI** library

members in solution. Snapshots of the last 50-ns in MD simulations of the probes show that **Mal-peg_n-FI** (**Figure 3.12A**) displays considerably more flexibility than **Mal-pro_n-FI** (**Figure 3.12B**), which can help explain the results observed in cell surface labeling experiments. More specifically, the root-mean-square deviation (RMSD) values from the equilibrium structure between the shortest spacer and the longest spacer for the **Mal-peg_n-FI** series increases more than 5-fold, whereas for the **Mal-pro_n-FI** series there is only a 2-fold increase (**Figure 3.12C**).

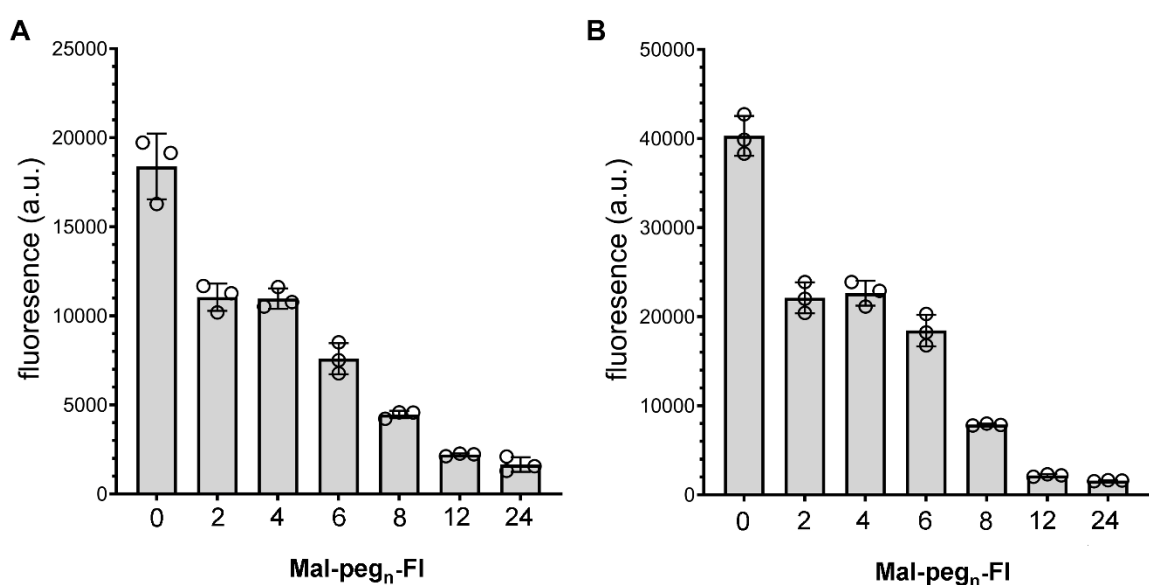


Figure 3.11 Flow cytometry analysis of (A) *S. aureus* (USA300) and (B) *S. aureus* (SCO1) treated overnight with 1 mM of D-cystine, reduced with DTT (5 mM), and incubated with designated accessibility probes. Data are represented as mean \pm SD ($n = 3$).

We proceeded to investigate the role of surface biopolymers on PG accessibility. There are two main surface biopolymers on *S. aureus* cells known as lipoteichoic acids (LTA) and wall teichoic acids (WTA).⁴²⁻⁴⁵ WTA is highly anionic and forms a dense glycan layer that is covalently attached to the stem peptide (**Figure 3.1**). Previous reports have described the influence of WTA on bacteriophage susceptibility,⁴⁶ antibody binding,⁵ antibiotic resistance (e.g.,

daptomycin),⁴⁷ and recognition by innate immune proteins that bind to PG (e.g., Peptidoglycan Recognition Protein).⁴⁸ Inhibitors of WTA biosynthesis, such as tunicamycin, have been developed as anti-infective agents.⁴⁹⁻⁵² Tunicamycin inhibits TarO, which is responsible for the first step in WTA biosynthesis.⁵³

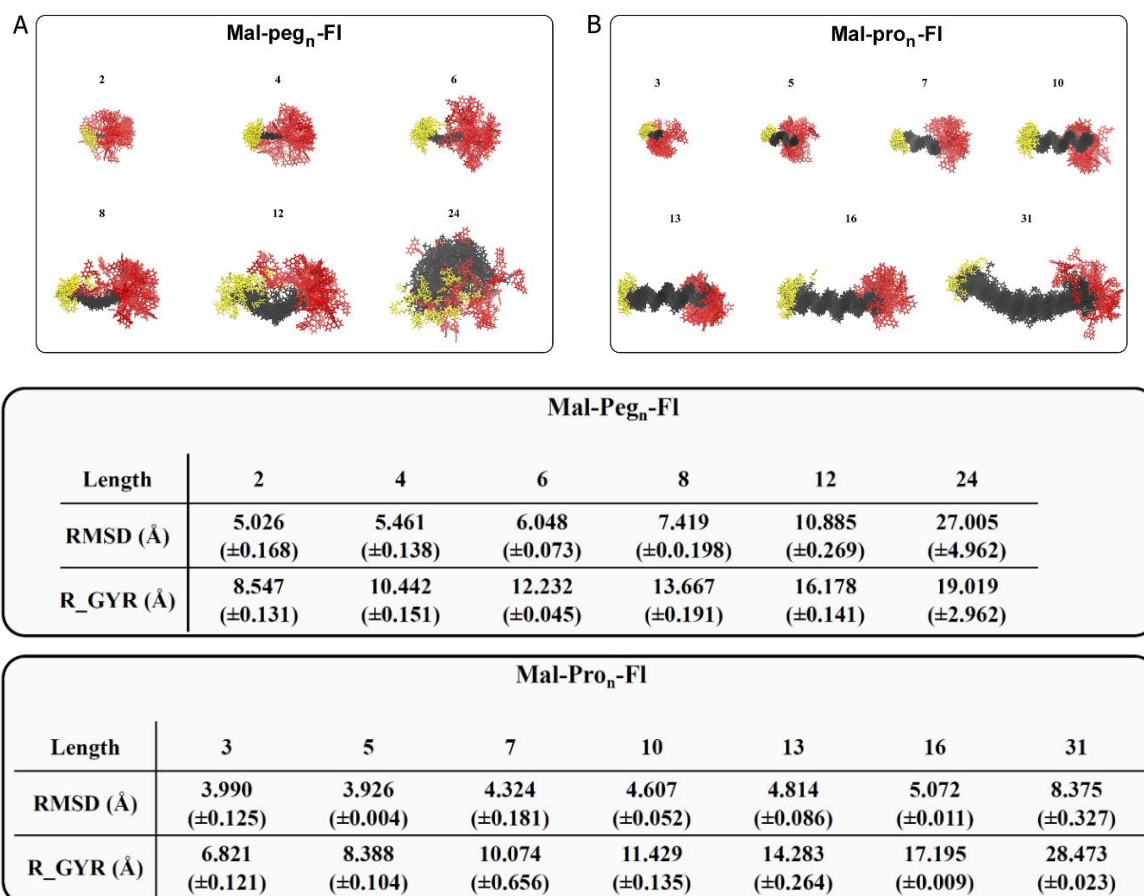


Figure 3.12 Molecular dynamics simulations of (A) PEG-based and (B) Pro-based accessibility probes in solution. Depicted are overlaid snapshots of every 1-ns during the last 50-ns of the simulation. Yellow represents the maleimide terminus, dark grey represents the spacer regions, and red represents the fluorescein terminus. (C) Summary of the root mean square deviation and radius of gyration for all systems (100 ns).

We sought to gain a more systematic description of the impact of WTA on accessibility to *S. aureus* PG by using a *tarO* deletion strain and tunicamycin-based WTA inhibition. Both modes of WTA disruption resulted in large increases in cellular labeling with the accessibility probes (**Figure 3.13**). For example, fluorescence levels in *S. aureus* (*tarO*) treated with the 36-atom long spacer, **Mal-peg₁₂-FI**, was higher than *S. aureus* (WT) treated with **Mal-FI**.

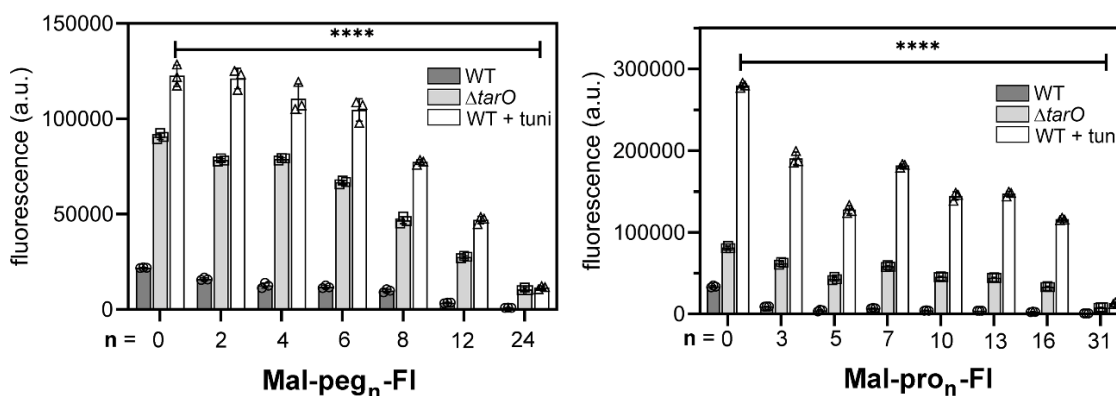


Figure 3.13 WT *S. aureus* (ATCC 25923) cells were incubated with 1 mM of D-cystine (dark bars), co-incubated with tunicamycin (tuni, 0.1 μ g/mL) and 1 mM of D-cystine (grey bars), or *S. aureus* ($\Delta tarO$) were incubated with 1 mM of D-cystine alone (white bars) overnight. Next, cells were reduced with DTT (5 mM), and incubated with 25 μ M of designated accessibility probes. Data are represented as mean \pm SD ($n = 3$).

Tunicamycin treatment yielded higher overall levels of cellular fluorescence in a concentration dependent manner (**Figure 3.14A**). There was minimal additive effect when $\Delta tarO$ cells were treated with tunicamycin (**Figure 3.14A**). The boost in cellular fluorescence was more pronounced with rigid spacers as demonstrated by the ratio of cellular fluorescence when treated with **Mal-pro₁₃-FI** and **Mal-FI**. In the absence of tunicamycin treatment, cellular fluorescence of **Mal-pro₁₃-FI** was

~6.5% relative to **Mal-FI** and this ratio jumped to ~40% upon tunicamycin treatment.

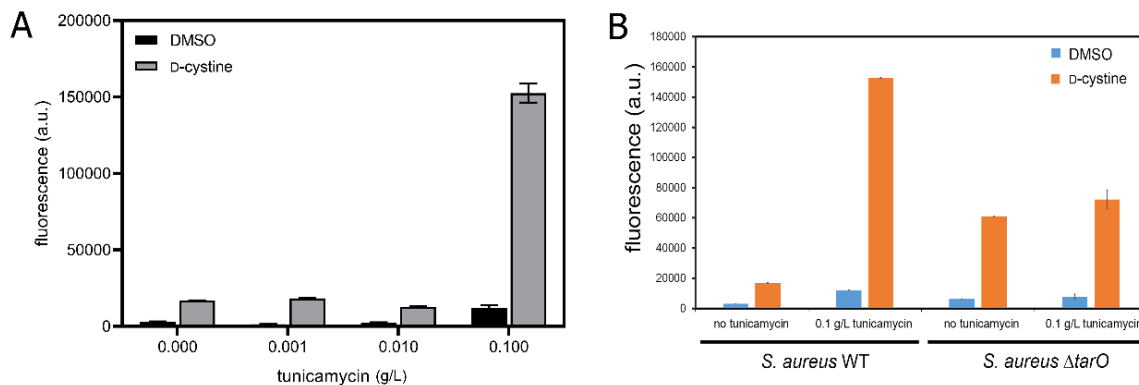


Figure 3.14 (A) Flow cytometry analysis of *S. aureus* (ATCC 25923) treated overnight with 1 mM of D-cystine or DMSO in the presence of given concentrations of tunicamycin. The next day cells were washed with PBS, reduced with DTT (5 mM), and incubated with 25 μ M of Mal-FI. (B) Flow cytometry analysis of *S. aureus* (ATCC 25923) and *S. aureus* ($\Delta tarO$) treated overnight with 1 mM of D-cystine or DMSO in the presence of absence of 0.1 μ g/L of tunicamycin. The next day cells were washed with PBS, reduced with DTT (5 mM), and incubated with 25 μ M of Mal-FI. Data are represented as mean \pm SD (n = 3).

Additionally, we also tested a series of maleimide-modified fluorophores in *S. aureus* (WT) and *S. aureus* (*tarO*) to evaluate the role of the fluorophore in the PG labeling (**Figure 3.15**). Our results showed that two other fluorophores (**AF488** and **AF647**) behaved similar to fluorescein in having a low labeling level in the absence of D-amino acid modification and an increase in the absence of WTA in comparison to WT when treated with D-cystine. Two other fluorophores (**BODIPY** and **Cy5**) resulted in considerable non-specific labeling.

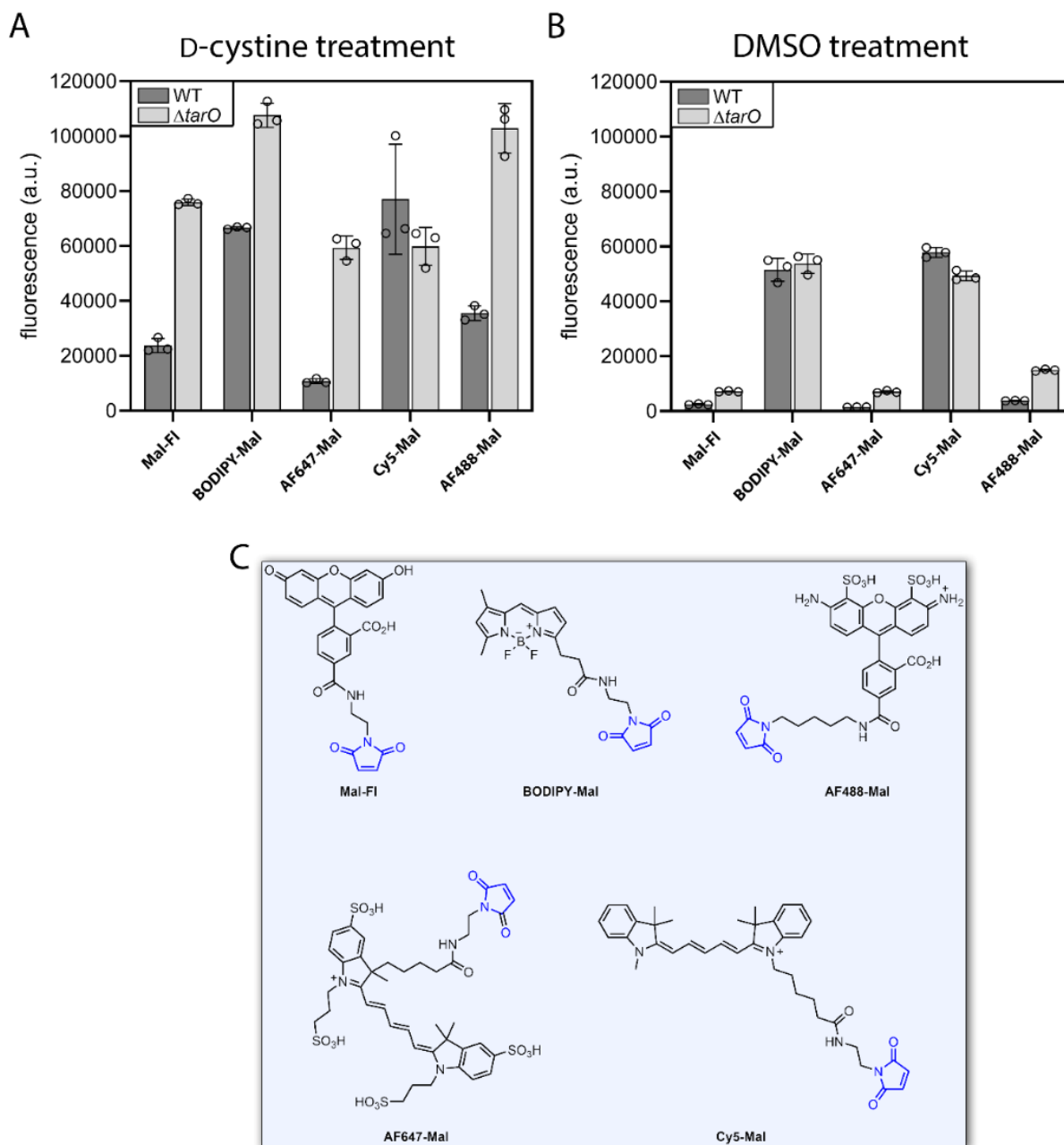


Figure 3.15 Flow cytometry analysis of *S. aureus* (ATCC 25923) and *S. aureus* ($\Delta tarO$) treated overnight with (A) 1 mM of D-cystine or (B) DMSO, reduced with DTT (5 mM), and incubated with designated accessibility probes. Data are represented as mean \pm SD ($n = 3$). (C) Chemical structures of the five fluorophores tested.

We next set out to test how robust the concept of this assay is by changing the reactive partners. Instead of thiol and maleimide, we assembled a panel of probes centered on an azide-modified D-lysine (**D-LysAz**) and DiBenzoCycloOctyne (DBCO) conjugated to a fluorescent handle (**Figure 3.16A**).⁵⁴⁻⁵⁵ This pair of reactive functional groups is bioorthogonal and readily forms a triazole covalent bond in the absence of metal catalysts. (**Figure 3.16B**)

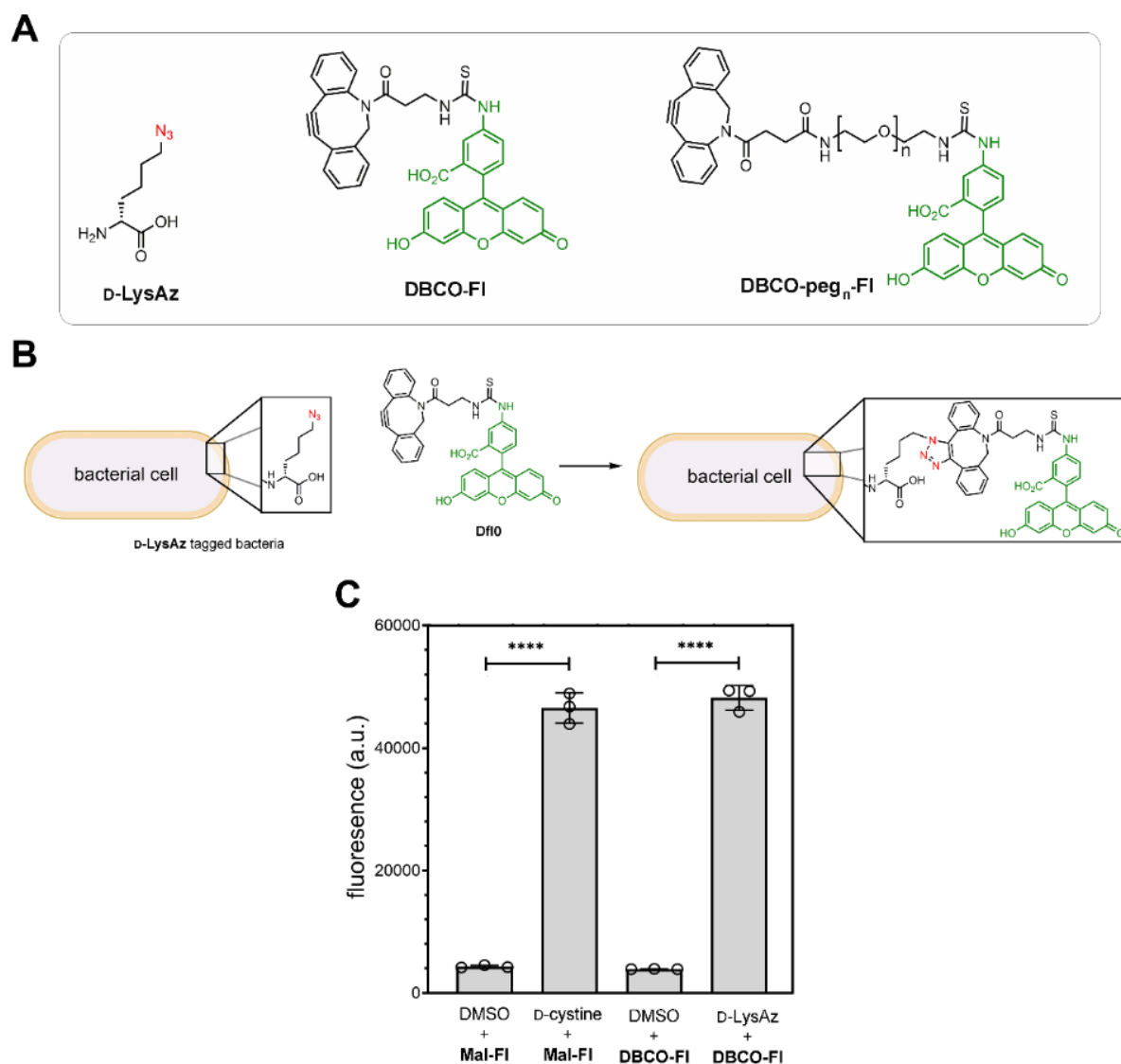


Figure 3.16 (A) Chemical structures of **D-LysAz**, **DBCO-FI**, and **DBCO-peg_n-FI**. (B) Schematic diagram of the PG labeling of live cells. (C) Flow cytometry analysis

of WT *S. aureus* (ATCC 25923) treated overnight with 1 mM of D-cystine or **D-LysAz** followed by a treatment with either 25 μ M of **Mal-FI** or **DBCO-FI**.

We found that *S. aureus* cells incubated with **D-LysAz** followed by treatment with **DBCO-FI** resulted in a ~12-fold increase in cellular fluorescence compared to cells not treated with the unnatural D-amino acid. Moreover, the fold increase in cellular fluorescence was very similar to the values observed using the D-cystine and **Mal-FI** pair. (**Figure 3.16C**) Cellular treatment with the enantiomer **L-LysAz** led to background fluorescence levels, another indication that fluorescence signals represent covalent modification of the PG scaffold (**Figure 3.17A**). In addition, mutanolysin analysis revealed a similar profile (**Figure 3.17B**) and confocal microscopy showed identical localization pattern (**Figure 3.17C**) to the thiol-maleimide pair.

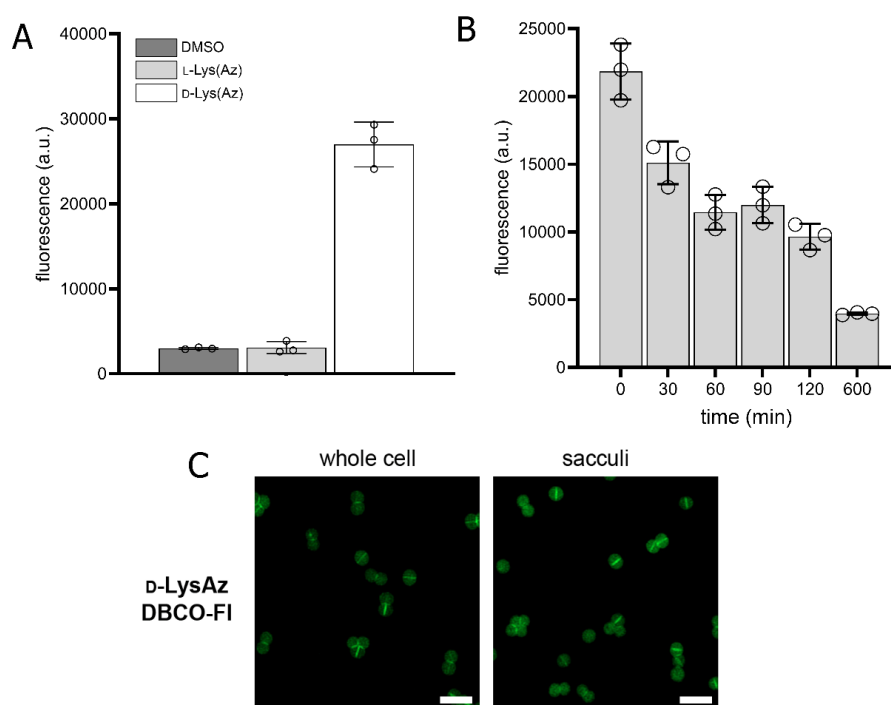


Figure 3.17 (A) Flow cytometry analysis of surface labeled *S. aureus* (ATCC 25923) treated overnight with 1 mM of **D-LysAz** or 1 mM of **L-LysAz** and incubated

with 25 μM of **DBCO-FI**. (B) Flow cytometry analysis of surface labeled *S. aureus* (ATCC 25923) treated overnight with 1 mM of **D-LysAz** and incubated with 25 μM of **DBCO-FI**. Cells were washed with PBS, and incubated with mutanolysin. Periodically, cells were fixed with formaldehyde and analyzed by flow cytometry. (C) Confocal microscopy analysis of surface labeled *S. aureus* (ATCC 25923) treated overnight with 1 mM of **D-LysAz** and incubated with 25 μM of **DBCO-FI**. Cells were washed with PBS, fixed with formaldehyde, and imaged. Data are represented as mean \pm SD ($n = 3$).

The effect of WTA on PG accessibility was evaluated for the bioorthogonal pair (**Figure 3.18**). Loss of WTA in the deletion strain resulted in a two-fold increase in cellular fluorescence across all spacer lengths. Co-incubation of cells with tunicamycin resulted in ~ 9 -fold increase in cellular fluorescence with the **DBCO-peg₃-FI** probe and a ~ 17 -fold increase with the longest **DBCO-peg₉-FI** probe. These results suggest that the assay platform is robust and the chemistry is not a factor in measuring access to the PG scaffold.

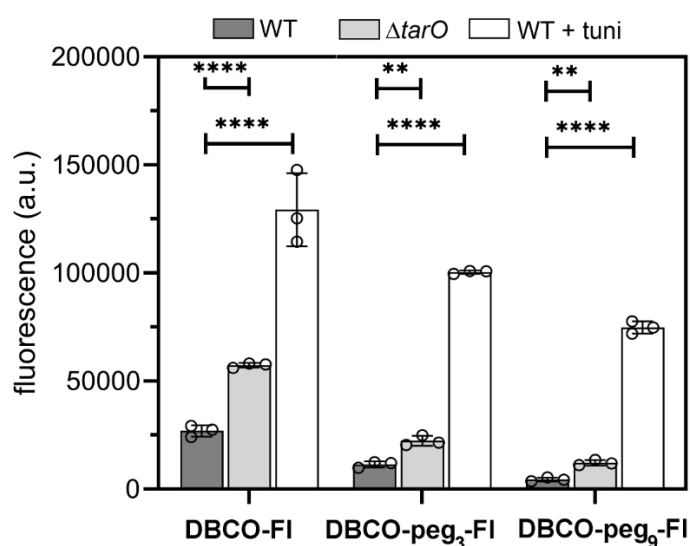


Figure 3.18 WT *S. aureus* (ATCC 25923) cells were incubated with 1 mM of **D-LysAz** alone (dark bars), co-incubated with tunicamycin (tuni, 0.1 $\mu\text{g}/\text{mL}$) and 1

mM of **D-LysAz** (grey bars), or *S. aureus* ($\Delta tarO$) were incubated with 1 mM of **D-LysAz** alone (white bars) overnight. Next, cells were treated with 25 μ M of designated accessibility probes. Data are represented as mean \pm SD ($n = 3$).

Next, we sought to evaluate the role of positively charged, branched polyethylenimine (BPEI) in potentiating β -lactam antibiotics against MRSA.⁵⁶⁻⁵⁷ Whereas tarO-null strain and tunicamycin pre-treatment results in cells lacking WTA, BPEI has been proposed to directly interact with WTA without inhibiting its biosynthesis. Binding of BPEI to WTA was suggested to result in the synergy of β -lactam antibiotics by causing delocalization of penicillin binding proteins. We reasoned that neutralization of WTA by BPEI could also alter accessibility of molecules to the PG scaffold. To test this, *S. aureus* cells were treated with BPEI and challenged with our probes (**Figure 3.19**). Our results reveal that BPEI improved the accessibility of smaller molecules to the PG, which likely plays a role in its synergistic activity with small molecule antibiotics. The increased accessibility appeared to be size dependent, as larger molecules did not permeate better when co-incubated with BPEI.

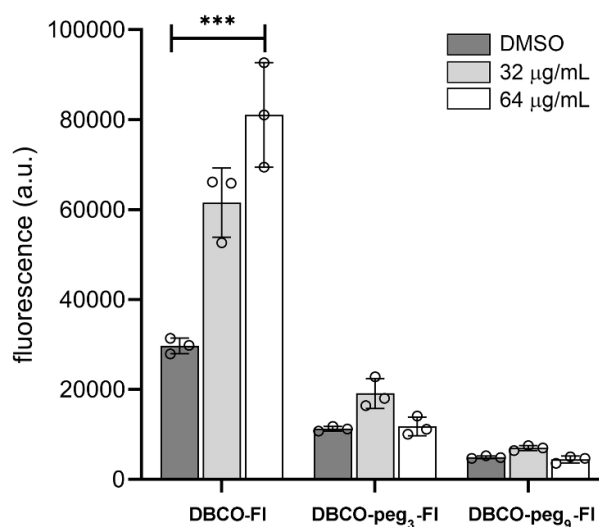


Figure 3.19 Flow cytometry analysis of WT *S. aureus* (ATCC 25923) treated overnight with 1 mM of **D-LysAz**, co-incubated with 0, 32, or 64 μ g/mL of BPEI at

stationary phase, followed by a treatment with 25 μM of designated probes. Data are represented as mean \pm SD ($n = 3$). P-values were determined by a two-tailed t-test (*denotes a p-value < 0.05 , ** < 0.01 , *** < 0.001 , ns = not significant).

We also set out to assess the effect of LTA on surface accessibility.⁵⁸⁻⁵⁹ Unlike WTA, LTA is anchored into the bacterial membrane *via* a glycolipid group. Although the roles of LTA have not been fully elucidated, LTA has been implicated in a diverse set of functions including interaction with host toll-like receptors,⁶⁰ organization of cell division machinery,⁶¹⁻⁶² and regulating biofilm formation.⁶³ The gene responsible for LTA biosynthesis, *ltaS*, is essential for growth of *S. aureus*⁶² but becomes conditionally essential when the chaperon ClpX is inactivated.⁶⁴ In our assay, we found that accessibility to the PG of cells lacking LTA was significantly increased (**Figure 3.20**). Deletion of *clpX* alone did not lead to an increase in the permeation of **DBCO-FI**, indicating that deletion of ClpX alone cannot account for the increased permeability.

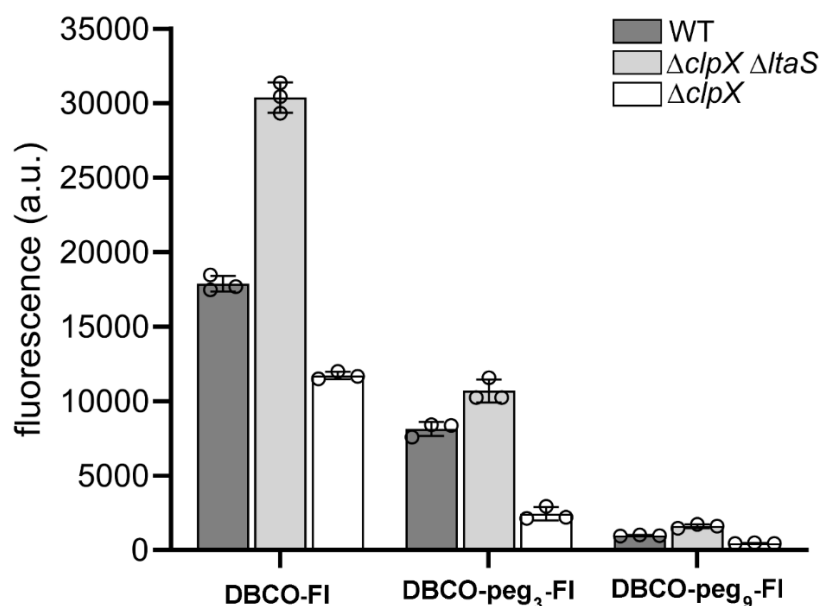


Figure 3.20 (B) Flow cytometry analysis of WT *S. aureus* (SA546), *S. aureus* ($\Delta clpX \Delta ltaS$), or *S. aureus* ($\Delta clpX$) treated overnight with 1 mM of **D-LysAz**,

followed by a treatment with 25 μM of designated probes. Data are represented as mean \pm SD ($n = 3$). P-values were determined by a two-tailed t-test (*denotes a p-value < 0.05 , ** < 0.01 , *** < 0.001 , ns = not significant).

We then investigated the role of LTA D-alanylation on surface accessibility using a small molecule inhibitor, amsacrine, that was previously described.⁵⁰ Introduction of a positively charged D-alanine within LTA results in the neutralization of the anionic teichoic acids. This modification has been shown to influence a number of biological functions including biofilm formation,⁶⁵⁻⁶⁶ sensitivity to antibiotics (e.g., antimicrobial peptides and daptomycin),^{58, 67-69} and recognition by human innate immune system.⁷⁰ However, its role in surface accessibility has not been evaluated. We found that treatment of *S. aureus* with amsacrine resulted in a modest increase in cellular fluorescence with **DBCO-peg₃-FI (Figure 3.21)**. Collectively, these results provide direct evidence that chemical or biochemical alterations to teichoic acids on the surface of bacteria can regulate the permeation of molecules. In turn, these results may reveal a new facet to the diverse ways that bacteria modulate access to essential components of the cell wall.

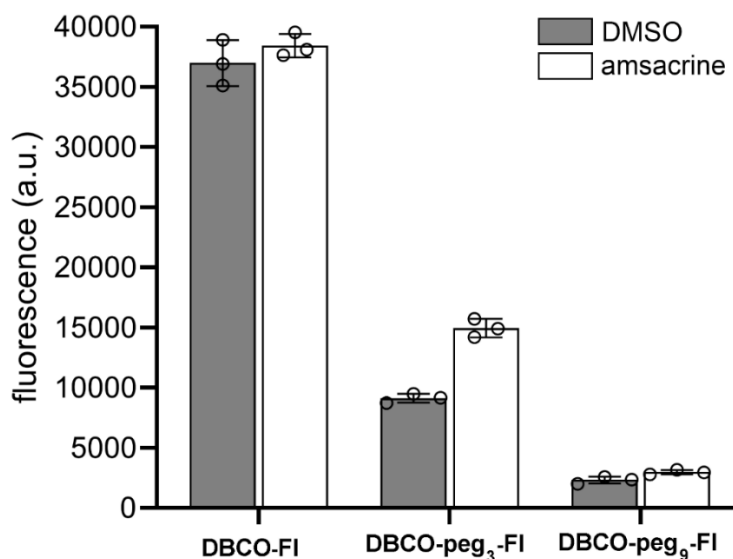


Figure 3.21 Flow cytometry analysis of WT *S. aureus* (ATCC 25923) treated overnight with 1 mM of **D-LysAz**, co-incubated with 0 or 10 $\mu\text{g/mL}$ of amsacrine

overnight, followed by a treatment with 25 μ M of designated probes. Data are represented as mean \pm SD ($n = 3$).

3.4 Conclusion

In conclusion, we have developed a novel fluorescence-based assay that reports on the accessibility of molecules to the surface of bacteria. Using *S. aureus* as a model organism, we showed that two distinct chemical handles (thiol and azide) were installed within the PG scaffold of *S. aureus*. Using two focused libraries in which each member contained a reactive handle and a fluorophore, we were able to show the effect of molecular size and flexibility on cellular accessibility. Molecules that are rigid, such as polyproline, displayed low access to the bacterial cell surface. Moreover, the presence of WTA (and to a less extent LTA), played a central role in regulating surface accessibility. Together, these results demonstrate that the assay outlined here is robust, potentially widely adaptable, and can play a significant role in elucidating dynamic features of bacterial cell surfaces.

3.5 Acknowledgements

Molecular dynamics studies, root mean square deviation, and radius of gyration calculations were provide by Seonghoon Kim and Wonpil Im. The computer resources for MD simulations were provided by the Center for Advanced Computation at Korea Institute for Advanced Study.

3.6 References

1. Sieradzki, K., Pinho, M. G., Tomasz, A. Inactivated pbp4 in highly glycopeptide-resistant laboratory mutants of *Staphylococcus aureus*. *J. Biol. Chem.* **1999**, *274*, 18942-18946.
2. Lienkamp, K., Kumar, K. N., Som, A., Nusslein, K., Tew, G. N. "Doubly selective" antimicrobial polymers: how do they differentiate between bacteria? *Chemistry.* **2009**, *15*, 11710-11714.
3. Mirouze, N., Ferret, C., Cornilleau, C., Carballido-Lopez, R. Antibiotic sensitivity reveals that wall teichoic acids mediate DNA binding during competence in *Bacillus subtilis*. *Nat. Commun.* **2018**, *9*, 5072.
4. Guariglia-Oropeza, V., Helmann, J. D. *Bacillus subtilis* sigma(V) confers lysozyme resistance by activation of two cell wall modification pathways, peptidoglycan O-acetylation and D-alanylation of teichoic acids. *J. Bacteriol.* **2011**, *193*, 6223-6232.
5. Gautam, S., Kim, T., Lester, E., Deep, D., Spiegel, D. A. Wall teichoic acids prevent antibody binding to epitopes within the cell wall of *Staphylococcus aureus* *ACS Chem. Biol.* **2016**, *11*, 25-30.
6. Egan, A. J. F., Errington, J., Vollmer, W. Regulation of peptidoglycan synthesis and remodelling *Nat. Rev. Microbiol.* **2020**, *18*, 446-460.
7. Weidenmaier, C., Peschel, A. Teichoic acids and related cell-wall glycopolymers in Gram-positive physiology and host interactions *Nat. Rev. Microbiol.* **2008**, *6*, 276-287.
8. Royet, J., Dziarski, R. Peptidoglycan recognition proteins: pleiotropic sensors and effectors of antimicrobial defences *Nat. Rev. Microbiol.* **2007**, *5*, 264-277.
9. Wolf, A. J., Underhill, D. M. Peptidoglycan recognition by the innate immune system *Nat. Rev. Immunol.* **2018**, *18*, 243-254.
10. Demchick, P., Koch, A. L. The permeability of the wall fabric of *Escherichia coli* and *Bacillus subtilis*. *J. Bacteriol.* **1996**, *178*, 768-773.
11. Sara, M., Sleytr, U. B. Molecular sieving through S layers of *Bacillus stearothermophilus* strains. *J. Bacteriol.* **1987**, *169*, 4092-4098.

12. Fura, J. M., Pidgeon, S. E., Birabaharan, M., Pires, M. M. Dipeptide-Based Metabolic Labeling of Bacterial Cells for Endogenous Antibody Recruitment. *ACS Infect. Dis.* **2016**, *2*, 302-309.
13. Caparros, M., Aran, V., de Pedro, M. A. Incorporation of S-[3H]methyl-D-cysteine into the peptidoglycan of ether-treated cells of Escherichia coli. *FEMS Microbiol. Lett.* **1992**, *72*, 139-146.
14. Cava, F., Lam, H., de Pedro, M. A., Waldor, M. K. Emerging knowledge of regulatory roles of D-amino acids in bacteria. *Cell Mol. Life Sci.* **2011**, *68*, 817-831.
15. de Pedro, M. A., Quintela, J. C., Holtje, J. V., Schwarz, H. Murein segregation in Escherichia coli. *J. Bacteriol.* **1997**, *179*, 2823-2834.
16. Schouten, J. A., Bagga, S., Lloyd, A. J., de Pascale, G., Dowson, C. G., Roper, D. I., Bugg, T. D. Fluorescent reagents for in vitro studies of lipid-linked steps of bacterial peptidoglycan biosynthesis: derivatives of UDPMurNAc-pentapeptide containing d-cysteine at position 4 or 5. *Mol. Biosyst.* **2006**, *2*, 484-491.
17. Siegrist, M. S., Swarts, B. M., Fox, D. M., Lim, S. A., Bertozzi, C. R. Illumination of growth, division and secretion by metabolic labeling of the bacterial cell surface. *FEMS Microbiol. Rev.* **2015**, *39*, 184-202.
18. Fura, J. M., Kearns, D., Pires, M. M. D-Amino Acid Probes for Penicillin Binding Protein-based Bacterial Surface Labeling. *J. Biol. Chem.* **2015**, *290*, 30540-30550.
19. Kuru, E., Hughes, H. V., Brown, P. J., Hall, E., Tekkam, S., Cava, F., de Pedro, M. A., Brun, Y. V., VanNieuwenhze, M. S. In Situ probing of newly synthesized peptidoglycan in live bacteria with fluorescent D-amino acids. *Angew. Chem. Int. Ed. Engl.* **2012**, *51*, 12519-12523.
20. Kuru, E., Tekkam, S., Hall, E., Brun, Y. V., Van Nieuwenhze, M. S. Synthesis of fluorescent D-amino acids and their use for probing peptidoglycan synthesis and bacterial growth in situ. *Nat. Protoc.* **2015**, *10*, 33-52.
21. Siegrist, M. S., Whiteside, S., Jewett, J. C., Aditham, A., Cava, F., Bertozzi, C. R. (D)-Amino acid chemical reporters reveal peptidoglycan dynamics of an intracellular pathogen. *ACS Chem. Biol.* **2013**, *8*, 500-505.

22. Lebar, M. D., May, J. M., Meeske, A. J., Leiman, S. A., Lupoli, T. J., Tsukamoto, H., Losick, R., Rudner, D. Z., Walker, S., Kahne, D. Reconstitution of peptidoglycan cross-linking leads to improved fluorescent probes of cell wall synthesis. *J. Am. Chem. Soc.* **2014**, *136*, 10874-10877.
23. Lupoli, T. J., Tsukamoto, H., Doud, E. H., Wang, T. S., Walker, S., Kahne, D. Transpeptidase-mediated incorporation of D-amino acids into bacterial peptidoglycan. *J. Am. Chem. Soc.* **2011**, *133*, 10748-10751.
24. Fura, J. M., Sabulski, M. J., Pires, M. M. D-amino acid mediated recruitment of endogenous antibodies to bacterial surfaces. *ACS Chem. Biol.* **2014**, *9*, 1480-1489.
25. Pidgeon, S. E., Pires, M. M. Cell Wall Remodeling of Staphylococcus aureus in Live Caenorhabditis elegans. *Bioconjug. Chem.* **2017**, *28*, 2310-2315.
26. Pidgeon, S. E., Fura, J. M., Leon, W., Birabaharan, M., Vezenov, D., Pires, M. M. Metabolic Profiling of Bacteria by Unnatural C-terminated D-Amino Acids. *Angew. Chem. Int. Ed. Engl.* **2015**, *54*, 6158-6162.
27. Apostolos, A. J., Pidgeon, S. E., Pires, M. M. Remodeling of Cross-bridges Controls Peptidoglycan Cross-linking Levels in Bacterial Cell Walls. *ACS Chem. Biol.* **2020**, *15*, 1261-1267.
28. Pidgeon, S. E., Apostolos, A. J., Nelson, J. M., Shaku, M., Rimal, B., Islam, M. N., Crick, D. C., Kim, S. J., Pavelka, M. S., Kana, B. D., Pires, M. M. L,D-Transpeptidase Specific Probe Reveals Spatial Activity of Peptidoglycan Cross-Linking. *ACS Chem. Biol.* **2019**, *14*, 2185-2196.
29. Liechti, G. W., Kuru, E., Hall, E., Kalinda, A., Brun, Y. V., VanNieuwenhze, M., Maurelli, A. T. A new metabolic cell-wall labelling method reveals peptidoglycan in Chlamydia trachomatis. *Nature.* **2014**, *506*, 507-510.
30. Sarkar, S., Libby, E. A., Pidgeon, S. E., Dworkin, J., Pires, M. M. In Vivo Probe of Lipid II-Interacting Proteins. *Angew. Chem. Int. Ed. Engl.* **2016**, *55*, 8401-8404.
31. Apostolos, A. J., Pidgeon, S. E., Pires, M. M. Remodeling of Crossbridges Controls Peptidoglycan Crosslinking Levels in Bacterial Cell Walls. *ACS Chem. Biol.* **2020**.

32. Gautam, S., Kim, T., Shoda, T., Sen, S., Deep, D., Luthra, R., Ferreira, M. T., Pinho, M. G., Spiegel, D. A. An Activity-Based Probe for Studying Crosslinking in Live Bacteria. *Angew. Chem. Int. Ed. Engl.* **2015**, *54*, 10492-10496.
33. Gautam, S., Kim, T., Spiegel, D. A. Chemical probes reveal an extraseptal mode of cross-linking in *Staphylococcus aureus*. *J. Am. Chem. Soc.* **2015**, *137*, 7441-7447.
34. Ngadjeua, F., Braud, E., Saidjalolov, S., Iannazzo, L., Schnappinger, D., Ehrt, S., Hugonnet, J. E., Mengin-Lecreulx, D., Patin, D., Etheve-Quelquejeu, M., Fonvielle, M., Arthur, M. Critical Impact of Peptidoglycan Precursor Amidation on the Activity of L,d-Transpeptidases from *Enterococcus faecium* and *Mycobacterium tuberculosis*. *Chemistry.* **2018**, *24*, 5743-5747.
35. Welsh, M. A., Taguchi, A., Schaefer, K., Van Tyne, D., Lebreton, F., Gilmore, M. S., Kahne, D., Walker, S. Identification of a Functionally Unique Family of Penicillin-Binding Proteins. *J. Am. Chem. Soc.* **2017**, *139*, 17727-17730.
36. Pereira, P. M., Filipe, S. R., Tomasz, A., Pinho, M. G. Fluorescence ratio imaging microscopy shows decreased access of vancomycin to cell wall synthetic sites in vancomycin-resistant *Staphylococcus aureus*. *Antimicrob. Agents. Chemother.* **2007**, *51*, 3627-3633.
37. De Jonge, B. L., Gage, D., Xu, N. The carboxyl terminus of peptidoglycan stem peptides is a determinant for methicillin resistance in *Staphylococcus aureus*. *Antimicrob. Agents. Chemother.* **2002**, *46*, 3151-3155.
38. Tom Dieck, S., Muller, A., Nehring, A., Hinz, F. I., Bartnik, I., Schuman, E. M., Dieterich, D. C. Metabolic labeling with noncanonical amino acids and visualization by chemoselective fluorescent tagging. *Curr. Protoc. Cell Biol.* **2012**, *Chapter 7*, Unit7 11.
39. tom Dieck, S., Kochen, L., Hanus, C., Heumuller, M., Bartnik, I., Nassim-Assir, B., Merk, K., Mosler, T., Garg, S., Bunse, S., Tirrell, D. A., Schuman, E. M. Direct visualization of newly synthesized target proteins in situ. *Nat. Methods.* **2015**, *12*, 411-414.
40. Dieterich, D. C., Hodas, J. J., Gouzer, G., Shadrin, I. Y., Ngo, J. T., Triller, A., Tirrell, D. A., Schuman, E. M. In situ visualization and dynamics of newly

- synthesized proteins in rat hippocampal neurons. *Nat. Neurosci.* **2010**, *13*, 897-905.
41. Apostolos, A. J., Ferraro, N. J., Dalesandro, B. E., Pires, M. M. SaccuFlow: A High-Throughput Analysis Platform to Investigate Bacterial Cell Wall Interactions. *ACS Infect Dis.* **2021**, *7*, 2483-2491.
 42. Atilano, M. L., Pereira, P. M., Yates, J., Reed, P., Veiga, H., Pinho, M. G., Filipe, S. R. Teichoic acids are temporal and spatial regulators of peptidoglycan cross-linking in *Staphylococcus aureus*. *Proc. Natl. Acad. Sci. U S A.* **2010**, *107*, 18991-18996.
 43. Xia, G., Kohler, T., Peschel, A. The wall teichoic acid and lipoteichoic acid polymers of *Staphylococcus aureus*. *Int. J. Med. Microbiol.* **2010**, *300*, 148-154.
 44. Swoboda, J. G., Campbell, J., Meredith, T. C., Walker, S. Wall teichoic acid function, biosynthesis, and inhibition. *Chembiochem.* **2010**, *11*, 35-45.
 45. Santa Maria, J. P., Jr., Sadaka, A., Moussa, S. H., Brown, S., Zhang, Y. J., Rubin, E. J., Gilmore, M. S., Walker, S. Compound-gene interaction mapping reveals distinct roles for *Staphylococcus aureus* teichoic acids. *Proc. Natl. Acad. Sci. U S A.* **2014**, *111*, 12510-12515.
 46. Eugster, M. R., Loessner, M. J. Wall teichoic acids restrict access of bacteriophage endolysin Ply118, Ply511, and PlyP40 cell wall binding domains to the *Listeria monocytogenes* peptidoglycan. *J. Bacteriol.* **2012**, *194*, 6498-6506.
 47. Bertsche, U., Weidenmaier, C., Kuehner, D., Yang, S. J., Baur, S., Wanner, S., Francois, P., Schrenzel, J., Yeaman, M. R., Bayer, A. S. Correlation of daptomycin resistance in a clinical *Staphylococcus aureus* strain with increased cell wall teichoic acid production and D-alanylation. *Antimicrob. Agents Chemother.* **2011**, *55*, 3922-3928.
 48. Vaz, F., Kounatidis, I., Covas, G., Parton, R. M., Harkiolaki, M., Davis, I., Filipe, S. R., Ligoxygakis, P. Accessibility to Peptidoglycan Is Important for the Recognition of Gram-Positive Bacteria in *Drosophila*. *Cell Rep.* **2019**, *27*, 2480-2492 e2486.

49. Matano, L. M., Morris, H. G., Hesser, A. R., Martin, S. E. S., Lee, W., Owens, T. W., Laney, E., Nakaminami, H., Hooper, D., Meredith, T. C., Walker, S. Antibiotic That Inhibits the ATPase Activity of an ATP-Binding Cassette Transporter by Binding to a Remote Extracellular Site. *J. Am. Chem. Soc.* **2017**, *139*, 10597-10600.
50. Pasquina, L., Santa Maria, J. P., Jr., McKay Wood, B., Moussa, S. H., Matano, L. M., Santiago, M., Martin, S. E., Lee, W., Meredith, T. C., Walker, S. A synthetic lethal approach for compound and target identification in *Staphylococcus aureus*. *Nat. Chem. Biol.* **2016**, *12*, 40-45.
51. Campbell, J., Singh, A. K., Santa Maria, J. P., Jr., Kim, Y., Brown, S., Swoboda, J. G., Mylonakis, E., Wilkinson, B. J., Walker, S. Synthetic lethal compound combinations reveal a fundamental connection between wall teichoic acid and peptidoglycan biosyntheses in *Staphylococcus aureus*. *ACS Chem. Biol.* **2011**, *6*, 106-116.
52. Suzuki, T., Campbell, J., Kim, Y., Swoboda, J. G., Mylonakis, E., Walker, S., Gilmore, M. S. Wall teichoic acid protects *Staphylococcus aureus* from inhibition by Congo red and other dyes. *J. Antimicrob. Chemother.* **2012**, *67*, 2143-2151.
53. Swoboda, J. G., Meredith, T. C., Campbell, J., Brown, S., Suzuki, T., Bollenbach, T., Malhowski, A. J., Kishony, R., Gilmore, M. S., Walker, S. Discovery of a small molecule that blocks wall teichoic acid biosynthesis in *Staphylococcus aureus*. *ACS Chem. Biol.* **2009**, *4*, 875-883.
54. Baskin, J. M., Prescher, J. A., Laughlin, S. T., Agard, N. J., Chang, P. V., Miller, I. A., Lo, A., Codelli, J. A., Bertozzi, C. R. Copper-free click chemistry for dynamic in vivo imaging. *Proc. Natl. Acad. Sci. U S A.* **2007**, *104*, 16793-16797.
55. Jewett, J. C., Sletten, E. M., Bertozzi, C. R. Rapid Cu-free click chemistry with readily synthesized biarylazacyclooctynones. *J. Am. Chem. Soc.* **2010**, *132*, 3688-3690.
56. Hill, M. A., Lam, A. K., Reed, P., Harney, M. C., Wilson, B. A., Moen, E. L., Wright, S. N., Pinho, M. G., Rice, C. V. BPEI-Induced Delocalization of PBP4 Potentiates beta-Lactams against MRSA. *Biochemistry.* **2019**, *58*, 3813-3822.

57. Foxley, M. A., Wright, S. N., Lam, A. K., Friedline, A. W., Strange, S. J., Xiao, M. T., Moen, E. L., Rice, C. V. Targeting Wall Teichoic Acid in Situ with Branched Polyethylenimine Potentiates beta-Lactam Efficacy against MRSA. *ACS Med. Chem. Lett.* **2017**, *8*, 1083-1088.
58. Brown, S., Xia, G., Luhachack, L. G., Campbell, J., Meredith, T. C., Chen, C., Winstel, V., Gekeler, C., Irazoqui, J. E., Peschel, A., Walker, S. Methicillin resistance in *Staphylococcus aureus* requires glycosylated wall teichoic acids. *Proc. Natl. Acad. Sci. U S A.* **2012**, *109*, 18909-18914.
59. Wood, B. M., Santa Maria, J. P., Jr., Matano, L. M., Vickery, C. R., Walker, S. A partial reconstitution implicates DltD in catalyzing lipoteichoic acid d-alanylation. *J. Biol. Chem.* **2018**, *293*, 17985-17996.
60. Schwandner, R., Dziarski, R., Wesche, H., Rothe, M., Kirschning, C. J. Peptidoglycan- and lipoteichoic acid-induced cell activation is mediated by toll-like receptor 2. *J. Biol. Chem.* **1999**, *274*, 17406-17409.
61. Oku, Y., Kurokawa, K., Matsuo, M., Yamada, S., Lee, B. L., Sekimizu, K. Pleiotropic roles of polyglycerolphosphate synthase of lipoteichoic acid in growth of *Staphylococcus aureus* cells. *J. Bacteriol.* **2009**, *191*, 141-151.
62. Grundling, A., Schneewind, O. Synthesis of glycerol phosphate lipoteichoic acid in *Staphylococcus aureus*. *Proc. Natl. Acad. Sci. U S A.* **2007**, *104*, 8478-8483.
63. Fedtke, I., Mader, D., Kohler, T., Moll, H., Nicholson, G., Biswas, R., Henseler, K., Gotz, F., Zahringer, U., Peschel, A. A *Staphylococcus aureus* ypfP mutant with strongly reduced lipoteichoic acid (LTA) content: LTA governs bacterial surface properties and autolysin activity. *Mol. Microbiol.* **2007**, *65*, 1078-1091.
64. Baek, K. T., Bowman, L., Millership, C., Dupont Sogaard, M., Kaeffer, V., Siljamaki, P., Savijoki, K., Varmanen, P., Nyman, T. A., Grundling, A., Frees, D. The Cell Wall Polymer Lipoteichoic Acid Becomes Nonessential in *Staphylococcus aureus* Cells Lacking the ClpX Chaperone. *mBio.* **2016**, *7*.
65. Fabretti, F., Theilacker, C., Baldassarri, L., Kaczynski, Z., Kropec, A., Holst, O., Huebner, J. Alanine esters of enterococcal lipoteichoic acid play a role in biofilm formation and resistance to antimicrobial peptides. *Infect. Immun.* **2006**, *74*, 4164-4171.

66. Wobser, D., Ali, L., Grohmann, E., Huebner, J., Sakinc, T. A novel role for D-alanylation of lipoteichoic acid of enterococcus faecalis in urinary tract infection. *PLoS One*. **2014**, *9*, e107827.
67. Kristian, S. A., Datta, V., Weidenmaier, C., Kansal, R., Fedtke, I., Peschel, A., Gallo, R. L., Nizet, V. D-alanylation of teichoic acids promotes group a streptococcus antimicrobial peptide resistance, neutrophil survival, and epithelial cell invasion. *J. Bacteriol.* **2005**, *187*, 6719-6725.
68. Peschel, A., Otto, M., Jack, R. W., Kalbacher, H., Jung, G., Gotz, F. Inactivation of the dlt operon in Staphylococcus aureus confers sensitivity to defensins, protegrins, and other antimicrobial peptides. *J. Biol. Chem.* **1999**, *274*, 8405-8410.
69. Bayer, A. S., Schneider, T., Sahl, H. G. Mechanisms of daptomycin resistance in Staphylococcus aureus: role of the cell membrane and cell wall. *Ann. N Y Acad. Sci.* **2013**, *1277*, 139-158.
70. Tabuchi, Y., Shiratsuchi, A., Kurokawa, K., Gong, J. H., Sekimizu, K., Lee, B. L., Nakanishi, Y. Inhibitory role for D-alanylation of wall teichoic acid in activation of insect Toll pathway by peptidoglycan of Staphylococcus aureus. *J. Immunol.* **2010**, *185*, 2424-2431.

3.7 Materials and Methods

Materials. All peptide related reagents (resin, coupling reagent, deprotection reagent, amino acids, and cleavage reagents) were purchased from ChemImpex or Broad Pharm. Bacterial strains *S. aureus* ATCC 25923, USA300, and *S. aureus* SCO1 were grown in lysogeny broth (LB). *S. aureus* $\Delta tarO$ was grown in LB supplemented with 150 $\mu\text{g}/\text{mL}$ spectinomycin. *S. aureus* SA546, $\Delta clpX$, and $\Delta clpX\Delta taS$ were grown in tryptic soy broth (TSB).

Flow Cytometry Analysis of *S. aureus* Treated with Thiol Analogue Panel. LB media containing 1 mM of each respective thiol analogue or dimethyl sulfoxide (DMSO) were prepared. *S. aureus* ATCC 25923 cells from an overnight culture were added to the medium (1:100 dilution) and allowed to grow overnight at 37 °C with shaking at 250 rpm. The cells were harvested at 4000 rpm and treated with 5 mM dithiothreitol (DTT) at the original culture volume for 5 min, to reverse any thiol oxidation that may have occurred. The cells were harvested at 4000 rpm and washed twice at the original culture volume with 1 \times phosphate-buffered saline (PBS) to remove residual DTT. The cells were then treated with 25 μM FAM maleimide, 6-isomer (**Mal-FI**) for 30 min at 37 °C, and protected from light. The samples were subsequently harvested at 4000 rpm and washed three times with PBS followed by fixation with 2% formaldehyde in 1 \times PBS for 30 min. The cells were washed once more to remove formaldehyde and then analyzed using the Attune NxT flow cytometer equipped with a 488 nm laser and a 525/40 nm bandpass filter. The data were analyzed using the Attune NXT Software.

Flow Cytometry Analysis of *S. aureus* Treated with Cystine Enantiomers. LB media containing either 1 mM D-cystine, L-cystine, or DMSO were prepared. *S. aureus* ATCC 25923 cells from an overnight culture were added to the medium (1:100 dilution) and allowed to grow overnight at 37 °C with shaking at 250 rpm. The cells were harvested at 4000 rpm and treated with 5 mM DTT at the original culture volume for 5 min, to reverse any thiol oxidation that may have occurred. The cells were harvested at 4000 rpm and washed twice at the original culture volume with 1 \times PBS to remove residual DTT. The cells were then treated with 25

μM **Mal-FI** for 30 min at 37 °C and protected from light. The samples were subsequently harvested at 4000 rpm and washed three times with PBS followed by fixation with 2% formaldehyde in 1x PBS for 30 min. The cells were washed once more to remove formaldehyde and then analyzed using the Attune NxT flow cytometer as described above.

Flow cytometry analysis of *S. aureus* treated with a Mal-FI titration. LB media containing 1mM of D-cystine was prepared. *S. aureus* ATCC 25923 cells from an overnight culture were added to the medium (1:100 dilution) and allowed to grow overnight at 37°C with shaking at 250 rpm. The cells were harvested at 4000 rpm and treated with 5 mM DTT at the original culture volume for 5 minutes, to reverse any thiol oxidation that may have occurred. The cells were harvested at 4000 rpm and washed twice at the original culture volume with 1X PBS to remove residual DTT. The cells were then treated with either 5, 10, 25, 50, or 100 μM **Mal-FI** for 30 minutes at 37°C and protected from light. The samples were subsequently harvested at 4000 rpm and washed three times with PBS followed by fixation with 2% formaldehyde in 1X PBS for 30 minutes. The cells were washed once more to remove formaldehyde and then analyzed using the Attune NxT flow cytometer as described above.

Enzymatic degradation of Whole Cell Samples. LB media containing either 1mM of D-cystine or **D-LysAz** were prepared. *S. aureus* ATCC 25923 cells were added to the LB medium (1:100) and allowed to grow overnight at 37°C with shaking at 250 rpm. The D-cystine treated cells were harvested at 4000 rpm and treated with 5 mM DTT, to reverse any thiol oxidation that may have occurred, at the original culture volume for 5 minutes. The cells were harvested at 4000 rpm and washed twice at the original culture volume with 1X PBS to remove residual DTT. The cells were then treated with 25 μM **Mal-FI** for 30 minutes at 37°C and protected from light. The samples were subsequently harvested at 4000 rpm and washed three times with 1X PBS. The **D-LysAz** treated cells were harvested at 4000 rpm and washed three times at the original culture volume with 1X PBS. The cells were then treated with 25 μM **DBCO-FI** for 30 minutes at 37°C and protected

from light. The samples were subsequently harvested at 4000 rpm and washed three times with 1X PBS. A zero time point sample was taken from both the **Mal-FI** and **DBCO-FI** treated cells before being subjected to treatment with either 50 µg/mL mutanolysin in 1X PBS or 500 µg/mL proteinase K in 50 mM TRIS HCl with 5 mM calcium chloride at pH 8. A portion of the cells were taken at 30, 60, 90, 120, and 600 minutes. At each time point, the collected bacteria resuspended in a final solution of 1X PBS containing 2% formaldehyde to quench the mutanolysin/proteinase K reaction. The cells were analyzed using the Attune NxT flow cytometer as described above.

BONCAT. LB media containing 1mM of L-azidohomoalanine was prepared. *S. aureus* ATCC 25923 cells were added to the LB medium (1:100) and allowed to grow overnight at 37°C with shaking at 250 rpm. The cells were harvested at 4000 rpm and washed three times with 1X PBS. The cells were then treated with 25 µM **DBCO-FI** for 30 minutes at 37°C and protected from light. The samples were subsequently harvested at 4000 rpm and washed three times with 1X PBS. A zero time point sample was taken before being subjected to treatment with either 50 µg/mL mutanolysin in 1X PBS or 500 µg/mL proteinase K in 50 mM TRIS HCl with 5 mM calcium chloride at pH 8. A portion of the cells were taken at 30, 60, 90, 120, and 150 minutes. At each time point, the sample was resuspended in a final solution of 1X PBS containing 2% formaldehyde to quench the mutanolysin/proteinase K reaction. The cells were analyzed using the Attune NxT flow cytometer as described above.

Peptidoglycan Isolation and Confocal Microscopy Analysis of *S. aureus*. LB media (25 mL) containing either 1 mM D-cystine, Nε -azido-D-lysine hydrochloride (**D-LysAz**), 100 µM **D-LysFI**, or DMSO were prepared. *S. aureus* ATCC 25923 cells were added to the LB medium (1:100) and allowed to grow overnight at 37 °C with shaking at 250 rpm. The D-cystine-treated cells were harvested at 4000 rpm and treated with 5 mM DTT, to reverse any thiol oxidation that may have occurred, at the original culture volume for 5 min. The cells were harvested at 4000 rpm and washed twice at the original culture volume with 1x PBS to remove

residual DTT. The cells were then treated with 25 μ M Mal-FI for 30 min at 37 °C and protected from light. The samples were subsequently harvested at 4000 rpm and washed three times with 1 \times PBS. The resulting pellet was resuspended in 1 \times PBS. Whole-cell samples were taken, subjected to fixation with 2% formaldehyde in 1 \times PBS, and analyzed via confocal microscopy. The remaining sample underwent the peptidoglycan isolation protocol. The **D-LysAz** treated cells were harvested at 4000 rpm and washed three times at the original culture volume with 1 \times PBS. The cells were then treated with 25 μ M fluorescein-DBCO (**DBCO-FI**) for 30 min at 37 °C and protected from light. The samples were subsequently harvested at 4000 rpm and washed three times with 1 \times PBS. The resulting pellet was resuspended in 1 \times PBS. Whole-cell samples were taken, subjected to fixation with 2% formaldehyde in 1 \times PBS, and analyzed via confocal microscopy. The remaining sample underwent the peptidoglycan isolation protocol. The **D-LysFI**- and DMSO-treated cells were harvested at 4000 rpm and washed three times at the original culture volume with 1 \times PBS. Whole-cell samples were taken, subjected to fixation with 2% formaldehyde in 1 \times PBS, and analyzed via confocal microscopy. The remaining sample underwent the peptidoglycan isolation protocol. To isolate the peptidoglycan, first, all four cell suspensions (D-cystine-, **D-LysAz**-, **D-LysFI**-, and DMSO-treated cells) were boiled for 25 min to induce cell death. The cells were subsequently harvested at 14000g. The samples were then treated with 15 mL of 5% sodium dodecyl sulfate (SDS) in deionized water and boiled for 25 min. The samples were then sedimented at 14000g and subjected to treatment with 15 mL of 4% SDS with boiling for 25 min. The samples were washed six times with deionized water to remove residual SDS. The resulting pellets were resuspended in 6 mL of 20 mM Tris HCl at pH 8 and treated with 133 μ g/mL DNase in 20 mM TRIS, pH 8, at 37 °C with shaking at 115 rpm for 24 h. After 24 h, 133 μ g/mL trypsin in 20 mM TRIS, pH 8, was added to each sample and that was incubated for 24 h at 37 °C with shaking at 115 rpm. The samples were then sedimented at 14000g after the 24 h time period. Both the whole-cell and isolated peptidoglycan samples were analyzed using the Zeiss 980 Airyscan Imaging System provided by the W. M. Keck Center for Cellular Imaging.

Enzymatic degradation of sacculi samples. LB media containing 1mM of D-cystine was prepared. *S. aureus* ATCC 25923 cells were added to the LB medium (1:100) and allowed to grow overnight at 37°C with shaking at 250 rpm. The D-cystine treated cells were harvested at 4000 rpm and treated with 5 mM DTT, to reverse any thiol oxidation that may have occurred, at the original culture volume for 5 minutes. The cells were harvested at 4000 rpm and washed twice at the original culture volume with 1X PBS to remove residual DTT. The cells were then treated with 25 µM **Mal-FI** for 30 minutes at 37°C and protected from light. The samples were subsequently harvested at 4000 rpm and washed three times with 1X PBS. The cells were then subjected to the peptidoglycan isolation described above. A zero time point sample of the sacculi was taken before being subjecting the sacculi to treatment with either 50 µg/mL mutanolysin in 1X PBS or 500 µg/mL proteinase K in 50 mM TRIS HCl with 5 mM calcium chloride at pH 8. A portion of the cells were taken at 30, 60, 90, 120, and 150 minutes. At each time point, the sample was resuspended in a final solution of 1X PBS containing 2% formaldehyde to quench the mutanolysin/proteinase K reaction. The cells were analyzed using the Attune NxT flow cytometer as described above.

Flow Cytometry Analysis of *S. aureus* Strains Treated with Mal-peg_n-FI and Mal-pro_n-FI Libraries. LB media containing 1 mM D-cystine were prepared. *S. aureus* ATCC 25923, *S. aureus* ATCC 25923 supplemented with 0.1 µg/mL tunicamycin, *S. aureus* $\Delta tarO$ supplemented with 150 µg/mL spectinomycin, USA300, or *S. aureus* SCO1 cells from overnight cultures were added to the medium (1:100 dilution) and allowed to grow overnight at 37 °C with shaking at 250 rpm. The cells were harvested at 4000 rpm and treated with 5 mM DTT at the original culture volume for 5 min, to reverse any thiol oxidation that may have occurred. The cells were harvested at 4000 rpm and washed twice at the original culture volume with 1x PBS to remove residual DTT. Each strain was then treated with both libraries, **Mal-peg_n-FI** and **Mal-pro_n-FI**, in parallel. All library members were used at a 25 µM concentration for 30 min at 37 °C and protected from light. The samples were subsequently harvested at 4000 rpm and washed three times with 1x PBS followed by fixation with 2% formaldehyde in 1x PBS for 30 min. The

cells were washed once more to remove formaldehyde and then analyzed using the Attune NxT flow cytometer as described above.

Tunicamycin scan. LB media containing 1mM of D-cystine were prepared. *S. aureus* ATCC 25923, *S. aureus* ATCC 25923 supplemented with 0.001, 0.01, or 0.1 $\mu\text{g}/\text{mL}$ tunicamycin, *S. aureus* ΔtarO supplemented with 150 $\mu\text{g}/\text{mL}$ spectinomycin, or *S. aureus* ΔtarO supplemented with 150 $\mu\text{g}/\text{mL}$ spectinomycin and 0.1 $\mu\text{g}/\text{mL}$ tunicamycin from overnight cultures were added to the medium (1:100 dilution) and allowed to grow overnight at 37°C with shaking at 250 rpm. The cells were harvested at 4000 rpm and treated with 5 mM DTT at the original culture volume for 5 minutes, to reverse any thiol oxidation that may have occurred. The cells were harvested at 4000 rpm and washed twice at the original culture volume with 1X PBS to remove residual DTT. The cells were then treated with 25 μM **Mal-FI** for 30 minutes at 37°C and protected from light. The samples were subsequently harvested at 4000 rpm and washed three times with 1X PBS followed by fixation with 2% formaldehyde in 1X PBS for 30 minutes. The cells were washed once more to remove formaldehyde and then analyzed using the Attune NxT flow cytometer as described above.

Flow cytometry analysis of *S. aureus* treated with a series of maleimide-modified fluorophores. LB media containing 1mM of D-cystine were prepared. *S. aureus* ATCC 25923 or *S. aureus* ΔtarO supplemented with 150 $\mu\text{g}/\text{mL}$ spectinomycin from overnight cultures were added to the medium (1:100 dilution) and allowed to grow overnight at 37°C with shaking at 250 rpm. The cells were harvested at 4000 rpm and treated with 5 mM DTT at the original culture volume for 5 minutes, to reverse any thiol oxidation that may have occurred. The cells were harvested at 4000 rpm and washed twice at the original culture volume with 1X PBS to remove residual DTT. The cells were then treated with 25 μM of each of the listed maleimide-modified fluorophores for 30 minutes at 37°C and protected from light. The samples were subsequently harvested at 4000 rpm and washed three times with 1X PBS followed by fixation with 2% formaldehyde in 1X PBS for

30 minutes. The cells were washed once more to remove formaldehyde and then analyzed using the Attune NxT flow cytometer as described above.

Chemistry comparison. LB media containing either 1mM of D-cystine or **D-LysAz** were prepared. *S. aureus* ATCC 25923 cells were added to the LB medium (1:100) and allowed to grow overnight at 37°C with shaking at 250 rpm. The D-cystine treated cells were harvested at 4000 rpm and treated with 5 mM DTT, to reverse any thiol oxidation that may have occurred, at the original culture volume for 5 minutes. The cells were harvested at 4000 rpm and washed twice at the original culture volume with 1X PBS to remove residual DTT. The cells were then treated with 25 µM **Mal-FI** for 30 minutes at 37°C and protected from light. The samples were subsequently harvested at 4000 rpm and washed three times with 1X PBS followed by fixation with 2% formaldehyde in 1X PBS for 30 minutes. The cells were washed once more to remove formaldehyde and then analyzed using the Attune NxT flow cytometer as described above. Concurrently the **D-LysAz** treated cells were harvested at 4000 rpm and washed three times at the original culture volume with 1X PBS. The cells were then treated with 25 µM **DBCO-FI** for 30 minutes at 37°C and protected from light. The samples were subsequently harvested at 4000 rpm and washed three times with 1X PBS followed by fixation with 2% formaldehyde in 1X PBS for 30 minutes. The cells were washed once more to remove formaldehyde and then analyzed using the Attune NxT flow cytometer as described above.

Flow cytometry analysis of *S. aureus* treated with azide enantiomers. LB media containing either 1mM of **D-LysAz**, N^ε-azido-L-lysine hydrochloride (**L-LysAz**), or DMSO were prepared. *S. aureus* ATCC 25923 cells were added to the LB medium (1:100) and allowed to grow overnight at 37°C with shaking at 250 rpm. The cells were harvested at 4000 rpm and washed three times at the original culture volume with 1X PBS. The cells were then treated with 25 µM **DBCO-FI** for 30 minutes at 37°C and protected from light. The samples were subsequently harvested at 4000 rpm and washed three times with 1X PBS followed by fixation with 2% formaldehyde in 1X PBS for 30 minutes. The cells were washed once

more to remove formaldehyde and then analyzed using the Attune NxT flow cytometer as described above.

Flow Cytometry Analysis of *S. aureus* Strains Lacking Wall Teichoic Acids Treated with the DBCO-peg_n-FI Library. LB media containing 1 mM **D-LysAz** were prepared. *S. aureus* ATCC 25923 cells supplemented with 0.1 µg/mL tunicamycin, *S. aureus* $\Delta tarO$ cells supplemented with 150 µg/mL spectinomycin, or *S. aureus* ATCC 25923 cells from overnight cultures were added to the medium (1:100 dilution) and allowed to grow overnight at 37 °C with shaking at 250 rpm. The cells were harvested at 4000 rpm and washed three times at the original culture volume with 1× PBS. Each strain was then treated with the **DBCO-peg_n-FI** library. All library members were used at a 25 µM concentration for 30 min at 37 °C and protected from light. The samples were subsequently harvested at 4000 rpm and washed three times with 1× PBS followed by fixation with 2% formaldehyde in 1× PBS for 30 min. The cells were washed once more to remove formaldehyde and then analyzed using the Attune NxT flow cytometer as described above.

Flow Cytometry Analysis of *S. aureus* Strains Treated with the DBCO-peg_n-FI Library after Surface Neutralization. LB media containing 1 mM **D-LysAz** were prepared. *S. aureus* ATCC 25923 cells from an overnight culture were added to the medium (1:100 dilution) and allowed to grow overnight at 37 °C with shaking at 250 rpm. Upon reaching stationary phase, the cells were harvested at 4000 rpm and washed three times at the original culture volume with 1× PBS. The cells were then resuspended in 1× PBS that contained DMSO, 32 µg/mL branched polyethylenimine (BPEI), or 64 µg/mL BPEI. That was allowed to incubate at 37 °C for 30 min with shaking at 250 rpm. Subsequently, the cells were harvested at 4000 rpm and washed three times with 1× PBS before treatment with the **DBCO-peg_n-FI** library. All library members were used at a 25 µM concentration for 30 min at 37 °C and protected from light. The samples were then harvested at 4000 rpm and washed three times with 1× PBS followed by fixation with 2% formaldehyde in

1× PBS for 30 min. The cells were washed once more to remove formaldehyde and then analyzed using the Attune NxT flow cytometer as described above.

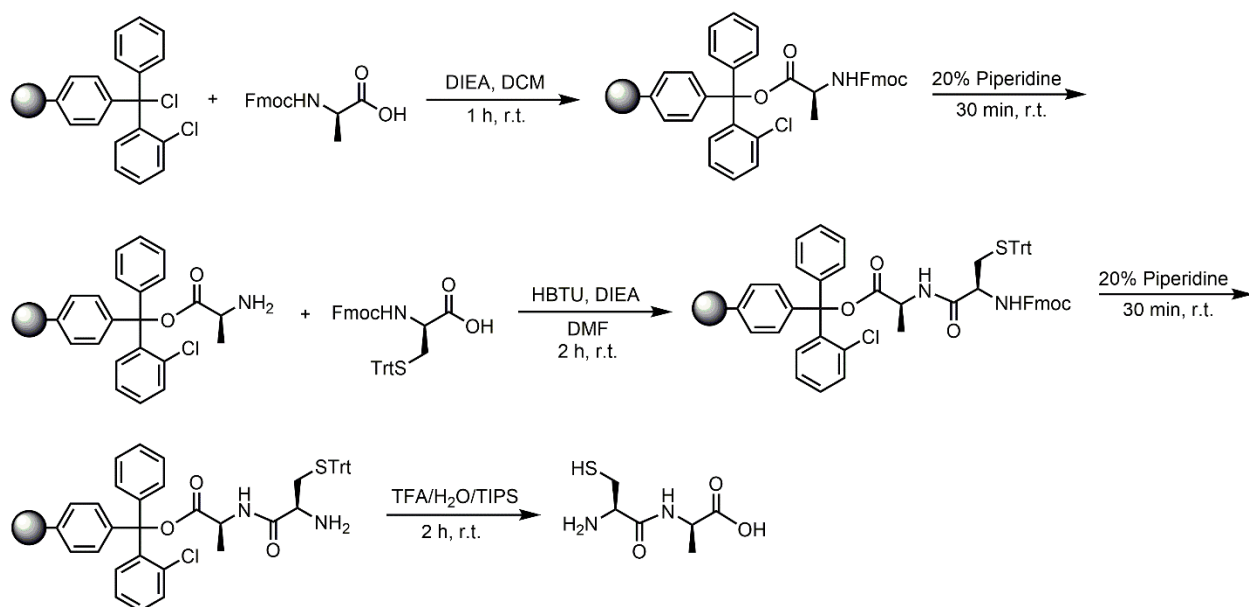
Flow Cytometry Analysis of *S. aureus* Strains Treated with the DBCO-peg_n-FI Library. TSB media containing 1 mM **D-LysAz** were prepared. *S. aureus* SA546, ΔclpX, or ΔclpXΔltaS cells from overnight cultures were added to the medium (1:100 dilution) and allowed to grow overnight at 37 °C with shaking at 250 rpm. The cells were harvested at 4000 rpm and washed three times at the original culture volume with 1× PBS. Each strain was then treated with the **DBCO-peg_n-FI** library. All library members were used at a 25 μM concentration for 30 min at 37 °C and protected from light. The samples were subsequently harvested at 4000 rpm and washed three times with 1× PBS followed by fixation with 2% formaldehyde in 1× PBS for 30 min. The cells were washed once more to remove formaldehyde and then analyzed using the Attune NxT flow cytometer as described above.

Flow Cytometry Analysis of *S. aureus* Strains Treated with the DBCO-peg_n-FI Library after Inhibition of D-Alanylation. LB media containing 1 mM **D-LysAz** were prepared. *S. aureus* ATCC 25923 cells supplemented with 10 μg/mL amsacrine or *S. aureus* ATCC 25923 cells from overnight cultures were added to the medium (1:100 dilution) and allowed to grow overnight at 37 °C with shaking at 250 rpm. The cells were harvested at 4000 rpm and washed three times at the original culture volume with 1× PBS. Each strain was then treated with the **DBCO-peg_n-FI** library. All library members were used at a 25 μM concentration for 30 min at 37 °C and protected from light. The samples were subsequently harvested at 4000 rpm and washed three times with 1× PBS followed by fixation with 2% formaldehyde in 1× PBS for 30 min. The cells were washed once more to remove formaldehyde and then analyzed using the Attune NxT flow cytometer as described above.

Computational Methods. Different polymerized states of **Mal-pro_n-FI** (n: 3, 5, 7, 10, 13, 16, 31) and **Mal-peg_n-FI** (n: 2, 4, 6, 8, 12, 24) were modeled and simulated to check the influences of the length and type of the spacer groups on the

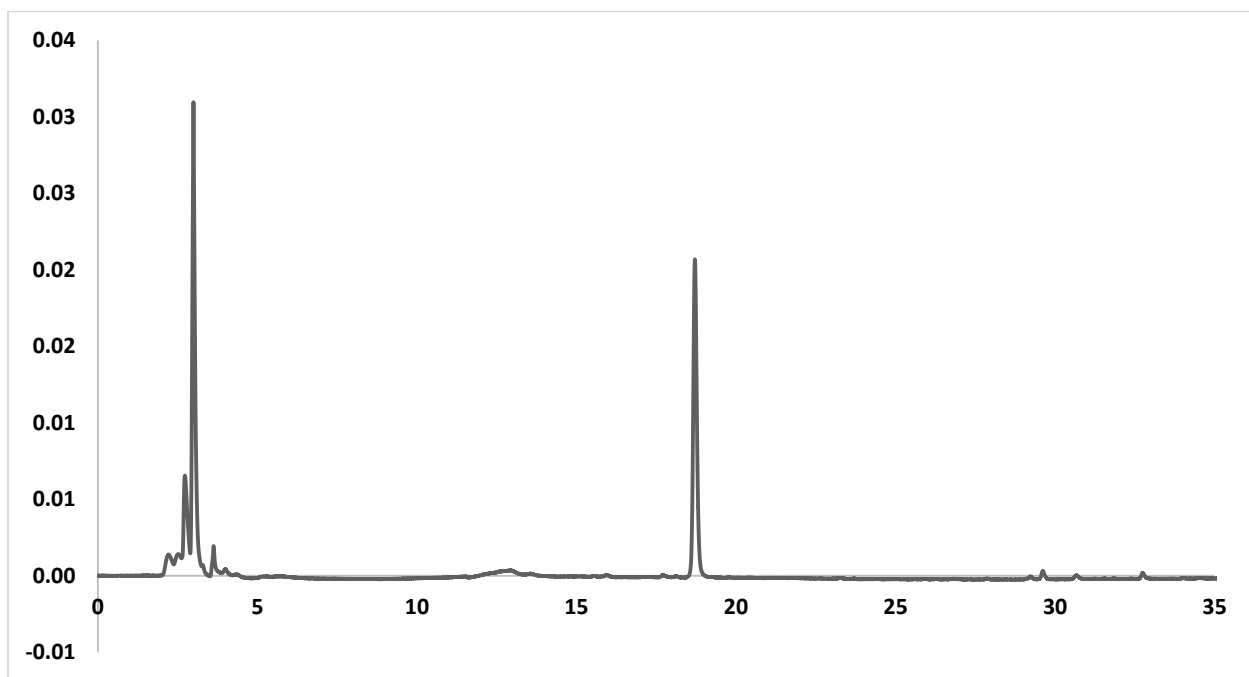
conformational variations of the probes. The force field parameters for maleimide (**Mal**) and fluorescein (**Fl**) groups and patches among moieties were generated and assembled by analogy from the CHARMM36 force field.¹⁻³ Each probe was solvated by an appropriate size of TIP3P⁴ box with neutralizing ions (Na⁺) following the CHARMM-GUI *Solution Builder* protocol.⁵ All simulations were performed using OpenMM-7.4.1 simulation package⁶ and the equilibration and production inputs generated by CHARMM-GUI *Input Generator*.⁷ For each system, after short minimization and 125-ps NVT (constant particle number, volume, and temperature) equilibration run, a 100-ns NPT (constant particle number, pressure, and temperature) production simulation was performed at 303.15 K and 1 bar. We performed two independent simulations for each system with different initial velocities to improve sampling and check the convergence.

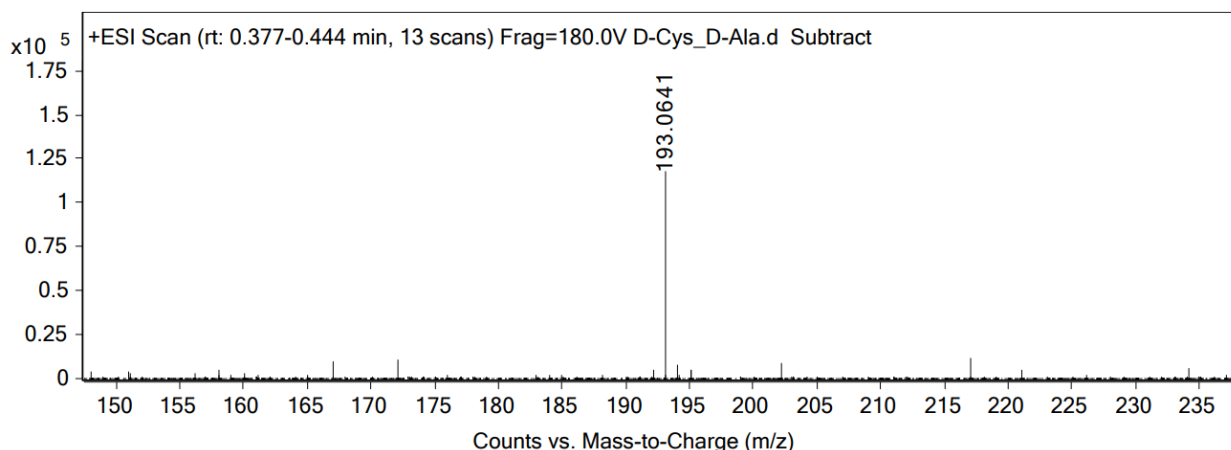
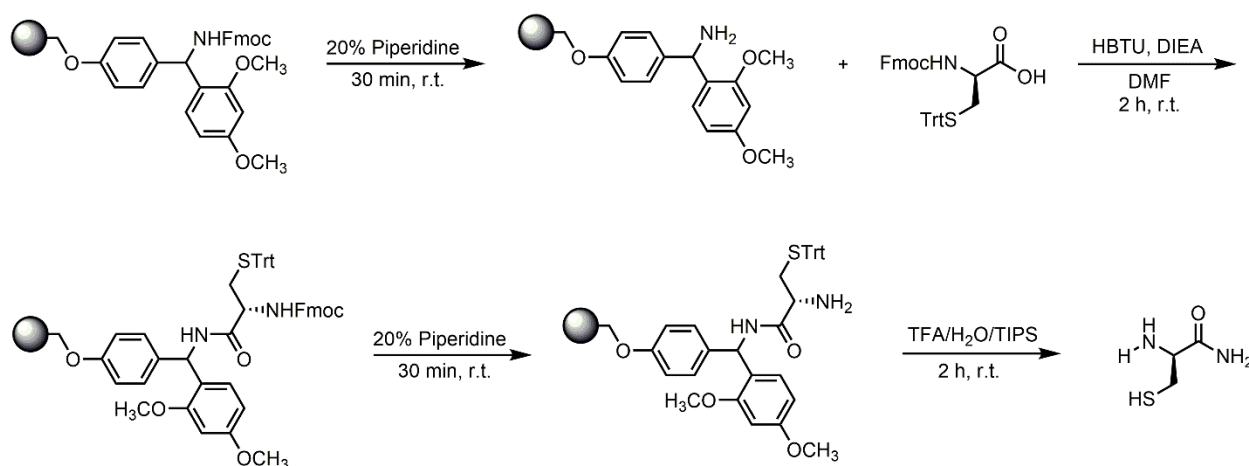
Scheme 3.1 Synthesis of D-Cys-D-Ala (dipeptide)



Fmoc-D-Alanine-OH (1.1 eq, 195 mg, 0.62 mmol) was added to a 25 mL peptide synthesis vessel charged with 2-Chlorotrityl chloride resin (500 mg, 0.57 mmol) and DIEA (4.4 eq, 0.436 mL, 2.50 mmol) in dry DCM (5mL). The resin was agitated for 1 h at ambient temperature and washed with MeOH and DCM (3 x 15 mL each). The Fmoc protecting group was removed with a 20% piperidine in DMF solution

(15 mL) for 30 minutes at ambient temperature, then washed as previously stated. Fmoc-D-Cysteine(Trt)-OH (2 eq, 667 mg, 1.14 mmol), HBTU (1.9 eq, 410 mg, 1.08 mmol), and DIEA (4 eq, 0.397 mL, 2.28 mmol) in DMF (15 mL) were added to the reaction vessel and agitated for 2 h at ambient temperature. After 2 h the resin was washed as previously stated and the Fmoc protecting group removal was also performed as described above followed by washing. The resin was added to a solution of TFA/H₂O/TIPS (95%, 2.5%, 2.5%, 20 mL) with agitation for 2 h at ambient temperature. The resin was filtered and the resulting solution was concentrated *in vacuo*. The residue was triturated with cold diethyl ether. The sample was analyzed for purity using a Waters 1525 Binary HPLC Pump using a Phenomenex Luna 5u C8(2) 100A (250 x 4.60 mm) column; gradient elution with H₂O/CH₃CN. Crude product was used.

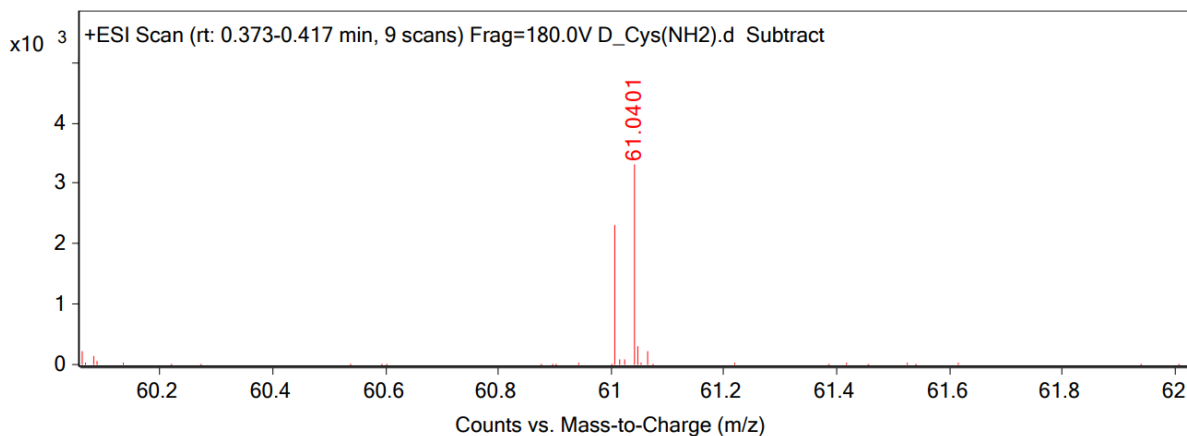


ESI-MS calculated $[M + H]^+$: 193.0641, found: 193.0641Scheme 3.2 Synthesis of D-Cys(NH₂)

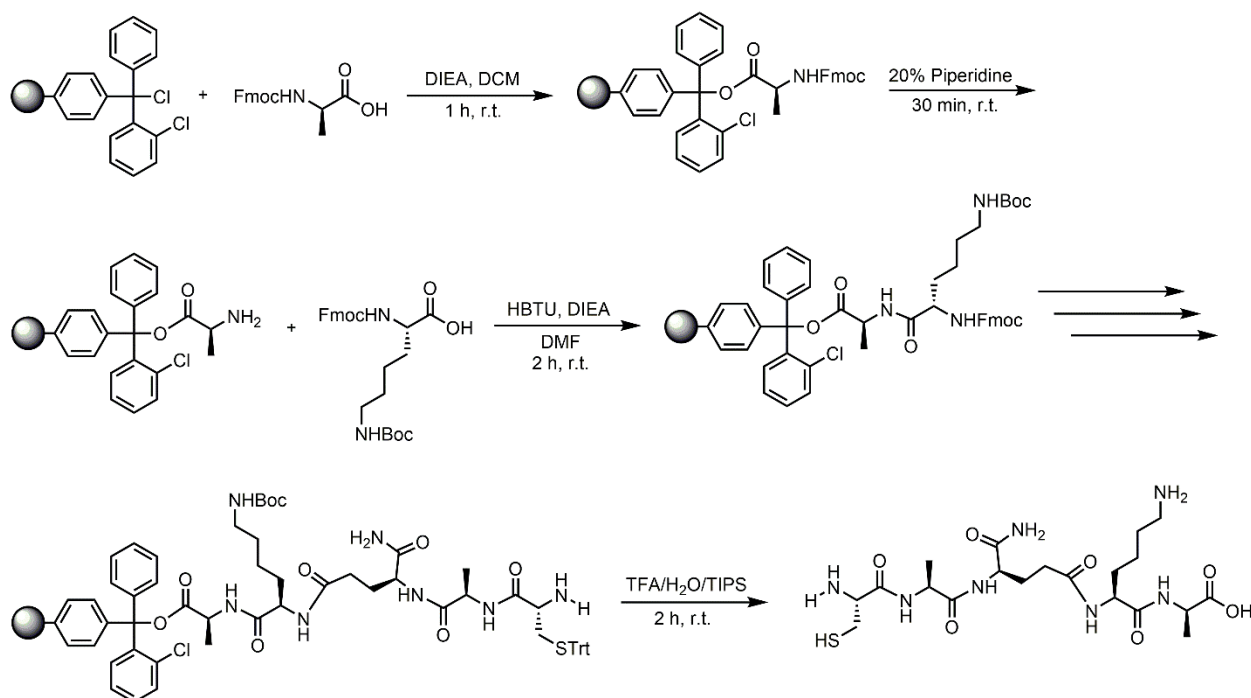
A 50 mL peptide synthesis vessel charged with rink amide resin (1000 mg, 0.45 mmol) underwent the Fmoc removal procedure and was washed as described above. Fmoc-D-Cysteine(Trt)-OH (1.5 eq, 395 mg, 0.67 mmol), HBTU (1.4 eq, 238 mg, 0.63 mmol), and DIEA (3 eq, 0.235 mL, 1.35 mmol) in DMF (20 mL) were added to the reaction vessel and agitated for 2 h at ambient temperature. After 2 h the resin was washed as previously stated and the Fmoc protecting group removal was also performed as described above followed by washing. The resin was added to a solution of TFA/H₂O/TIPS (95%, 2.5%, 2.5%, 20 mL) with agitation for 2 h at ambient temperature. The resin was filtered and the resulting solution

was concentrated *in vacuo*. The residue was triturated with cold diethyl ether. Crude product was used.

ESI-MS calculated $[M + 2H]^{2+}$: 61.0251, found: 61.0401

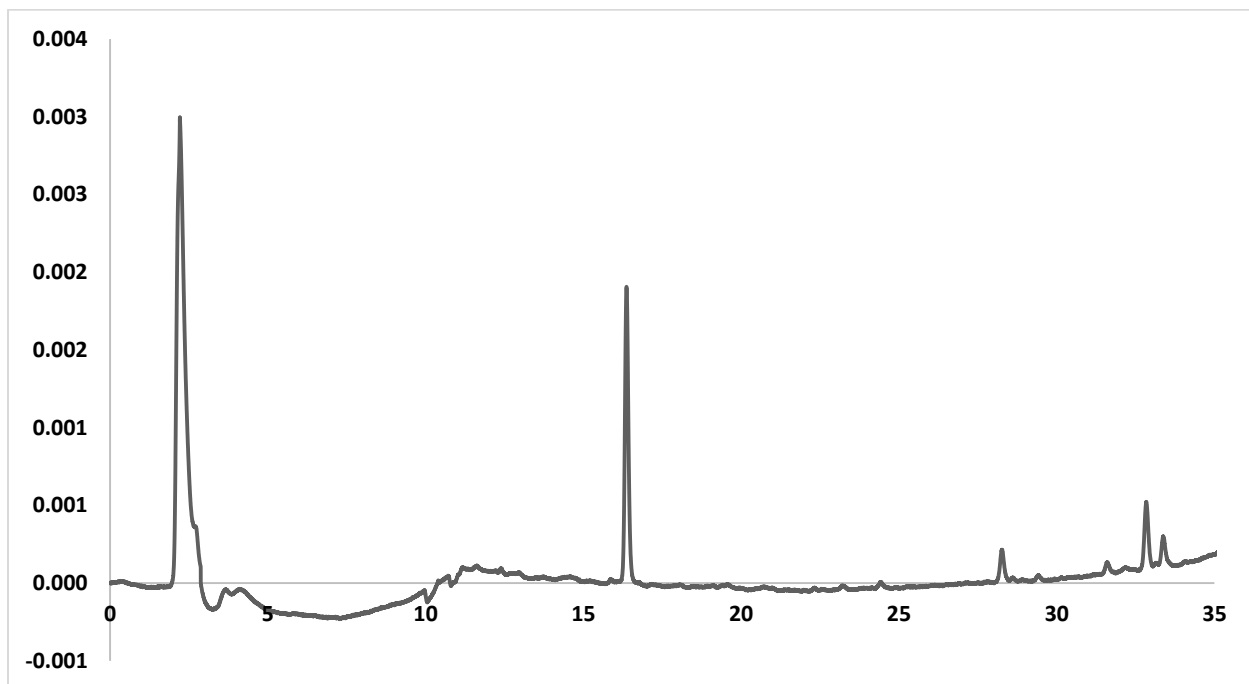


Scheme 3.3 Synthesis of cysteine modified tetrapeptide

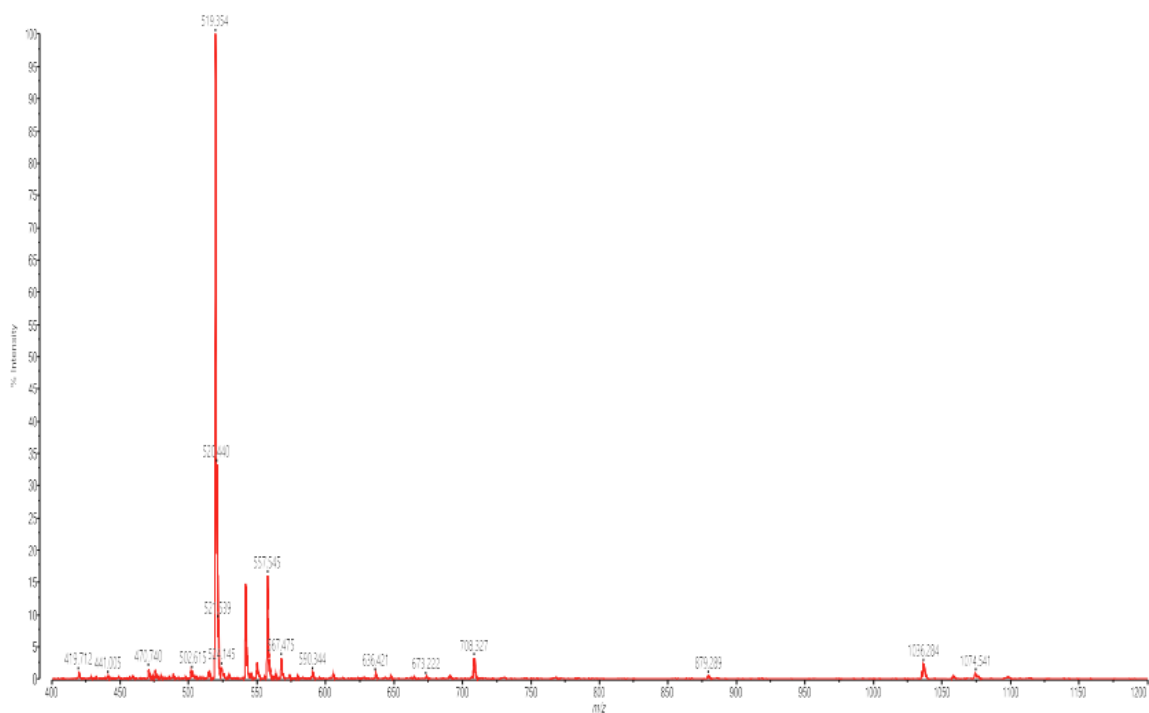


Fmoc-D-Alanine-OH (1.1 eq, 195 mg, 0.62 mmol) was added to a 25 mL peptide synthesis vessel charged with 2-Chlorotrityl chloride resin (500 mg, 0.57 mmol)

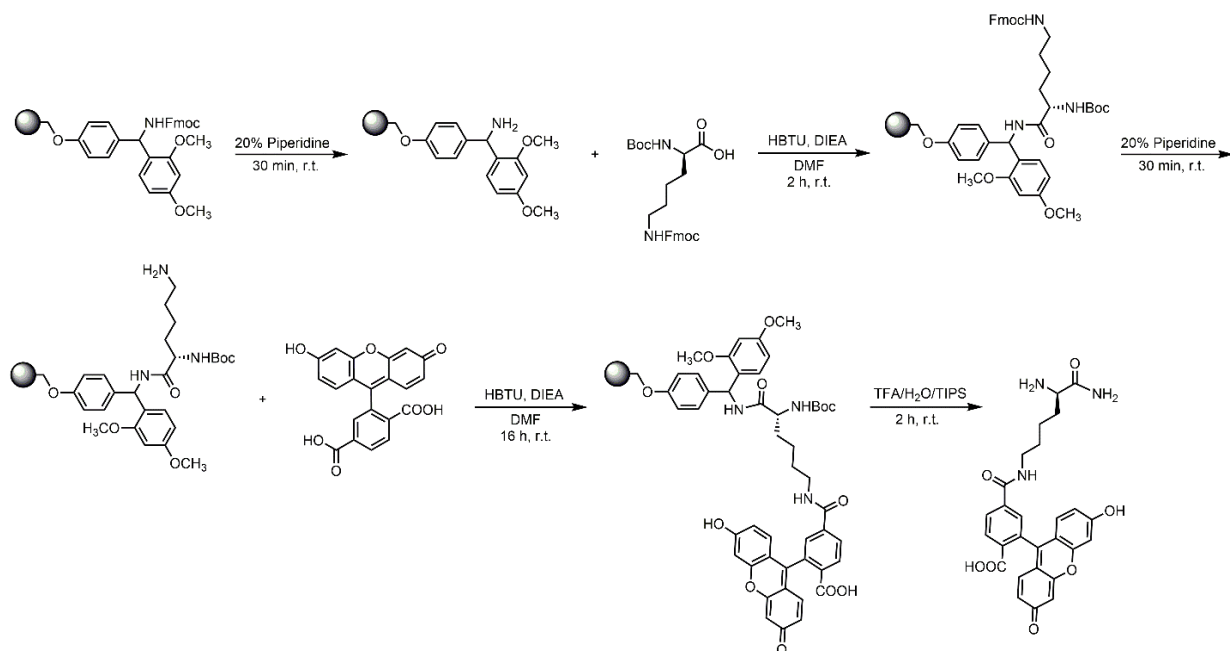
and DIEA (4.4 eq, 0.436 mL, 2.50 mmol) in dry DCM (5mL). The resin was agitated for 1 h at ambient temperature and washed as described above. The Fmoc protecting group was removed and the resin was washed as previously stated. Fmoc-L-Lysine(Boc)-OH (5 eq, 1335 mg, 2.85 mmol), HBTU (4.9 eq, 1059 mg, 2.79 mmol), and DIEA (10 eq, 0.992 mL, 5.70 mmol) in DMF (15 mL) were added to the reaction vessel and agitated for 2 h at ambient temperature. After 2 h the resin was washed as previously stated and the Fmoc protecting group removal was performed also as described above followed by washing. Fmoc-D-glutamic acid α -amide (1.5 eq, 157 mg, 0.85 mmol), HBTU (1.4 eq, 151 mg, 0.79 mmol), and DIEA (3 eq, 0.148 mL, 1.71 mmol) were added to the reaction vessel and agitated for 2 h at ambient temperature and washed as described above. The Fmoc deprotection and coupling procedure was repeated for Fmoc-L-Alanine-OH and Fmoc-L-Cysteine(Trt)-OH using the same equivalencies as used for Fmoc-L-Lysine(Boc)-OH. The Fmoc group was removed after the coupling of the last amino acid, Fmoc-L-Cysteine(Trt)-OH, and washed as before. The resin was then added to a solution of TFA/H₂O/TIPS (95%, 2.5%, 2.5%, 20 mL) with agitation for 2 h at ambient temperature. The resin was filtered and the resulting solution was concentrated *in vacuo*. The residue was triturated with cold diethyl ether. The compounds were purified using reverse phase HPLC using 95% H₂O/ 5% MeOH starting and gradient elution. The sample was analyzed for purity using a Waters 1525 Binary HPLC Pump using a Phenomenex Luna 5u C8(2) 100A (250 x 4.60 mm) column; gradient elution with H₂O/CH₃CN.



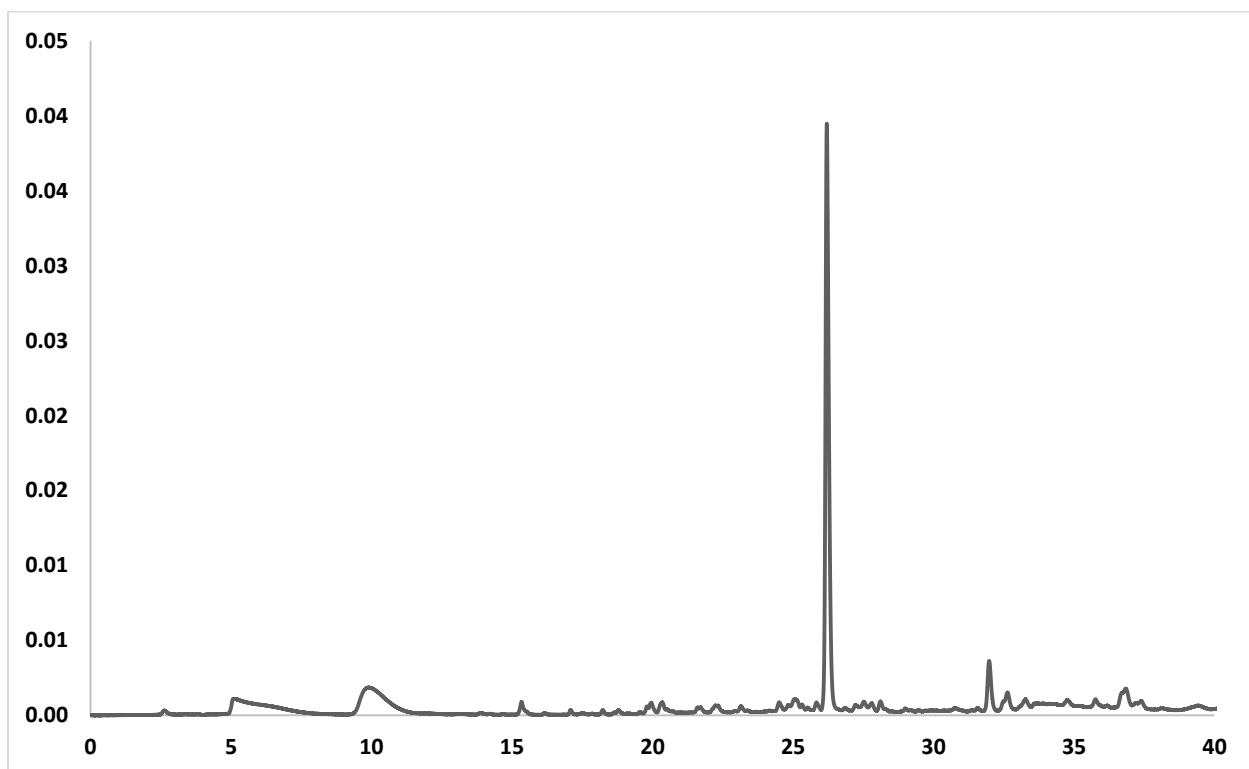
MALDI-TOF calculated $[M + H]^+$: 519.248, found: 519.354

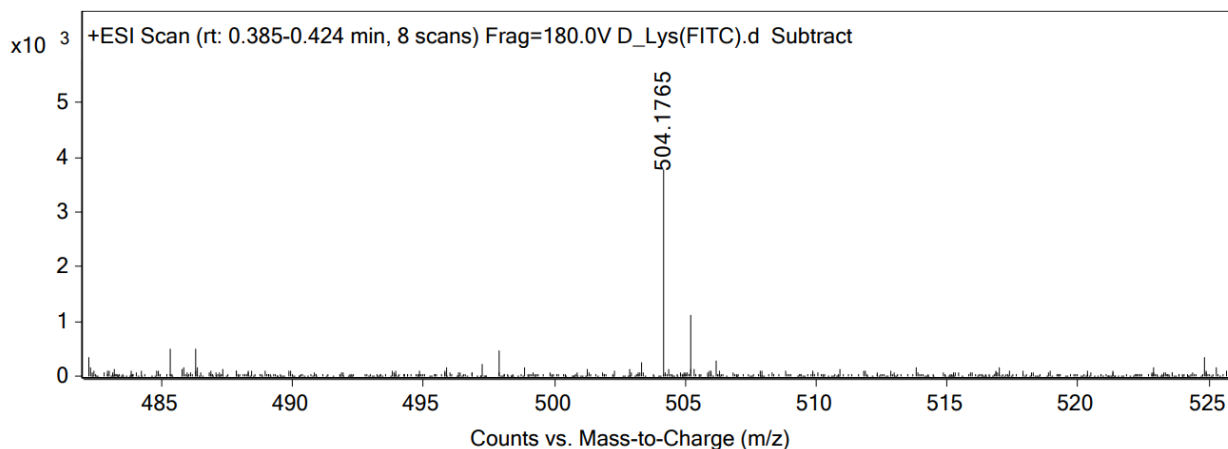
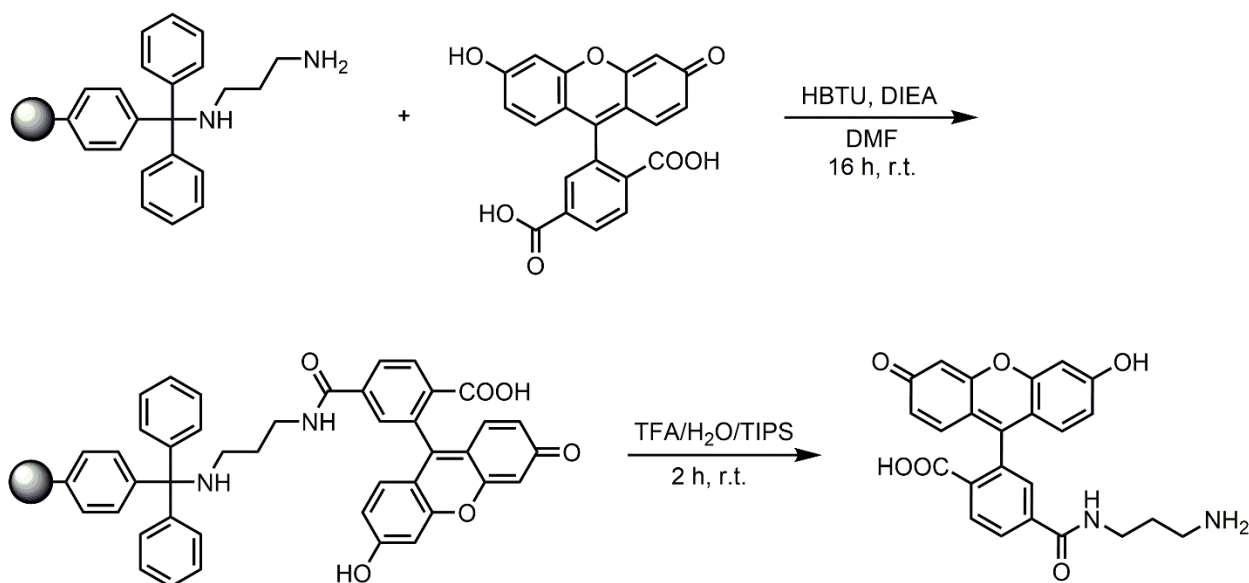


Scheme 3.4 Synthesis of D-LysFI



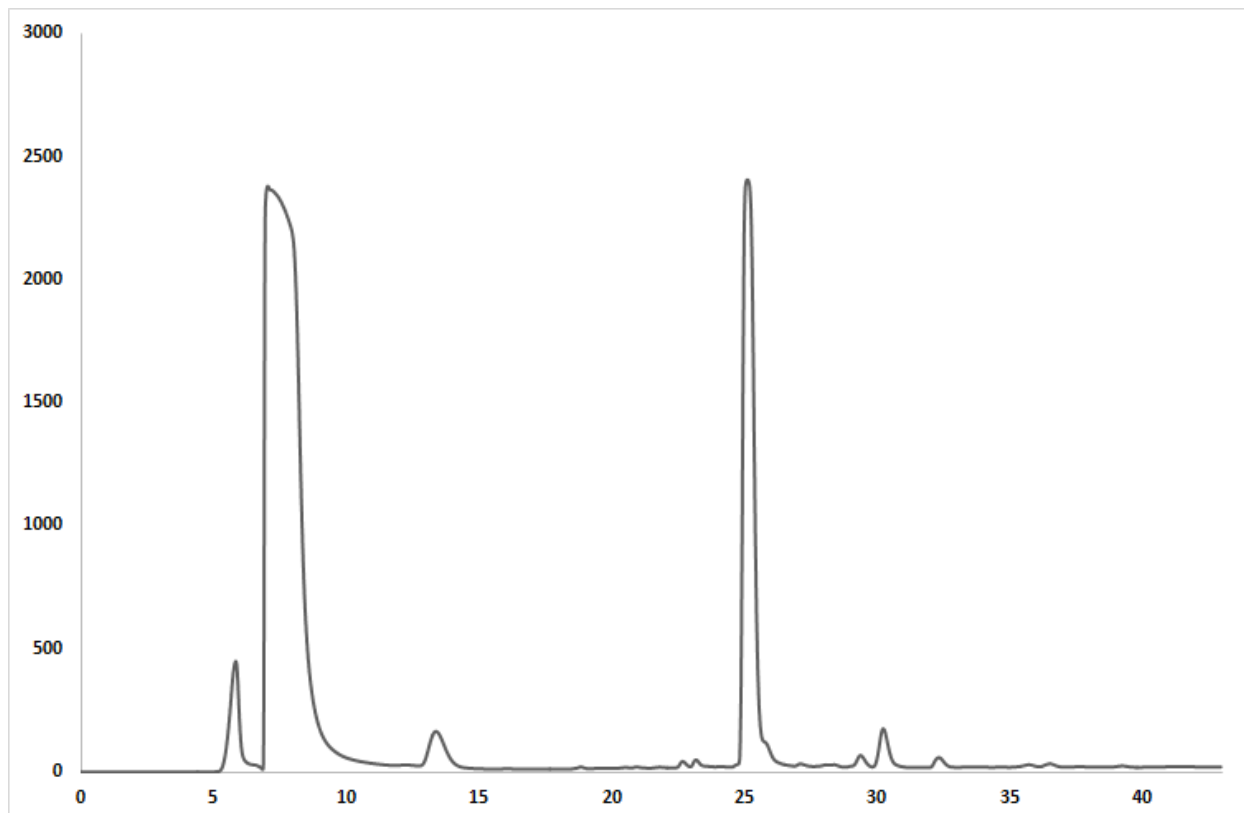
A 25 mL peptide synthesis vessel charged with rink amide resin (250 mg, 0.11 mmol) underwent the Fmoc removal procedure and was washed as described above. Boc-D-Lysine(Fmoc)-OH (5 eq, 257 mg, 0.55 mmol), HBTU (4.9 eq, 204 mg, 0.53 mmol), and DIEA (10 eq, 0.191 mL, 1.10 mmol) in DMF (15 mL) were added to the reaction vessel and agitated for 2 h at ambient temperature. After 2 h the resin was washed as previously stated and the Fmoc protecting group removal was also performed as described above followed by washing. The resin was coupled with 5,6-carboxyfluorescein (2 eq, 82 mg, 0.22 mmol), HBTU (1.9 eq, 79 mg, 0.20 mmol), and DIEA (4 eq, 0.076 mL, 0.44 mmol) in DMF (15 mL) and agitated for 16h at ambient temperature. The resin was washed as previously described and then added to a solution of TFA/H₂O/TIPS (95%, 2.5%, 2.5%, 20 mL) with agitation for 2 h at ambient temperature. The resin was filtered and the resulting solution was concentrated *in vacuo*. The residue was triturated with cold diethyl ether. The sample was analyzed for purity using a Waters 1525 Binary HPLC Pump using a Phenomenex Luna 5u C18(2) 100A (250 x 4.60 mm) column; gradient elution with H₂O/CH₃CN. Crude product was used.



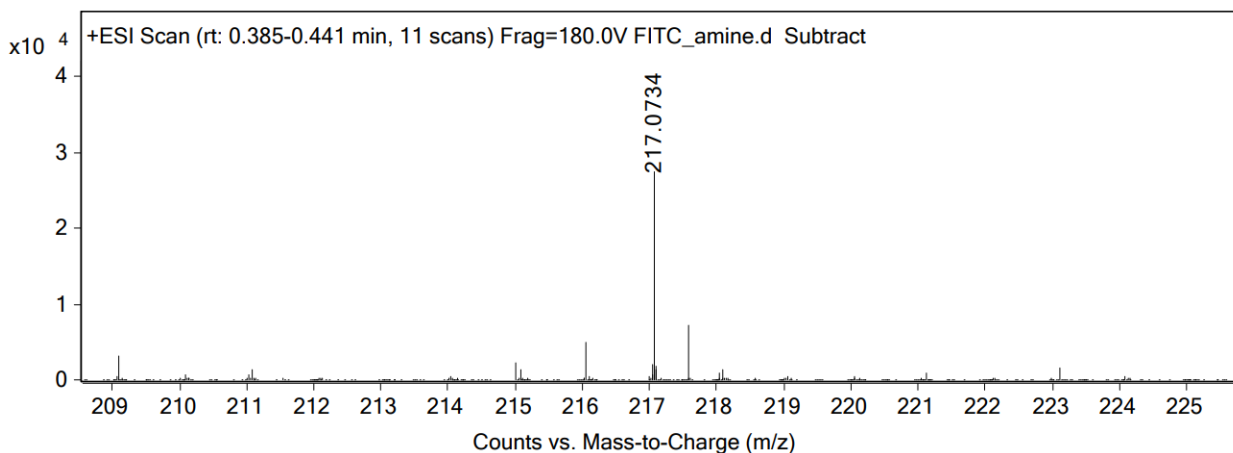
ESI-MS calculated $[M + H]^+$: 504.1765, found: 504.1765**Scheme 3.5 Synthesis of AmineFI**

5,6-carboxyfluorescein (2 eq, 206 mg, 0.55 mmol) was added to a 25 mL peptide synthesis vessel charged with 1,3-Diaminopropane trityl resin (500 mg, 0.27 mmol), HBTU (1.9 eq, 194 mg, 0.51 mmol), and DIEA (4 eq, 0.383 mL, 1.08 mmol). The resin was agitated for 16 h at ambient temperature. Then the resin was washed as previously described and then added to a solution of TFA/H₂O/TIPS (95%, 2.5%, 2.5%, 20 mL) with agitation for 2 h at ambient temperature. The resin

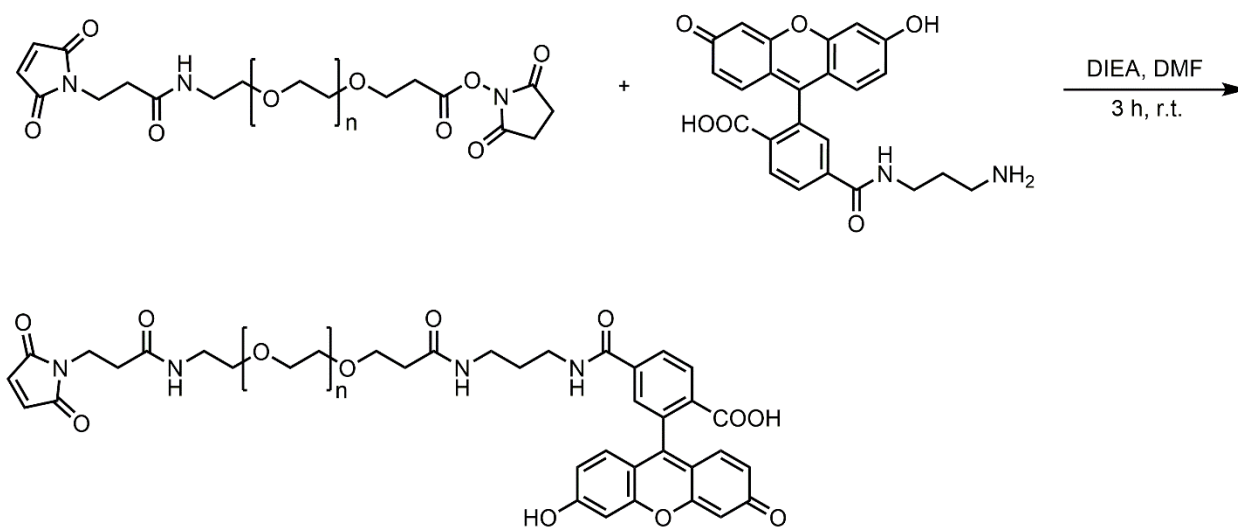
was filtered and the resulting solution was concentrated *in vacuo*. The residue was triturated with cold diethyl ether. The resulting sample was analyzed for purity using an Agilent 1200 HPLC with a Phenomenex Luna 5 μ C4 300Å (250 x 2.00 mm) column; gradient elution with H₂O/CH₃CN. Crude product was used for further synthesis of PEG based library.



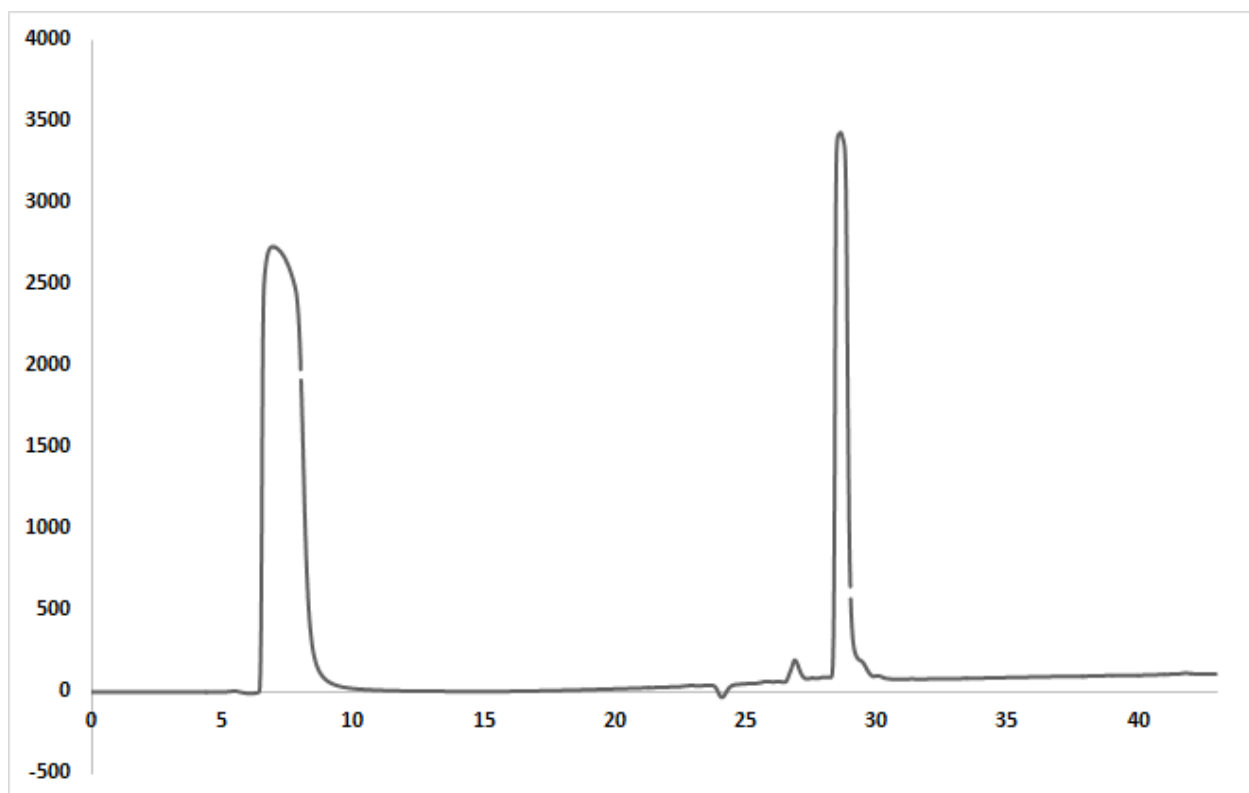
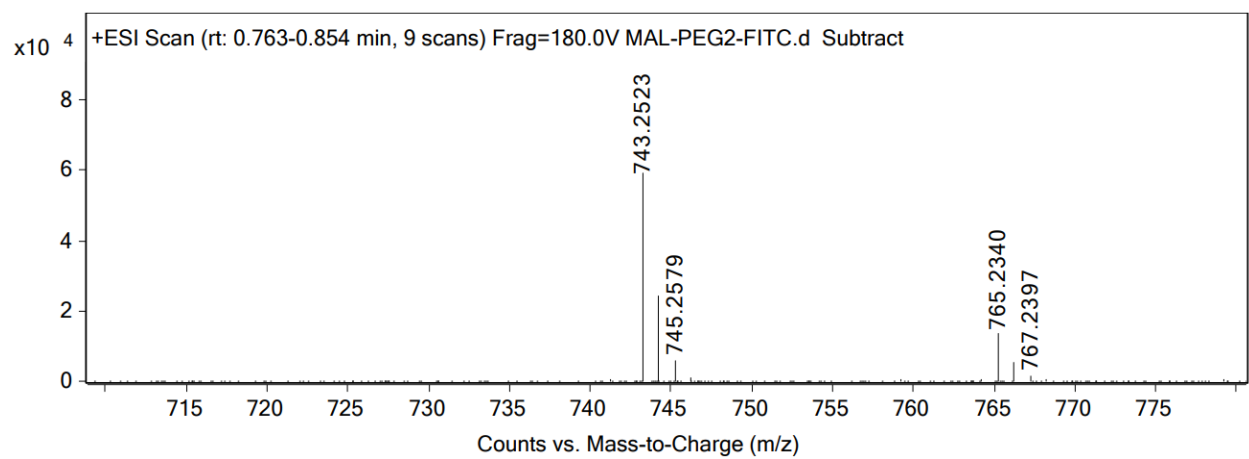
ESI-MS calculated $[M + 2H]^{2+}$: 217.0733, found: 217.0734

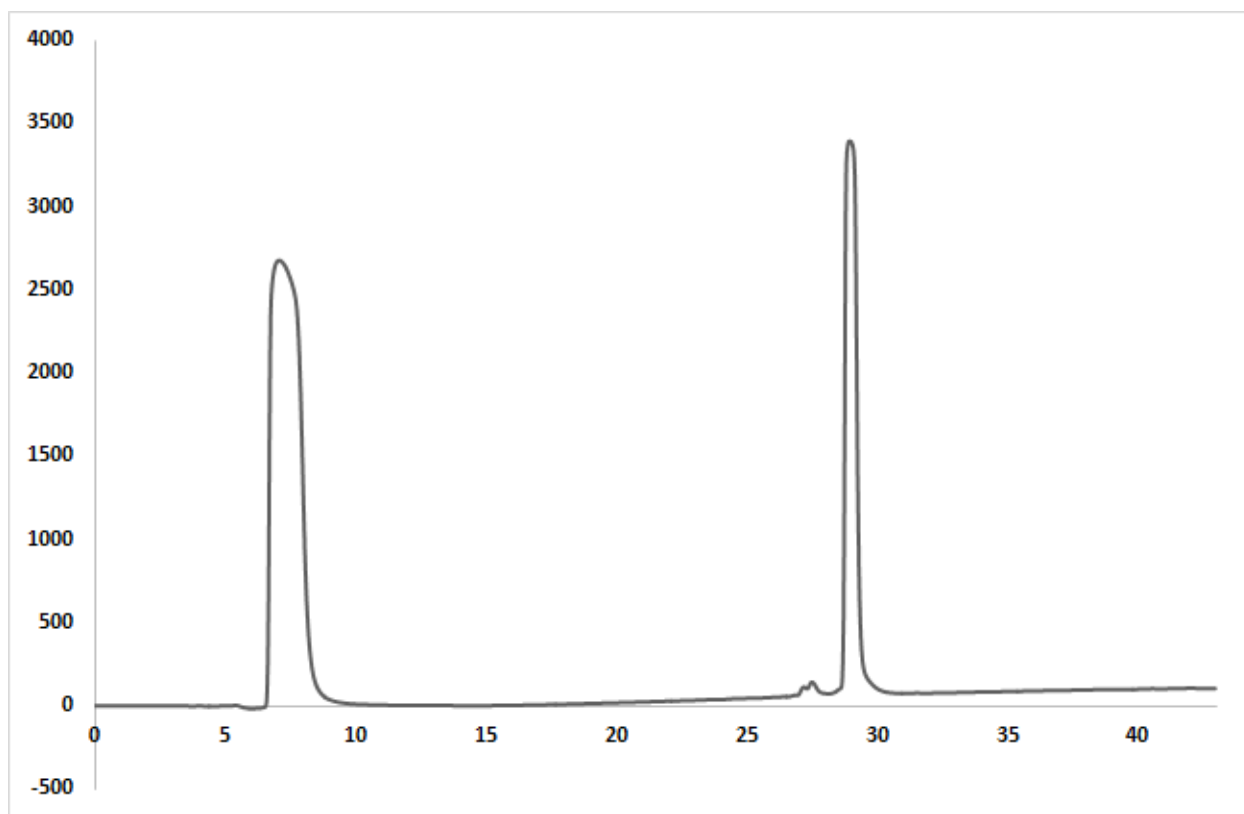
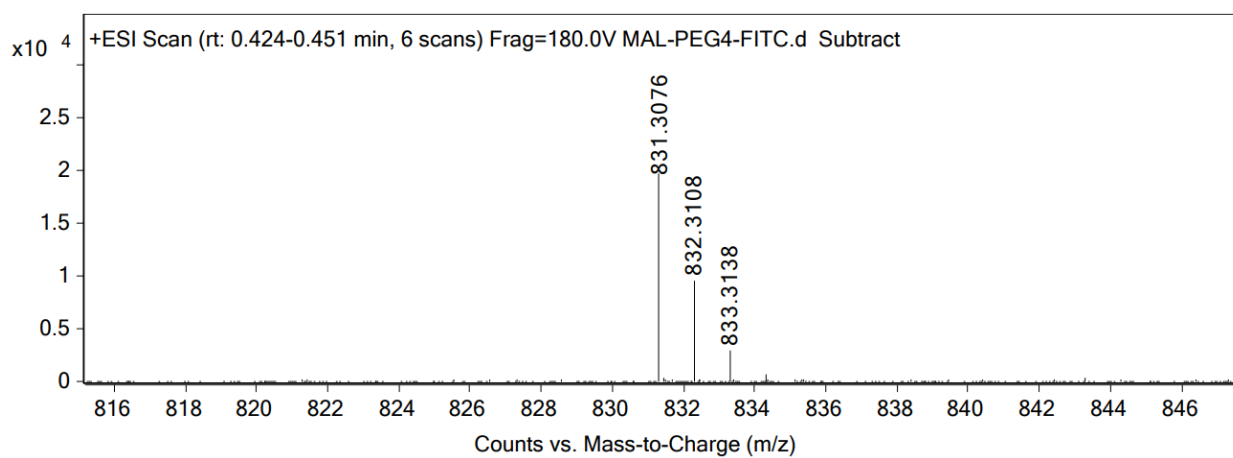


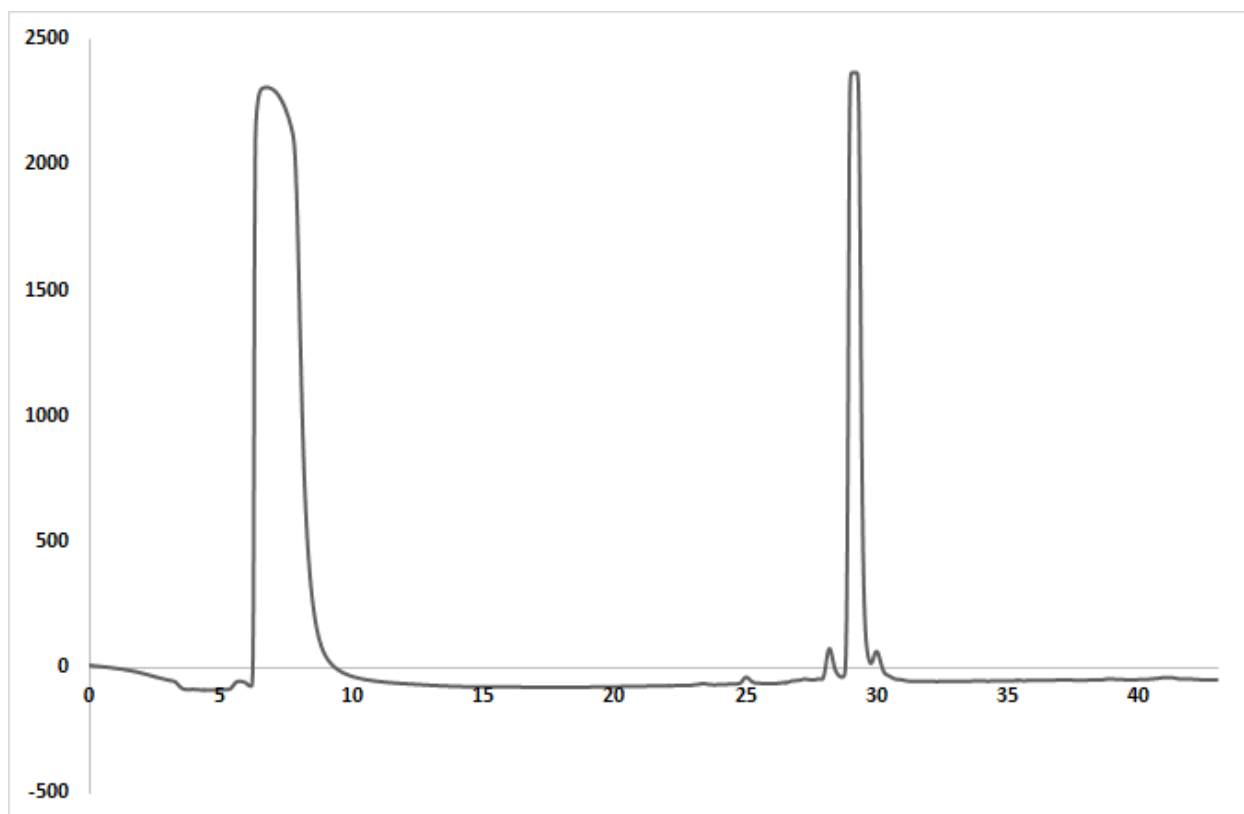
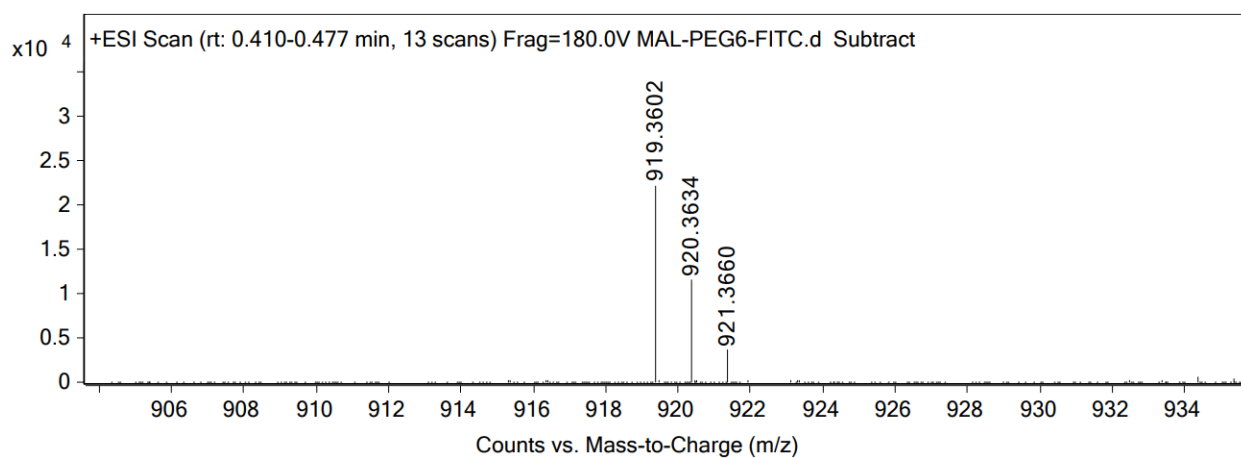
Scheme 3.6 Synthesis of Mal-peg_n-FI Library

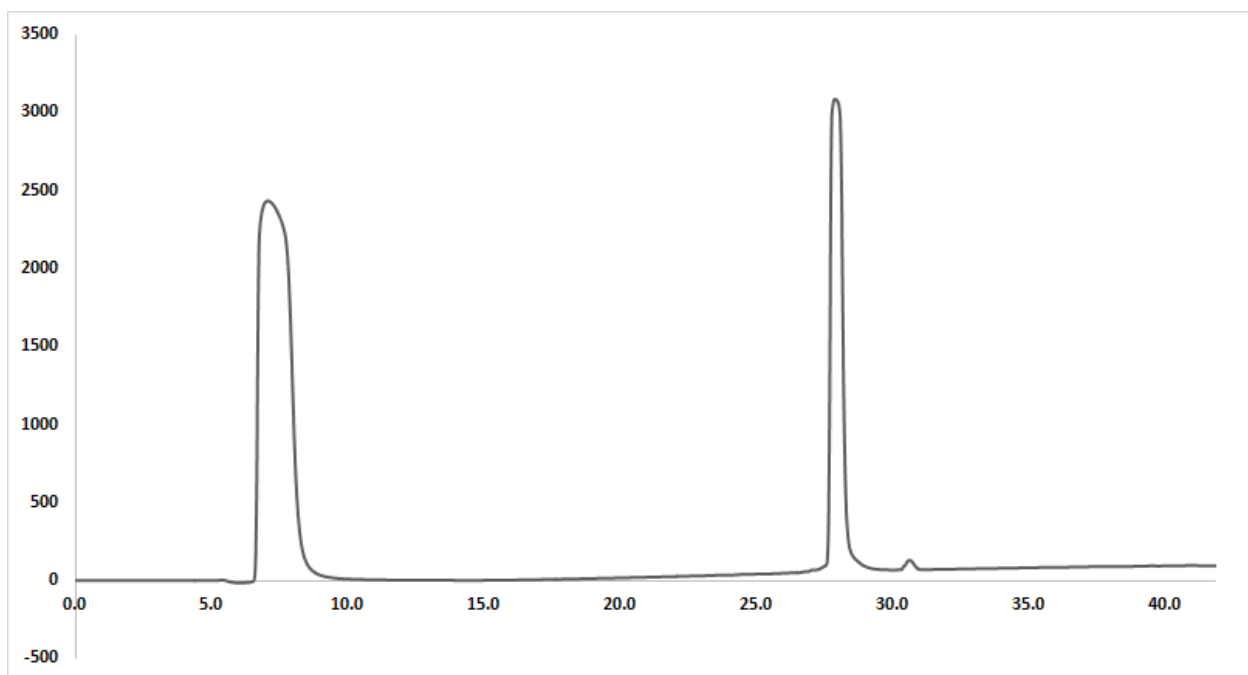
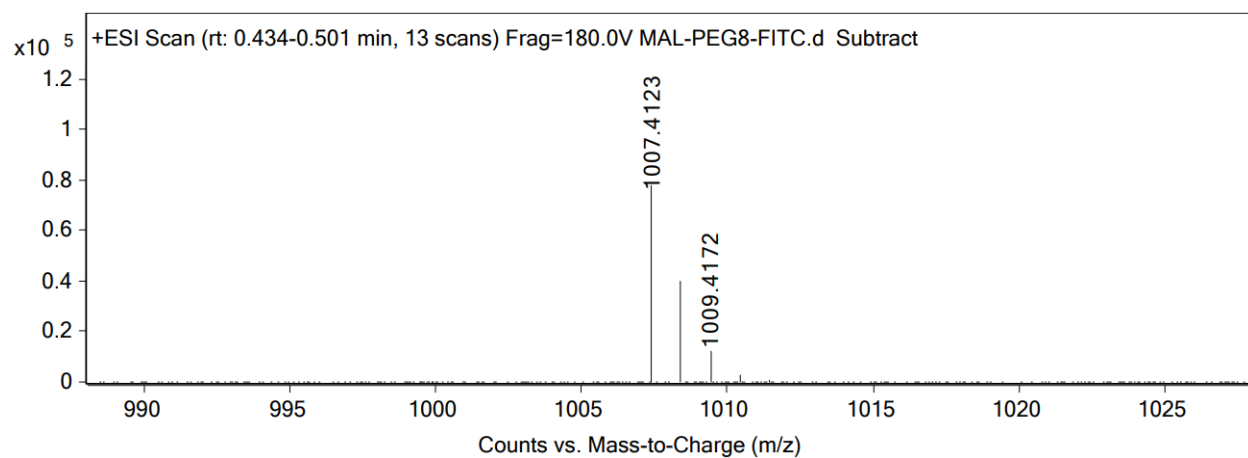


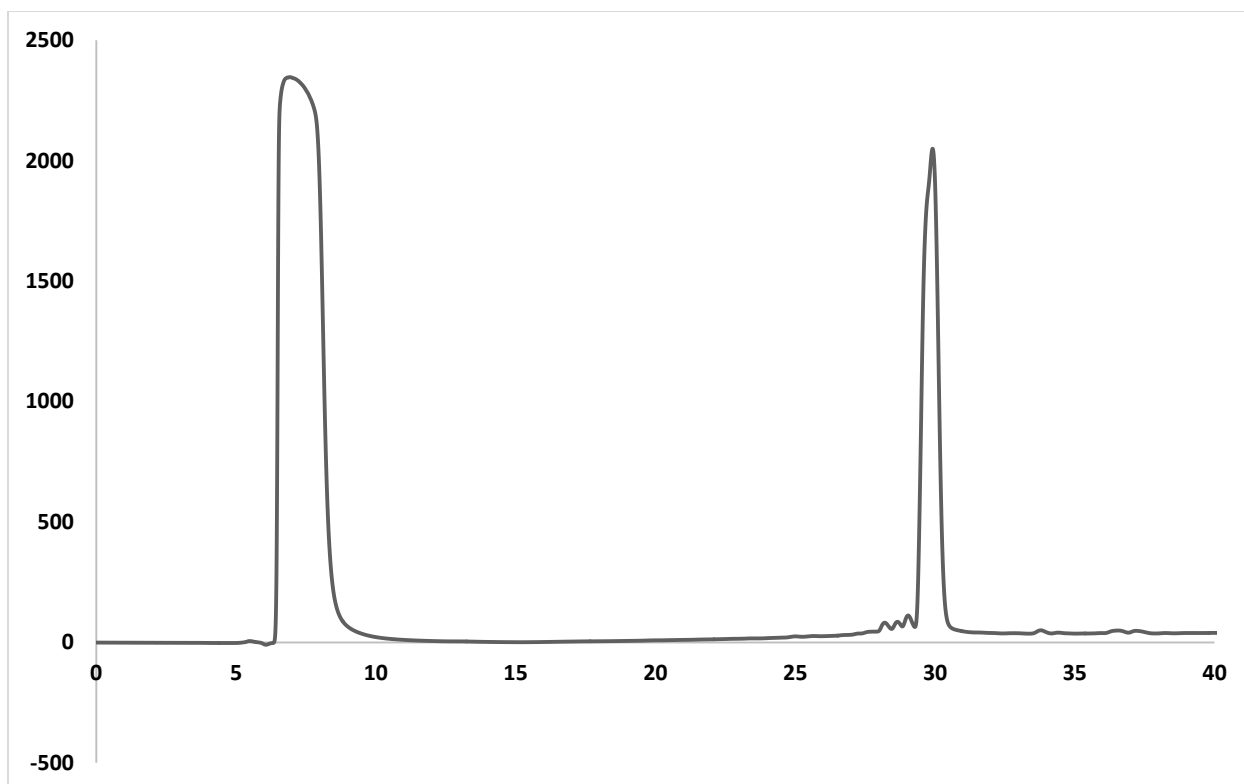
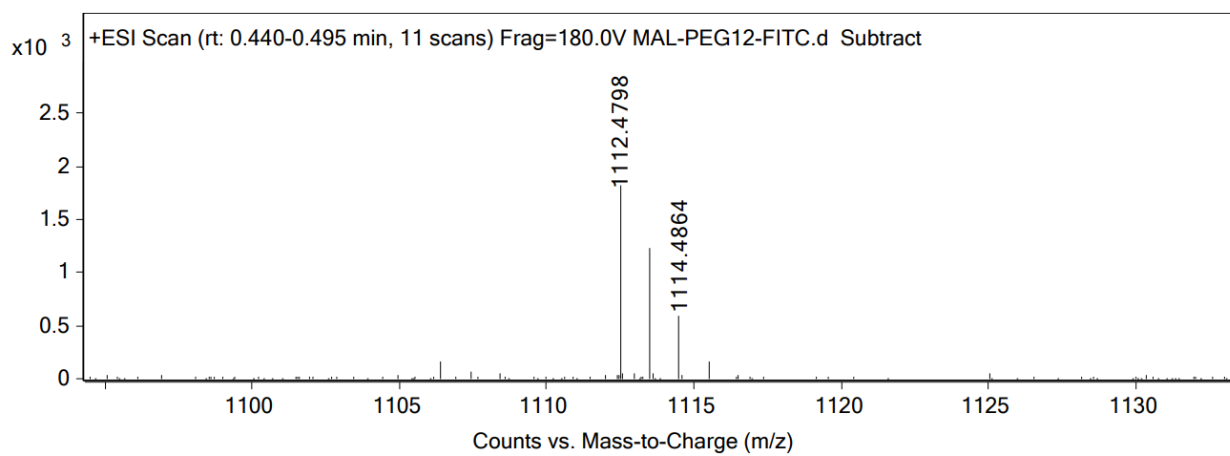
All library members were synthesized using the same method. Mal-amido-PEG_n-NHS ($n = 2, 4, 6, 8, 24, 10$ mg) or Mal-PEG₁₂-NHS was added to **AmineFI** (3 eq) dissolved in dry DMF and DIEA (3 eq). This was allowed to react for 3 h with agitation. The reaction mix was purified using reverse phase HPLC using 70% H₂O/ 30% MeOH starting and gradient elution. The resulting sample was analyzed for purity using an Agilent 1200 HPLC with a Phenomenex Luna 5 μ C4 300Å (250 x 2.00 mm) column; gradient elution with H₂O/CH₃CN.

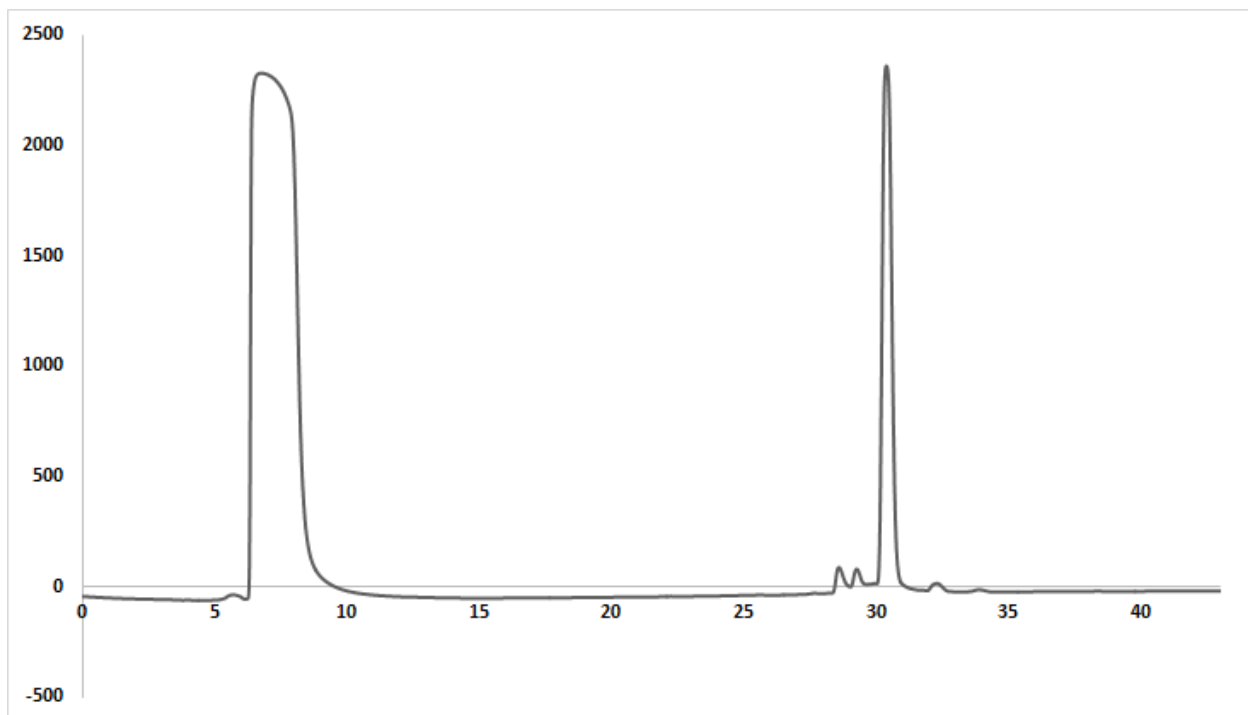
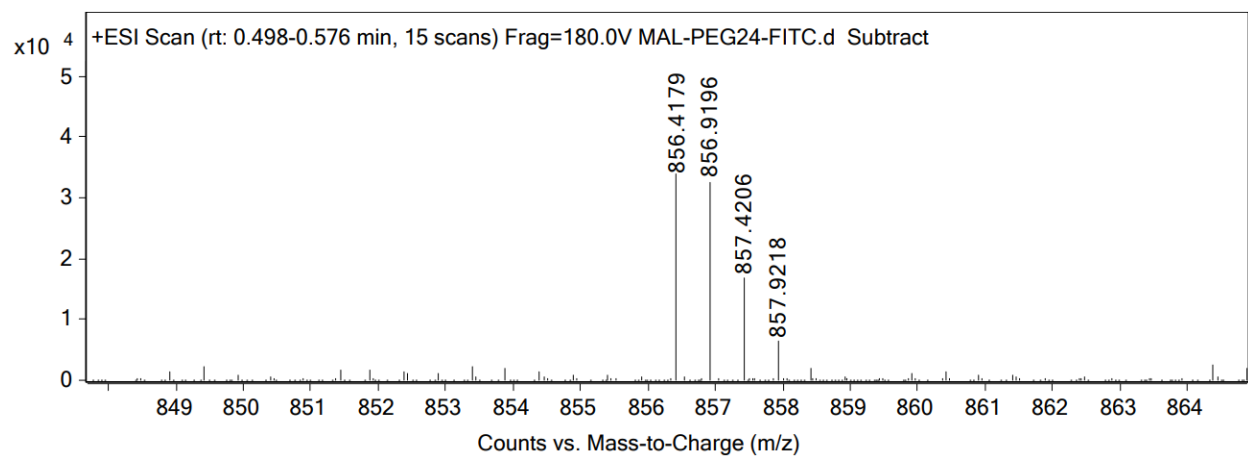
Mal-peg₂-FI**ESI-MS calculated [M + H]⁺: 743.2558, found: 743.2523**

Mal-peg₄-FI**ESI-MS calculated [M + H]⁺: 831.3083, found: 831.3076**

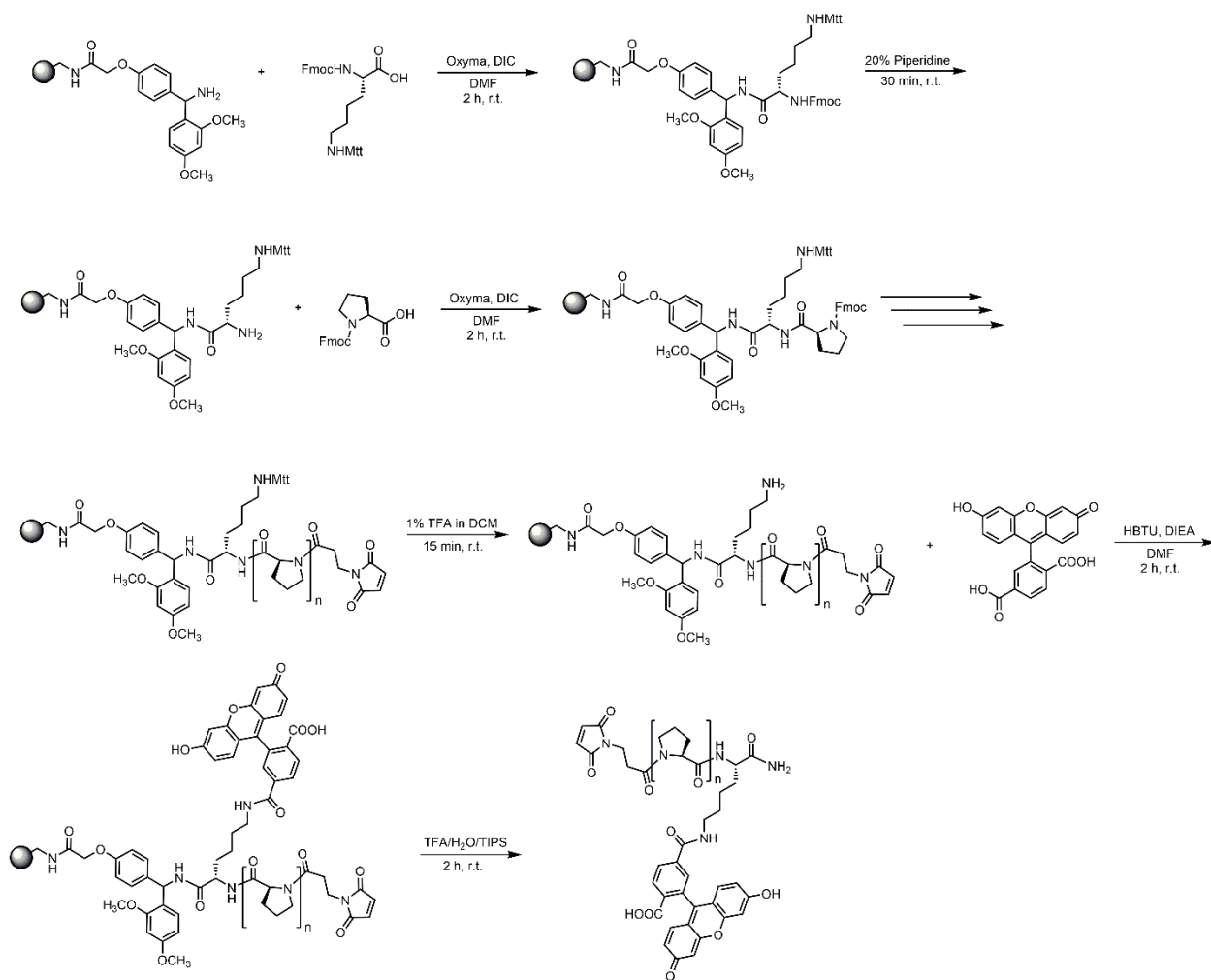
Mal-peg₆-FI**ESI-MS calculated [M + H]⁺: 919.3607, found: 919.3602**

Mal-peg₈-FI**ESI-MS calculated [M + H]⁺: 1007.4131, found: 1007.4123**

Mal-peg₁₂-FI**ESI-MS calculated [M + H]⁺: 1112.4809, found: 1112.4798**

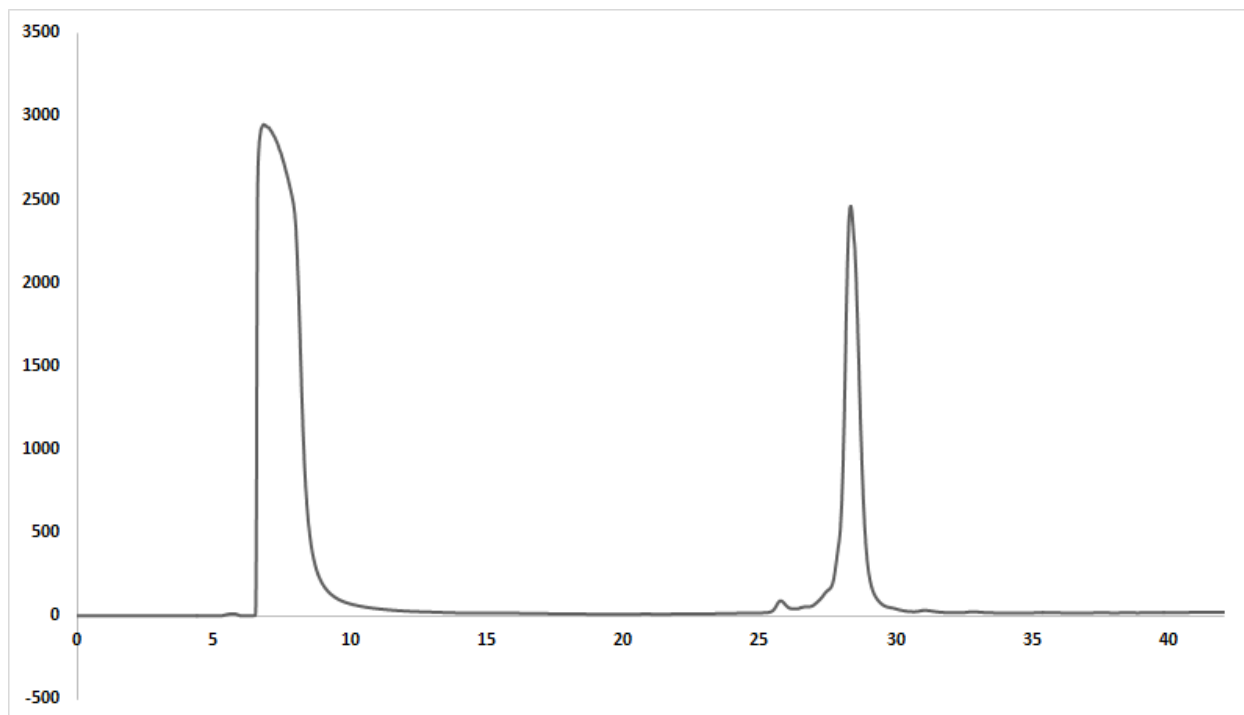
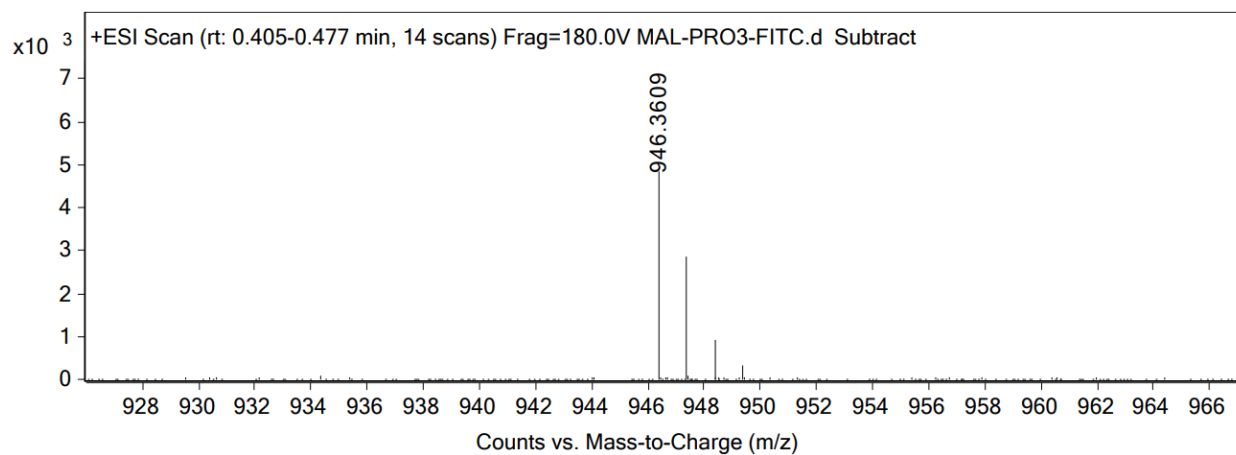
Mal-peg24-FI**ESI-MS calculated $[M + 2H]^{2+}$: 856.4199, found: 856.4179**

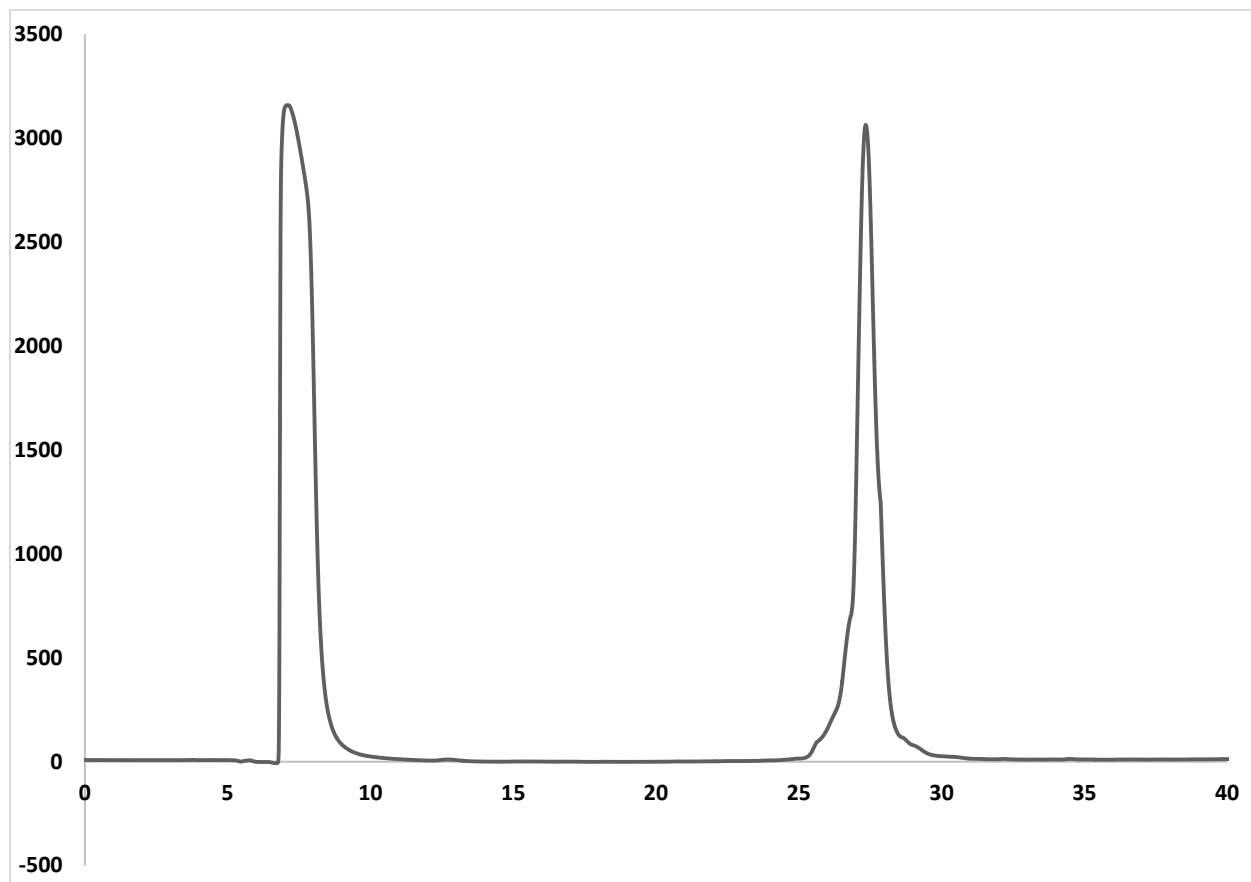
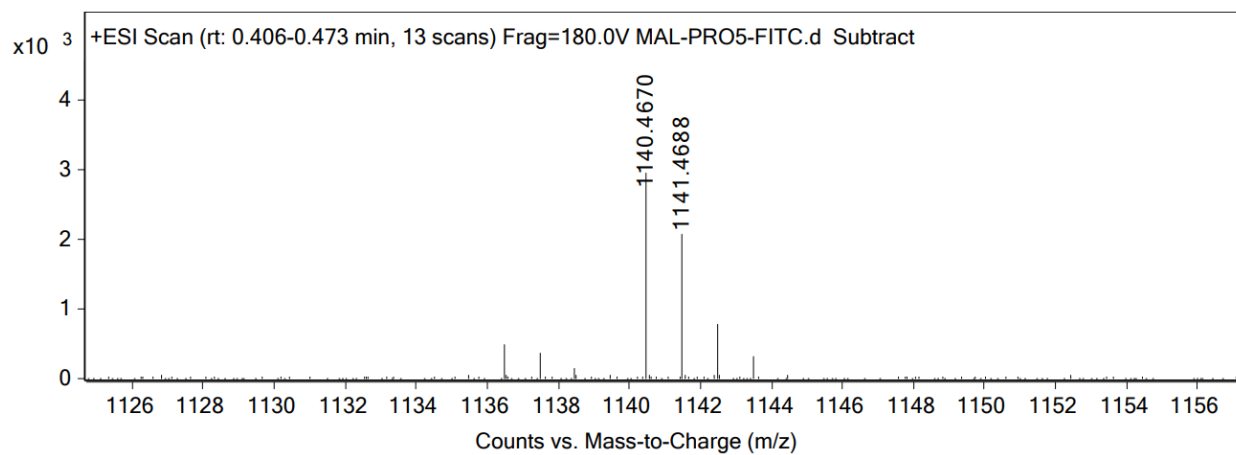
Scheme 3.7 Synthesis of Mal-pro_n-FI Library

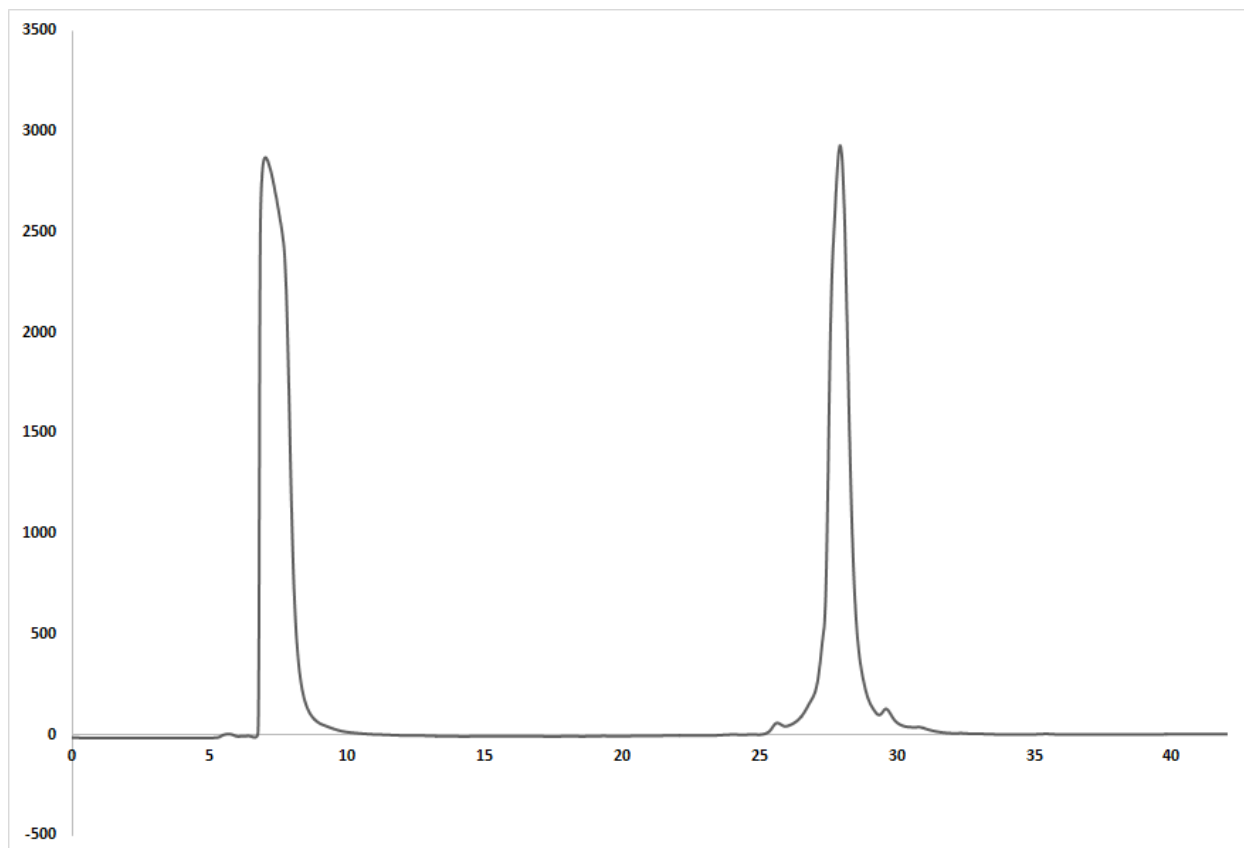
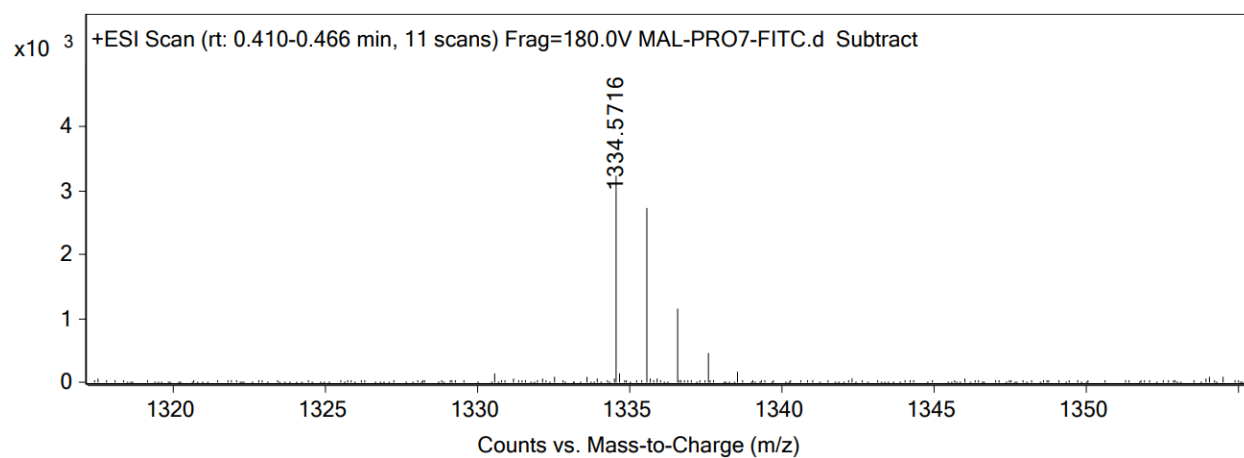


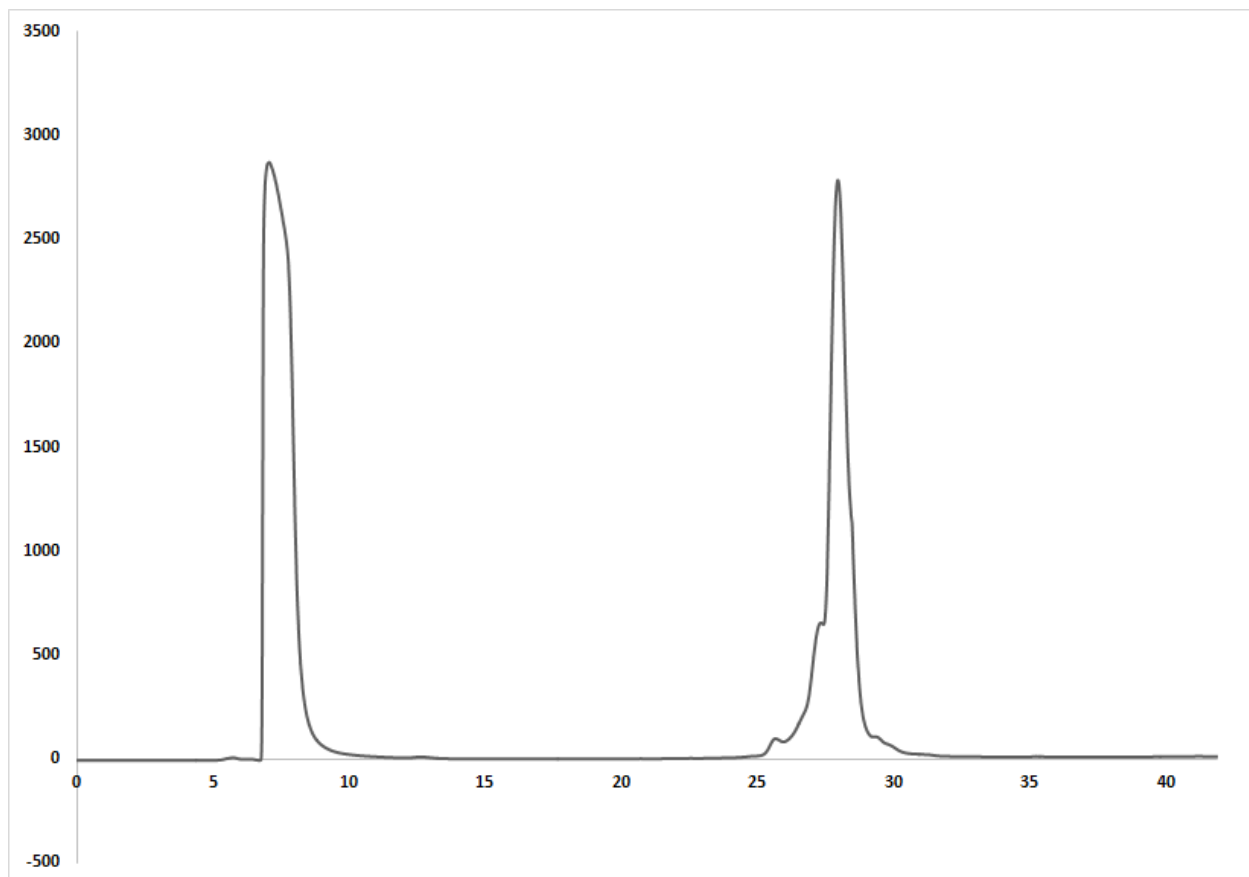
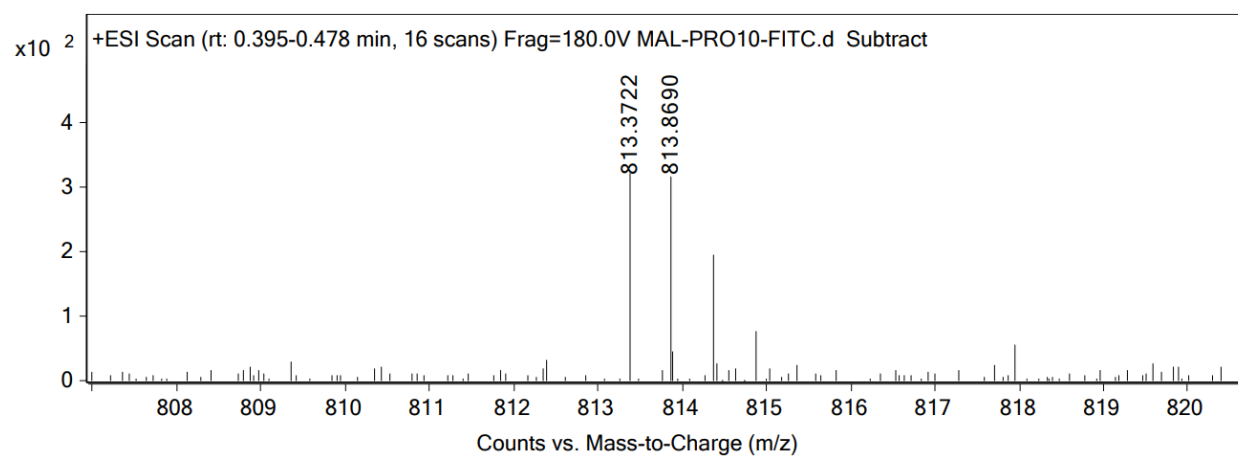
Fmoc-L-Lysine(Mtt)-OH (2 eq, 1124 mg, 1.80 mmol), Oxyma Pure (2 eq, 255 mg, 1.80mmol), and DIC (2 eq, 0.278 mL, 1.80 mmol) were added to a 50 mL peptide synthesis vessel charged with H-Rink amide ChemMatrix resin (2000 mg, 0.90 mmol) in DMF (20mL). The resin was agitated for 2 h at ambient temperature and washed as described above. The Fmoc protecting group was removed and the resin was washed as previously stated. Fmoc-L-Proline-OH (5 eq, 1518 mg, 4.50 mmol), Oxyma Pure (5 eq, 639 mg, 4.50 mmol), and DIC (5 eq, 0.696 mL, 4.50 mmol) in DMF (20 mL) were added to the reaction vessel and agitated for 5 minutes at ambient temperature. The resin was then drained and immediately after Fmoc-L-Proline-OH (5 eq, 1518 mg, 4.50 mmol), Oxyma Pure (5 eq, 639 mg, 4.50

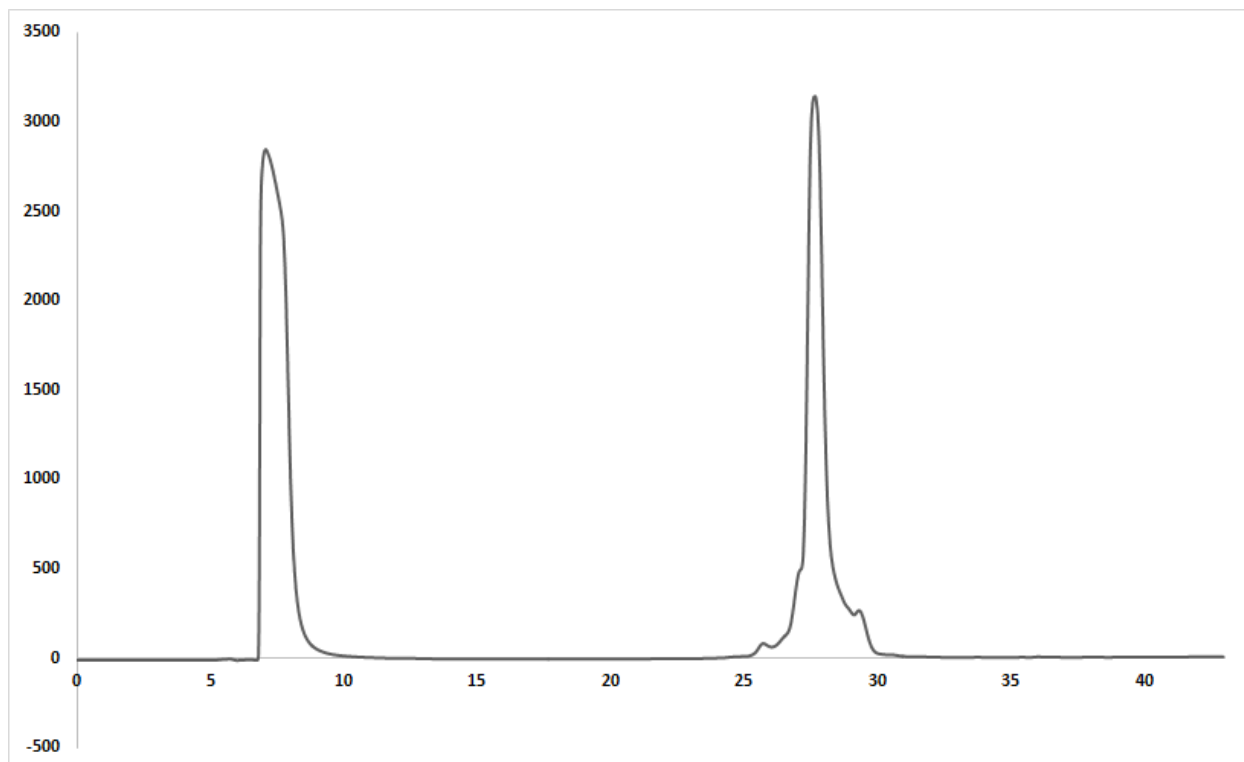
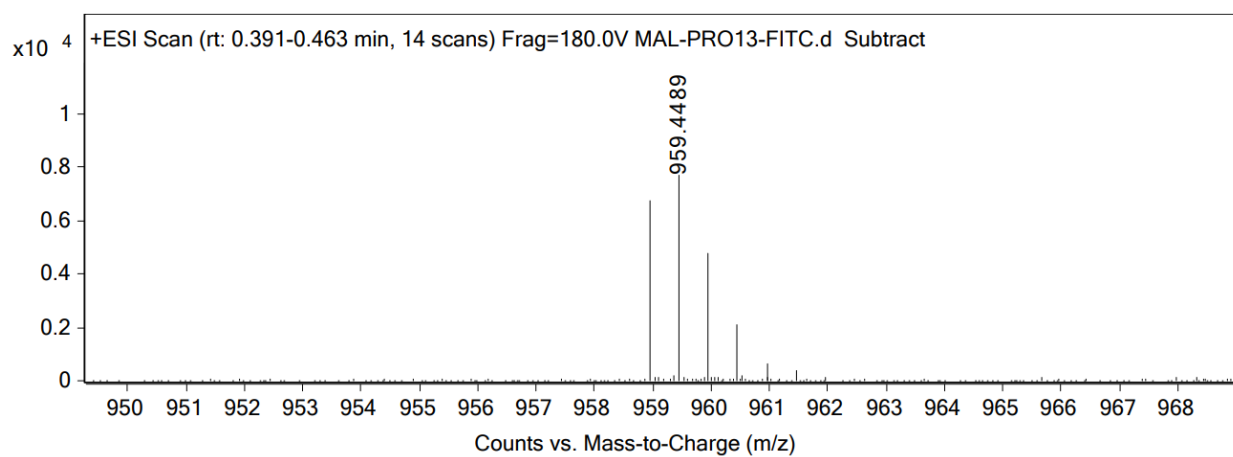
mmol), and DIC (5 eq, 0.696 mL, 4.50 mmol) in DMF (20 mL) were added to the reaction vessel and that was allow to react with agitation for 2 h at ambient temperature. After 2 h the resin was washed as previously stated. The Fmoc deprotection, previously described, and coupling procedure, at the same equivalencies, was repeated for all subsequent Fmoc-L-Proline-OH residues added to reach the desired n lengths. The resin was split off at n = 3, 5, 7, 10, 13, 16, and 31 proline residues. Once the polyproline segments were built, each resin pool could undergo the Fmoc removal procedure. To the resin 3-maleimidopropionic acid (3 eq), Oxyma Pure (3 eq), and DIC (3 eq) were added and agitated for 2 h at ambient temperature. The resin was washed as described above. Next the Mtt protecting group of the lysine residue was removed by adding a TFA cocktail solution (1% TFA in DCM) to the resin and agitating for 15 minutes. The solution was drained, and this procedure was repeated five additional times. The solution was then drained, rinsed with DMF, and washed as previously described. Finally the resin was coupled with 5,6-carboxyfluorescein (2 eq), HBTU (1.9 eq), and DIEA (4 eq) in DMF (20 mL) and agitated for 16h at ambient temperature. The resin was washed as previously described and then added to a solution of TFA/H₂O/TIPS (95%, 2.5%, 2.5%, 20 mL) with agitation for 2 h at ambient temperature. The resin was filtered and the resulting solution was concentrated in vacuo. The residue was trituated with cold diethyl ether. The compounds were purified using reverse phase HPLC 70% H₂O/ 30% MeOH starting and gradient elution. The resulting sample was analyzed for purity using an Agilent 1200 HPLC with a Phenomenex Luna 5 μ C4 300Å (250 x 2.00 mm) column; gradient elution with H₂O/CH₃CN.

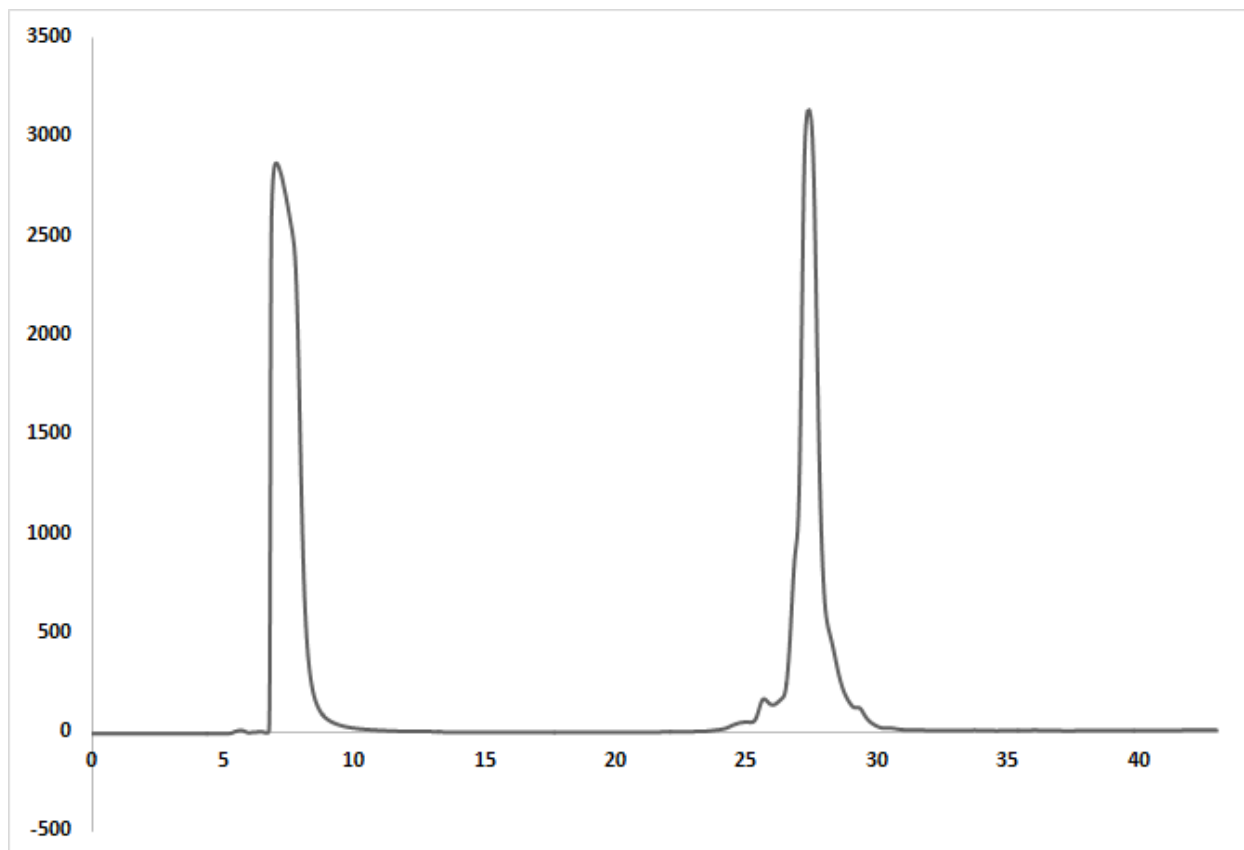
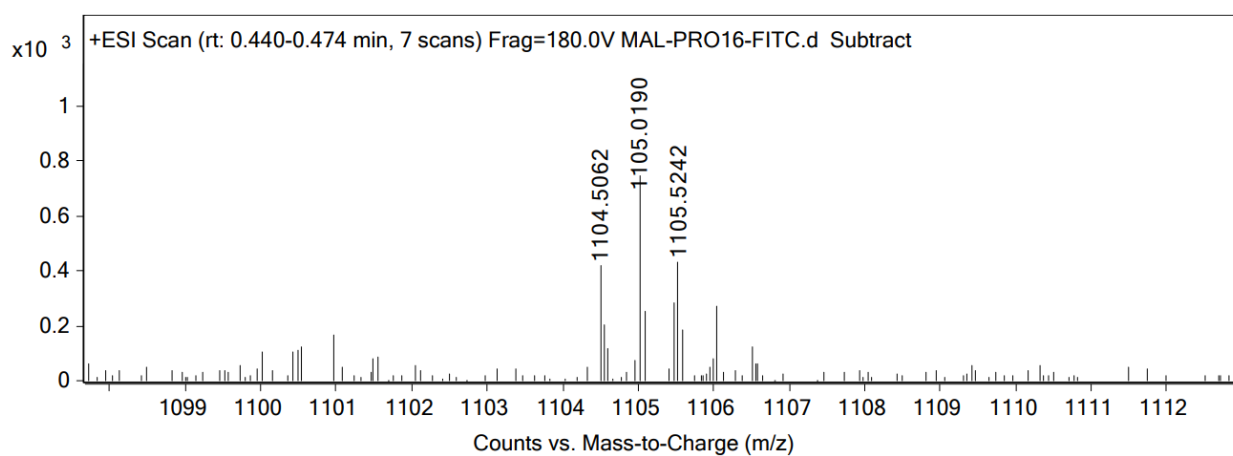
Mal-pro₃-FI**ESI-MS calculated [M + H]⁺: 946.3617, found: 946.3609**

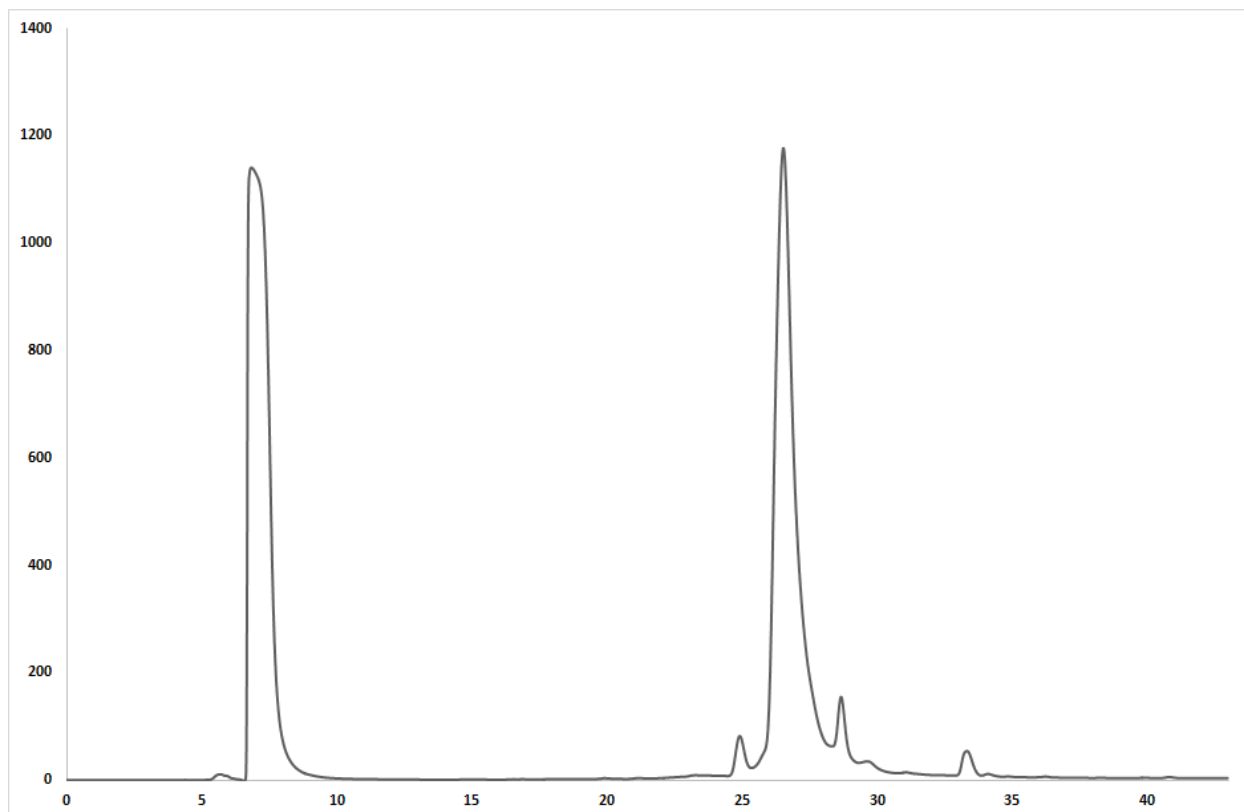
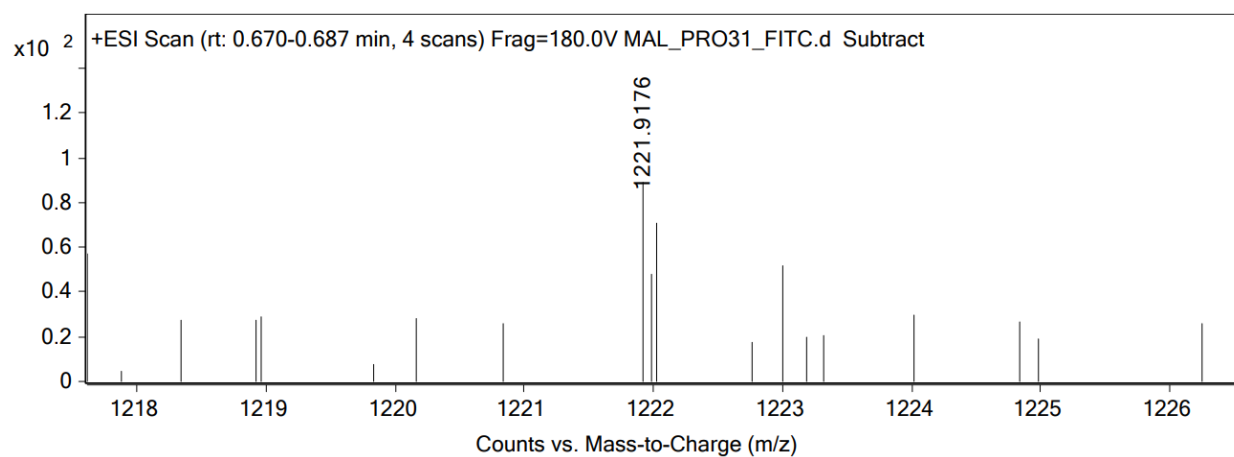
Mal-pro5-FI**ESI-MS calculated $[M + H]^+$: 1140.4672, found: 1140.4670**

Mal-pro7-FI**ESI-MS calculated $[M + H]^+$: 1334.5727, found: 1334.5716**

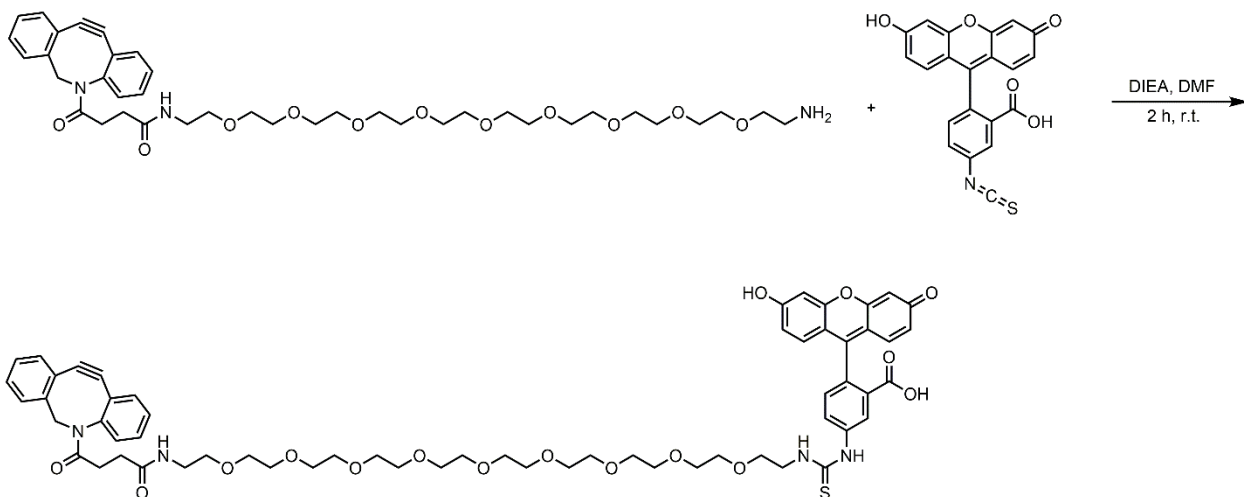
Mal-pro₁₀-FI**ESI-MS calculated $[M + 2H]^{2+}$: 813.8611, found: 813.8690**

Mal-pro₁₃-FI**ESI-MS calculated $[M + 2H]^{2+}$: 959.4403, found: 959.4489**

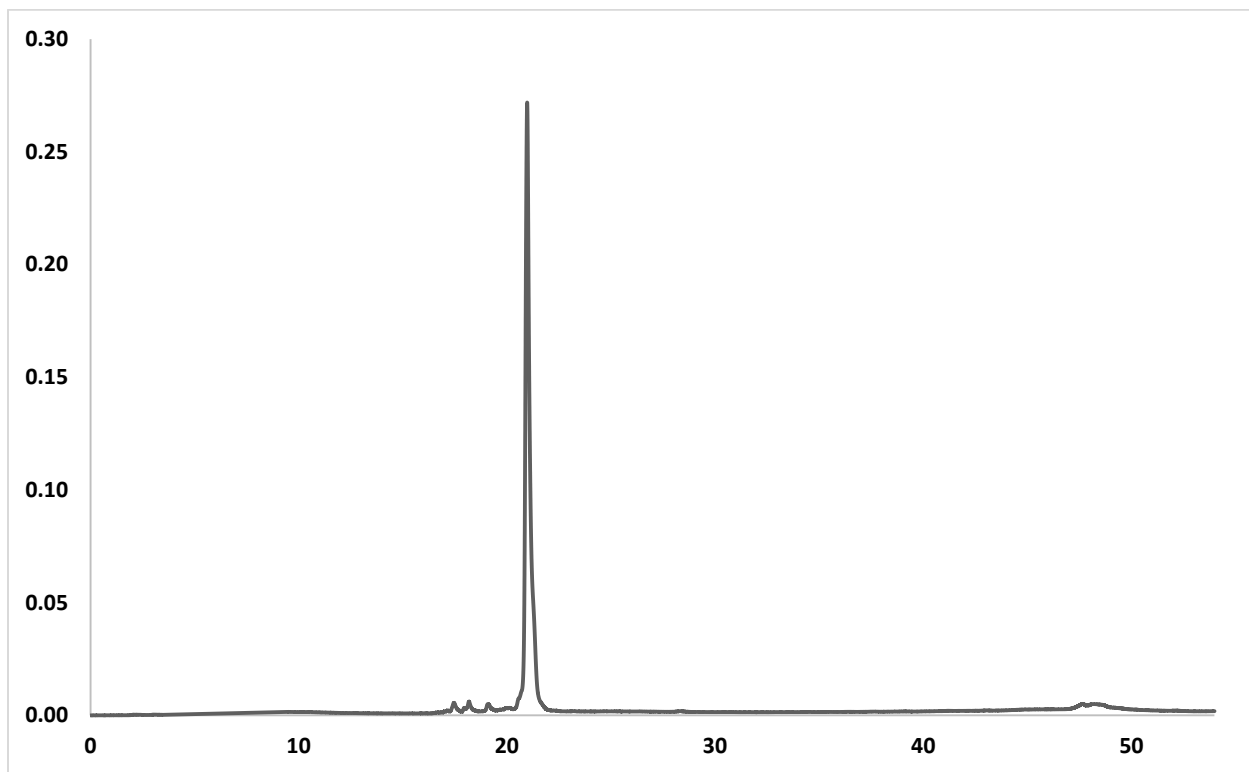
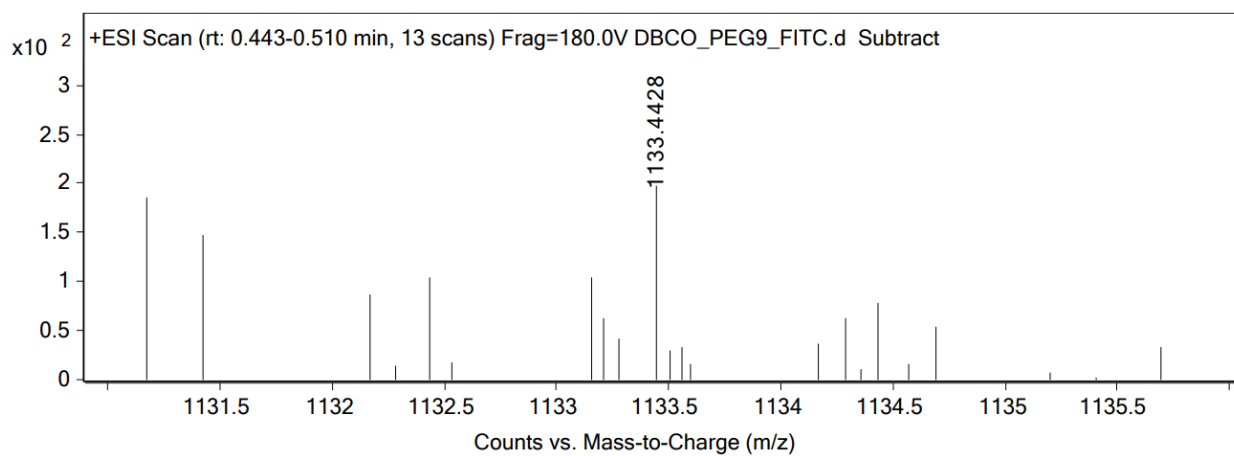
Mal-pro₁₆-FI**ESI-MS calculated [M + H]⁺: 1104.5274, found: 1104.5062**

Mal-pro₃₁-FI**ESI-MS calculated $[M + 3H]^{3+}$: 1221.9512, found: 1221.9176**

Scheme 3.8 Synthesis of DBCO-peg₉-FI



DBCO-PEG₉-amine was added to fluorescein isothiocyanate isomer I (2 eq) and DIEA (2 eq) in DMF and allowed to react at ambient temperature for 2 h. The reaction mix was purified using reverse phase HPLC using 70% H₂O/ 30% MeOH starting and gradient elution. The sample was analyzed for purity using a Waters 1525 Binary HPLC Pump using a Phenomenex Luna 5u C8(2) 100A (250 x 4.60 mm) column; gradient elution with H₂O/CH₃CN (DMSO signal has been subtracted).

DBCO-peg₉-FI**ESI-MS calculated [M + H]⁺: 1133.4423, found:1133.4428**

3.8 References for Material and Methods

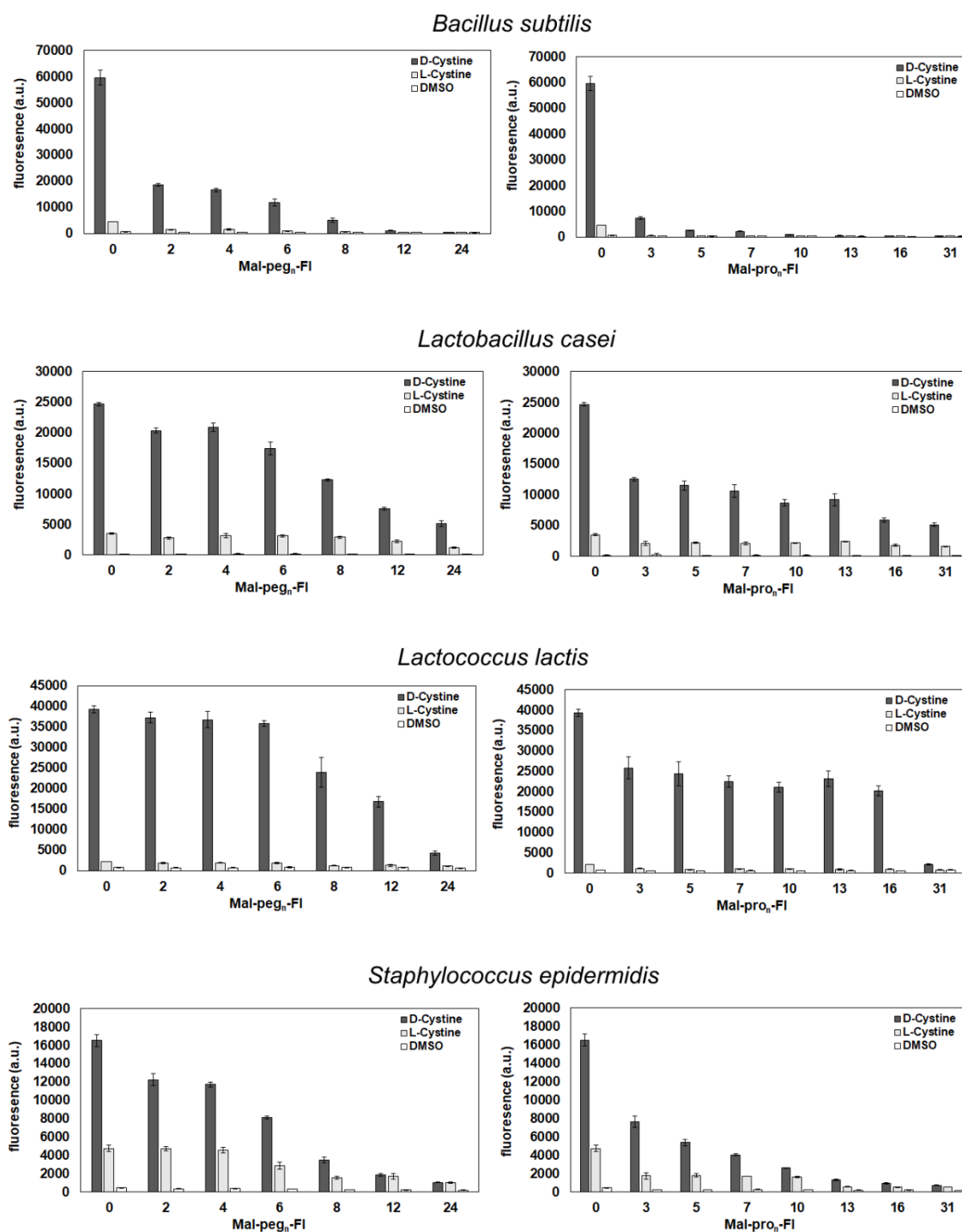
1. Guvench, O.; Mallajosyula, S. S.; Raman, E. P.; Hatcher, E.; Vanommeslaeghe, K.; Foster, T. J.; Jamison, F. W., 2nd; Mackerell, A. D., Jr., CHARMM additive all-atom force field for carbohydrate derivatives and its utility in polysaccharide and carbohydrate-protein modeling. *J Chem Theory Comput* **2011**, 7 (10), 3162-3180.
2. Best, R. B.; Zhu, X.; Shim, J.; Lopes, P. E.; Mittal, J.; Feig, M.; Mackerell, A. D., Jr., Optimization of the additive CHARMM all-atom protein force field targeting improved sampling of the backbone phi, psi and side-chain chi(1) and chi(2) dihedral angles. *J Chem Theory Comput* **2012**, 8 (9), 3257-3273.
3. Vanommeslaeghe, K.; MacKerell, A. D., Jr., Automation of the CHARMM General Force Field (CGenFF) I: bond perception and atom typing. *J Chem Inf Model* **2012**, 52 (12), 3144-54.
4. Jorgensen, W. L.; Chandrasekhar, J.; Madura, J. D.; Impey, R. W.; Klein, M. L., Comparison of Simple Potential Functions for Simulating Liquid Water. *Journal of Chemical Physics* **1983**, 79 (2), 926-935.
5. Jo, S.; Kim, T.; Iyer, V. G.; Im, W., CHARMM-GUI: a web-based graphical user interface for CHARMM. *J Comput Chem* **2008**, 29 (11), 1859-65.
6. Eastman, P.; Swails, J.; Chodera, J. D.; McGibbon, R. T.; Zhao, Y.; Beauchamp, K. A.; Wang, L. P.; Simmonett, A. C.; Harrigan, M. P.; Stern, C. D.; Wiewiora, R. P.; Brooks, B. R.; Pande, V. S., OpenMM 7: Rapid development of high performance algorithms for molecular dynamics. *PLoS Comput Biol* **2017**, 13 (7), e1005659.
7. Lee, J.; Cheng, X.; Jo, S.; MacKerell, A. D.; Klauda, J. B.; Im, W., CHARMM-GUI Input Generator for NAMD, Gromacs, Amber, Openmm, and CHARMM/OpenMM Simulations using the CHARMM36 Additive Force Field. *Biophys J* **2016**, 110 (3), 641a-641a.

3.9 Extensions

Demonstrated in this chapter is a systematic characterization of accessibility to the surface of the PG layer in the Gram-positive organism *S. aureus*. Also demonstrated is the power of this assay to identify how the flexibility of a molecule impacts its ability to reach a surface target and the key features of the cell wall of *S. aureus* that interfere with surface accessibility. Using this same system we aim to investigate the surface accessibility of various Gram-positive bacteria. In keeping with our initial study, a thiol functional group was chosen to be installed within bacterial PG. The cysteine-based label chosen was based on the results obtained with *S. aureus*. The oxidized form of D-cysteine, D-cystine, had appreciable incorporation levels that resulted in robust reporter molecule signals when tested in *S. aureus*.

Accessibility to the bacterial PG layer by molecules introduced to the extracellular space should be tied to the incoming molecules physiochemical properties (e.g. flexibility, size, and charge). As previously described on this chapter, we assembled two libraries of probes in order to investigate the accessibility to the PG layer in various Gram-positive organisms. One library contained a flexible polar polyethylene glycol (PEG) spacer and the other a rigid polyproline spacer of varying lengths. All members of both libraries displayed a reactive maleimide moiety and a fluorophore, fluorescein. Surface accessibility was assessed for all the following organisms: *Bacillus subtilis*, *Lactobacillus casei*, *Lactococcus lactis*, *Staphylococcus epidermidis*, *Streptococcus pyogenes*, *Enterococcus faecalis*, and *Listeria monocytogenes*. This covers both commensal bacteria and those that are pathogenic. The assay was performed as detailed previously in this chapter, bacterial cells were grown overnight in the presence of D-cystine, the enantiomer, L-cystine, or DMSO to promote incorporation throughout the PG scaffold. After growth overnight, due to the oxidizing nature of the culture media, cells were treated with the reducing agent dithiothreitol (DTT) to unmask the free thiols on the PG which were expected to exist primarily as disulfides. To remove excess reducing agent, cells were washed with phosphate

buffered saline (PBS) and incubated with either maleimide-modified fluorescein (**Mal-FI**) or members of both libraries (**Mal-peg_n-FI** or **Mal-pro_n-FI**). Cellular fluorescence levels were then quantified by flow cytometry. (**Figure 3.22**)



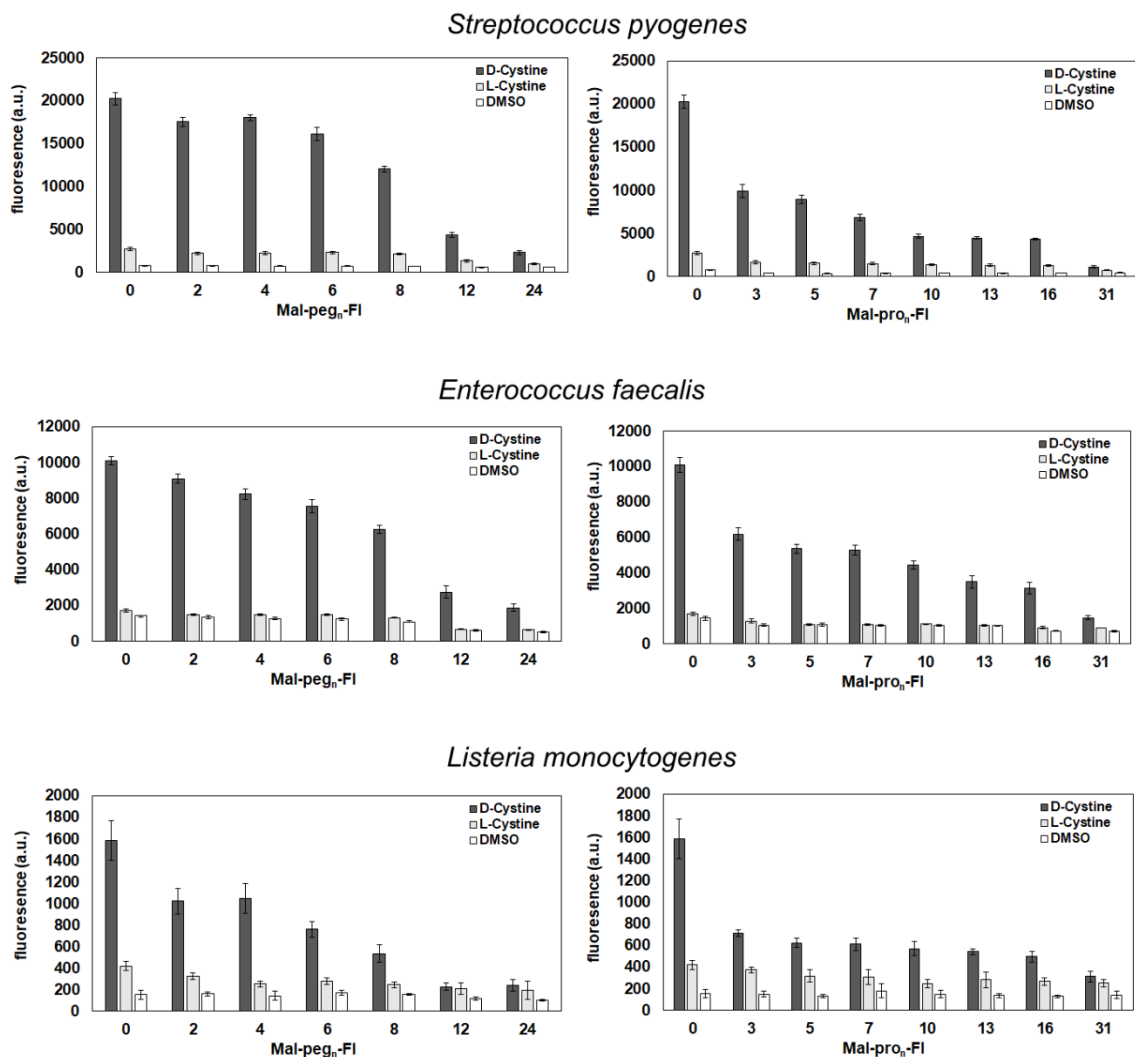


Figure 3.22 Gram-positive organism scan after treatment with 1mM D-cystine or L-cystine, reduced with DTT (5 mM), and incubated with 25 μ M of designated accessibility probes. Analysis was performed *via* flow cytometry.

Similar to the profiles seen for multiple strains of *S. aureus*, a striking difference in surface accessibility can be seen between the two libraries for most of the organisms tested. The increasing length of the PEG spacer in the **Mal-peg_n-FI** probes resulted in a gradual decrease in fluorescence, whereas the **Mal-pro_n-FI** probes resulted in a sharper decrease of fluorescence. Treatment with L-cystine,

which is not expected to be processed by PG biosynthesis machinery, resulted in minimal fluorescence increase.

In an effort to translate the assay to Gram-negative bacteria, work is being done to perform BioOrthogonal Non-Canonical Amino acid Tagging (BONCAT) in *Escherichia coli* (*E. coli*) using L-azidohomoalanine (AHA), which is an analog of L-methionine.¹⁻³ The substrate flexibility of methionyl-tRNA synthetase allows for the incorporation of AHA into proteins that are newly synthesized during cell growth, including those that are in the outer membrane and potentially surface exposed. These azide tagged cells can then be tested in the accessibility assay however with a new library. The new library being built consists of a DiBenzoCycloOctyne (DBCO) reactive moiety and a fluorescein as the reporter. The linker between the two is either a rigid polyproline or a flexible Gly-Gly-Gly-Ser repeating unit. (**Figure 3.23**)

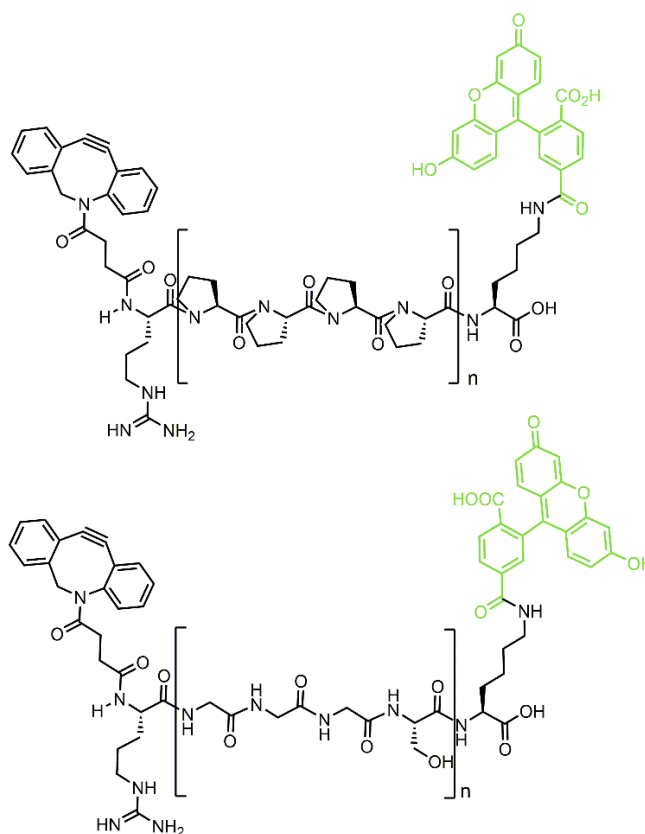


Figure 3.23 Structural depictions of the new accessibility library, where n= number of repeating linker units.

The synthesis of both libraries was accomplished on solid support using standard peptide coupling procedures. However, DBCO is acid sensitive and prone to a rearrangement that results in an inactive form of the molecule. Moreover, there is no shift in molecular weight after rearrangement so it can be easily missed. Unfortunately during synthesis we encountered this rearrangement, as evidenced by the loss of UV-VIS spectra integrity (critical wavelengths: 290 nm and 309 nm for DBCO). (**Figure 3.24**) To use DBCO in our synthesis it requires either a resin that can be cleaved in low acid conditions, high acid conditions with a special protecting group, or for it to be conjugated to the peptide in solution.⁴⁻⁶

Effort is also being made to apply the accessibility assay to mycobacteria. It has been shown that mycobacteria can process a modified trehalose sugar and metabolically incorporate it into the mycomembrane as either an arabinogalactan (AG) linked mycolate, trehalose monomycolate (TMM), or trehalose dimycolate (TDM).⁷⁻¹² Interestingly TMM can be metabolically processed into TDM and an AG-linked mycolate. Trehalose probes, 2-trehalose-azido and 6-trehalose-azido, have been obtained from a collaborator and preliminary incorporation assays have been run. *Mycobacterium smegmatis* are grown to mid-log (OD₆₀₀ 0.8-1.2), diluted with media to OD₆₀₀ 0.4, and incubated with either sugar for 4 hours. These cells are subsequently harvested and labeled with 25 μ M **DBCO-FI**. The eventual aim will be to label the trehalose-azide incorporated cells with the DBCO-based library and gauge accessibility to the mycomembrane surface. (**Figure 3.25**)

Another application of the DBCO functionalized library involves the use of the assay platform SaccuFlow described in Chapter 5. While the current assay can depict accessibility to the surface of peptidoglycan in whole cells, that is really describing molecule permeation through the surface polymers and proteins. A SaccuFlow type assay can describe instead the permeation of molecules through the peptidoglycan matrix itself. The assay would entail metabolically labeling the peptidoglycan of live cells with **D-LysAZ**, harvesting the intact peptidoglycan layer or sacculi from those cells, treating that sacculi with the DBCO-based library, and analyzing the fluorescence signal of the sacculi on the flow cytometer.

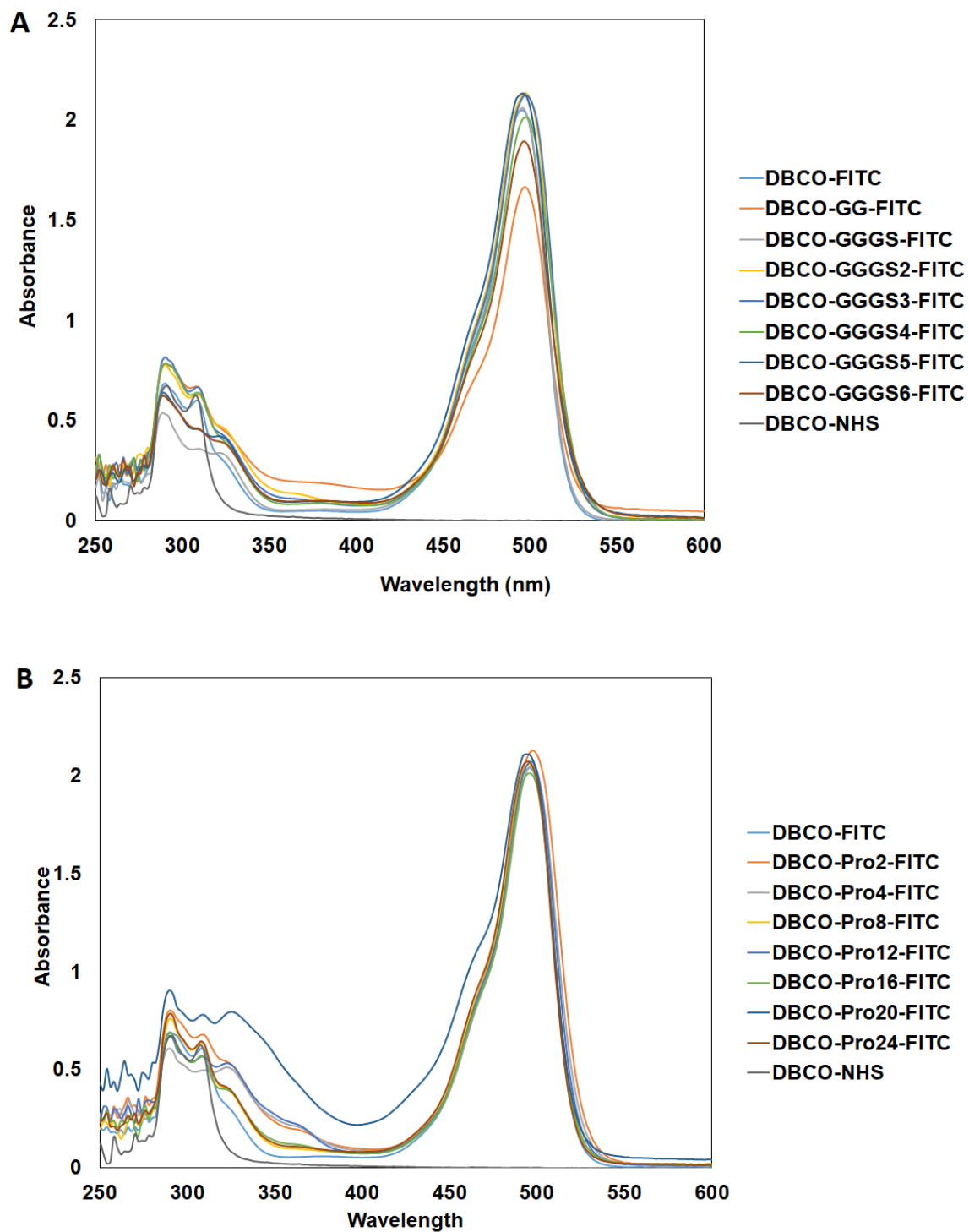


Figure 3.24 UV-VIS spectra of the DBCO library (A) GGGs-based and (B) proline-based. Critical wavelengths: 290 nm and 309 nm for DBCO.

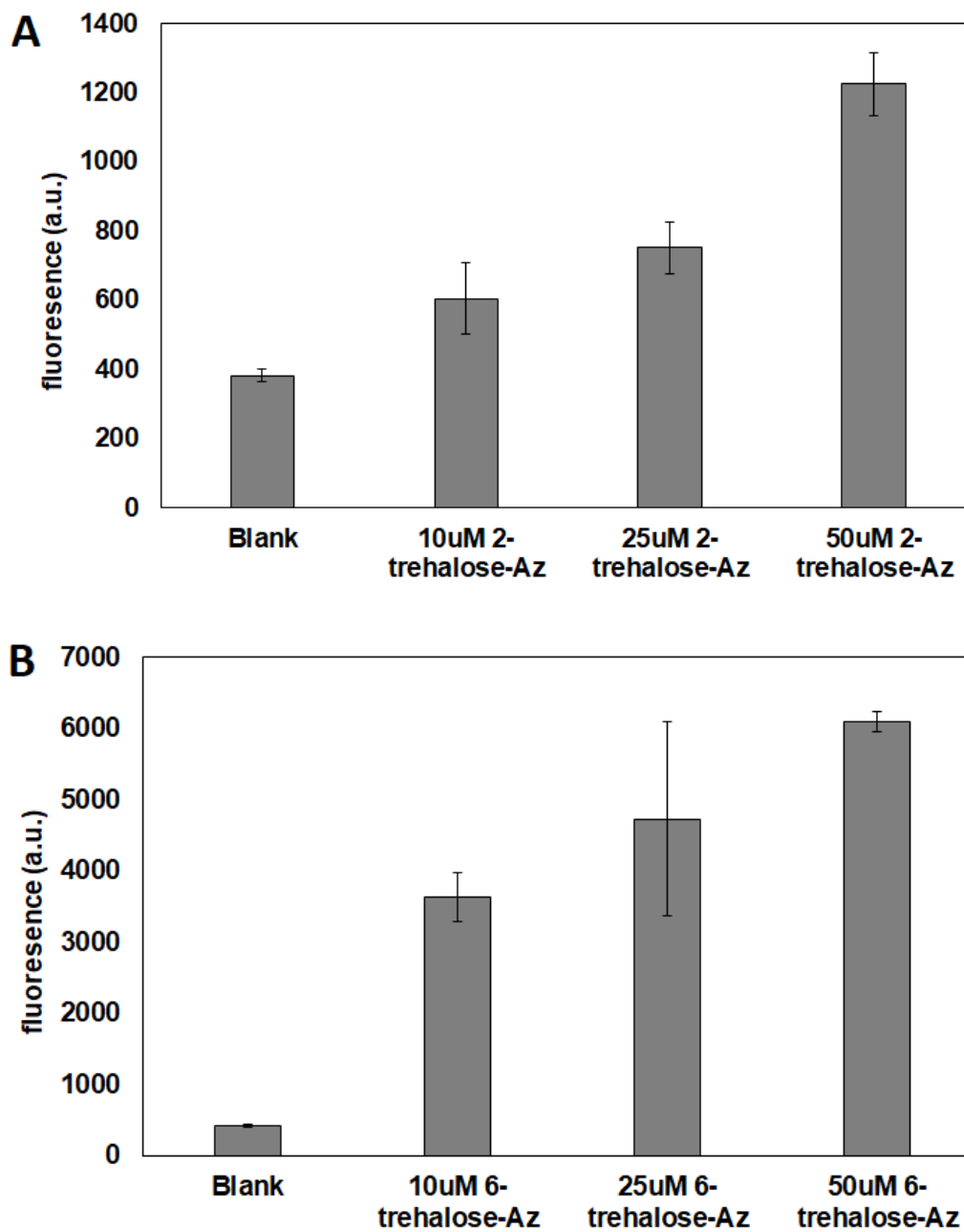


Figure 3.25 Flow cytometry analysis of *Mycobacterium smegmatis* treated with increasing concentrations of azido modified trehalose, (A) 2-trehalose-azido and (B) 6-trehalose-azido, after labeling with 25 μ M **DBCO-FITC**.

3.10 References for Extensions

1. Tom Dieck, S., Muller, A., Nehring, A., Hinz, F. I., Bartnik, I., Schuman, E. M., Dieterich, D. C. Metabolic labeling with noncanonical amino acids and visualization by chemoselective fluorescent tagging. *Curr. Protoc. Cell Biol.* **2012**, Chapter 7, Unit 7.11.
2. Tom Dieck, S., Kochen, L., Hanus, C., Heumuller, M., Bartnik, I., Nassim-Assir, B., Merk, K., Mosler, T., Garg, S., Bunse, S., Tirrell, D. A., Schuman, E. M. Direct visualization of newly synthesized target proteins in situ. *Nat. Methods.* **2015**, 12, 411-414.
3. Dieterich, D. C., Hodas, J. J., Gouzer, G., Shadrin, I. Y., Ngo, J. T., Triller, A., Tirrell, D. A., Schuman, E. M. In situ visualization and dynamics of newly synthesized proteins in rat hippocampal neurons. *Nat. Neurosci.* **2010**, 13, 897-905.
4. Wang, X.; Gobbo, P.; Suchy, M.; Workentin, M. S.; Hudson, R. H. E., Peptide-decorated gold nanoparticles via strain-promoted azide-alkyne cycloaddition and post assembly deprotection. *RSC Advances* **2014**, 4 (81), 43087-43091.
5. Yoshida, S.; Hatakeyama, Y.; Johmoto, K.; Uekusa, H.; Hosoya, T., Transient protection of strained alkynes from click reaction via complexation with copper. *J Am Chem Soc* **2014**, 136 (39), 13590-3.
6. Chigrinova, M.; McKay, C. S.; Beaulieu, L. P.; Udachin, K. A.; Beauchemin, A. M.; Pezacki, J. P., Rearrangements and addition reactions of biarylazacyclooctynones and the implications to copper-free click chemistry. *Org Biomol Chem* **2013**, 11 (21), 3436-41.
7. Dai, T.; Xie, J.; Zhu, Q.; Kamariza, M.; Jiang, K.; Bertozzi, C. R.; Rao, J., A Fluorogenic Trehalose Probe for Tracking Phagocytosed Mycobacterium tuberculosis. *J Am Chem Soc* **2020**, 142 (36), 15259-15264.
8. Kamariza, M.; Shieh, P.; Ealand, C. S.; Peters, J. S.; Chu, B.; Rodriguez-Rivera, F. P.; Babu Sait, M. R.; Treuren, W. V.; Martinson, N.; Kalscheuer, R.; Kana, B. D.; Bertozzi, C. R., Rapid detection of Mycobacterium tuberculosis in sputum with a solvatochromic trehalose probe. *Sci Transl Med* **2018**, 10 (430).

9. Rodriguez-Rivera, F. P.; Zhou, X.; Theriot, J. A.; Bertozzi, C. R., Visualization of mycobacterial membrane dynamics in live cells. *J Am Chem Soc* **2017**, *139* (9), 3488-3495.
10. Swarts, B. M.; Holsclaw, C. M.; Jewett, J. C.; Alber, M.; Fox, D. M.; Siegrist, M. S.; Leary, J. A.; Kalscheuer, R.; Bertozzi, C. R., Probing the mycobacterial trehalome with bioorthogonal chemistry. *J Am Chem Soc* **2012**, *134* (39), 16123-6.
11. Kavunja, H. W.; Biegas, K. J.; Banahene, N.; Stewart, J. A.; Piligian, B. F.; Groenevelt, J. M.; Sein, C. E.; Morita, Y. S.; Niederweis, M.; Siegrist, M. S.; Swarts, B. M., Photoactivatable Glycolipid Probes for Identifying Mycolate-Protein Interactions in Live Mycobacteria. *J Am Chem Soc* **2020**, *142* (17), 7725-7731.
12. Fiolek, T. J.; Banahene, N.; Kavunja, H. W.; Holmes, N. J.; Rylski, A. K.; Pohane, A. A.; Siegrist, M. S.; Swarts, B. M., Engineering the Mycomembrane of Live Mycobacteria with an Expanded Set of Trehalose Monomycolate Analogues. *Chembiochem* **2019**, *20* (10), 1282-1291.

Chapter 4. Transposon Screen of Surface Accessibility in *Staphylococcus aureus*

4.1 Abstract

Bacterial cell walls represent one of the most prominent targets of antibacterial agents. These agents include natural products (e.g., vancomycin) and proteins stemming from the innate immune system (e.g., peptidoglycan-recognition proteins and lysostaphin). Among bacterial pathogens that infect humans, *Staphylococcus aureus* (*S. aureus*) continues to impose a tremendous healthcare burden across the globe. *S. aureus* has evolved countermeasures that can directly restrict the accessibility of innate immune proteins, effectively protecting itself from threats that target key cell wall components. We recently described a novel assay that directly reports on the accessibility of molecules to the peptidoglycan layer within the bacterial cell wall of *S. aureus*. The assay relies on site-specific chemical remodeling of the peptidoglycan with a bioorthogonal handle. Here, we disclose the application of our assay to a screen of a nonredundant transposon mutant library for susceptibility of the peptidoglycan layer with the goal of identifying genes that contribute to the control of cell surface accessibility. We discovered several genes that resulted in higher accessibility levels to the peptidoglycan layer and showed that these genes modulate sensitivity to lysostaphin. These results indicate that this assay platform can be leveraged to gain further insight into the biology of bacterial cell surfaces.

4.2 Introduction

Bacterial resistance to antibiotics has become an imminent threat to global health and must be met with an antibiotic pipeline revitalization or, in lieu of that, alternative methods to combat bacterial infections. Intrinsic resistance is a multifactorial phenomenon but sometimes it can be mediated by a simple lack of accessibility to the bacterial targets.¹⁻³ Recent efforts have led to the discovery of molecules that can potentiate antibiotics by improving permeation to and across the bacterial cell surface. For example, Gram-negative pathogens can be sensitized by co-treatment with polymyxins (and similar outer membrane

destabilizers), which improve permeation of antimicrobials through the bacterial cell wall.⁴⁻⁸ Likewise, positively charged Branched PolyEthylenImine (BPEI) has been shown to potentiate β -lactam antibiotics against the Gram-positive pathogen methicillin resistant *Staphylococcus aureus* (MRSA).⁹⁻¹⁰ It was proposed that BPEI neutralization of negatively charged polymers on the bacterial cell surface improved permeability.¹¹ These examples demonstrate that improved permeation to the essential cell wall components can be a powerful modality of reducing intrinsic resistance to small molecule antibacterials and immune proteins.¹²

The cell walls of bacteria are complex in structure and composition. For the Gram-positive bacterium, *Staphylococcus aureus* (*S. aureus*), the cell wall is composed of a thick peptidoglycan (PG) scaffold that is shielded by proteins and other biomacromolecules (**Figure 4.1**).¹³ The proteins are covalently anchored onto the PG *via* the transpeptidase, sortase A.¹⁴⁻¹⁵ The cell surface is further functionalized by wall teichoic acids (WTAs), which are anionic glycopolymers that are covalently anchored onto the PG, and lipoteichoic acids (membrane anchored).¹⁶ The restricted accessibility afforded by teichoic acids and other surface-bound macromolecules has been implicated in the virulence of Staphylococci. In *Drosophila*, it was recently discovered that the accessibility of peptidoglycan recognition proteins (PGRPs) to PG plays a determinant role in the host immunity to infection.¹⁷ Removal of WTAs resulted in considerably increased accessibility of PGRPs to the PG and predisposed *S. aureus* to PGRP-mediated immunity. Additionally, it has been found that WTA-deficient *S. aureus* fails to colonize the nasal cavities of rats.¹⁸ More recently, it was established that *Staphylococcus epidermidis* shift from a commensal to pathogen lifestyle upon expression of *S. aureus*-like WTAs.¹⁹ Aside from modulating immunity, PG accessibility can potentially impact drug discovery based on the fact that a number of FDA approved antibiotics work by inhibiting steps in the bacterial PG biosynthesis pathway.²⁰⁻²¹ The essential nature of accessibility to the PG scaffold by immune proteins and antibiotics alike means that there is a need to better understand the genes that control surface accessibility.

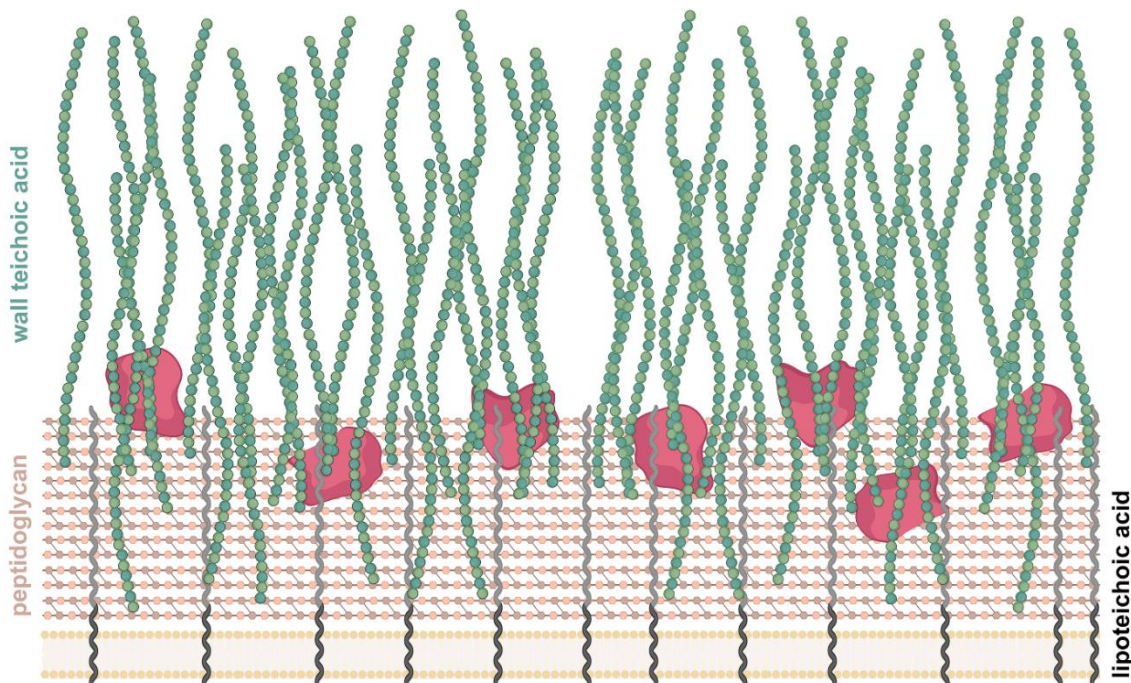


Figure 4.1 Schematic representation of the surface of Gram-positive bacteria. The PG scaffold is heavily decorated with a number of biomacromolecules, including WTAs, LTAs, and proteins. These features can reduce the permeation of extracellular proteins and molecules to the PG scaffold, which can modulate host immunity and the potency of antibacterial agents.

Among Gram-positive pathogens, *S. aureus* has proven to be particularly challenging to treat; it is a formidable foe, as it is well suited to evade attacks by the host immune system²² and it is a pathogen that can readily become resistant to standard of care therapies.²³ The difficulty in finding new efficacious antibiotics against *S. aureus* highlights the need to explore less conventional therapeutic approaches such as antibiotic adjuvants or immunotherapies.²⁴⁻²⁹ For example, adjuvants can potentiate antibiotics by improving their accessibility to their cognate molecular targets. Likewise, anti-infective immunotherapeutics (e.g., antibody recruiting agents developed by our lab^{24-27, 29}) work by targeting specific macromolecules on bacterial cell surfaces. Despite the pivotal role of surface accessibility in bacterial pathogenesis, to date there has not been a systematic

analysis of the genes that control penetration of biomacromolecules across cell surfaces of *S. aureus*; information that can directly impact current therapies and the development of alternative treatments. To address this, we performed a screen against a non-redundant transposon mutant library using a robust assay that reports on surface accessibility in *S. aureus*.

4.3 Results and Discussion

We set out to comprehensively screen nonessential genes in *S. aureus* for their ability to alter accessibility to the PG scaffold. The basis of the screening assay is site-specific incorporation of a bioorthogonal handle *via* metabolic remodeling of bacterial PG.¹¹ More specifically, an unnatural amino acid (**D-LysAz**) is supplemented in the media, inoculated with *S. aureus*, and cultured overnight (**Figure 4.2A**). During PG biosynthesis and assembly, transpeptidases catalyze the replacement of the 5th position D-alanine on the stem peptide within the bacterial PG scaffold for **D-LysAz**, thus leading to the covalent installation of the azido-handle (**Figure 4.2B**). With the azido group installed through the entire PG scaffold, treatment of cells with a complementary DiBenzoCycloOctyne (DBCO) handle conjugated to fluorescein (**DBCOfl**) leads to the specific tagging of the bacterial PG with fluorescent moieties (**Figure 4.2C**).³⁰⁻³¹ We previously showed that cellular fluorescence levels reflect the ability of molecules to reach the PG scaffold and consequently result in a covalent tag. We hypothesized that this reporter assay could be leveraged to identify genes that modulate PG accessibility in *S. aureus*, thus revealing genes that have implications in immunity and drug discovery. By screening a non-redundant library of transposon mutants, we reasoned that any mutants exhibiting increased cellular fluorescence levels could identify potential genetic alterations that result in higher surface accessibility.

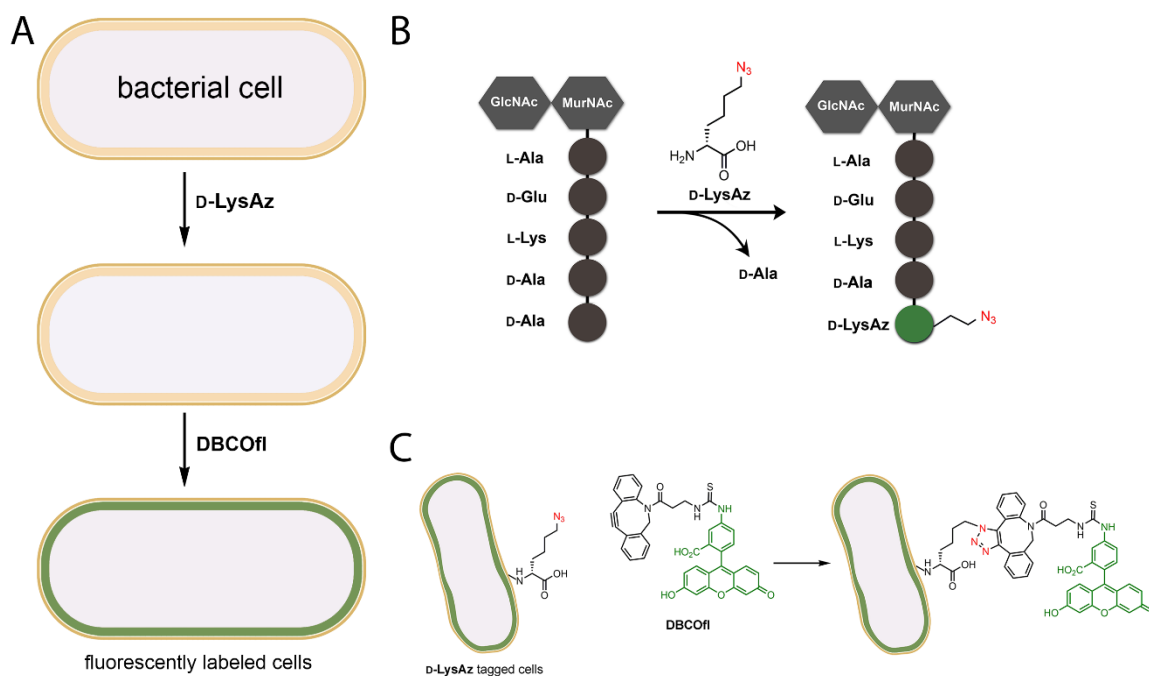


Figure 4.2 (A) Live cell labeling with **D-LysAz** and **DBCOfl**. Cells are analyzed by the flow cytometer to quantify modification with **DBCOfl**. (B) The unnatural amino acid (**D-LysAz**) is enzymatically installed in place of the terminal D-alanine on the stem peptide within the bacterial PG during cellular growth. (C) Chemical structures depicting the reaction between the azido moiety and DBCO.

First, we demonstrated that the assay performed as expected in wildtype (WT) *S. aureus* cells by supplementing the PG label (**D-LysAz**) during overnight culture. Subsequent treatment with **DBCOfl** resulted in cellular fluorescence levels that were ~6-fold and ~8-fold higher than no amino acid and the **L-LysAz**, respectively (**Figure 4.3A**). We³²⁻³³ and others³⁴⁻³⁷ had previously demonstrated that the enantiomeric **L-LysAz** does not incorporate into the growing PG scaffold of bacteria. These results confirm that cellular fluorescence increases in a manner that is dependent on PG remodeling with azido handles.

To demonstrate the effect of surface accessibility, a similar labeling protocol was performed with *tarO*-deleted *S. aureus*, which results in WTA-free *S. aureus* cells.^{16, 38-39} Fluorescence levels of $\Delta tarO$ *S. aureus* labeled with **D-LysAz** were

~2-fold higher than WT cells (**Figure 4.3A**). These results are consistent with previous findings showing that WTAs control the accessibility of immunoproteins to the PG.^{17, 40-41}

We then performed an additional set of experiments to confirm that the fluorescent reporter handle reached the PG scaffold. Our research lab recently described an assay (SaccuFlow) that combines the quantification of flow cytometry with the analysis of bacterial sacculi.¹¹ Similar to the whole cell assay described in Figure 2, *S. aureus* cells were treated with **D-LysAz** followed by **DBCOfl**. Instead of analyzing the whole cell, the sacculus was isolated using a standard isolation procedure which includes boiling of cells with SDS (to solubilize biomacromolecules) and treatment with trypsin (to remove proteins anchored on the PG scaffold). Following these steps, the isolated sacculi are analyzed on the flow cytometer. As expected, fluorescence levels of sacculi from cells treated with a combination of **D-LysAz** and **DBCOfl** were ~12-fold and ~9-fold higher than sacculi from cells treated with DMSO or **L-LysAz**, respectively (**Figure 4.3B**). Confocal microscopy confirmed that the whole cells and the isolated sacculi retained the expected size and shape of the fluorescently labeled cells and biomacromolecule, respectively (**insets of Figure 4.3**).

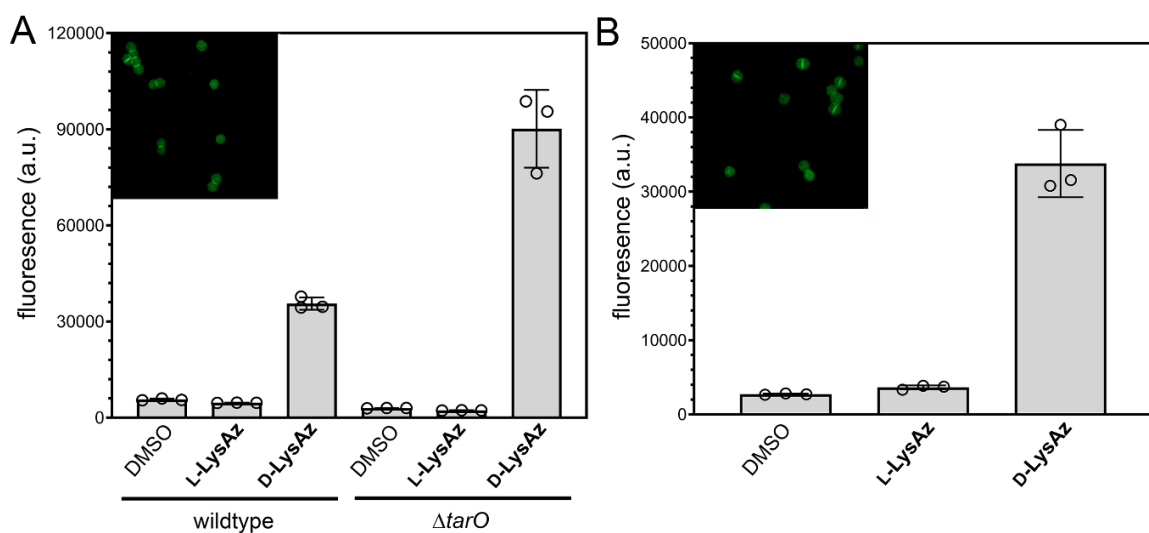


Figure 4.3 (A) Flow cytometry analysis of WT *S. aureus* (ATCC 25923) or *S. aureus* ($\Delta tarO$) treated overnight with DMSO, 1 mM of **L-LysAz**, or 1 mM of **D-LysAz** followed by a treatment with 25 μ M of **DBCOfl**. Inset, confocal microscopy of the WT cells tagged with and treated with **D-LysAz** followed by a treatment with 25 μ M of **DBCOfl**. (B) Sacculi isolated from WT *S. aureus* (ATCC 25923). WT cells were incubated with 1 mM of **D-LysAz**, 1 mM of **L-LysAz**, or DMSO alone overnight. Next, the cells were treated with 25 mM of **DBCO-FI** and subjected to a sacculi isolation protocol. The resulting sacculi were analyzed by flow cytometry. *Inset*, confocal microscopy of the sacculi from WT cells that were treated with **D-LysAz** followed by a treatment with 25 μ M of **DBCOfl**. Data are represented as mean \pm SD (n = 3).

To confirm the metabolic labeling step did not alter cellular viability, a growth curve analysis was performed by monitoring the optical density at 600 nm (**Figure 4.4**). Consistent with our prior results using D-amino acid labeling at the concentrations used in our assay, cellular viability was not impacted. Together, these results show that the combination of PG labeling with **D-LysAz** and treatment with the **DBCOfl** in the media results in the fluorescence tagging of bacterial PG in a manner that reports on cell surface accessibility.

We next shifted our efforts to demonstrate the utility of the surface accessibility assay by screening a library of *S. aureus* transposon mutants to identify genes that could play important roles in controlling permeation to the *S. aureus* cell surface. To this end, a transposon (Tn) insertion mutant library was used as the platform of the screen, which contained 1952 individual strains each with a single insertion within a nonessential gene in *S. aureus* USA300. A major advantage of using the transposon mutant library is the potential to identify genes that were not previously purported to have biological roles related to accessibility, thus revealing new targets for the development of adjuvant agents. Before screening the entire library, the assay was benchmarked in a 384-well format and it was found that the assay could be readily miniaturized (**Figure 4.5**).

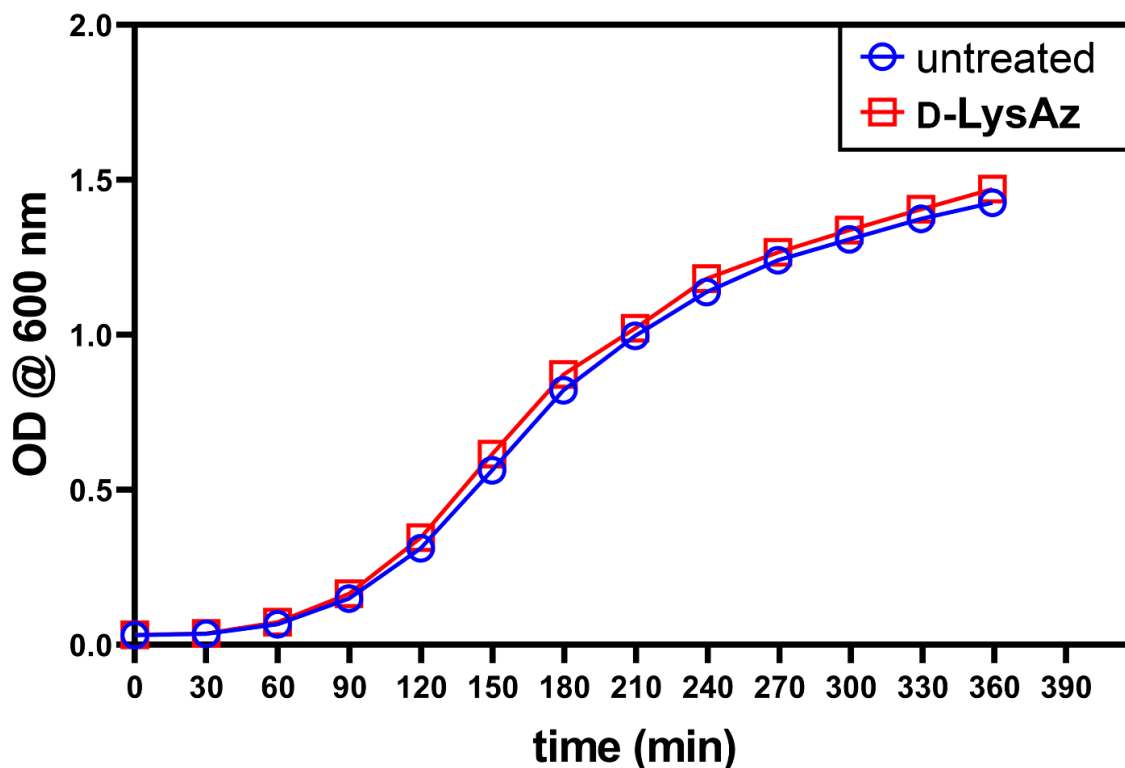


Figure 4.4 Cellular viability of wildtype (WT) *S. aureus* (ATCC 25923) overtime as tracked by optical density (OD) readings at 600 nm. Media containing 1mM **D-LysAz** or DMSO was inoculated by an overnight culture of WT *S. aureus* cells and allowed to grow with shaking at 37°C.

Next, the entire library was screened using the combination of **D-LysAz** and **DBCOfl** (**Figure 4.6A**). While most transposon mutants did not significantly display altered labeling levels, several transposants exhibited elevated fluorescence levels (defined as 33%+ above the average and denoted by the green line). These results suggest that those genes may potentially play a role in surface accessibility.

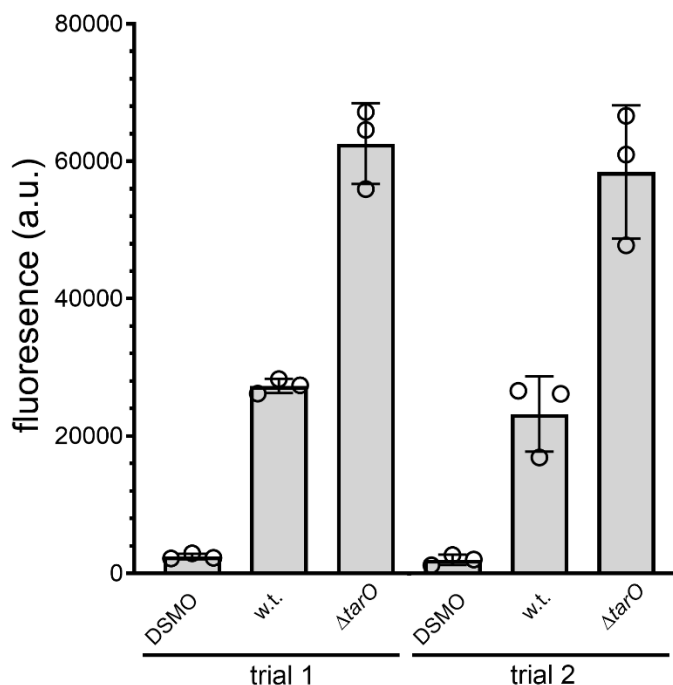


Figure 4.5 Flow cytometry analysis of WT *S. aureus* (ATCC 25923) and $\Delta tarO$ grown in a 384-well plate with media containing 1 mM of **D-LysAz**, 1 mM of **L-LysAz**, or DMSO overnight, followed by a treatment with 25 μ M of **DBCofI**. Cells were analyzed in the 384-well plates using flow cytometry. Two independent trials were performed to demonstrate the stability of the assay. Data are represented as mean \pm SD ($n = 3$).

The 24 transposants with the highest increase in cellular fluorescence were re-assayed in triplicate and transposon mutants that consistently labeled at a higher level than wild-type were selected (**Figure 4.7**). These results showed that four transposants were confirmed to play a determinant role in the accessibility of **DBCofI** to the cell surface, namely SAUSA300_1989, SAUSA300_1984, SAUSA300_1992, and SAUSA300_1467. SAUSA300_1989 and SAUSA300_1992 have been annotated as *agrB* and *agrA*, respectively.⁴² Their protein products play a central role in processing autoinducing peptides in *S. aureus*. Relatedly, the protein product of SAUSA300_1984 (*mroQ*) acts within the

Agr pathway.⁴³ Moreover, the protein product of SAUSA300_1467 (IpdA) has been shown to have a role in branched-chain fatty acid biosynthesis.⁴⁴

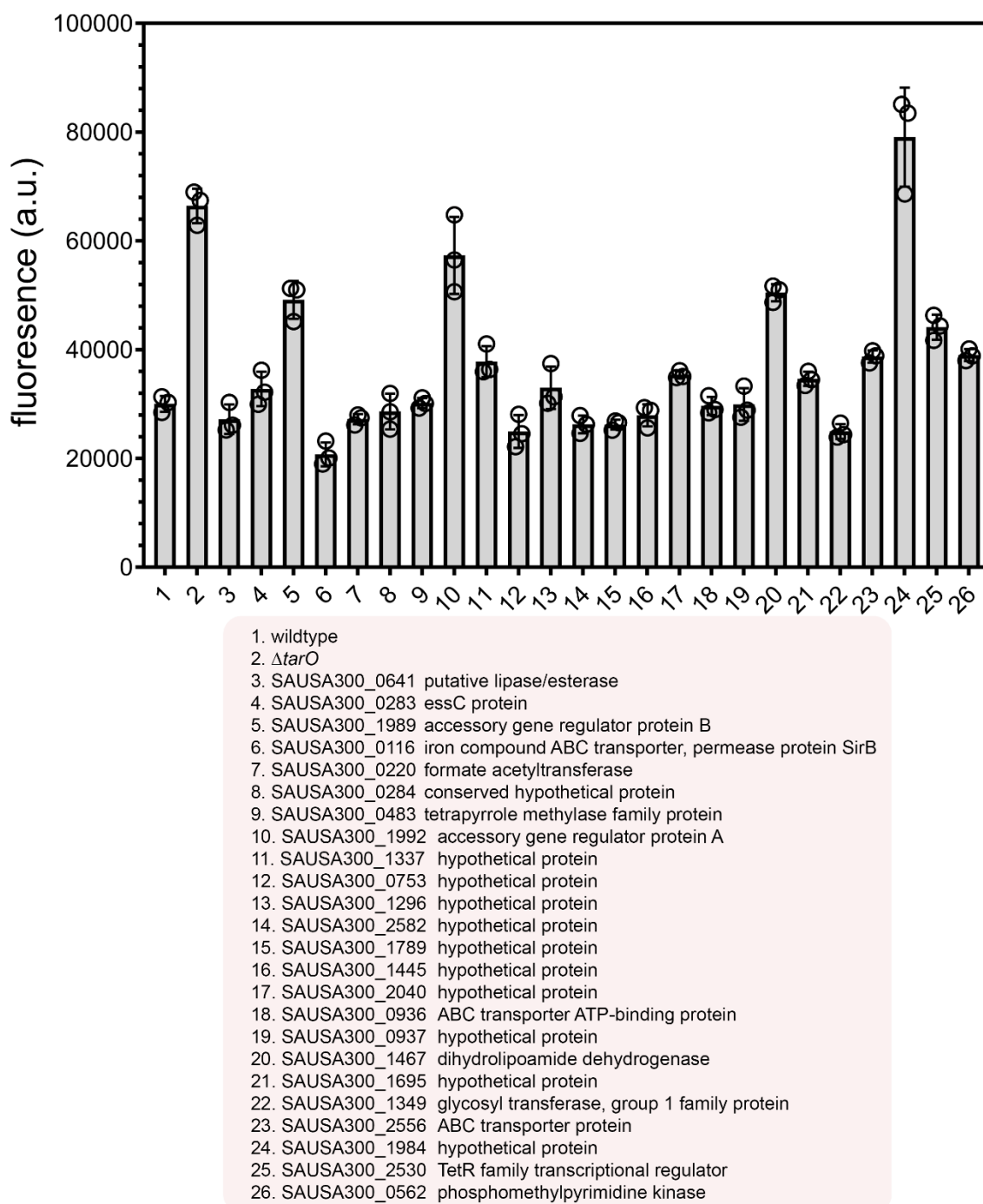


Figure 4.7 Flow cytometry analysis of designated *S. aureus* strains selected from the transposon screen. Cells were grown overnight with 1 mM of **D-LysAz** and

treated the next day with 25 μM of **DBCOfl**. Data are represented as mean \pm SD (n = 3).

The selected transposants were also tested for labeling with a second fluorescent probe (**DBCOaf488**) in order to determine the role of the fluorophore in PG labeling (**Figure 4.8**). The labeling pattern of the **DBCOaf488** mirrored that of **DBCOfl** with the mutants labeling at a higher level than WT.

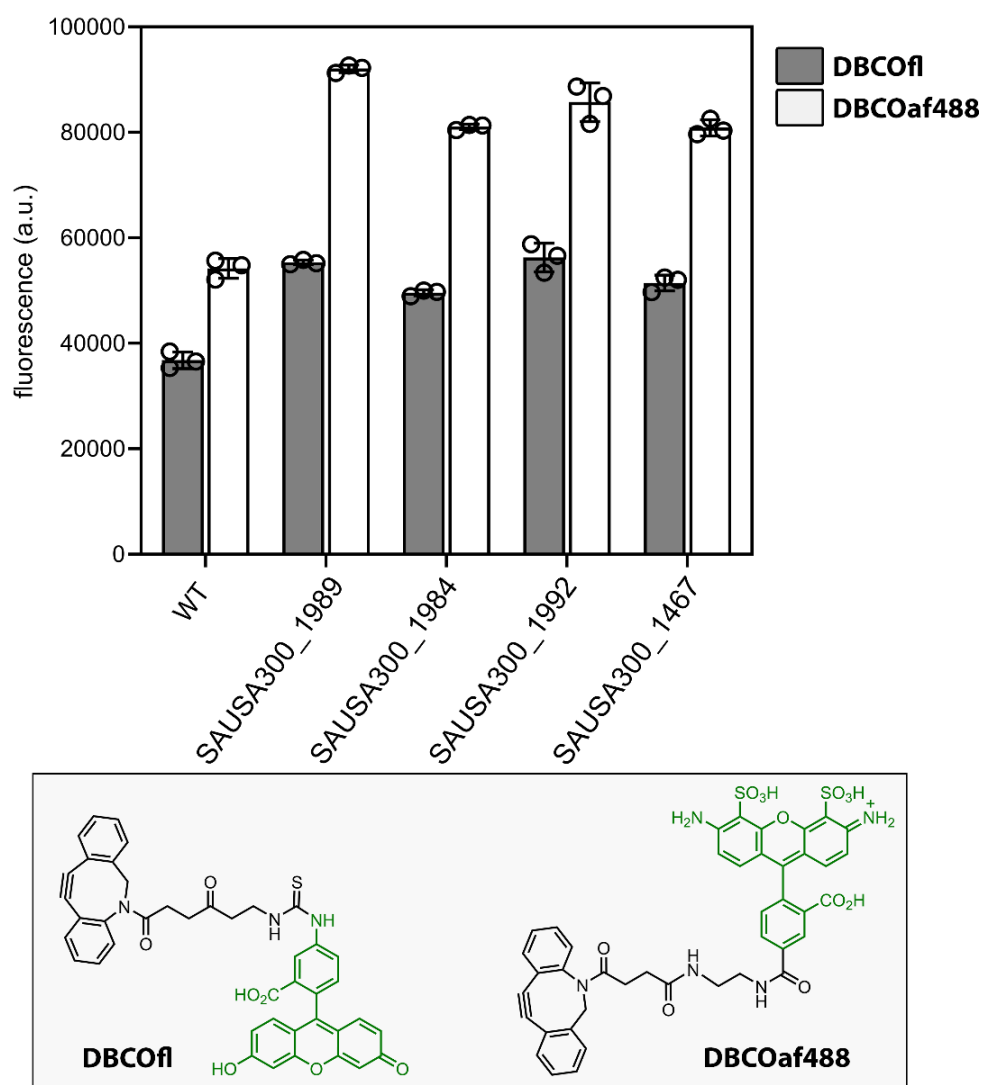


Figure 4.8 Flow cytometry analysis of WT *S. aureus* and selected transposants after treatment with two different fluorescent probes. The cells were grown overnight with 1 mM **D-LysAz**, subsequently labeled with either 25 μM **DBCOfl** or

DBCOaf488, and analyzed by flow cytometry. Data are represented as mean \pm SD (n = 3).

Similarly, we evaluated the impact of a spacer length between the DBCO handle and the fluorescein moiety across the transposants. A polyethylene glycol spacer was inserted between DBCO and fluorescein (**DBCOpegFl**) to test how a larger molecule would compare to the smaller **DBCOfl**. It was observed that increasing the size of the probe resulted in similar profile to that of **DBCOfl**, which indicates that the effect of increased fluorescence in the transposants as compared to WT is relevant for different sized probes (**Figure 4.9**).

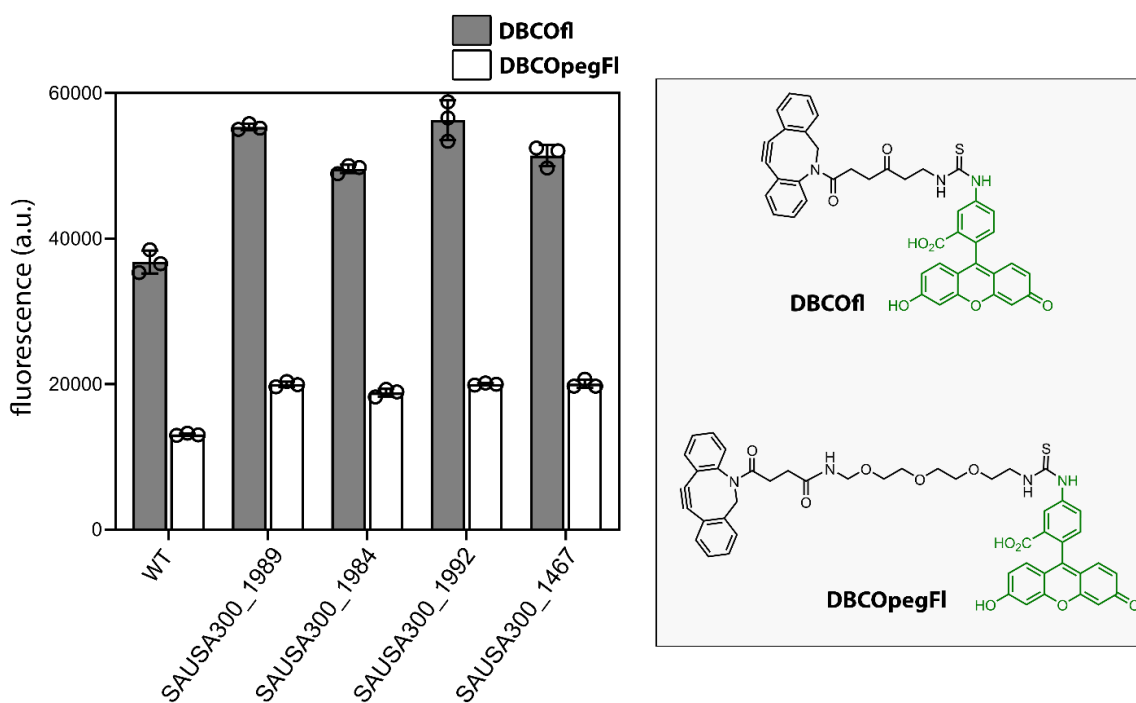


Figure 4.9 Flow cytometry analysis of WT *S. aureus* cells and selected transposants after being grown overnight with 1 mM **D-LysAz** and labeled the next day with either 25 μ M **DBCOfl** or **DBCOpegFl**. Data are represented as mean \pm SD (n = 3).

To assess the overall morphology of the transposants scanning electron microscopy (SEM) imaging was performed, which showed that the general morphology of these strains was similar to that of the WT cells (**Figure 4.10**).

Finally, the identified hits were tested for their susceptibility to a larger molecular weight protein, lysostaphin, which needs to reach the PG layer to impart its antimicrobial activity (**Figure 4.6B**). We reasoned that genes that impact surface accessibility may be able to modulate the activity of lysostaphin by increasing its access to its target biomacromolecule, the bacterial PG. Lysostaphin is a bacteriocin that cleaves the pentaglycine cross-bridges found in the cell walls of *S. aureus*, leading to bacterial lysis.⁴⁵

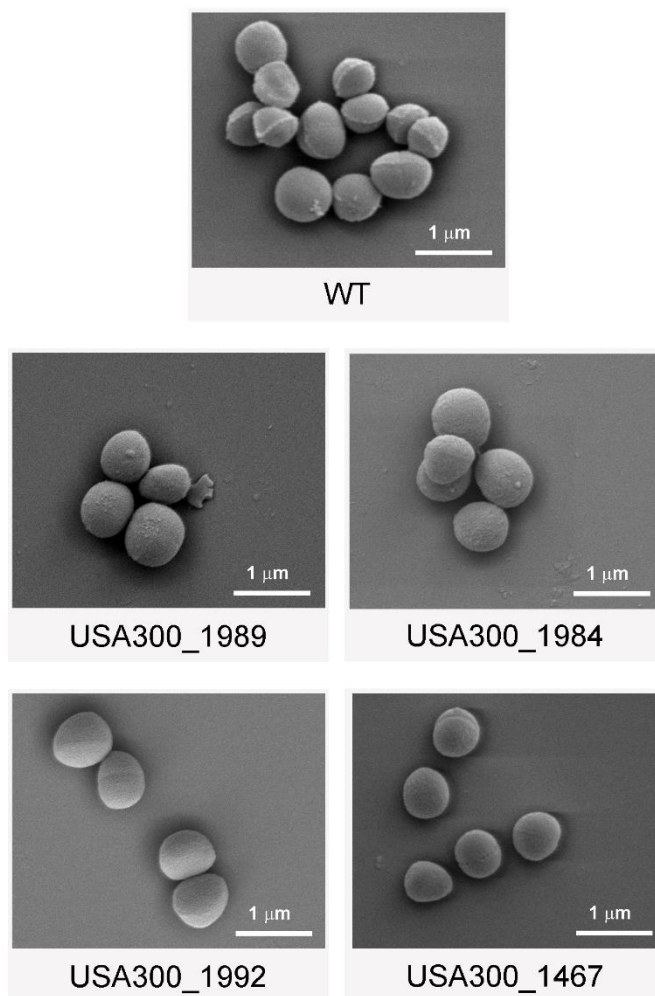


Figure 4.10 Scanning electron microscopy (SEM) images of WT *S. aureus* and selected transposants after overnight growth.

Challenge with lysostaphin showed that disruption to those genes resulted in altered sensitivity, which suggests the possibility that surface accessibility is playing a role lysostaphin activity. Together, this pilot screen confirmed the ability of the assay to be miniaturized to formats that are compatible with high-throughput screening and it reveals potential genes that may control surface accessibility of *S. aureus*.

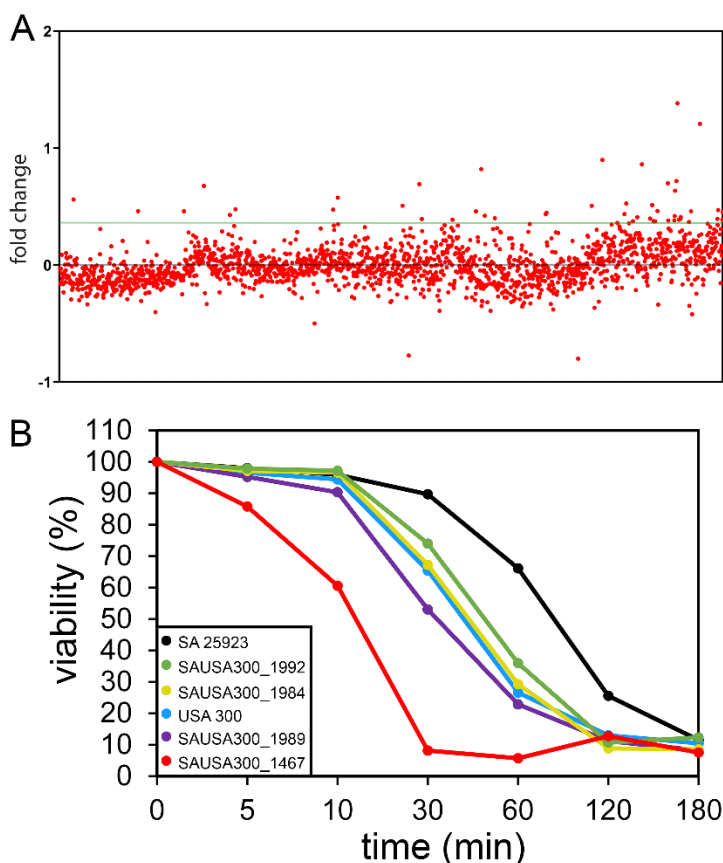


Figure 4.6 (A) Flow cytometry analysis of transposon library in *S. aureus* (ATCC 25923) treated overnight with 1 mM of **D-LysAz**, followed by a treatment with 25 μ M of **DBCOfl**. Fluorescence levels were normalized to the average levels across all transposon mutants. Fold change refers to the ratio of fluorescence of the strain

relative to the library average. Black line represents the zero point (average) and the green line represents +0.33-fold change above the average, which we designated as potential hits. (B) Percent viability of designated transposon mutants and wild-type strains of *S. aureus* when challenged with 5 µg/mL of lysostaphin. Measurement of cellular viability was performed by analyzing the optical density at 600 nm and at each time point the optical density value was compared to the initial optical density reading.

4.4 Conclusion

In conclusion, we have shown the application of our novel assay that reports on accessibility to the PG in identifying genes that potentially control permeation to the bacterial cell surface in *S. aureus*. Using site-selective incorporation of a bioorthogonal handle and a corresponding reactive fluorescent probe, we were able to screen a transposon mutant library in effort to discern any genetic variations that led to an increase in fluorescence labeling thus signaling a possible increase in permeability. The screen revealed four transposants that consistently labeled at a higher level when compared to WT cells and some of these identified hits showed increased susceptibility to the bacteriocin, lysostaphin. The protein products of these transposants can potentially be considered new targets to develop potentiators for antibacterial therapies. Overall, we have demonstrated the use of our PG accessibility assay in a high-throughput screen and identified genes that may control access to the cell wall surface in *S. aureus*.

4.5 Materials and Methods

Materials. The fluorescent probes were purchased from Click Chemistry Tools, Lumiprobe, and Conju-Probe. The amino acids were purchased from ChemImpex. Wildtype (WT) *S. aureus* (ATCC 25923) and the transposon mutant library (Nebraska Transposon Mutant Library [NTML] purchased from BEI Resources) were grown in lysogeny broth (LB). *S. aureus* $\Delta tarO$ was grown in LB supplemented with 150 µg/mL spectinomycin.

Flow cytometry analysis of labeled whole cells. LB media containing either 1mM of **D-LysAz**, 1mM **L-LysAz**, or DMSO were prepared. WT *S. aureus* or $\Delta tarO$ (supplemented with 150 $\mu\text{g}/\text{mL}$ spectinomycin) cells were added to the LB medium (1:100) and allowed to grow overnight at 37°C with shaking at 250 rpm. The cells were harvested at 4000 rpm and washed three times at the original culture volume with 1X PBS. The cells were then treated with 25 μM **DBCOfl** for 30 minutes at 37°C and protected from light. The samples were subsequently harvested at 4000 rpm and washed three times with 1X PBS followed by fixation with 2% formaldehyde in 1X PBS for 30 minutes. The cells were analyzed using the Attune NxT flow cytometer equipped with a 488 nm laser and 525/40 nm bandpass filter. The data were analyzed using the Attune NXT Software.

Sacculi isolation protocol and flow cytometry analysis. The following sacculi isolation protocol was adapted from an existing protocol.⁴⁶ LB media containing either 1mM of **D-LysAz**, 1mM **L-LysAz**, or DMSO were prepared in a deep 96-well culture plate. WT *S. aureus* cells were added to the LB medium (1:100) and allowed to grow overnight at 37°C with shaking at 250 rpm. The cells were harvested at 4000 rpm and washed three times at the original culture volume with 1X PBS. The cells were then treated with 25 μM **DBCOfl** for 30 minutes at 37°C and protected from light. The samples were subsequently harvested at 4000 rpm and washed three times with 1X PBS. The final cell pellets were resuspended in 0.25% SDS in 0.1 M Tris HCl at pH 6.8 at the original culture volume, the plate was wrapped in foil to seal it, and placed in boiling water (plate will float) for 30 minutes. After 30 minutes the cell matter was harvested at 4000 rpm for 10 minutes and washed three times with 1X PBS. The final pellet was resuspended at the original culture volume in DI water, the plate was wrapped in foil to seal it, and sonicated in a bath sonicator (plate will float) for 30 minutes. The cell matter was harvested at 4000 rpm for 10 minutes and the resulting pellet was resuspended at half the original culture volume in 15 $\mu\text{g}/\text{mL}$ of DNase and 60 $\mu\text{g}/\text{mL}$ of RNase in 0.1 M Tris HCl at pH 6.8. This was allowed to incubate for 1 hour with shaking (150 rpm) at 37°C. After an hour, at half the culture volume, 50 $\mu\text{g}/\text{mL}$ of trypsin in DI water was added and allowed to incubate for an additional hour. After an hour the

plate was wrapped in foil to seal it and boiled in a water bath for 5 minutes to inactivate the enzymes. The cell matter was harvested at 4000 rpm for 10 minutes and washed once with DI water. The resulting pellet is the isolated sacculi and it was analyzed using the Attune NxT flow cytometer as described above.

Viability analysis. LB media containing either 1mM of **D-LysAz** or DMSO were prepared. WT *S. aureus* cells were added to the LB medium (1:100) and allowed to grow at 37°C with shaking at 250 rpm. At each of the designated time points the optical density at 600 nm was recorded.

384-well plate labeling benchmark. 35 μ L of LB media was transferred by a liquid handling system into a 384-well plate (120 μ L max capacity). Each well was inoculated with either WT *S. aureus* or $\Delta tarO$ (supplemented with 150 μ g/mL spectinomycin). Inoculated plates were allowed incubate for 8 hours with shaking at 37°C. 75 μ L of fresh LB media containing 1mM of **D-LysAz** was transferred by a liquid handling system into a deep 384-well plate (240 μ L max capacity). After 8 hours, the newly prepared plate was inoculated and allowed to incubate overnight with shaking at 37°C. The cells were then harvested at 4000 rpm and washed three times with 1X PBS. The pellets were then resuspended at the original culture volume (75 μ L) and 10 μ L of cells were transferred to a new 384-well plate (120 μ L max capacity) containing **DBCOfl** for a final concentration of 25 μ M and allowed to incubate for 30 minutes at 37°C. After 30 minutes the samples were fixed with 2% formaldehyde and analyzed using the Attune NxT flow cytometer as described above.

Transposon Mutant Screen. 35 μ L of LB media was transferred by a liquid handling system into each well of the desired number of 384-well plates (120 μ L max capacity). A 384 pin replicator was used to inoculate the prepared plates from the NTML glycerol stock plates. Inoculated plates were allowed incubate for 8 hours with shaking at 37°C. 75 μ L of fresh LB media containing 1mM of **D-LysAz** was transferred by a liquid handling system into each well of the desired number of deep 384-well plates (240 μ L max capacity). After 8 hours, the newly prepared plates were inoculated and allowed to incubate overnight with shaking at 37°C.

The cells were then harvested at 4000 rpm and washed three times with 1X PBS. The pellets were then resuspended at the original culture volume (75 μ L) and 10 μ L of cells were transferred to new 384-well plates (120 μ L max capacity) containing **DBCofl** for a final concentration of 25 μ M and allowed to incubate for 30 minutes at 37°C. After 30 minutes the samples were fixed with 2% formaldehyde and analyzed using the Attune NxT flow cytometer as described above.

Triplicate screen of selected transposants. The triplicate screen of the identified hits was performed as described. LB media containing 1mM of **D-LysAz** was prepared. Identified hits grown overnight were added to the LB medium (1:100) and allowed to grow overnight at 37°C with shaking at 250 rpm. The cells were harvested at 4000 rpm and washed three times at the original culture volume with 1X PBS. The cells were then treated with 25 μ M **DBCofl** for 30 minutes at 37°C and protected from light. The samples were subsequently harvested at 4000 rpm and washed three times with 1X PBS followed by fixation with 2% formaldehyde in 1X PBS for 30 minutes. The cells were then analyzed using the Attune NxT flow cytometer as described above.

Fluorophore and length scan. LB media containing 1mM of **D-LysAz** was prepared. WT *S. aureus* or the transposants identified as hits, after an initial overnight growth, were added to the LB medium (1:100) and allowed to grow overnight at 37°C with shaking at 250 rpm. The cells were harvested at 4000 rpm and washed three times at the original culture volume with 1X PBS. The cells were then treated with 25 μ M of either **DBCofl**, **DBCOfaf488**, or **DBCOfpegfl** for 30 minutes at 37°C (protected from light). Then the samples were harvested at 4000 rpm and washed three times with 1X PBS. This was followed by fixation with 2% formaldehyde in 1X PBS for 30 minutes. The cells were then analyzed using the Attune NxT flow cytometer as described above.

Scanning electron microscopy (SEM). WT *S. aureus* and the transposants identified as hits were grown overnight at 37°C in LB media. The cells were then harvested at 4000 rpm and the resulting pellets were resuspended in a fixative

solution of 2% glutaraldehyde and 4% paraformaldehyde in sodium cacodylate buffer. The fixed samples were put onto glass coverslips and left at 4 degrees overnight. Next the samples were washed to remove fixative three times for 10 minutes with 0.1M cacodylate buffer. Samples were then treated with 2% osmium tetroxide for 30-60 minutes, washed twice for 10 min with 0.1M cacodylate buffer, and then washed once distilled H₂O. Next the samples were dehydrated in graded ethanol series (30% EtOH for 10 min, 50% EtOH for 10 min, 70% EtOH for 10 min, 95% EtOH for 10 min, 100% EtOH for 10 min) and critical point dried. Finally, the coverslips were mounted on stubs with silver paint or carbon stickers and sputter coated with gold paladium. The samples were then imaged using a Zeiss Sigma HD.

Susceptibility of Transposon Mutants. Identified hits from the triplicate screen in addition to WT *S. aureus* and USA300 were grown overnight in LB media. After growth cells were washed 3 times with 1X PBS and resuspended in buffer and the optical density at 600 nm was measured, constituting the zero time point. Next 5 µg/mL of lysostaphin was introduced to each sample and allowed to incubate at 37°C with shaking at 250 rpm. The optical density at 600 nm was taken at each designated time point (5, 10, 30, 60, 120, 180 mins). Percent of initial optical density was calculated and graphed to represent the decrease in viability of cells over time.

4.6 References

1. Cox, G., and Wright, G. D. (2013) Intrinsic antibiotic resistance: mechanisms, origins, challenges and solutions, *Int J Med Microbiol* 303, 287-292.
2. Martinez, J. L. (2014) General principles of antibiotic resistance in bacteria, *Drug Discov Today Technol* 11, 33-39.
3. Nuri, R., Shprung, T., and Shai, Y. (2015) Defensive remodeling: How bacterial surface properties and biofilm formation promote resistance to antimicrobial peptides, *Biochim Biophys Acta* 1848, 3089-3100.
4. French, S., Farha, M., Ellis, M. J., Sameer, Z., Cote, J. P., Cotroneo, N., Lister, T., Rubio, A., and Brown, E. D. (2020) Potentiation of Antibiotics against Gram-Negative Bacteria by Polymyxin B Analogue SPR741 from Unique Perturbation of the Outer Membrane, *ACS Infect Dis* 6, 1405-1412.
5. Vaara, M., and Porro, M. (1996) Group of peptides that act synergistically with hydrophobic antibiotics against gram-negative enteric bacteria, *Antimicrob Agents Chemother* 40, 1801-1805.
6. Klobucar, K., Cote, J. P., French, S., Borrillo, L., Guo, A. B. Y., Serrano-Wu, M. H., Lee, K. K., Hubbard, B., Johnson, J. W., Gaulin, J. L., Magolan, J., Hung, D. T., and Brown, E. D. (2021) Chemical Screen for Vancomycin Antagonism Uncovers Probes of the Gram-Negative Outer Membrane, *ACS Chem Biol* 16, 929-942.
7. Vaara, M. (1992) Agents that increase the permeability of the outer membrane, *Microbiol Rev* 56, 395-411.
8. Stokes, J. M., MacNair, C. R., Ilyas, B., French, S., Cote, J. P., Bouwman, C., Farha, M. A., Sieron, A. O., Whitfield, C., Coombes, B. K., and Brown, E. D. (2017) Pentamidine sensitizes Gram-negative pathogens to antibiotics and overcomes acquired colistin resistance, *Nat Microbiol* 2, 17028.
9. Hill, M. A., Lam, A. K., Reed, P., Harney, M. C., Wilson, B. A., Moen, E. L., Wright, S. N., Pinho, M. G., and Rice, C. V. (2019) BPEI-Induced Delocalization of PBP4 Potentiates beta-Lactams against MRSA, *Biochemistry* 58, 3813-3822.
10. Lam, A. K., Panlilio, H., Pusavat, J., Wouters, C. L., Moen, E. L., Brennan, R. E., and Rice, C. V. (2020) Expanding the Spectrum of Antibiotics Capable of Killing

Multidrug-Resistant *Staphylococcus aureus* and *Pseudomonas aeruginosa*, *ChemMedChem* 15, 1421-1428.

11. Ferraro, N. J., and Pires, M. M. (2021) Systematic Assessment of Accessibility to the Surface of *Staphylococcus aureus*, *ACS Chem Biol* Under review.

12. Lambert, P. A. (2002) Cellular impermeability and uptake of biocides and antibiotics in Gram-positive bacteria and mycobacteria, *J Appl Microbiol* 92 Suppl, 46S-54S.

13. Vollmer, W., Blanot, D., and de Pedro, M. A. (2008) Peptidoglycan structure and architecture, *FEMS Microbiol Rev* 32, 149-167.

14. Maresso, A. W., and Schneewind, O. (2008) Sortase as a target of anti-infective therapy, *Pharmacol Rev* 60, 128-141.

15. Nelson, J. W., Chamessian, A. G., McEnaney, P. J., Murelli, R. P., Kazmierczak, B. I., and Spiegel, D. A. (2010) A biosynthetic strategy for re-engineering the *Staphylococcus aureus* cell wall with non-native small molecules, *ACS Chem Biol* 5, 1147-1155.

16. Weidenmaier, C., and Peschel, A. (2008) Teichoic acids and related cell-wall glycopolymers in Gram-positive physiology and host interactions, *Nat Rev Microbiol* 6, 276-287.

17. Vaz, F., Kounatidis, I., Covas, G., Parton, R. M., Harkiolaki, M., Davis, I., Filipe, S. R., and Ligoxygakis, P. (2019) Accessibility to Peptidoglycan Is Important for the Recognition of Gram-Positive Bacteria in *Drosophila*, *Cell Rep* 27, 2480-2492 e2486.

18. Weidenmaier, C., Kokai-Kun, J. F., Kristian, S. A., Chanturiya, T., Kalbacher, H., Gross, M., Nicholson, G., Neumeister, B., Mond, J. J., and Peschel, A. (2004) Role of teichoic acids in *Staphylococcus aureus* nasal colonization, a major risk factor in nosocomial infections, *Nat Med* 10, 243-245.

19. Du, X., Larsen, J., Li, M., Walter, A., Slavetinsky, C., Both, A., Sanchez Carballo, P. M., Stegger, M., Lehmann, E., Liu, Y., Liu, J., Slavetinsky, J., Duda, K. A., Krismer, B., Heilbronner, S., Weidenmaier, C., Mayer, C., Rohde, H., Winstel, V., and Peschel, A. (2021) *Staphylococcus epidermidis* clones express

Staphylococcus aureus-type wall teichoic acid to shift from a commensal to pathogen lifestyle, *Nat Microbiol* 6, 757-768.

20. Royet, J., and Dziarski, R. (2007) Peptidoglycan recognition proteins: pleiotropic sensors and effectors of antimicrobial defences, *Nat Rev Microbiol* 5, 264-277.

21. Wolf, A. J., and Underhill, D. M. (2018) Peptidoglycan recognition by the innate immune system, *Nat Rev Immunol* 18, 243-254.

22. Foster, T. J. (2005) Immune evasion by staphylococci, *Nat Rev Microbiol* 3, 948-958.

23. Lowy, F. D. (2003) Antimicrobial resistance: the example of *Staphylococcus aureus*, *J Clin Invest* 111, 1265-1273.

24. Feigman, M. S., Kim, S., Pidgeon, S. E., Yu, Y., Ongwae, G. M., Patel, D. S., Regen, S., Im, W., and Pires, M. M. (2018) Synthetic Immunotherapeutics against Gram-negative Pathogens, *Cell Chem Biol* 25, 1185-1194 e1185.

25. Fura, J. M., Pidgeon, S. E., Birabaharan, M., and Pires, M. M. (2016) Dipeptide-Based Metabolic Labeling of Bacterial Cells for Endogenous Antibody Recruitment, *ACS Infect Dis* 2, 302-309.

26. Fura, J. M., and Pires, M. M. (2015) D-amino carboxamide-based recruitment of dinitrophenol antibodies to bacterial surfaces via peptidoglycan remodeling, *Biopolymers* 104, 351-359.

27. Fura, J. M., Sabulski, M. J., and Pires, M. M. (2014) D-amino acid mediated recruitment of endogenous antibodies to bacterial surfaces, *ACS Chem Biol* 9, 1480-1489.

28. Fura, J. M., Sarkar, S., Pidgeon, S. E., and Pires, M. M. (2017) Combatting Bacterial Pathogens with Immunomodulation and Infection Tolerance Strategies, *Curr Top Med Chem* 17, 290-304.

29. Sabulski, M. J., Pidgeon, S. E., and Pires, M. M. (2017) Immuno-targeting of *Staphylococcus aureus* via surface remodeling complexes, *Chem Sci* 8, 6804-6809.

30. Baskin, J. M., Prescher, J. A., Laughlin, S. T., Agard, N. J., Chang, P. V., Miller, I. A., Lo, A., Codelli, J. A., and Bertozzi, C. R. (2007) Copper-free click chemistry for dynamic in vivo imaging, *Proc Natl Acad Sci U S A* 104, 16793-16797.
31. Jewett, J. C., Sletten, E. M., and Bertozzi, C. R. (2010) Rapid Cu-free click chemistry with readily synthesized biarylazacyclooctynones, *J Am Chem Soc* 132, 3688-3690.
32. Apostolos, A. J., Pidgeon, S. E., and Pires, M. M. (2020) Remodeling of Crossbridges Controls Peptidoglycan Crosslinking Levels in Bacterial Cell Walls, *ACS Chem Biol*.
33. Pidgeon, S. E., Apostolos, A. J., Nelson, J. M., Shaku, M., Rimal, B., Islam, M. N., Crick, D. C., Kim, S. J., Pavelka, M. S., Kana, B. D., and Pires, M. M. (2019) L,D-Transpeptidase Specific Probe Reveals Spatial Activity of Peptidoglycan Cross-Linking, *ACS Chem Biol* 14, 2185-2196.
34. Welsh, M. A., Taguchi, A., Schaefer, K., Van Tyne, D., Lebreton, F., Gilmore, M. S., Kahne, D., and Walker, S. (2017) Identification of a Functionally Unique Family of Penicillin-Binding Proteins, *J Am Chem Soc* 139, 17727-17730.
35. Gautam, S., Kim, T., Shoda, T., Sen, S., Deep, D., Luthra, R., Ferreira, M. T., Pinho, M. G., and Spiegel, D. A. (2015) An Activity-Based Probe for Studying Crosslinking in Live Bacteria, *Angew Chem Int Ed Engl* 54, 10492-10496.
36. Gautam, S., Kim, T., and Spiegel, D. A. (2015) Chemical probes reveal an extraseptal mode of cross-linking in *Staphylococcus aureus*, *J Am Chem Soc* 137, 7441-7447.
37. Ngadjewa, F., Braud, E., Saidjalolov, S., Iannazzo, L., Schnappinger, D., Ehrt, S., Hugonnet, J. E., Mengin-Lecreulx, D., Patin, D., Etheve-Quellejeu, M., Fonvielle, M., and Arthur, M. (2018) Critical Impact of Peptidoglycan Precursor Amidation on the Activity of L,d-Transpeptidases from *Enterococcus faecium* and *Mycobacterium tuberculosis*, *Chemistry*.
38. D'Elia, M. A., Millar, K. E., Beveridge, T. J., and Brown, E. D. (2006) Wall teichoic acid polymers are dispensable for cell viability in *Bacillus subtilis*, *J Bacteriol* 188, 8313-8316.

39. Swoboda, J. G., Meredith, T. C., Campbell, J., Brown, S., Suzuki, T., Bollenbach, T., Malhowski, A. J., Kishony, R., Gilmore, M. S., and Walker, S. (2009) Discovery of a small molecule that blocks wall teichoic acid biosynthesis in *Staphylococcus aureus*, *ACS Chem Biol* 4, 875-883.
40. Gautam, S., Kim, T., Lester, E., Deep, D., and Spiegel, D. A. (2016) Wall teichoic acids prevent antibody binding to epitopes within the cell wall of *Staphylococcus aureus*, *ACS Chem Biol* 11, 25-30.
41. Eugster, M. R., and Loessner, M. J. (2012) Wall teichoic acids restrict access of bacteriophage endolysin Ply118, Ply511, and PlyP40 cell wall binding domains to the *Listeria monocytogenes* peptidoglycan, *J Bacteriol* 194, 6498-6506.
42. Novick, R. P., Projan, S. J., Kornblum, J., Ross, H. F., Ji, G., Kreiswirth, B., Vandenesch, F., and Moghazeh, S. (1995) The agr P2 operon: an autocatalytic sensory transduction system in *Staphylococcus aureus*, *Mol Gen Genet* 248, 446-458.
43. Cosgriff, C. J., White, C. R., Teoh, W. P., Grayczyk, J. P., and Alonzo, F., 3rd. (2019) Control of *Staphylococcus aureus* Quorum Sensing by a Membrane-Embedded Peptidase, *Infect Immun* 87.
44. Singh, V. K., Sirobhusanam, S., Ring, R. P., Singh, S., Gatto, C., and Wilkinson, B. J. (2018) Roles of pyruvate dehydrogenase and branched-chain alpha-keto acid dehydrogenase in branched-chain membrane fatty acid levels and associated functions in *Staphylococcus aureus*, *J Med Microbiol* 67, 570-578.
45. Grundling, A., and Schneewind, O. (2006) Cross-linked peptidoglycan mediates lysostaphin binding to the cell wall envelope of *Staphylococcus aureus*, *J Bacteriol* 188, 2463-2472.
46. Kühner, D., Stahl, M., Demircioglu, D. *et al.* (2014) From cells to muropeptide structures in 24 h: Peptidoglycan mapping by UPLC-MS. *Sci Rep* 4, 7494.

Chapter 5. SaccuFlow – A High-throughput Analysis Platform to Investigate Bacterial Cell Wall Interactions

Adapted from: Apostolos, A. J.; Ferraro, N. J.; Dalesandro, B. E.; Pires, M. M., SaccuFlow: A High-Throughput Analysis Platform to Investigate Bacterial Cell Wall Interactions. *ACS Infect Dis* **2021**, 7 (8), 2483-2491.

5.1 Abstract

Bacterial cell walls are formidable barriers that protect bacterial cells against external insults and oppose internal turgor pressure. While cell wall composition is variable across species, peptidoglycan is the principal component of all cell walls. Peptidoglycan is a mesh-like scaffold composed of crosslinked strands that can be heavily decorated with anchored proteins. The biosynthesis and remodeling of peptidoglycan must be tightly regulated by cells because disruption to this biomacromolecule is lethal. This essentiality is exploited by the human innate immune system in resisting colonization and by a number of clinically relevant antibiotics that target peptidoglycan biosynthesis. Evaluation of molecules or proteins that interact with peptidoglycan can be a complicated and, typically, qualitative effort. We have developed a novel assay platform (SaccuFlow) that preserves the native structure of bacterial peptidoglycan and is compatible with high-throughput flow cytometry analysis. We show that the assay is facile and versatile as demonstrated by its compatibility with sacculi from Gram-positive bacteria, Gram-negative bacteria, and mycobacteria. Finally, we highlight the utility of this assay to assess the activity of sortase A from *Staphylococcus aureus* against potential anti-virulence agents.

5.2 Introduction

Bacterial cell walls have many functions but none more important than acting as a protective barrier from potentially harsh external elements and attacks from host defense mechanisms.¹⁻² Bacteria can be categorized based on the type of cell wall they possess and there are distinctive features of each that can pose a challenge, or opportunity, for the host the immune system or antibiotics.³⁻⁴ In the

case of Gram-positive bacteria, their cell wall is composed of a thick peptidoglycan (PG) sacculus layer followed by a cytoplasmic membrane. PG is a mesh-like polymer made up of repeating disaccharide units of N-acetylglucosamine (GlcNAc) and N-acetylmuramic acid (MurNAc). Attached to each MurNAc unit is a short peptide, referred to as the stem peptide, that ranges from 3 to 5 amino acids in length. The stem pentapeptide sequence is typically L-Ala-iso-D-Glu-L-Lys (or meso-diaminopimelic acid [m-DAP])-D-Ala-D-Ala, although there are considerable variations in the primary sequence.⁵

Crosslinking can occur between neighboring stem peptides and the degree to which the PG is crosslinked can influence the cell wall rigidity and integrity.² The thick PG layer in Gram-positive bacteria is generally believed to be a permeability barrier to molecules in the extracellular space.⁶⁻⁹ While most small molecules can potentially sieve through the PG, there is evidence that the PG is a formidable barrier for the permeation of larger molecules.¹⁰⁻¹² This feature has significant implications for molecules with intracellular and cell membrane targets; one example being the membrane attack complex (MAC), a product of the complement system that targets bacterial cell membranes. The MAC is prevented from reaching the cytoplasmic membrane of Gram-positive bacteria due in part to its inability to penetrate through the PG layer.¹³⁻¹⁴ Gram-positive pathogens can also alter the composition of their PG to become resistant to specific classes of antibiotics. For example, both *Staphylococcus aureus* (*S. aureus*) and *Enterococcus faecium* can alter the PG structure to resist the antibacterial actions of vancomycin.¹⁵⁻¹⁷ Due to its critical role in bacterial cell survival, PG is often the target of antibiotics and components of the human immune system.^{4, 18-19} Clinically and industrially important antibacterial agents (e.g., β -lactams, teixobactin, vancomycin, bacitracin, and moenomycin) target components of the PG biosynthesis as integral parts of their mechanism of actions. Similarly, components of the human immune system (e.g., lysozyme, LysM-displaying proteins, and PG recognition proteins [PGRPs]) must reach the PG to impart their response onto the invading bacterial pathogen.

Despite the importance of characterizing interactions with the PG scaffold of bacteria, there are limited methods to investigate the specific binding of molecules to PG. More specifically, there is a clear need for a method to determine PG binding interactions that (1) retains the natural composition of native PG, (2) is applicable to all types of bacteria, (3) preserves the polymeric nature of native PG, (4) is readily attainable in high yields, and (5) is compatible with quantitative, high-throughput analysis platforms. There are several challenges with obtaining PG samples for analysis. The use of synthetic PG mimics provides some advantages such as sample homogeneity and the ability to install specific changes to the PG primary sequence. In fact, a number of important contributions to the field have been made using synthetic PG mimics.²⁰⁻²⁴ Our own group has extensively used synthetic PG mimics in studying cell wall biosynthesis and remodeling.²⁵⁻²⁶ However, there are severe drawbacks to using synthetic analogs, including the lack of commercially available building blocks for the disaccharide units and m-DAP. In addition, there is potential for the loss of polyvalent interactions, which are prevalent in PG-binding molecules, using monomeric PG analogs. Alternatively, PG fragments can be obtained by digesting isolated native PG (sacculi) with a hydrolase enzyme and performing chromatography.²⁷⁻²⁸ This last-resort method is fraught with challenges due to the difficulty in the separation of fragments, convoluted characterization of fragments (e.g., site of amidation), and low yields. Finally, the use of intact cells to study PG interactions has advantages in terms of retaining the polymeric nature and preservation of the native composition (even if variable across the PG scaffold). However, isolation of the effect of PG interaction alone in the background of surface bound proteins and other potential biomacromolecules is a major hurdle. Herein, we report a new method (SaccuFlow) that uses sacculi isolated directly from Gram-positive, Gram-negative, or mycobacterial organisms in combination with flow cytometry to assay PG binding interactions. To the best of our knowledge, flow cytometry has not yet been systematically used to evaluate isolated bacterial PG and/or its interactions with binding partners.

5.3 Results and Discussion

We reasoned that murein sacculus from bacteria, which is a single macromolecular scaffold made of PG, would provide a superior platform to analyze PG interactions due to its ease of isolation and proper mimicry of the PG composition and structure. While sacculi analysis has been implemented for decades, these studies have focused primarily on mass spectrometry analysis of digested low molecular weight PG fragments²⁹⁻³¹ and low-throughput qualitative analyses techniques (e.g., confocal microscopy³² and pull-down assays³³). We envisioned that a higher-throughput and quantitative sacculus analysis platform could be achieved by performing the analysis using flow cytometry. Sacculi should be readily detected *via* flow cytometry because its size resembles that of the bacterial cell.³⁴ Significantly, sacculi preparations are routinely performed with relative ease from almost any type of bacteria with these isolation steps.

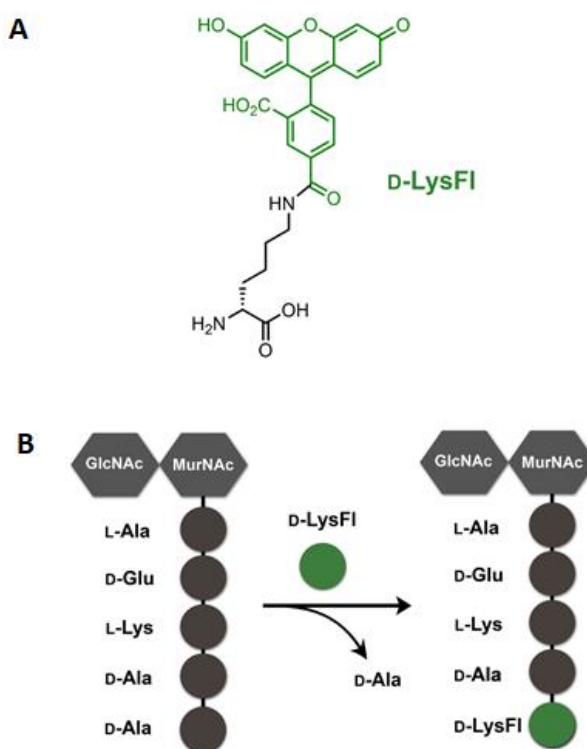


Figure 5.1 (A) Chemical structure of **D-LysFI**. (B) Cartoon representation of the metabolic swapping of the terminal D-ala from the bacterial PG with the exogenously supplied **D-LysFI**.

Initially, we set out to benchmark the detection of bacterial sacculi from a Gram-positive organism using a standard flow cytometer. We chose to site selectively tag the sacculi with a fluorescent handle by metabolic labeling of the PG scaffold. Our research group³⁵⁻³⁹, and others^{26, 35, 37, 38, 40-47} have previously demonstrated that co-incubation of unnatural D-amino acids, including those modified with fluorophores, metabolically label PG of live bacteria cells. More specifically, fluorescein conjugated D-Lys (**D-LysFI**) from the culture media is expected to replace the 5th position D-alanine of the PG stem peptide of *S. aureus* during the biosynthesis and remodeling of new PG (**Figure 5.1A-B**). Generally, 1-2 % of the stem peptides in the PG scaffold of *S. aureus* is labeled when cells are treated overnight with the D-amino acid label under the assay conditions. Bacterial sacculi were isolated using standard procedures from whole cells, which were expected to yield fluorescently labeled sacculi (**Figure 5.2**).

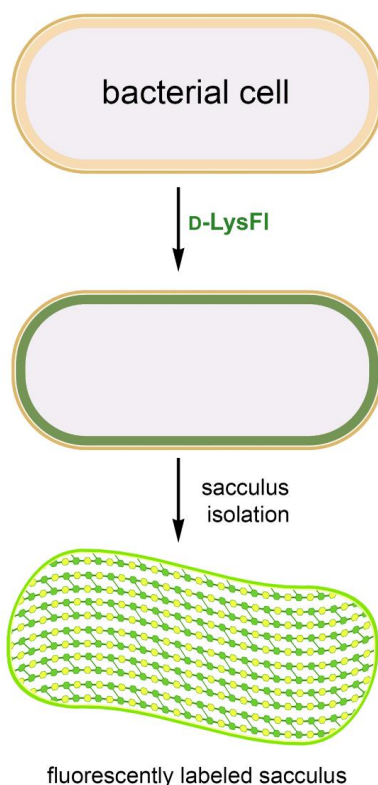


Figure 5.2 Assay workflow of SaccuFlow for the labeling of sacculi.

Our results revealed that labeled sacculi formed a tight population of events that could readily be distinguished from background debris (**Figure 5.3A**). Most significantly, fluorescence levels of sacculi from cells treated with **D-LysFI** were 17-fold higher than cells treated with the control amino acid **L-LysFI** (**Figure 5.3B**). Unlike **D-LysFI**, its enantiomer does not become incorporated as part of the bacterial PG scaffold.

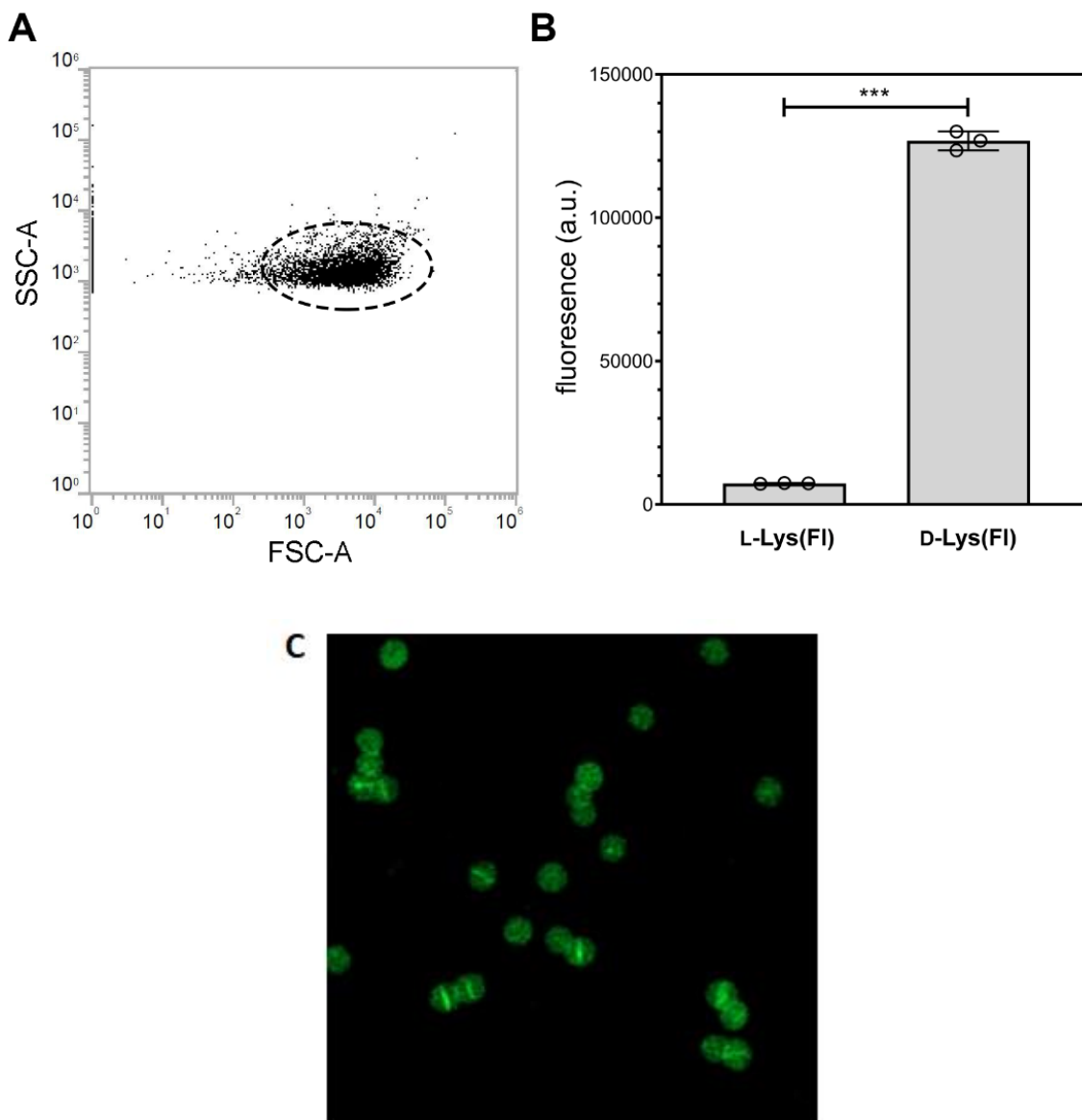


Figure 5.3 (A) Side and forward scatter plot of *S. aureus* sacculi. (B) Flow cytometry analysis of sacculi isolated from *S. aureus* (ATCC 25923) treated overnight with 500 μ M of **D-LysFI** or **L-LysFI**. Data are represented as mean \pm SD ($n = 3$). P -values were determined by a two-tailed t -test (* denotes a p -value < 0.05 , ** < 0.01 , *** < 0.001 , ns = not significant). (C) Confocal microscopy of sacculi isolated from *S. aureus* (ATCC 25923) that was treated with 100 μ M **D-LysFI** overnight.

The same sacculi was imaged using confocal microscopy, thus confirming that the sample analyzed was primarily fluorescent sacculi (**Figure 5.3C**). A **D-LysFI** concentration dependent labeling pattern of the isolated PG was also observed (**Figure 5.4A**). Next, a series of additional experiments were performed to confirm that the events being detected on the flow cytometer were, indeed, *S. aureus* sacculi. Sacculi labeled with **D-LysFI** were subjected to treatment with two PG hydrolases: lysozyme and mutanolysin (**Figure 5.4B**). As expected, treatment with mutanolysin resulted in a time-dependent reduction in fluorescence levels due to the release of PG fragments. O-acetylation of *S. aureus* PG renders it insensitive to lysozyme digestion and, likewise, lysozyme treatment.⁴⁸ Digestion by mutanolysin was also found to be concentration dependent (**Figure 5.4C**).

To show the versatility of the tagged sacculi in a flow cytometry platform, we prepared sacculi from organisms that had been co-incubated with either **D-** or **L-LysAz** (**Figure 5.5**). We anticipated that **D-LysAz** treated cells would provide a bioorthogonal click handle on the PG scaffold that could be covalently linked to a variety of compounds containing the corresponding reactive moieties. Subsequent treatment with cyclooctynes should result in strain-promoted alkyne-azide cycloaddition (SPAAC) ligation with azide groups on the sacculi.⁴⁹⁻⁵⁰

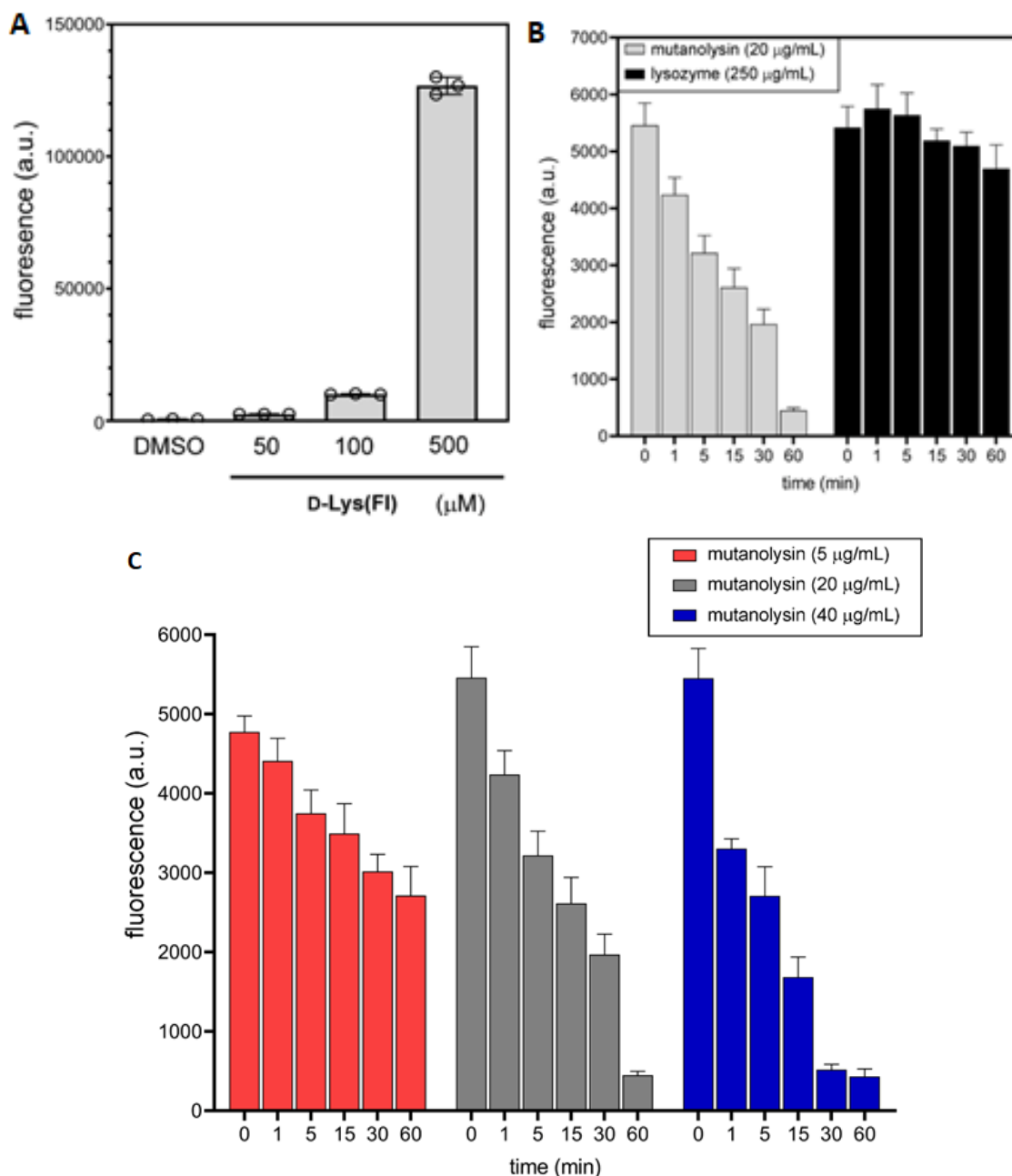


Figure 5.4 (A) Flow cytometry analysis of sacculi isolated from *S. aureus* (ATCC 25923) treated overnight with varying concentrations of **D-LysFI**. (B) Flow cytometry analysis of sacculi isolated from *S. aureus* (ATCC 25923) treated overnight with 500 μM of **D-LysFI** and incubated with either mutanolysin or lysozyme. (C) Fluorescence read out of sacculi isolated from *S. aureus* (ATCC 25923) that was treated with 100 μM **D-LysFI** overnight and subjected to

degradation by increasing concentrations of mutanolysin overtime. Data are represented as mean +/- SD (n = 3).

For this assay, azide-tagged sacculi isolated from *S. aureus* were incubated with dibenzocyclooctyne (DBCO) linked to fluorescein. Our results showed increase in of ~8-fold in sacculi fluorescence when cells were treated with **D-LysAz**, which is consistent with the successful ligation of fluorescein mediated by SPAAC (**Figure 5.6A**). Strikingly, after chemical removal of the wall teichoic acids (WTA), an increase in fluorescence was observed with the small fluorescently labeled handle (**Figure 5.6B**). WTA is an anionic polymer that is covalently anchored onto PG of some Gram-positive organisms.⁵¹⁻⁵⁴ It is well established that WTA can block or impede interaction of extracellular molecules with the PG scaffold. These results highlight the role that surface biopolymers play in accessibility to the PG scaffold and further demonstrates the ability to use flow cytometry to systematically assess this important feature related to bacterial cell wall biology.

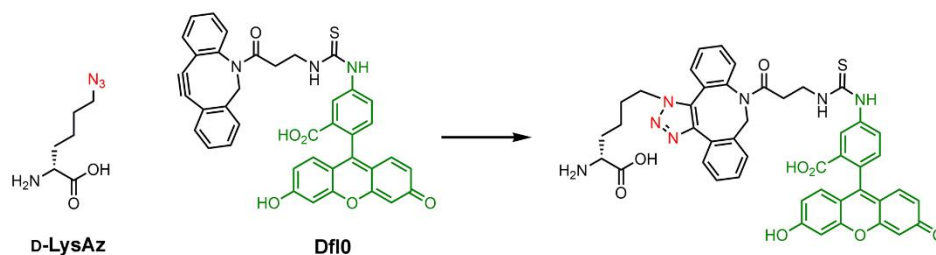


Figure 5.5 Chemical structures representing the SPAAC reaction between azide and a strained alkyne in DBCO.

Similarly, to test the applicability of this method to mycobacterial and Gram-negative organisms, *Mycobacterium smegmatis* (*M. smegmatis*) and *Escherichia coli* (*E. coli*) were grown in media supplemented with either **D-** or **L-LysAz** and their sacculi were harvested following the standard procedures for each classification.

The isolated PG was then treated with **Dfl0** and analyzed by flow cytometry, showing that only sacculi from cells that had been treated with **D-LysAz** labeled extensively with **Dfl0** (**Figure 5.7**). This highlights the adaptability of SaccuFlow to bacterial species of varied classifications.

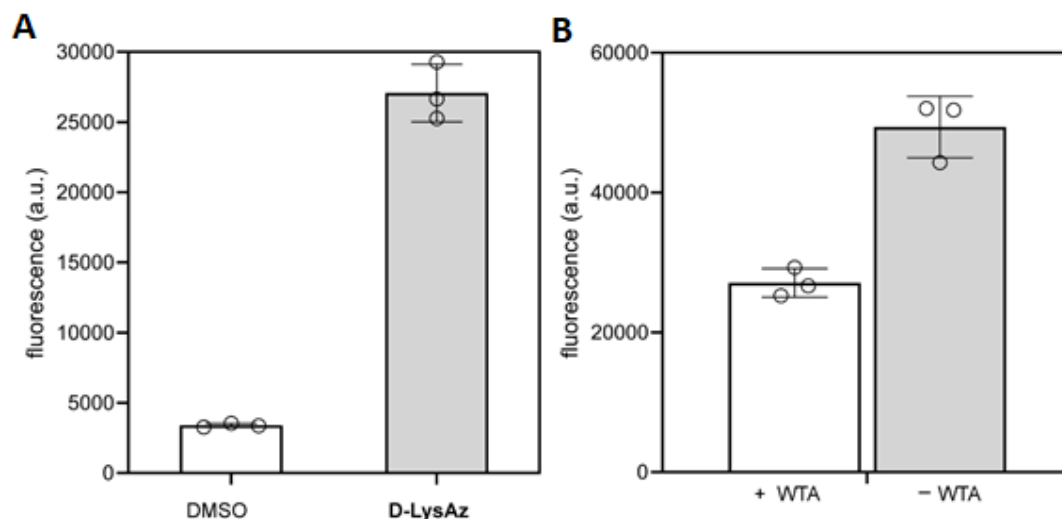


Figure 5.6 (A) Flow cytometry analysis of sacculi isolated from *S. aureus* (ATCC 25923) treated overnight with 1 mM of **D-LysAz** or DMSO. Subsequently, sacculi were incubated with 25 μ M of **Dfl0**. (B) Flow cytometry analysis of sacculi isolated from *S. aureus* (ATCC 25923) treated overnight with 1 mM of **D-LysAz**. Where noted, sacculi were chemically treated to remove WTA. Subsequently, sacculi were incubated with 25 μ M of **Dfl0**. Data are represented as mean \pm SD ($n = 3$).

Having shown that SaccuFlow was operational and facile, we then set out to demonstrate that it could report on features related to PG-binding antibiotics. Vancomycin, a glycopeptide antibiotic that specifically hydrogen-binds the D-Ala-D-Ala fragment of the stem peptide, conjugated to BODIPY (**VBD**)⁵⁵ was analyzed for binding using SaccuFlow. As anticipated, *S. aureus* sacculi demonstrated ~8-

fold BODIPY fluorescence over background, suggesting that vancomycin bound to isolated PG was detectable by flow cytometry (**Figure 5.8**).

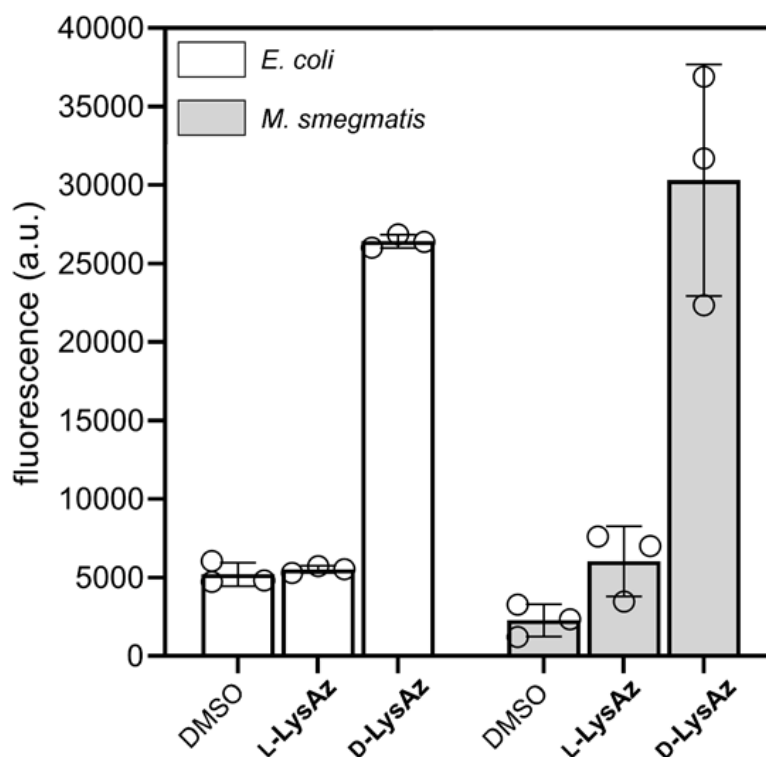


Figure 5.7 Fluorescence read-out of sacculi isolated from *E. coli* BW25113 or *M. smegmatis* WT that was incubated with 1 mM L- or D-LysAz overnight, and subsequently treated with 25 μ M Df10. Data are represented as mean \pm SD (n = 3).

To show that fluorescence levels were reflective of specific binding interactions, bacterial sacculi was treated with a synthetic analog of the PG, L-Lys-D-Ala-D-Ala. As expected, increasing concentrations of L-Lys-D-Ala-D-Ala led to decreasing fluorescence levels associated with the decrease in binding events of VBD to sacculi (**Figure 5.9**). To show the versatility of this assay amongst other strains, we isolated *Bacillus subtilis* (*B. subtilis*) sacculi from a wildtype (WT) strain and from a strain lacking *dacA* (*dacA* Δ), the gene responsible for the D-alanyl-D-

alanine carboxypeptidase.⁵⁶ **VBD** would be expected to bind *dacAΔ B. subtilis* sacculi to a higher level in comparison to WT, as lack of the carboxypeptidase would present additional D-Ala-D-Ala binding points for **VBD**. Our results demonstrate a ~3-fold increase in binding of **VBD** to *dacAΔ* sacculi as compared to WT, as monitored by SaccuFlow (**Figure 5.10A**).

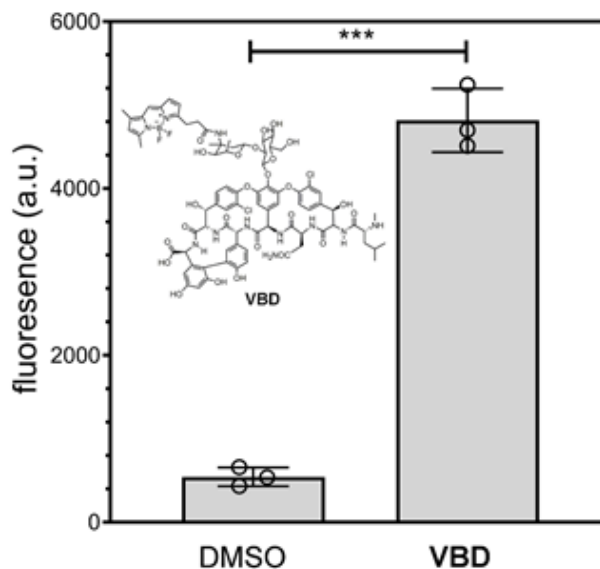


Figure 5.8 Flow cytometry analysis of sacculi isolated from *S. aureus* (ATCC 25923). Subsequently, sacculi were treated with **VBD** (4 $\mu\text{g}/\text{mL}$) or DMSO. Data are represented as mean \pm SD ($n = 3$). P -values were determined by a two-tailed t -test (* denotes a p -value < 0.05 , ** < 0.01 , *** < 0.001 , ns = not significant).

Next, sacculi samples were isolated from an *Enterococci faecium* (*E. faecium*) strain that has a vancomycin inducible resistant phenotype based on activation of the membrane receptor VanS.⁵⁷⁻⁵⁸ The outcome of this activation is the intracellular removal of the terminal D-alanine in the PG precursor, which should reduce the bindings available to **VBD**. Consistent with this phenotypic switch, analysis of VRE sacculi showed that there was a significant decrease in fluorescence associated with VRE pre-treated with vancomycin (**Figure 5.10B**).

Together, these results confirm that SaccuFlow can be readily adopted to monitor and quantify interactions of PG-binding molecules, which can have applicability in studying drug resistance or establish therapeutic interventions.

We tested the ability of the SaccuFlow assay to evaluate the processing and remodeling of PG. More specifically, we evaluated the possibility of tracking the activity of the enzyme sortase A from *S. aureus*. Sortase A is a transpeptidase that recognizes the sorting sequence LPXTG (where X is any amino acid) and thereby anchors proteins that contain this sequence onto the bacterial PG.⁵⁹⁻⁶⁰ *S. aureus* utilizes sortase A to heavily decorate the surface of the PG with proteins capable of improving host colonization and interfering with human immune response. Therefore, sortase A is considered an attractive drug target and small molecules that inhibit sortase A could prove to be promising anti-virulence agents.

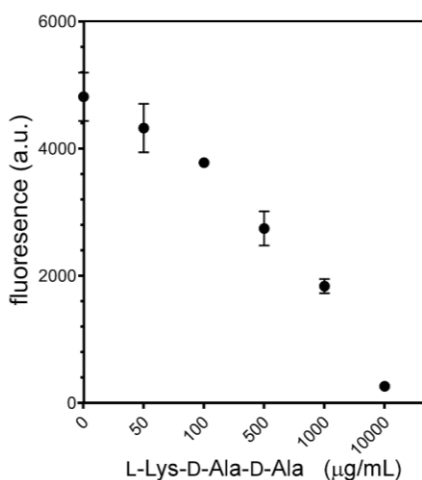


Figure 5.9 Flow cytometry analysis of sacculi isolated from *S. aureus* (ATCC 25923). Subsequently, sacculi were treated with **VBD** (2 µg/mL) and increasing concentrations of L-Lys-D-Ala-D-Ala. Data are represented as mean +/- SD (n = 3).

Prior efforts to investigate sortase A activity have generally used minimal peptide mimics of PG (e.g., penta-glycine), which may not be entirely representative of the features of the PG (or its lipid anchored precursor). For our

assay, sacculi isolated from *S. aureus* were incubated with purified sortase A originating from *S. aureus* and a sorting signal substrate modified with a fluorophore. We monitored the fluorescence of the sacculi over time *via* flow cytometry and, as expected, observed an increase in fluorescence as sortase A linked the fluorescent sorting signal substrate to the isolated PG (**Figure 5.11**). Further, sacculi treated with methanethiosulfonate (MTSET), a covalent inhibitor of sortase⁶¹, or no sortase at all, demonstrated fluorescence that was at background levels (**Figure 5.11**). These results provide clear demonstration that SaccuFlow can be utilized to investigate processing of PG in a quantitative manner.

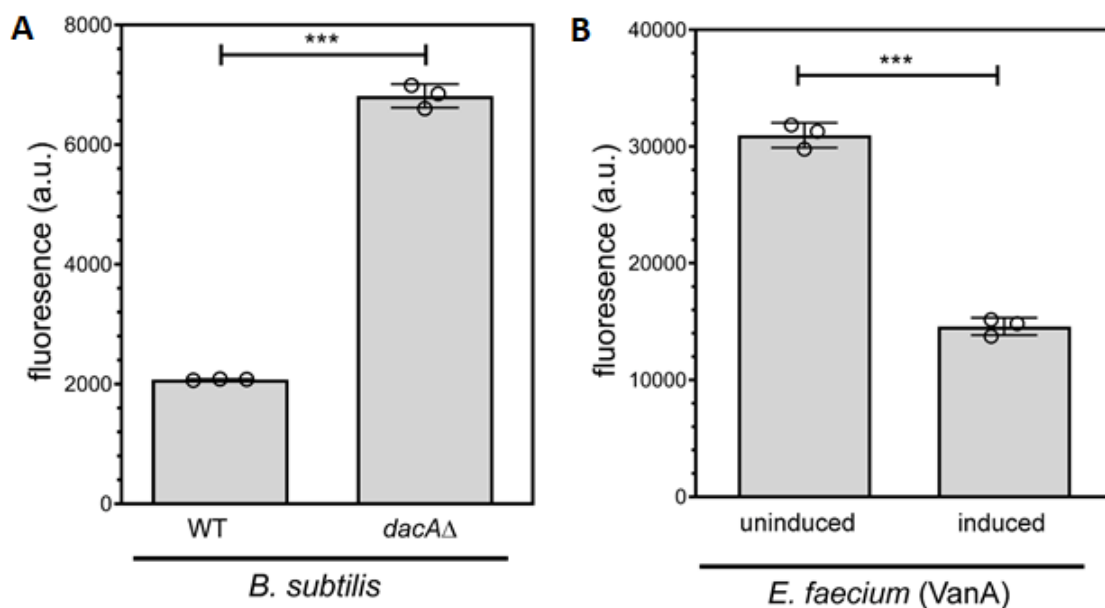


Figure 5.10 (A) Flow cytometry analysis of sacculi isolated from *B. subtilis* (WT and *dacA*Δ). Subsequently, sacculi were treated with **VBD** (2 μg/mL). (B) Flow cytometry analysis of sacculi isolated from *E. faecium* *vanA* (with and without pre-incubation of vancomycin). Subsequently, sacculi were treated with **VBD** (4 μg/mL). Data are represented as mean +/- SD (n = 3). *P*-values were determined by a two-tailed *t*-test (* denotes a *p*-value < 0.05, ** < 0.01, *** < 0.001, ns = not significant).

Finally, to demonstrate the high-throughput capability of SaccuFlow, we used the established parameters of the sortase A assay to determine the ability of a library of 1,280 pharmacologically active compounds to inhibit sortase A activity (LOPAC 1280 library). Using isolated *S. aureus* sacculi, sortase A, and the fluorescent sorting signal substrate, we monitored the fluorescence readout of the sacculi against individual members of the compound library. We predicted that a reduction in fluorescence would correspond to a reduction of sortase A activity.

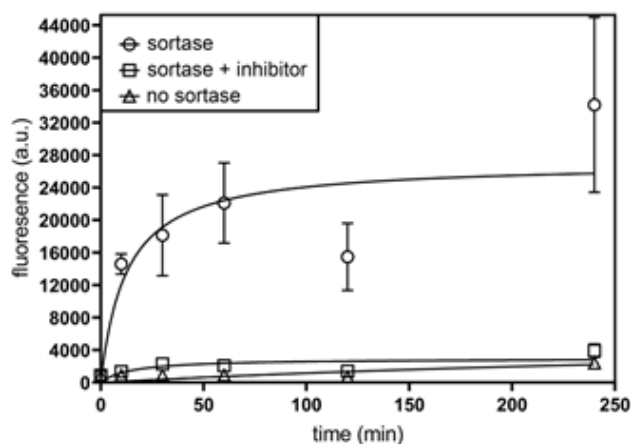


Figure 5.11 Time course analysis of sortase activity using isolated sacculi from *S. aureus* (ATCC 25923) in the presence of the fluorescent sorting signal substrate (100 μ M). Flow cytometry analysis of sacculi treated with sortase, the covalent inhibitor MTSET (1 mM), and in the absence of sortase.

Our screening results revealed a total of 18 compounds as potential inhibitors of sortase (**Figure 5.12A**). Of interest, amsacrine, which was previously reported to inhibit Mycobacterial topoisomerases⁶² as well as D-alanylation of teichoic acids in *S. aureus*⁶³, was identified as a potential inhibitor. We further tested the ability of amsacrine to inhibit sortase A in a titration assay, which showed a reduction in fluorescence levels in a concentration-dependent manner (**Figure 5.12B**). This pilot screen demonstrated the feasibility of SaccuFlow to be

miniaturized and used in a high-throughput screen. Moreover, these results highlight the potential of SaccuFlow to assess essential enzyme operations within the PG scaffold and identify substrates or inhibitors of those enzymes of interest, paving the way to the discovery of potential therapeutics against these validated drug targets.

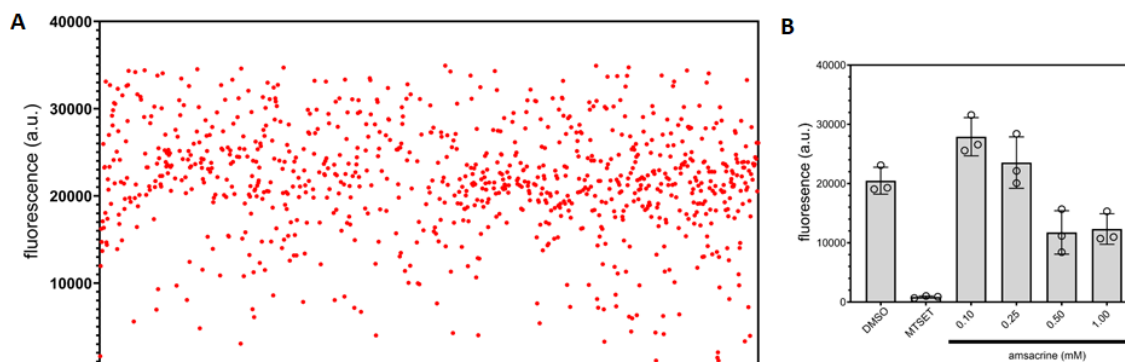


Figure 5.12 (A) Screening of LOPAC 1280 library using 384-well format. Individual dots represent members of the library in the presence of isolated sacculi and sorting signal substrate (100 μ M). (B) Flow cytometry analysis of sortase activity in the presence of designated conditions. Data are represented as mean \pm SD ($n = 3$).

5.4 Conclusion

In conclusion, we have described the implementation of a new flow cytometry assay (SaccuFlow) that makes use of the mechanical strength and native composition of bacterial sacculi. By adopting the assay to flow cytometry, we showed that it is possible to gain quantitative information on interactions of molecules with PG. Moreover, versatility of the assay platform was demonstrated by analyzing sacculi from three different species of Gram-positive bacteria, one Gram-negative bacterium, and a mycobacterium. Binding studies with fluorescently labeled vancomycin showed that SaccuFlow can reveal PG interaction dynamics, including phenotypic changes due to drug resistance. Finally, enzymatic processing of PG by sortase A was performed to highlight the

versatility of this assay in studying PG biology. Given the important nature of PG binding molecules, including several clinically relevant antibiotics and components of the innate immune system, we expect that this assay platform will find wide usage across microbiology studies.

5.5 Materials and Methods

Materials. All peptide related reagents (resin, coupling reagent, deprotection reagent, amino acids, and cleavage reagents) were purchased from ChemImpex or BroadPharm. Bacterial strains *Staphylococcus aureus* (*S. aureus*), *Bacillus subtilis* (*B. subtilis*), *B. subtilis dacAΔ*, and *Escherichia coli* (*E. coli*) were grown in lysogeny broth, *Enterococcus faecium* (*E. faecium*) was grown in tryptic soy broth, *Mycobacterium smegmatis* (*M. smegmatis*) were grown in lysogeny broth supplemented with 0.05% Tween 80 for all experiments.

Peptidoglycan Isolation of *S. aureus*. Lysogeny broth (LB, 25 mL) containing 1 mM D- or L-Lys-azido, 50, 100, or 500 μM D-Lys(FITC), 500 μM L-Lys(FITC), or no supplemented probe was prepared. *S. aureus* bacteria were added to the LB medium (1:100) and allowed to grow overnight at 37°C with shaking at 250 rpm. The cells were harvested and then resuspended in 1X PBS, boiled for 25 min, and then centrifuged at 14,000g for 15 min at 4°C. Cells were then placed in 15 mL of 5% (w/v) sodium dodecyl sulfate (SDS) and boiled for 25 min followed by centrifugation at 14,000g for 15 min at 4°C. Following centrifugation, cells were boiled again in 25 mL of 4% (w/v) SDS for 15 min followed by centrifugation using same parameters as before. Cells were then washed 6 times with 60 °C DI water to remove all SDS. After washing, cells were resuspended in 6 mL of 20 mM Tris buffer (pH 8.0). Pellets were treated with 800 μg DNase for 24 h followed by trypsin (800 μg) for another 24 h (37°C shaking at 115 rpm). Pellets were boiled for 25 min followed by centrifugation at 14,000g for 15 min at 4°C, resuspended in 2 mL of 1X PBS, and further diluted for analysis by flow cytometry. In samples where wall teichoic acid removal was desired the pellets after the last centrifugation step were resuspended 1 M HCl and incubated for 4 h at 37°C with shaking. The pellet was harvested by centrifugation for 10 min at 4,000 rpm and washed with ddH₂O

until the pH of the supernatant reached 6-7. The final pellet was resuspended in 1X PBS, and further diluted for analysis by flow cytometry with an Attune NxT flow cytometer, equipped with a 488 nm laser and 525/40 nm bandpass filter. The data were analyzed using the Attune NXT Software.

Peptidoglycan Isolation of *B. subtilis* and *B. subtilis dacΔ*. LB was supplemented with 1X kanamycin during the growth of the *B. subtilis dacAΔ*. The rest of the isolation protocol follows that of the *S. aureus* isolation protocol detailed above.

Peptidoglycan Isolation of *E. faecium*. Tryptic soy broth (TSB) was supplemented with 16 µg/mL of vancomycin in order to induce the resistance phenotype during the growth of the *E. faecium*. The rest of the isolation protocol follows that of the *S. aureus* isolation protocol detailed above.

Peptidoglycan Isolation of *E. coli*. LB (100 mL) containing 1 mM D- or L-Lys-azido, or no supplemented probe was prepared. *E. coli* BW25113 bacteria were added to the LB medium (1:100) and allowed to grow overnight at 37°C with shaking at 250 rpm. The cells were chilled on ice, then harvested at 8,000g for 10 min at 4°C. The resulting pellet was resuspended in 3 mL of 1% (w/v) NaCl, then added slowly to 6 mL of 8% SDS that was in a boiling water bath with a stir bar. Samples were boiled for 5 h, followed by incubation at room temperature with continued stirring overnight. The following morning, samples were boiled for 2 h and then pelleted at 100,000g for 10 min at 25°C. Resulting pellets were suspended in 3 mL of 4% SDS, boiled for 2 h with stirring. Samples were collected using the same parameters and washed 5 times with sterile DI H₂O to remove all SDS. Pellets were resuspended in 1 mL of 1X PBS and 200 µg/mL of trypsin was added followed by incubation at 37°C with shaking at 115 rpm for 2 h. A second dose of trypsin was added, and samples were incubated overnight. The following morning, one-tenth volume of 10% SDS was added and samples were placed in an oil bath at 100°C for 2 h. Sacculi were collected as before, and washed 3X with sterile DI H₂O to remove residual SDS. The final pellet was lyophilized and resuspended in 400 µL of H₂O for further analysis by flow cytometry.

Peptidoglycan Isolation of *M. smegmatis*. LB (100 mL) with 0.05% Tween 80 containing 1 mM D- or L-Lys-azido, or no supplemented probe was prepared. *M. smegmatis* bacteria were added to the LB medium (1:100) and allowed to grow overnight at 37°C with shaking at 250 rpm. Cells were then harvested at 14,000g for 15 min at 4°C and washed 1X in a minimal volume of 1X PBS. Pellets were resuspended in 10 mM NH₄HCO₃ with a protease inhibitor cocktail (Sigma SRE005-1BO). This suspension was lysed using a tip sonicator (Fisher Scientific) at 60% amplitude for 60 seconds, with at least 60 seconds on ice in between. This was repeated for 5 cycles. The sonicate was digested with 10 µg/mL DNase and RNase for 1 h at 4°C, then harvested at 27,000g for 30 min at 4°C. The pellet was resuspended in PBS with 2% SDS and incubated for 1 h at 50°C with constant stirring. This was collected using the same centrifugal parameters and the SDS process was repeated 2X. The resulting pellet was resuspended in PBS with 1% SDS and 0.1 mg/mL Proteinase K at 45°C for 1 h with stirring. The sample was then heated to 90°C for 1 h and collected as above. This step at 90°C was repeated 2X. The sample was washed 2X with PBS and 4X with dH₂O. This yielded mycolic-arabinogalactan-peptidoglycan (mAGP). The final mAGP sample was lyophilized and resuspended in H₂O for further SPAAC chemistry and analysis by flow cytometry.

Enzymatic Degradation. Isolated 100 µM D-Lys(FITC) labeled *S. aureus* sacculi samples were pelleted in a 96-well plate at 4,000 rpm for 4 min and then resuspended in a 1X PBS solution containing either 5, 20, or 40 µg/mL mutanolysin or 250 µg/mL lysozyme and allowed to incubate at 37°C, however a zero time point was taken before any samples were subjected to enzyme treatment. A portion of the cells were then taken at 1, 5, 15, 30, and 60 minutes. At each time point, the collected bacteria were resuspended solution of 1X PBS containing 4% formaldehyde to quench the enzymatic activity. Samples were analyzed by flow cytometry as described above.

SPAAC Reaction with Isolated Sacculi. Isolated sacculi samples (50 µL) were pelleted in a 96-well plate at 4,000 rpm for 4 min and then resuspended in a 1X

PBS solution containing 25 μM **Df10**. Plates were incubated at 37°C for 30 min and washed 3X with 1X PBS by centrifugation as before to remove excess FITC. Samples were then diluted 10-fold for analysis by flow cytometry as described above.

Vancomycin-BODIPY (VBD) Binding Assays. Isolated *S. aureus* sacculi samples were pelleted in a 96-well plate at 4,000 rpm for 4 min and then resuspended in a 1X PBS solution containing either 2 $\mu\text{g}/\text{mL}$ **VBD** alone or 2 $\mu\text{g}/\text{mL}$ **VBD** in conjunction with either 50, 100, 500, 1000, or 10000 $\mu\text{g}/\text{mL}$ of the L-Lys-D-Ala-D-Ala peptide. The plates were incubated for 30 min at 37°C and after incubation the samples were immediately subjected to analysis by flow cytometry as described above. Isolated *B. subtilis* and *B. subtilis* *dacA* Δ sacculi samples were pelleted in a 96-well plate at 4,000 rpm for 4 min and then resuspended in a 1X PBS solution containing 4 $\mu\text{g}/\text{mL}$ **VBD** and incubated for 30 min at 37°C. After incubation samples were washed with 1X PBS and subjected to analysis by flow cytometry as described above. *E. faecium* (noninduced and induced) sacculi samples were pelleted in a 96-well plate at 4,000 rpm for 4 min and then resuspended in a 1X PBS solution containing 4 $\mu\text{g}/\text{mL}$ **VBD** and incubated for 30 min at 37°C. After incubation samples were immediately subjected to analysis by flow cytometry as described above.

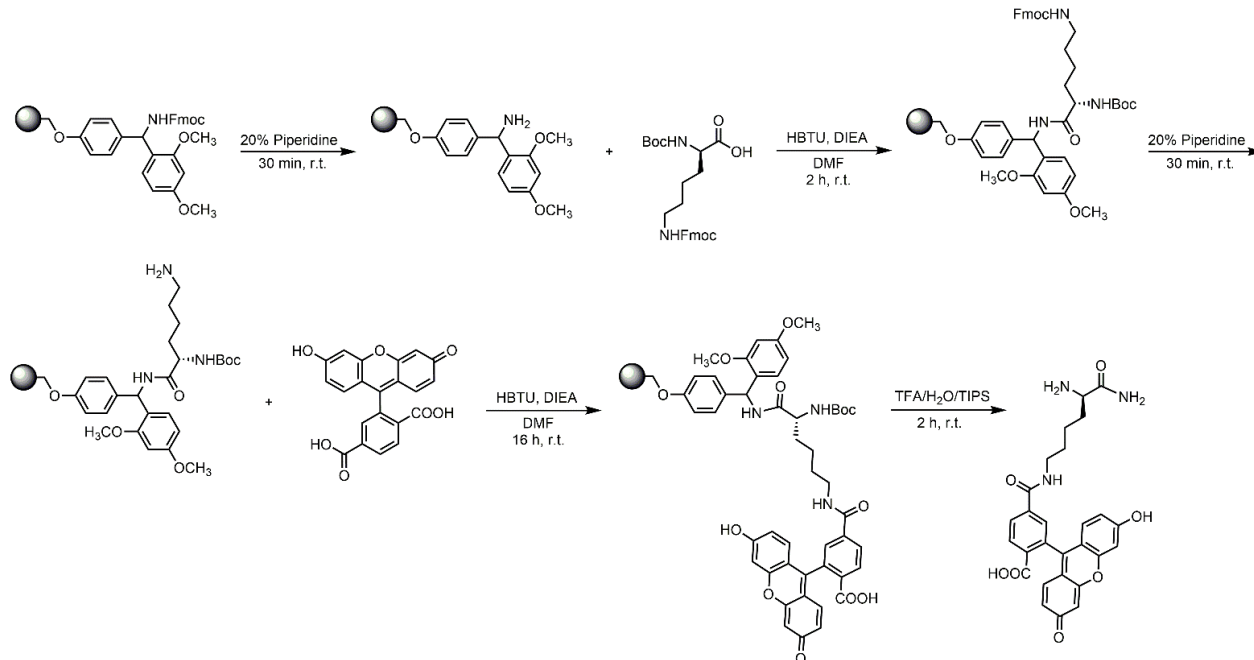
Sortase A Expression and Purification. The plasmid for sortase A from *S. aureus* was obtained from Addgene: pET28a-SrtAdelta59. Competent BL21 (DE3) *E. coli* were transformed with the plasmid. *E. coli* cells containing the plasmid from an overnight culture were diluted 1:100 and grown at 37°C until the OD₆₀₀ was 0.4-0.6. At this time, Isopropyl- β -D-thiogalactopyranoside (IPTG) was added to a concentration of 0.5 mM and the cultures were shook at 25°C for 16 h. Cells were collected at 3,000g for 30 min and resuspended in 50 mM Tris-HCl, pH 7.5, and 150 mM NaCl. Pellets were then recollected and lysed in cold lysis buffer (50 mM Tris-HCl, pH 7.5, 150 mM NaCl, 5 mM MgCl₂, 10 mM imidazole, 10% vol/vol glycerol, 1 mg ml⁻¹ DNase and 1 mg ml⁻¹ lysozyme). Cells were lysed using an ultrasonic cell sonicator and the lysate was separated from cellular debris by

centrifugation at 20,000g for 30 min at 4°C. The supernatant was loaded onto a Ni-NTA agarose resin and eluted with 500 mM imidazole in buffer (50 mM Tris-HCl pH 7.5, 150 mM NaCl, and 10% vol/vol glycerol). The eluted protein was dialyzed against buffer without imidazole, aliquoted (protein concentration determined by Bradford assay), and stored at –20°C until use.

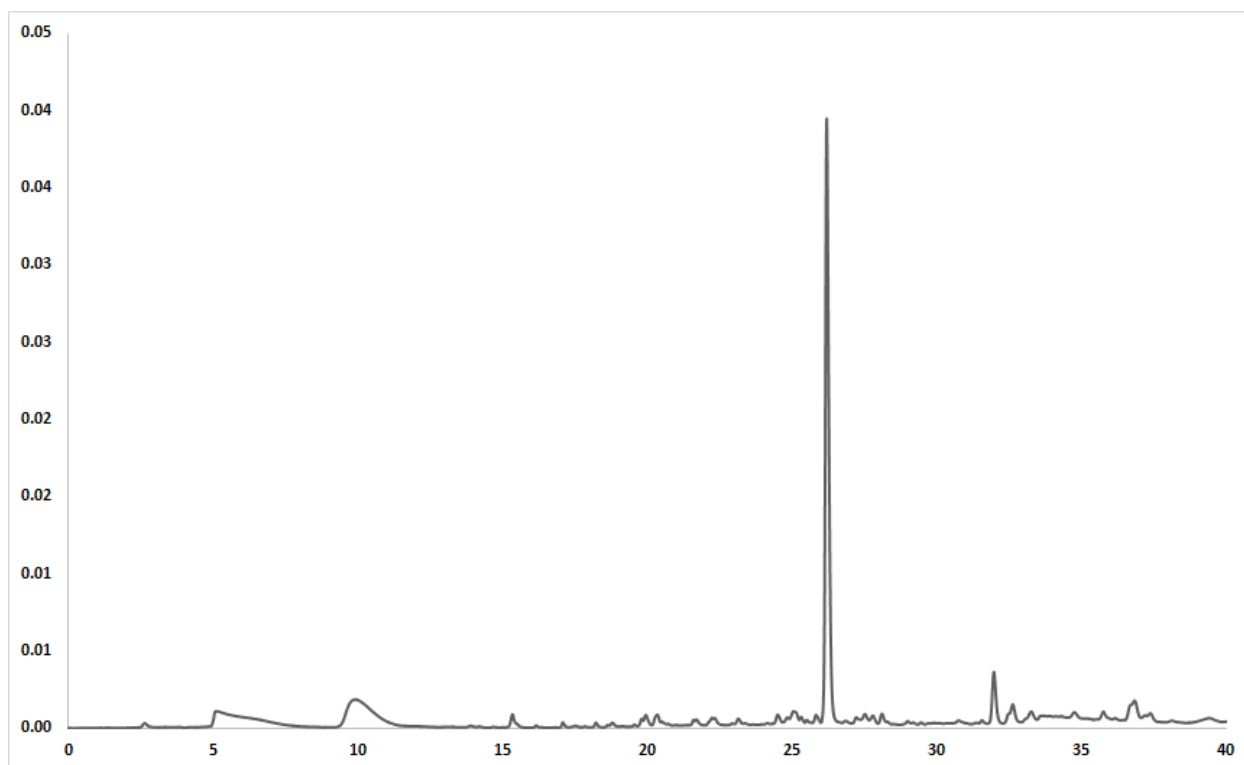
Sortase A Enzymatic Assays. Isolated *S. aureus* sacculi samples were incubated with 20 uM sortase A, 100 uM sorting signal substrate, and 1X sortase buffer (10X contains 500 mM Tris-HCl, pH 7.5, 1.5 M NaCl, 100 mM CaCl₂). Samples that contained the covalent inhibitor, MTSET, were run at a concentration of 1 mM. All were shook at room temperature for the given time. At each time point, 20 uL were taken out of the reaction, quenched with 0.1% TFA, and washed 3X with 100 mM Tris, 5 mM EDTA, pH 7 and freshly added 8 M urea. Samples were resuspended in a final volume of 120 uL 1X PBS and analyzed by flow cytometry as described above.

For the high-throughput scan using the LOPAC library of 1,280 small molecule compounds, the same conditions were used. However, sortase was incubated with 1 mM of the compound library and let incubate at room temperature for 20 minutes before addition of sacculi, FI-LPMTG (sorting signal), and buffer. After the addition of the remaining reaction components, samples were shook at room temperature for 4 h before being quenched with 0.1% TFA, then washed in buffer with 8M urea as above. Samples were resuspended in a final volume of 100 uL 1X PBS and analyzed by flow cytometry as described above.

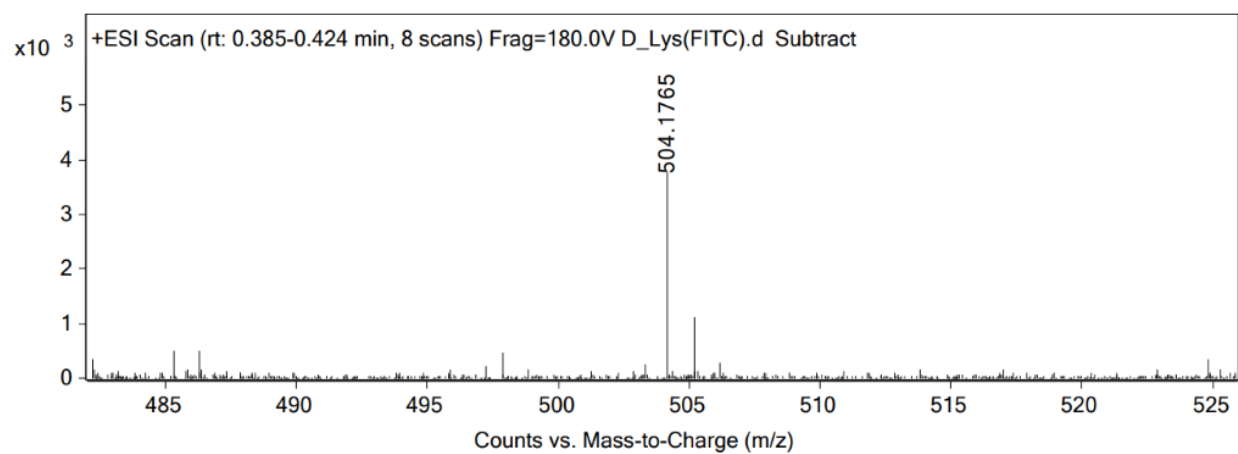
Scheme S1. Synthesis of D-LysFI (shown) and L-LysFI

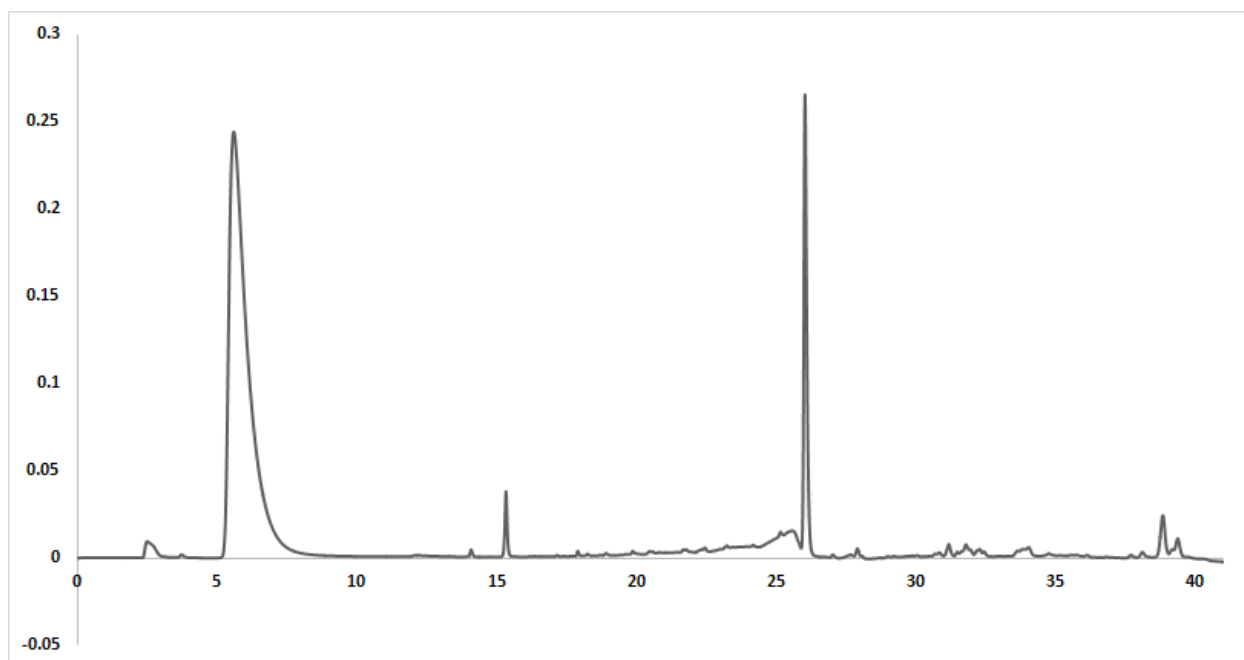


A 25 mL peptide synthesis vessel charged with rink amide resin (250 mg, 0.11 mmol) underwent the Fmoc removal procedure and was washed as described above. Boc-D-Lysine(Fmoc)-OH (5 eq, 257 mg, 0.55 mmol), HBTU (4.9 eq, 204 mg, 0.53 mmol), and DIEA (10 eq, 0.191 mL, 1.10 mmol) in DMF (15 mL) were added to the reaction vessel and agitated for 2 h at ambient temperature. After 2 h the resin was washed as previously stated and the Fmoc protecting group removal was also performed as described above followed by washing. The resin was coupled with 5,6-carboxyfluorescein (2 eq, 82 mg, 0.22 mmol), HBTU (1.9 eq, 79 mg, 0.20 mmol), and DIEA (4 eq, 0.076 mL, 0.44 mmol) in DMF (15 mL) and agitated for 16h at ambient temperature. The resin was washed as previously described and then added to a solution of TFA/H₂O/TIPS (95%, 2.5%, 2.5%, 20 mL) with agitation for 2 h at ambient temperature. The resin was filtered and the resulting solution was concentrated *in vacuo*. The residue was triturated with cold diethyl ether. The sample was analyzed for purity using a Waters 1525 Binary HPLC Pump using a Phenomenex Luna 5u C8(2) 100A (250 x 4.60 mm) column; gradient elution with H₂O/CH₃CN.

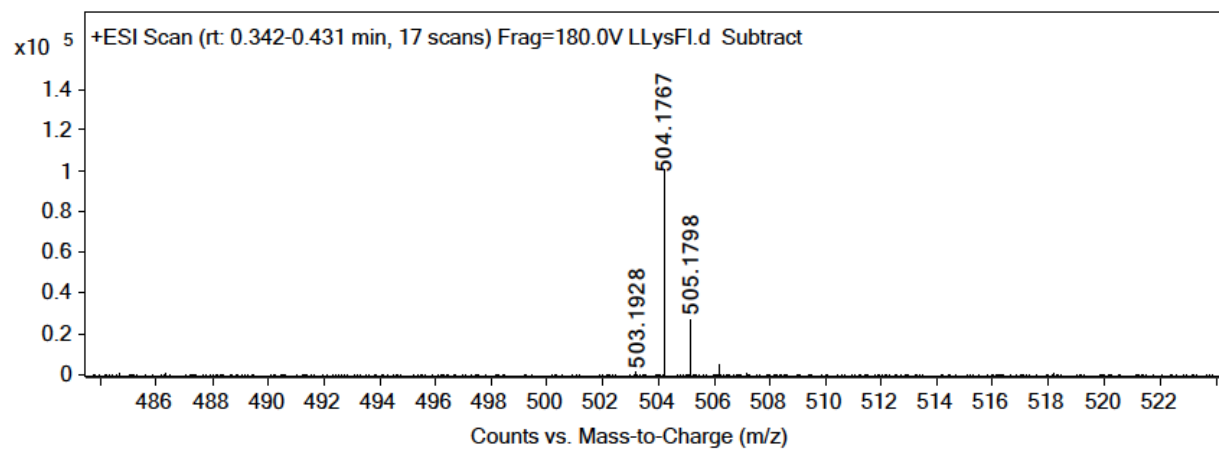
D-LysFI

ESI-MS calculated $[M + H]^+$: 504.1765, found: 504.1765

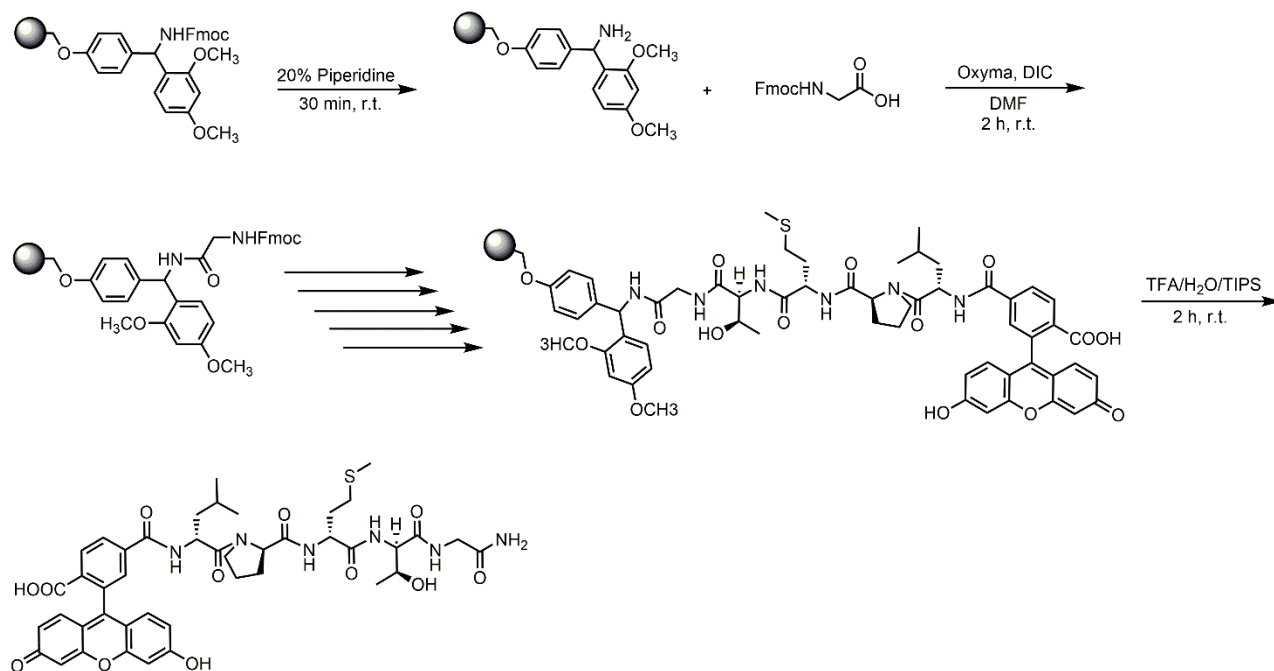


L-LysFI

ESI-MS calculated [M + H]⁺: 504.1765, found: 504.1767

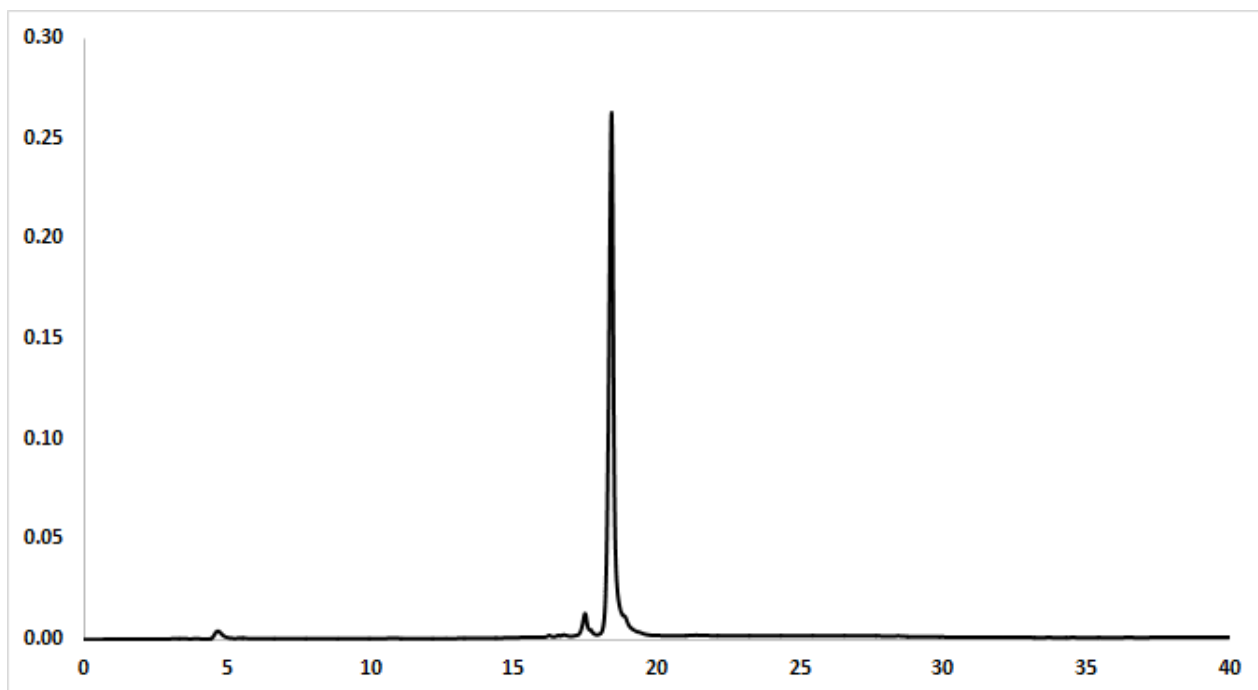


Scheme S3. Synthesis of FI-LPMTG

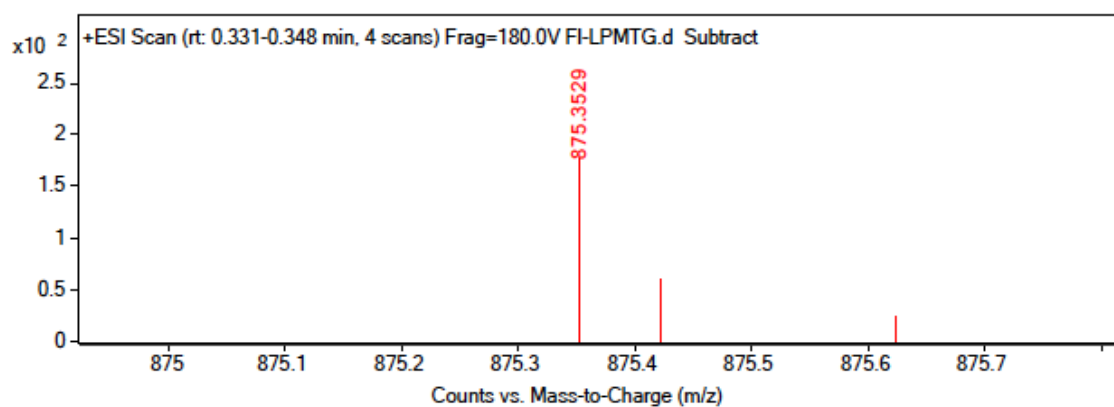


A 25 mL synthetic vessel was charged with 500 mg (0.27 mmol) of Fmoc-Rink amide resin. The Fmoc protecting group was removed with a 20% piperidine in DMF solution (15 mL) for 30 minutes at ambient temperature, then washed with MeOH and DCM (3 x 15 mL each). Fmoc-glycine-OH (3 eq, 240 mg, 0.810 mmol), Oxyma (3 eq, 115 mg, 0.810 mmol), and DIC (3 eq, 126 μ L, 0.810 mmol) in DMF (15 mL) was added to the reaction vessel and agitated for 2 hours at ambient temperature and washed as previously stated. The Fmoc removal and coupling procedure was repeated as before using the same equivalencies with Fmoc-L-threonine(tBu)-OH, Fmoc-L-methionine-OH, Fmoc-L-proline-OH, and Fmoc-L-leucine-OH. The Fmoc group of L-leucine was deprotected and resin coupled with 5,6-carboxyfluorescein (2 eq, 203 mg, 0.810 mmol), HBTU (2 eq, 201 mg, 0.810 mmol), and DIEA (4 eq, 187 μ L, 1.08 mmol) in DMF (15 mL) shaking over-night. The resin was washed as previously described. To remove the peptide from resin, a TFA cocktail solution (95 % TFA, 2.5% TIPS, and 2.5 % DCM) was added to the resin with agitation for 2 hours protected from light. The resin was filtered and resulting solution was concentrated *in vacuo*. The peptide was triturated with cold diethyl ether and purified using reverse phase HPLC using H₂O/MeOH to yield **FI-**

LPMTG. The sample was analyzed for purity using a Waters 1525 Binary HPLC Pump using a Phenomenex Luna 5u C8(2) 100A (250 x 4.60 mm) column; gradient elution with H₂O/CH₃CN.



ESI-MS calculated [M + H]⁺: 875.3280, found: 875.3529



5.6 Acknowledgements

Alexis J. Apostolos performed the D-Lys(FITC) labeling of *S. aureus* and sacculi isolation, D-Lys(AZ) labeling of the Gram-negative and mycobacteria and sacculi isolation, sortase isolation and expression, sortase inhibitor screen. Brianna Dalesandro synthesized the FITC-LPMTG peptide.

5.7 References

1. Vollmer, W.; Blanot, D.; de Pedro, M. A., Peptidoglycan structure and architecture. *FEMS Microbiol Rev* **2008**, 32 (2), 149-67.
2. Silhavy, T. J.; Kahne, D.; Walker, S., The bacterial cell envelope. *Cold Spring Harb Perspect Biol* **2010**, 2 (5), a000414.
3. Royet, J.; Dziarski, R., Peptidoglycan recognition proteins: pleiotropic sensors and effectors of antimicrobial defences. *Nat Rev Microbiol* **2007**, 5 (4), 264-77.
4. Wolf, A. J.; Underhill, D. M., Peptidoglycan recognition by the innate immune system. *Nat Rev Immunol* **2018**, 18 (4), 243-254.
5. Egan, A. J. F.; Errington, J.; Vollmer, W., Regulation of peptidoglycan synthesis and remodelling. *Nat Rev Microbiol* **2020**, 18 (8), 446-460.
6. Brown, D. G.; May-Dracka, T. L.; Gagnon, M. M.; Tommasi, R., Trends and exceptions of physical properties on antibacterial activity for Gram-positive and Gram-negative pathogens. *J Med Chem* **2014**, 57 (23), 10144-61.
7. O'Shea, R.; Moser, H. E., Physicochemical properties of antibacterial compounds: implications for drug discovery. *J Med Chem* **2008**, 51 (10), 2871-8.
8. Richter, M. F.; Drown, B. S.; Riley, A. P.; Garcia, A.; Shirai, T.; Svec, R. L.; Hergenrother, P. J., Predictive compound accumulation rules yield a broad-spectrum antibiotic. *Nature* **2017**, 545 (7654), 299-304.
9. Cloud-Hansen, K. A.; Peterson, S. B.; Stabb, E. V.; Goldman, W. E.; McFall-Ngai, M. J.; Handelsman, J., Breaching the great wall: peptidoglycan and microbial interactions. *Nat Rev Microbiol* **2006**, 4 (9), 710-6.
10. Demchick, P.; Koch, A. L., The permeability of the wall fabric of *Escherichia coli* and *Bacillus subtilis*. *J Bacteriol* **1996**, 178 (3), 768-73.
11. Dijkstra, A. J.; Keck, W., Peptidoglycan as a barrier to transenvelope transport. *J Bacteriol* **1996**, 178 (19), 5555-62.
12. Scherrer, R.; Gerhardt, P., Molecular sieving by the *Bacillus megaterium* cell wall and protoplast. *J Bacteriol* **1971**, 107 (3), 718-35.

13. Berends, E. T.; Dekkers, J. F.; Nijland, R.; Kuipers, A.; Soppe, J. A.; van Strijp, J. A.; Rooijackers, S. H., Distinct localization of the complement C5b-9 complex on Gram-positive bacteria. *Cell Microbiol* **2013**, 15 (12), 1955-68.
14. Lambert, P. A., Cellular impermeability and uptake of biocides and antibiotics in Gram-positive bacteria and mycobacteria. *J Appl Microbiol* **2002**, 92 Suppl, 46S-54S.
15. Arthur, M.; Courvalin, P., Genetics and mechanisms of glycopeptide resistance in enterococci. *Antimicrob Agents Chemother* **1993**, 37 (8), 1563-71.
16. Bugg, T. D.; Wright, G. D.; Dutka-Malen, S.; Arthur, M.; Courvalin, P.; Walsh, C. T., Molecular basis for vancomycin resistance in *Enterococcus faecium* BM4147: biosynthesis of a depsipeptide peptidoglycan precursor by vancomycin resistance proteins VanH and VanA. *Biochemistry* **1991**, 30 (43), 10408-15.
17. Pereira, P. M.; Filipe, S. R.; Tomasz, A.; Pinho, M. G., Fluorescence ratio imaging microscopy shows decreased access of vancomycin to cell wall synthetic sites in vancomycin-resistant *Staphylococcus aureus*. *Antimicrob Agents Chemother* **2007**, 51 (10), 3627-33.
18. Bush, K., Antimicrobial agents targeting bacterial cell walls and cell membranes. *Rev Sci Tech* **2012**, 31 (1), 43-56.
19. de Kruijff, B.; van Dam, V.; Breukink, E., Lipid II: a central component in bacterial cell wall synthesis and a target for antibiotics. *Prostaglandins Leukot Essent Fatty Acids* **2008**, 79 (3-5), 117-21.
20. Asong, J.; Wolfert, M. A.; Maiti, K. K.; Miller, D.; Boons, G. J., Binding and Cellular Activation Studies Reveal That Toll-like Receptor 2 Can Differentially Recognize Peptidoglycan from Gram-positive and Gram-negative Bacteria. *J Biol Chem* **2009**, 284 (13), 8643-53.
21. Fuda, C.; Heseck, D.; Lee, M.; Morio, K.; Nowak, T.; Mobashery, S., Activation for catalysis of penicillin-binding protein 2a from methicillin-resistant *Staphylococcus aureus* by bacterial cell wall. *J Am Chem Soc* **2005**, 127 (7), 2056-7.

22. Grimes, C. L.; Ariyananda Lde, Z.; Melnyk, J. E.; O'Shea, E. K., The innate immune protein Nod2 binds directly to MDP, a bacterial cell wall fragment. *J Am Chem Soc* **2012**, 134 (33), 13535-7.
23. Guan, R.; Roychowdhury, A.; Ember, B.; Kumar, S.; Boons, G. J.; Mariuzza, R. A., Structural basis for peptidoglycan binding by peptidoglycan recognition proteins. *Proc Natl Acad Sci U S A* **2004**, 101 (49), 17168-73.
24. Ngadjeua, F.; Braud, E.; Saidjalolov, S.; Iannazzo, L.; Schnappinger, D.; Ehrt, S.; Hugonnet, J. E.; Mengin-Lecreulx, D.; Patin, D.; Etheve-Quellejeu, M.; Fonvielle, M.; Arthur, M., Critical Impact of Peptidoglycan Precursor Amidation on the Activity of L,D-Transpeptidases from *Enterococcus faecium* and *Mycobacterium tuberculosis*. *Chemistry* **2018**, 24 (22), 5743-5747.
25. Apostolos, A. J.; Pidgeon, S. E.; Pires, M. M., Remodeling of Crossbridges Controls Peptidoglycan Crosslinking Levels in Bacterial Cell Walls. *ACS Chem Biol* **2020**.
26. Pidgeon, S. E.; Apostolos, A. J.; Nelson, J. M.; Shaku, M.; Rimal, B.; Islam, M. N.; Crick, D. C.; Kim, S. J.; Pavelka, M. S.; Kana, B. D.; Pires, M. M., L,D-Transpeptidase Specific Probe Reveals Spatial Activity of Peptidoglycan Cross-Linking. *ACS Chem Biol* **2019**, 14 (10), 2185-2196.
27. Desmarais, S. M.; Tropini, C.; Miguel, A.; Cava, F.; Monds, R. D.; de Pedro, M. A.; Huang, K. C., High-throughput, Highly Sensitive Analyses of Bacterial Morphogenesis Using Ultra Performance Liquid Chromatography. *J Biol Chem* **2015**, 290 (52), 31090-100.
28. Mesnage, S.; Dellarole, M.; Baxter, N. J.; Rouget, J. B.; Dimitrov, J. D.; Wang, N.; Fujimoto, Y.; Hounslow, A. M.; Lacroix-Desmazes, S.; Fukase, K.; Foster, S. J.; Williamson, M. P., Molecular basis for bacterial peptidoglycan recognition by LysM domains. *Nat Commun* **2014**, 5, 4269.
29. Desmarais, S. M.; De Pedro, M. A.; Cava, F.; Huang, K. C., Peptidoglycan at its peaks: how chromatographic analyses can reveal bacterial cell wall structure and assembly. *Mol Microbiol* **2013**, 89 (1), 1-13.

30. Lee, T. K.; Meng, K.; Shi, H.; Huang, K. C., Single-molecule imaging reveals modulation of cell wall synthesis dynamics in live bacterial cells. *Nat Commun* **2016**, 7, 13170.
31. Sharif, S.; Singh, M.; Kim, S. J.; Schaefer, J., Staphylococcus aureus peptidoglycan tertiary structure from carbon-13 spin diffusion. *J Am Chem Soc* **2009**, 131 (20), 7023-30.
32. Yahashiri, A.; Jorgenson, M. A.; Weiss, D. S., Bacterial SPOR domains are recruited to septal peptidoglycan by binding to glycan strands that lack stem peptides. *Proc Natl Acad Sci U S A* **2015**, 112 (36), 11347-52.
33. Baik, J. E.; Jang, Y. O.; Kang, S. S.; Cho, K.; Yun, C. H.; Han, S. H., Differential profiles of gastrointestinal proteins interacting with peptidoglycans from *Lactobacillus plantarum* and *Staphylococcus aureus*. *Mol Immunol* **2015**, 65 (1), 77-85.
34. Koch, A. L., The exoskeleton of bacterial cells (the sacculus): still a highly attractive target for antibacterial agents that will last for a long time. *Crit Rev Microbiol* **2000**, 26 (1), 1-35.
35. Fura, J. M.; Kearns, D.; Pires, M. M., D-Amino Acid Probes for Penicillin Binding Protein-based Bacterial Surface Labeling. *J Biol Chem* **2015**, 290 (51), 30540-50.
36. Fura, J. M.; Pires, M. M., D-amino carboxamide-based recruitment of dinitrophenol antibodies to bacterial surfaces via peptidoglycan remodeling. *Biopolymers* **2015**, 104 (4), 351-9.
37. Pidgeon, S. E.; Fura, J. M.; Leon, W.; Birabaharan, M.; Vezenov, D.; Pires, M. M., Metabolic Profiling of Bacteria by Unnatural C-terminated D-Amino Acids. *Angew Chem Int Ed Engl* **2015**, 54 (21), 6158-62.
38. Pidgeon, S. E.; Pires, M. M., Cell Wall Remodeling of *Staphylococcus aureus* in Live *Caenorhabditis elegans*. *Bioconjug Chem* **2017**, 28 (9), 2310-2315.
39. Sarkar, S.; Libby, E. A.; Pidgeon, S. E.; Dworkin, J.; Pires, M. M., In Vivo Probe of Lipid II-Interacting Proteins. *Angew Chem Int Ed Engl* **2016**, 55 (29), 8401-4.

40. Kuru, E.; Hughes, H. V.; Brown, P. J.; Hall, E.; Tekkam, S.; Cava, F.; de Pedro, M. A.; Brun, Y. V.; VanNieuwenhze, M. S., In Situ probing of newly synthesized peptidoglycan in live bacteria with fluorescent D-amino acids. *Angew Chem Int Ed Engl* **2012**, 51 (50), 12519-23.
41. Kuru, E.; Tekkam, S.; Hall, E.; Brun, Y. V.; Van Nieuwenhze, M. S., Synthesis of fluorescent D-amino acids and their use for probing peptidoglycan synthesis and bacterial growth in situ. *Nat Protoc* **2015**, 10 (1), 33-52.
42. Siegrist, M. S.; Whiteside, S.; Jewett, J. C.; Aditham, A.; Cava, F.; Bertozzi, C. R., (D)-Amino acid chemical reporters reveal peptidoglycan dynamics of an intracellular pathogen. *ACS Chem Biol* **2013**, 8 (3), 500-5.
43. Siegrist, M. S.; Swarts, B. M.; Fox, D. M.; Lim, S. A.; Bertozzi, C. R., Illumination of growth, division and secretion by metabolic labeling of the bacterial cell surface. *FEMS Microbiol Rev* **2015**, 39 (2), 184-202.
44. Lebar, M. D.; May, J. M.; Meeske, A. J.; Leiman, S. A.; Lupoli, T. J.; Tsukamoto, H.; Losick, R.; Rudner, D. Z.; Walker, S.; Kahne, D., Reconstitution of peptidoglycan cross-linking leads to improved fluorescent probes of cell wall synthesis. *J Am Chem Soc* **2014**, 136 (31), 10874-7.
45. Lupoli, T. J.; Tsukamoto, H.; Doud, E. H.; Wang, T. S.; Walker, S.; Kahne, D., Transpeptidase-mediated incorporation of D-amino acids into bacterial peptidoglycan. *J Am Chem Soc* **2011**, 133 (28), 10748-51.
46. Fura, J. M.; Sabulski, M. J.; Pires, M. M., D-amino acid mediated recruitment of endogenous antibodies to bacterial surfaces. *ACS Chem Biol* **2014**, 9 (7), 1480-9.
47. Apostolos, A. J.; Pidgeon, S. E.; Pires, M. M., Remodeling of Cross-bridges Controls Peptidoglycan Cross-linking Levels in Bacterial Cell Walls. *ACS Chem Biol* **2020**, 15 (5), 1261-1267.
48. Bera, A.; Herbert, S.; Jakob, A.; Vollmer, W.; Gotz, F., Why are pathogenic staphylococci so lysozyme resistant? The peptidoglycan O-acetyltransferase OatA is the major determinant for lysozyme resistance of *Staphylococcus aureus*. *Mol Microbiol* **2005**, 55 (3), 778-87.

49. Baskin, J. M.; Prescher, J. A.; Laughlin, S. T.; Agard, N. J.; Chang, P. V.; Miller, I. A.; Lo, A.; Codelli, J. A.; Bertozzi, C. R., Copper-free click chemistry for dynamic in vivo imaging. *Proc Natl Acad Sci U S A* **2007**, 104 (43), 16793-7.
50. Jewett, J. C.; Sletten, E. M.; Bertozzi, C. R., Rapid Cu-free click chemistry with readily synthesized biarylazacyclooctynones. *J Am Chem Soc* **2010**, 132 (11), 3688-90.
51. Atilano, M. L.; Pereira, P. M.; Yates, J.; Reed, P.; Veiga, H.; Pinho, M. G.; Filipe, S. R., Teichoic acids are temporal and spatial regulators of peptidoglycan cross-linking in *Staphylococcus aureus*. *Proc Natl Acad Sci U S A* **2010**, 107 (44), 18991-6.
52. Xia, G.; Kohler, T.; Peschel, A., The wall teichoic acid and lipoteichoic acid polymers of *Staphylococcus aureus*. *Int J Med Microbiol* **2010**, 300 (2-3), 148-54.
53. Swoboda, J. G.; Campbell, J.; Meredith, T. C.; Walker, S., Wall teichoic acid function, biosynthesis, and inhibition. *Chembiochem* **2010**, 11 (1), 35-45.
54. Santa Maria, J. P., Jr.; Sadaka, A.; Moussa, S. H.; Brown, S.; Zhang, Y. J.; Rubin, E. J.; Gilmore, M. S.; Walker, S., Compound-gene interaction mapping reveals distinct roles for *Staphylococcus aureus* teichoic acids. *Proc Natl Acad Sci U S A* **2014**, 111 (34), 12510-5.
55. DeDent, A. C.; McAdow, M.; Schneewind, O., Distribution of protein A on the surface of *Staphylococcus aureus*. *J Bacteriol* **2007**, 189 (12), 4473-84.
56. Popham, D. L.; Gilmore, M. E.; Setlow, P., Roles of low-molecular-weight penicillin-binding proteins in *Bacillus subtilis* spore peptidoglycan synthesis and spore properties. *J Bacteriol* **1999**, 181 (1), 126-32.
57. Arthur, M.; Molinas, C.; Courvalin, P., The VanS-VanR two-component regulatory system controls synthesis of depsipeptide peptidoglycan precursors in *Enterococcus faecium* BM4147. *J Bacteriol* **1992**, 174 (8), 2582-91.
58. Koteva, K.; Hong, H. J.; Wang, X. D.; Nazi, I.; Hughes, D.; Naldrett, M. J.; Buttner, M. J.; Wright, G. D., A vancomycin photoprobe identifies the histidine kinase VanSsc as a vancomycin receptor. *Nat Chem Biol* **2010**, 6 (5), 327-9.
59. Maresso, A. W.; Schneewind, O., Sortase as a target of anti-infective therapy. *Pharmacol Rev* **2008**, 60 (1), 128-41.

60. Nelson, J. W.; Chamessian, A. G.; McEnaney, P. J.; Murelli, R. P.; Kazmierczak, B. I.; Spiegel, D. A., A biosynthetic strategy for re-engineering the *Staphylococcus aureus* cell wall with non-native small molecules. *ACS Chem Biol* **2010**, 5 (12), 1147-55.
61. Ton-That, H.; Schneewind, O., Anchor structure of staphylococcal surface proteins. IV. Inhibitors of the cell wall sorting reaction. *J Biol Chem* **1999**, 274 (34), 24316-20.
62. Szafran, M. J.; Kolodziej, M.; Skut, P.; Medapi, B.; Domagala, A.; Trojanowski, D.; Zakrzewska-Czerwinska, J.; Sriram, D.; Jakimowicz, D., Amsacrine Derivatives Selectively Inhibit Mycobacterial Topoisomerase I (TopA), Impair *M. smegmatis* Growth and Disturb Chromosome Replication. *Front Microbiol* **2018**, 9, 1592.
63. Pasquina, L.; Santa Maria, J. P., Jr.; McKay Wood, B.; Moussa, S. H.; Matano, L. M.; Santiago, M.; Martin, S. E.; Lee, W.; Meredith, T. C.; Walker, S., A synthetic lethal approach for compound and target identification in *Staphylococcus aureus*. *Nat Chem Biol* **2016**, 12 (1), 40-5.